U.S. DEPARTMENT OF COMMERCE
National Technical Information Service
PB-282 784

Use of Dredgings for Landfill. Technical Report No. 5. Behavior of Dredged Materials in Diked Containment Areas

Northwestern Univ, Evanston, Ill Dept of Civil Engineering

Prepared for

Municipal Environmental Research Lab -Cincinnati, Ohio

May 78

TECHNICAL REPORT DATA
(Please read Instructions on the reverse before completing)

1. REPORT NO. EPA-600/2-78-088f	2.	3. PB 282 784
4. TITLE AND SUBTITLE USE OF DREDGINGS FOR LANDFILL Technical Report No. 5 Behavior of Dredged Materials in Diked Containment Areas		5. REPORT DATE May 1978 (Issuing Date) 6. PERFORMING ORGANIZATION CODE
7. AUTHOR(S) Raymond J. Krizek, Abdelsalam M. Salem		8. PERFORMING ORGANIZATION REPORT NO.
9. PERFORMING ORGANIZATION NAME AND ADDRESS Department of Civil Engineering The Technological Institute Northwestern University Evanston, Illinois 60201		10. PROGRAM ELEMENT NO. 1BC611 11. CONTRACT/GRANT NO. R-800948
12. SPONSORING AGENCY NAME AND ADDRESS Municipal Environmental Research Laboratory--Cin.,OH Office of Research and Development U.S. Environmental Protection Agency Cincinnati, Ohio 45268		13. TYPE OF REPORT AND PERIOD COVERED Final 14. SPONSORING AGENCY CODE EPA/600/14

15. SUPPLEMENTARY NOTES Project Officers: Clifford Risley, Phone (312) 353-2200, and Richard P. Traver, Phone (201) 321-6677 8-340-6677. See also Technical Reports No. 1, 2, 3, & 4, EPA-600/2-78-088b, c, d, & e, available from the National Technical Information Service, Springfield, VA.

16. ABSTRACT The behavioral characteristics of hydraulically placed maintenance dredgings were investigated during an extensive four-year field and laboratory experimental program. The field work, which took place primarily at four disposal areas near Toledo, Ohio, consisted of (a) periodic vane shear strength determinations, (b) obtaining undisturbed tube samples for subsequent laboratory tests, and (c) the measurement of in situ permeability values. The laboratory testing program included the evaluation of time-dependent (a) volume changes by means of slurry consolidation, conventional consolidation and long-term secondary compression tests, (b) strength determinations by use of a miniature vane, fall cone, and unconfined compression tests, and (c) various classification tests. Based on an extensive series of classification tests, it was found that the characteristics of the dredged materials deposited in each of the four sites were essentially the same, thereby enabling data from the different sites to be synthesized and interpreted as representative of one large site spanning a time period of almost a decade.

17. KEY WORDS AND DOCUMENT ANALYSIS

a. DESCRIPTORS	b. IDENTIFIERS/OPEN ENDED TERMS	c. COSATI Field/Group
Dredging, Dredges, Sediments, Harbors, Dikes, Channels (waterways), Excavation, Spoil, Waterways (watercourses), Channel stabilization	Landfills	13B 68C

18. DISTRIBUTION STATEMENT Release to public	19. SECURITY CLASS *(This Report)* UNCLASSIFIED	21. NO. OF PAGES 349
	20. SECURITY CLASS *(This page)* UNCLASSIFIED	22. PRICE A15-A01

E A Form 2220-1 (9-73)

REPRODUCED BY
NATIONAL TECHNICAL
INFORMATION SERVICE
U. S. DEPARTMENT OF COMMERCE
SPRINGFIELD, VA. 22161

TYPING GUIDE SHEET
BEGIN FIRST LINE OF TEXT HERE
CENTER OF PAGE
TOP OF IMAGE AREA
DROPPED HEAD BEGIN SECTIONS HERE

EPA-600/2-78-088f
May 1978

USE OF DREDGINGS FOR LANDFILL

Technical Report No. 5
Behavior of Dredged Materials in Diked Containment Areas

6-1/2"
9-1/8"

by

Raymond J. Krizek
Abdelsalam M. Salem
The Technological Institute
Northwestern University
Evanston, Illinois 60201

Grant No. R-800948 (15070-GCK)

Project Officers

Clifford Risley
U.S. Environmental Protection Agency
Region V
Chicago, Illinois 60604

Richard Traver
Storm and Combined Sewer Section
Wastewater Research Division
Municipal Environmental Research Laboratory (Cincinnati)
Edison, New Jersey 08817

MUNICIPAL ENVIRONMENTAL RESEARCH LABORATORY
OFFICE OF RESEARCH AND DEVELOPMENT
U.S. ENVIRONMENTAL PROTECTION AGENCY
CINCINNATI, OHIO 45268

BOTTOM OF IMAGE AREA, OUTSIDE DIMENSION FOR TABLES AND ILLUSTRATIONS
BEGIN LAST LINE OF TEXT
3/8"
PAGE NUMBER
EPA-287 (Cin.)
(4-76)

TYPING GUIDE SHEET
BEGIN FIRST LINE OF TEXT HERE
CENTER OF PAGE
TOP OF IMAGE AREA
DROPPED HEAD. BEGIN SECTIONS HERE

DISCLAIMER

This report has been reviewed by the Municipal Environmental Research Laboratory, U.S. Environmental Protection Agency, and approved for publication. Approval does not signify that the contents necessarily reflect the views and policies of the U.S. Environmental Protection Agency, nor does mention of trade names or commercial products constitute endorsement or recommendation for use.

6-1/2"
9-1/8"
BEGIN LAST LINE OF TEXT
BOTTOM OF IMAGE AREA OUTSIDE DIMENSION FOR TABLES AND ILLUSTRATIONS
3/8"
PAGE NUMBER
EPA-287 (Cin.)
(4-70)

FOREWORD

The Environmental Protection Agency was created because of increasing public and government concern about the dangers of pollution to the health and welfare of the American people. Noxious air, foul water, and spoiled land are tragic testimony to the deterioration of our natural environment. The complexity of that environment and the interplay between its components require a concentrated and integrated attack on the problem.

Research and development is that necessary first step in problem solution and it involves defining the problem, measuring its impact, and searching for solutions. The Municipal Environmental Research Laboratory develops new and improved technology and systems for the prevention, treatment, and management of wastewater and solid and hazardous waste pollutant discharges from municipal and community sources, for the preservation and treatment of public drinking water supplies, and to minimize the adverse economic, social, health, and aesthetic effects of pollution. This publication is one of the products of that research; a most vital communications link between the researcher and the user community.

The need to protect the ecology of the Great Lakes and the other waterways of the United States has led to a variety of problems concerned with the dredging and disposal of increasing volumes of polluted dredge spoil in areas of high population density and industrial development. One commonly used alternative to open water disposal is to place these polluted sediments in diked containment areas to form landfills of marginal value. However, due to the high costs involved, the scarcity of land, and other environmental and economic considerations, these landfills should desirably serve some useful purpose. Accordingly, this study was directed toward evaluating quantitatively the engineering characteristics of dredged materials as they affect their potential usefulness in a landfill.

Francis T. Mayo, Director
Municipal Environmental Research
Laboratory

SUMMARY

In many cases environmental and economic considerations have dictated that maintenance dredgings be placed in nearby diked containment areas to form landfills of marginal value. Since many of these dredged materials are organic clayey silts with high water contents, the potential usefulness of the resulting landfills is governed to a large extent by the time-consuming processes of drainage, consolidation, and shear strength development. Accordingly, the behavioral characteristics of hydraulically placed maintenance dredgings were investigated during an extensive four-year field and laboratory experimental program. The field work, which took place primarily at four disposal areas near Toledo, Ohio, consisted of (a) periodic vane shear strength determinations, (b) obtaining undisturbed tube samples for subsequent laboratory tests, and (c) the measurement of in-situ permeability values. One of the field sites was instrumented with settlement plates and piezometers before and during the disposal process, and time-dependent settlements and pore water pressures were monitored during the entire two-year history of this site. The laboratory testing program included the evaluation of time-dependent (a) volume changes by means of slurry consolidation, conventional consolidation, and long-term secondary compression tests, (b) strength determinations by use of a miniature vane, fall cone, and unconfined compression tests, and (c) various classification tests. Based on an extensive series of classification tests, it was found that the characteristics of the dredged materials deposited

in each of the four sites were essentially the same, thereby enabling data from the different sites to be synthesized and interpreted as representative of one large site spanning a time period of almost a decade.

Data from about a dozen slurry consolidation tests and more than sixty conventional consolidation tests were used to develop convenient empirical relationships among the compression index, coefficient of consolidation, coefficient of volume compressibility, coefficient of permeability, consolidation pressure, void ratio, and index properties of these materials. Two long-term slurry consolidation tests and eight long-term conventional consolidation tests were conducted to study the secondary compression-log time response, which exhibits a consistent, but unusual, pattern wherein the rate of secondary compression, after remaining constant with log time for a considerable period of time, increases and forms a second S-shaped curve similar to that normally associated with primary consolidation. Secondary compressions were found to be very significant, often comprising more than one-half of the total settlement; although results from the slurry consolidation tests yielded lower proportions of secondary to total compressions, the total compression per unit height of specimen was nearly the same for both tests. The parameters which characterize the secondary and total compressions, including the coefficient of secondary compression, were correlated with the index properties and consolidation pressure. A combination of data from several types of laboratory and field tests indicates that the coefficient of permeability decreases from about 10^{-4} to 10^{-9} cm/sec as the void ratio decreases from approximately 10 to 1.

Due to the manner of placement, the coarse materials settle near the inflow pipe while the fines accumulate in the vicinity of the outflow weir; grain size analyses show that the percent clay increases from virtually none at the discharge pipe to about 40 percent near the overflow weir, and similar results were found for silt. A synthesis of shear strength data from four different sites, together with the deposition histories of these sites and the basic assumption that the materials in each site are essentially similar, allowed the development of a fairly comprehensive relationship for shear strength as a function of both time and space for a hypothetical, geometrically similar, site over a period of about ten years. Various empirical relationships were established to provide guidance in estimating the strength of similar dredgings. The observed settlements at several locations in the instrumented landfill were found to agree reasonably well with settlements predicted from a mathematical model that accounts for both consolidation and desiccation of the materials, as well as impeded bottom drainage and a nonhomogeneous distribution of mechanical properties in the vertical direction. The average dry density increased about 4 percent per year and the average shear strength increased about 3.5 kN/m^2 (0.5 psi) per year for at least the first eight years after deposition of the dredgings. Unless steps are taken to accelerate the dewatering of such landfills, their relatively low bearing capacity, as well as the associated settlements, limit to large extent the use of these sites for purposes other than wildlife refuges, parks, recreational areas, parking lots, and access roads to buildings that are supported on appropriate foundations which extend below the deposited dredged materials.

TABLE OF CONTENTS

Page

SUMMARY iv

LIST OF FIGURES xiii

LIST OF TABLES xx

LIST OF SYMBOLS xxi

ACKNOWLEDGMENTS xxv

CHAPTER 1 INTRODUCTION. 1

CHAPTER 2 BACKGROUND. 5
- DREDGING AND DISPOSAL CYCLE 5
- FIELD STUDY 8
  - Field Sites. 11
  - Test Locations 13
- LABORATORY STUDY. 14
- FIELD INSTRUMENTATION AT PENN 7 SITE. 15
- SUMMARY 17

CHAPTER 3 MATERIAL CHARACTERIZATION 18
- BACKGROUND AND DEFINITIONS. 18
  - Atterberg Limits 19
    - Liquid Limit. 20
    - Plastic Limit 21
    - Shrinkage Limit 21
    - Plasticity Chart. 22
  - Particle Size and Gradation. 22
  - Activity 23
  - Organic Content. 24
  - Mineralogy and Chemistry 25
- MATERIALS TESTED AND TEST PROCEDURES. 25
- RESULTS AND ANALYSIS. 27
  - Natural Water Content. 34
  - Variation of Liquid Limit and Plastic Limit with Clay Content 34

Page

Variation of Plasticity Index with Percent Clay. 36

Relationship Between Plasticity Index and Liquid Limit. 37

Variation of Limits and Plasticity Index with Activity 38

Particle Size Characteristics. 38

Organic Matter 40

Chemistry. 42

Mineralogy 42

CONCLUSIONS 43

CHAPTER 4 SLURRY CONSOLIDATION. 44

MATERIALS TESTED. 44

EXPERIMENTAL PROCEDURE. 45

Description of Equipment 49

Loading Scheme 49

ANALYSIS OF RESULTS 52

Void Ratio versus Pressure 52

Comparison with a Clay Soil. 57

Relationship Between Compression Index and Liquid Limit. 58

Conventional Consolidation Tests on Consolidated Slurry Samples. 61

Coefficient of Consolidation 63

Coefficient of Volume Compressibility. 64

Coefficient of Permeability. 67

Shear Strength 70

SIGNIFICANCE OF RESULTS 74

CONCLUSIONS 75

CHAPTER 5 PRIMARY CONSOLIDATION AND COMPRESSIBILITY 76

MATERIALS TESTED. 76

EXPERIMENTAL PROCEDURE. 77

ANALYSIS OF RESULTS 78

Void Ratio versus Consolidation Pressure . . . 78

Compression Index. 80

Page

Constrained Modulus. 83

Coefficient of Consolidation 88

Coefficient of Volume Compressibility. 90

Coefficient of Permeability. 92

VARIATION OF CONSOLIDATION CHARACTERISTICS WITH DEPTH 96

CONCLUSIONS 96

CHAPTER 6 SECONDARY CONSOLIDATION 104

BRIEF BACKGROUND. 105

EXPERIMENTAL PROGRAM. 107

Sampling Procedures. 107

Experimental Procedure for Slurry Consolidation Tests. 108

Experimental Procedure for Conventional Consolidation Tests 108

EXPERIMENTAL RESULTS. 109

Patterns from Slurry Consolidation Tests . . . 109

Patterns from Conventional Consolidation Tests 112

Comparison of Behavior Patterns. 115

INTERPRETATION. 118

Variation with Natural Water Content 119

Variation with Consolidation Pressure. 119

Variation with Compression Index 122

Determination of Parameters. 122

Observed and Calculated Deformations 126

Variation of Parameters with Natural Water Content 126

Variation of t_k with Percent Clay. 129

EXAMPLE PROBLEM 129

CONCLUSIONS 131

CHAPTER 7 PERMEABILITY AND DRAINAGE 133

EXPERIMENTAL PROGRAM. 133

Drainage 134

Equipment and Procedures. 134

Analysis of Results 136

Page

Direct Permeability. 143

Conventional Consolidation 144

Slurry Consolidation 144

Field Tests. 145

Electro-osmosis. 146

POTENTIAL INFLUENCE OF ORGANIC CONTENT AND GAS GENERATION 150

SYNTHESIS OF RESULTS. 152

CONCLUSIONS 152

CHAPTER 8 SHEAR STRENGTH. 155

TEST PROGRAM. 155

Field Tests. 155

Laboratory Tests 158

Laboratory Vane 160

Penetration Test (Fall Cone). 160

Unconfined Compression Test 162

Field and Laboratory Results 162

ANALYSIS OF RESULTS 189

Correlation between Shear Strength and Index Properties. 189

Comparison between Field and Laboratory Strengths 191

Variation of Shear Strength with Depth 192

Variation of Strength with Horizontal Distance. 194

Variation of Strength with Time. 194

Sensitivity. 200

Correlations between Secant Modulus and Index Properties. 206

CONCLUSIONS 206

CHAPTER 9 FIELD MEASUREMENTS 209

FOUNDATION SOILS. 210

General Description. 210

Topography 210

Underlying Soil. 211

Page

Permeability 212
Shallow Infiltration Tests. 214
Deep Well Tests 214
Results 217
SETTLEMENT PLATE-PIEZOMETER UNITS 218
Locations. 218
Description of Unit. 220
Methods of Installation. 223
Dry Foundation Soil 223
Submerged Foundation Soil 223
Dredging Slurry 224
Methods of Monitoring. 226
Measurement of Risers Above Water Surface . 226
Measurement of Calibrated Risers. 227
Conventional Level Measurements 227
Piezometric Heads. 227
Results 227
TRAVERSE AND LEVEL SURVEY OF DIKE. 233
SURVEY OF GRID IN LANDFILL 235
SUMMARY AND RECOMMENDATIONS. 237

CHAPTER 10 EXPERIMENTAL PROBLEMS 242
LOGISTICS. 242
SAMPLING 243
Inflow Pipe 247
Fill and Foundation Materials 247
Observation Wells 249
Bottom Sediments and Overflow Weir. 251
INSTALLATION OF OBSERVATION WELLS. 251
INSTALLATION OF SETTLEMENT PLATES. 252
FIELD EVAPORATION TESTS. 254
WATER QUALITY STUDY. 254
SUMMARY. 255

Page

CHAPTER 11 SYNTHESIS OF RESULTS. 257

SETTLEMENTS. 258

Model Based on Classical Theory of Consolidation 259

Model Based on Consolidation and Desiccation. 264

STORAGE CAPACITY OF CONTAINMENT AREAS. 268

Experimental Program. 270

Analysis and Interpretation of Results. . . . 271

RELATIONSHIPS BETWEEN DRY DENSITY, SHEAR STRENGTH, AND TIME. 278

PARTICLE SIZE DISTRIBUTION 281

Actual Variations 282

Longitudinal Line. 282

Vicinity of Discharge Pipe 284

Theoretical Variations. 285

Vicinity of Inflow Pipe. 285

Open Water Domain. 288

PRELIMINARY COST STUDY 292

USES OF RESULTING LANDFILLS. 293

SUMMARY. 294

CHAPTER 12 SUMMARY AND CONCLUSIONS 297

REFERENCES 301

APPENDIX DESCRIPTIONS OF SAMPLES 307

LIST OF FIGURES

Figure		Page
2-1	Aerial Views of Toledo Disposal Areas.	9
2-2	Test Locations at Toledo Disposal Areas.	10
2-3	Cumulative Volumes of Dredgings Deposited in Toledo Disposal Areas	12
2-4	Coordinate System at Penn 7.	14
2-5	Locations of Observation Wells and Permeability Tests.	16
3-1	Plasticity Relationships	35
3-2	Variation of Atterberg Limits and Plasticity Index with Activity.	39
3-3	Atterberg Limits versus Organic Content for Various Dredged Materials.	41
4-1	Slurry Consolidometer Apparatus.	50
4-2	Cross-section of Slurry Consolidometer	51
4-3	Slurry Consolidometer Sample Removal System.	53
4-4	Typical Plots of Void Ratio versus Time.	54
4-5	Void Ratio versus Consolidation Pressure Curves for Twelve Slurry Consolidation Tests.	55
4-6	Comparison of Several Typical Curves of Void Ratio versus Consolidation Pressure.	59
4-7	Compression Index versus Liquid Limit for Slurry Consolidation.	60
4-8	Void Ratio versus Consolidation Pressure Curves for Two Conventional Consolidation Tests	62
4-9	Average Coefficient of Consolidation versus Consolidation Pressure for Slurry Consolidation	65
4-10	Coefficient of Consolidation versus Consolidation Pressure for Slurry and Conventional Consolidation Tests.	66
4-11	Average Coefficient of Volume Compressibility versus Consolidation Pressure for Slurry Consolidation. . .	68

Figure	Page
4-12 Average Coefficient of Permeability versus Consolidation Pressure for Slurry Consolidation 69
4-13 Average Coefficient of Permeability versus Average Void Ratio for Slurry Consolidation. 71
4-14 Coefficient of Permeability versus Void Ratio for Slurry and Conventional Consolidation Tests. 72
4-15 Shear Strength versus Water Content. 73
5-1 Typical Deformation-Time Response Curves 79
5-2 Variation of Compression Index with Natural Water Content and Liquid Limit 82
5-3 Typical Plots of Constrained Tangent Modulus versus Consolidation Stress 85
5-4 Variation of Modulus Number with Different Material Properties 87
5-5 Average Coefficient of Consolidation versus Consolidation Pressure for Conventional Consolidation . . . 89
5-6 Average Coefficient of Volume Compressibility versus Consolidation Pressure for Conventional Consolidation 91
5-7 Coefficient of Permeability versus Void Ratio for Conventional Consolidation 93
5-8 Average Coefficient of Permeability versus Consolidation Pressure for Conventional Consolidation . . . 95
5-9 Consolidation Test Data for Samples from Location 1 at Riverside Site. 97
5-10 Consolidation Test Data for Samples from Location 6 at Riverside Site. 98
5-11 Consolidation Test Data for Samples from Location 8 at Riverside Site. 99
5-12 Consolidation Test Data for Samples from Location 3 at Island Site 100
5-13 Consolidation Test Data for Samples from Location 1 at Penn 8 Site 101

Figure Page

5-14 Consolidation Test Data for Samples from Location 2 at Penn 8 Site 102

6-1 Consolidation-Time Response of Slurry Samples. 110

6-2 Primary Consolidation of Conventional Samples. 113

6-3 Secondary Compression of Conventional Samples. 114

6-4 Coefficient of Secondary Compression versus Natural Water Content. 120

6-5 Coefficient of Secondary Compression versus Consolidation Pressure. 121

6-6 Relationships Between Void Ratio and Consolidation Pressure 123

6-7 Coefficient of Secondary Compression versus Compression Index 124

6-8 Method for Determining Parameters from Typical Consolidation Curve 125

6-9 Determination of Parameters for Dredging Samples . . . 127

6-10 Variation of Parameters with Natural Water Content . . 128

6-11 Variation of t_k with Percent Clay. 130

7-1 Particle Size Distribution Curves. 135

7-2 Rates of Drainage by Gravity and Vacuum Methods. . . . 137

7-3 Data from Gravity Drainage Tests 141

7-4 Permeability as a Function of Void Ratio or Water Content. 142

7-5 Summary of Values for Coefficient of Permeability. . . 153

8-1 Photographs of Field Vane and Its Use. 159

8-2 Photographs of Laboratory Test Devices 161

8-3 Strength Profiles at Location 3 of Island Site (1973). 163

8-4 Strength Profiles at Location 1 of Penn 8 Site (1973). 164

8-5 Strength Profiles at Location 2 of Penn 8 Site (1973). 165

Figure Page

8-6 Strength Profiles at Location 1 of Riverside Site (1973). 166

8-7 Strength Profiles at Location 6 of Riverside Site (1973). 167

8-8 Strength Profiles at Location 8 of Riverside Site (1973). 168

8-9 Strength Profiles at Location 3 of Island Site (1974). 169

8-10 Strength Profiles at Location 1 of Penn 8 Site (1974). 170

8-11 Strength Profiles at Location 2 of Penn 8 Site (1974). 171

8-12 Strength Profiles at Location 1 of Riverside Site (1974). 172

8-13 Strength Profiles at Location 6 of Riverside Site (1974). 173

8-14 Strength Profiles at Location 8 of Riverside Site (1974). 174

8-15 Strength Profiles at Location 2/10 of Penn 7 Site (May 1974) 175

8-16 Strength Profiles at Location 5/8 of Penn 7 Site (May 1974) 176

8-17 Strength Profiles at Location 5/10 of Penn 7 Site (May 1974) 177

8-18 Strength Profiles at Location 5/13 of Penn 7 Site (May 1974) 178

8-19 Strength Profiles at Location 8/10 of Penn 7 Site (May 1974) 179

8-20 Strength Profiles at Location 8/13 of Penn 7 Site (May 1974) 180

8-21 Strength Profiles at Location 12/10 of Penn 7 Site (May 1974) 181

8-22 Strength Profiles at Location 15/10 of Penn 7 Site (May 1974) 182

8-23 Strength Profiles at Location 16/12 of Penn 7 Site (May 1974) 183

Figure | Page

8-24 Typical Unconfined Compression Test Data from Penn 8 (1974). 184

8-25 Variation of Shear Strength with Natural Water Content. 185

8-26 Variation of Shear Strength with Dry Density 186

8-27 Variation of Shear Strength with Liquidity Index . . . 187

8-28 Summary of Field Vane Strength Profiles. 193

8-29 Average Field Vane Strength versus Horizontal Distance 195

8-30 Average Field Vane Strength versus Time. 199

8-31 Rate of Change of Average Strength versus Distance from Discharge Pipe. 201

8-32 Sensitivity versus Natural Water Content 203

8-33 Sensitivity versus Dry Density 204

8-34 Sensitivity versus Liquidity Index 205

8-35 Relationships between Secant Modulus and Different Material Properties. 207

9-1 Grain Size Curves of Foundation Soils. 213

9-2 Photographs of Field Permeability Tests. 216

9-3 Locations of Settlement Plates and Piezometers 219

9-4 Construction Details of Settlement Plate-Piezometer Unit 222

9-5 Photographs of Settlement Plate Installation 225

9-6 Settlement and Piezometric Head versus Time at Location 2/10. 228

9-7 Settlement and Piezometric Head versus Time at Location 5/8 229

9-8 Settlement and Piezometric Head versus Time at Location 5/10. 230

Figure		Page
9-9	Settlement and Piezometric Head versus Time at Location 5/13.	231
9-10	Settlement and Peizometric Head versus Time at Location 15/10	232
9-11	Plan View of Penn 7 with Locations of Benchmarks and Reference Points	234
9-12	Longitudinal Section along the Centerline of Dike. . .	236
9-13	Variations in Topography of Penn 7 during Disposal Operation.	238
9-14	Longitudinal Section along Base Line of Penn 7	239
10-1	Conditions Associated with Inflow Pipe	244
10-2	Sampling Difficulties.	245
10-3	Rapid Growth of Vegetation	246
10-4	Piston Sampling Operation.	248
10-5	Installation of Wells.	250
11-1	Assumed Initial and Final Conditions for Typical Layer of Dredgings	261
11-2	Comparison between Observed Settlements and Predictions Based on Classical Consolidation Theory . .	263
11-3	Comparison between Observed Settlements and Predictions of Mathematical Model	266
11-4	Increase in Dry Density with Time.	273
11-5	Increase in Maximum Dry Density with Compactive Effort	276
11-6	Development of Shear Strength with Dry Density and Time	280
11-7	Spatial Variations of Average Grain Size Characteristics.	283
11-8	Observed and Predicted Values for Spatial Variation of Mean Grain Size	287

Figure Page

11-9 Assumed Conditions for Development of Model to Characterize Spatial Distribution of Mean Grain Size 289

A-1 Test Locations at Toledo Disposal Areas. 308

A-2 Sampling Locations in Vicinity of Inflow Pipe at Riverside. 309

LIST OF TABLES

Table		Page
3-1	Index Properties of Tested Samples	28
3-2	Summary of Grain Size Analysis	31
3-3	Organic Carbon and Loss on Ignition for Various Dredgings	32
3-4	Qualitative Mineralogical Analyses	33
4-1	Summary of Materials Tested	46
4-2	Characteristics of Materials Tested	47
4-3	Chemical Analyses of Effluents	48
5-1	Summary of Empirical Coefficients for Permeability Relationships	94
6-1	Proportions of Compression Components	116
7-1	Coefficient of Permeability from Short-Term Drainage Tests	139
7-2	Coefficient of Permeability from Direct Tests	139
7-3	Coefficient of Permeability from Single-Load Consolidation Tests	139
7-4	Average Electro-osmotic Coefficient of Permeability and Flow Efficiency	147
7-5	Comparison of Dewatering Rates with and without an Electrical Gradient	149
8-1	Values of Coefficients	188
9-1	Coefficient of Permeability for Foundation Soil	217
9-2	Base Elevations of Settlement Plate Units	221
A-1	Summary of "E" Samples	310

LIST OF SYMBOLS

A = activity

a_L, b_L = empirical coefficients in correlations between shear strength and liquidity index

a_v = coefficient of compressibility

a_w, b_w = empirical coefficients in correlations between shear strength and natural water content

a_γ, b_γ = empirical coefficients in correlations between shear strength and dry density

B = average width of disposal area

C_a = coefficient of secondary compression

C_c = compression index

C_u = coefficient of uniformity

c_v = coefficient of consolidation

$\bar{c}_v$ = average coefficient of consolidation

D = particle diameter

D_P = equivalent diameter for which P percent (by weight) of the soil is finer

E_c = compactive effort

E_{sec} = secant modulus

e = void ratio

e_o = initial void ratio

$\bar{e}$ = average void ratio

H = thickness of test specimen or soil stratum

H_f = thickness of foundation soil

h = length of drainage path (equal to one-half the sample or layer thickness for double drainage or the total thickness for single drainage)
h_f = height of fall for a particle in suspension
i = hydraulic gradient
k = coefficient of permeability
k_e = electro-osmotic coefficient of permeability
k_f = coefficient of permeability for foundation soil
k_h = coefficient of permeability in horizontal direction
k_v = coefficient of permeability in vertical direction
$\bar{k}$ = average coefficient of permeability
LI = liquidity index
ℓ = distance between overflow weir and inlet pipe
M = constrained tangent modulus
m = modulus number
m_v = coefficient of volume compressibility
$\bar{m}_v$ = average coefficient of volume compressibility
PI = plasticity index
p = consolidation stress
p_a = atmospheric pressure
p_c = preconsolidation stress
p_o = initial effective stress in a soil stratum
Q = discharge per unit time from disposal area
q = intensity of load on stratum in field
r = radial distance measured from end of inlet pipe
S = sensitivity or settlement
s = undisturbed shear strength

s_{avg} = average shear strength

s_{fc} = shear strength determined by fall cone

s_{fv} = shear strength determined by field vane

$s_{\ell v}$ = shear strength determined by laboratory vane

s_r = remolded shear strength

s_{uc} = shear strength determined by unconfined compression test

T = time factor

t = time

t_k = empirically determined coefficient in secondary compression analysis

U = degree of consolidation

v = settling velocity of particle

v_x = average velocity of flow at a distance x from inlet pipe

$\bar{v}$ = average voltage gradient across the sample

w_L = liquid limit

w_n = natural water content

w_p = plastic limit

X = distance of test location from overflow weir

x = distance of test location from inlet pipe

α_p = coefficient of primary compressibility

β = coefficient of transpiration

γ_d = dry density

γ_f = unit weight of suspending fluid

γ_s = unit weight of soil particles

γ_w = unit weight of water

$\Delta\epsilon_a$ = increment of axial strain

ΔH = reduction in specimen or stratum thickness

Δp = pressure increment

$\varepsilon(f)$ = ultimate or final strain

$\varepsilon(t)$ = strain at time, t

η = absolute viscosity

θ = angle (measured at inlet pipe) corresponding to effective flow area

ACKNOWLEDGMENTS

This report represents the combined efforts and genuine cooperation of a multitude of individuals and organizations. With a sincere hope that all appropriate credits will be enumerated and a humble apology for any omissions, grateful acknowledgments are extended to:

The Environmental Protection Agency for supporting the major portion of the work under Grants 15070-GCK and R-800948

Northwestern University for the many ways it has cost-shared in this effort

John Mulhern, EPA Office of Research and Monitoring in Washington, D. C., for his administrative assistance and advice

Clifford Risley and Stephen Poloncsik, Region V Office of EPA, for their role in monitoring this project

Various offices and personnel of the U. S. Army Corps of Engineers, but particularly Ken C. Powell and the personnel of the Toledo Field Office, for their whole-hearted cooperation in almost every request made of them

Soil Testing Services for the loan of several items of field equipment

Dr. Jorj O. Osterberg for his advice on various aspects of the sampling and testing program

Dr. Arley G. Franklin for his help in interpreting some of the data

Dr. Gabor M. Karadi for his supervision of some aspects of the field work and his assistance in evaluating the permeability test data

Dominic M. Delle Grazie, Hugo K. Koller, and Theophille Felton for their assistance and advice in constructing the various pieces of equipment needed for this work

M. Salah Abdelhamid, Dimitrios K. Atmatzidis, Amr S. Azzouz, Rafael Blazquez, Manuel Casteleiro, Vincente Cuellar, Abdulmohsen W. Dhowian, Houssam H. El-Moursi, Ali A. Elzaroughi, Max W. Giger, Jau S. Jin, Jose L. Monte, Kutay I. Ozydin, Jack Rosenfarb, Rudolfo Semrau, Nejat Seyhun, and John R. Wiesneth for their conscientious attitudes and whole-hearted efforts in performing the many laborious tasks associated with the laboratory and field phases of this work.

CHAPTER 1

INTRODUCTION

Until recently most of the bottom sediments dredged from the harbors and channels of deep water ports in the United States were deposited in open waters at selected disposal areas located sufficiently near the source of the dredged material to minimize hauling costs, but far enough away to avoid interference with water intakes, beaches, and other facilities. However, concerns for the protection of the environment, as well as economic considerations, have dictated that open water disposal be abandoned in certain cases. Although there are several possible alternative methods for the disposal of maintenance dredgings, the currently used major alternative to open water disposal is to deposit the dredgings within diked containment areas. In the case of polluted sediments, such a procedure has been found to satisfactorily prevent the pollutants from reaching the open waters, and in some areas it is actually more economical than open water disposal. A major problem associated with the use of diked disposal areas is concerned with the ultimate productive use of such landfills for community and industrial development projects.

Two main issues contribute to the existence of this problem. First, there is a continually increasing demand for more areas to dispose of dredged material and the land in urban areas surrounding most harbors is usually expensive, as well as difficult to locate; accordingly, worthless land created by the disposal of dredgings simply can not be tolerated, and landfills must play a positive role in the forthcoming systems of urban and regional development. Second, since these dredgings usually have a high water content and contain substantial amounts of clay-like and/or organic materials, as well as various concentrations of pollutants, the usefulness, effectiveness, and economy of the resulting landfills are strongly dependent on the time-consuming processes of drainage, consolidation, and shear strength development.

In general, the use of landfill for industrial or residential construction involves the consideration of both settlement and stability with respect to time. Since relatively little is known about the behavioral characteristics of dredged materials, the primary effort in this research program is directed toward establishing relationships among index properties, time, and engineering properties to provide urban and regional planners with appropriate input information on which they can base their judgment regarding the potential usefulness of landfills composed of dredged materials. Although this study centers around the Great Lakes (and more specifically the harbor at Toledo, Ohio), it is reasonable to anticipate that the results will be applicable to any area in which the dredged materials are similar.

Within the Toledo harbor area, four diked disposal sites extending over a time span of about 10 years were studied. Piston tube sampling, the field measurement of shear strength, and an extensive series of laboratory tests were conducted each year, although not at every site. Since the dredged material deposited in each site was essentially dredged from the same general vicinity, the resulting data from each site can be synthesized to deduce the behavioral pattern (such as time-dependent increases in dry density, settlement, shear strength, etc) of a single representative site over a period of 10 years. In addition, one of the field sites was observed during its entire two-year history of dredge spoil deposition; settlement plates and piezometers were installed and monitored to obtain data on rates of settlement and pore pressure dissipation.

Chapter 2 presents some background information on typical dredging and disposal operations for a hopper dredge, the anticipated behavior of a diked containment area composed of dredged materials, the expected trends in the variations of certain engineering properties, a description of the field sites studied, and locations of the test positions. The results of characterization and classification tests are interpreted in Chapter 3 to establish correlations among the different properties, such as liquid limit, plastic limit, plasticity index, percent clay, and activity, and the dredged materials investigated are placed in perspective with commonly encountered soils that exhibit similar behavior.

The work in Chapter 4 is directed toward evaluating the consolidation characteristics of several typical dredging slurries that are too soft and/or too fluid to test by conventional means, and the resulting data are analyzed to develop empirical relationships among the compression index, coefficient of consolidation, coefficient of permeability, and coefficient of volume compressibility. Chapter 5 includes the results obtained from an extensive experimental program to investigate the primary consolidation and compressibility characteristics of dredging samples taken from four disposal sites, and the results are interpreted to establish empirical relationships among the consolidation and compressibility parameters and various index properties. Reported in Chapter 6 are the results of several long-term tests to study the secondary compression characteristics of dredged materials and their variation with consolidation stress, natural water content, and compression index.

Described in Chapter 7 is the work undertaken to assess the permeability and drainage characteristics of dredge spoil and to provide quantitative orders of magnitude for these properties; results from several series of laboratory and field tests are reported, and correlations are deduced among different variables. Chapter 8 deals with an extensive laboratory and field investigation of the time-dependent development of shear strength in a typical landfill composed of dredged materials; comparisons are made between field and laboratory values, and correlations are established among shear strength, sensitivity, secant modulus, and various index properties.

Chapter 9 describes the field instrumentation that was installed at one site, the methods used to monitor its response, and a summary of the results obtained; also included is an evaluation of the horizontal and vertical movements of the dike surrounding the site. The difficulties and hardships encountered during the different phases of the field work are discussed in Chapter 10. Chapter 11 synthesizes the results obtained in the various phases, and Chapter 12 summarizes the conclusions that may be deduced from this study with special reference to the potential usefulness of dredged materials for landfill.

CHAPTER 2

BACKGROUND

This chapter includes a general background of the dredging and disposal cycle as it pertains to the hydraulic placement and subsequent desiccation and consolidation of dredged materials in a diked containment area. Also described briefly are the locations and dimensions of four disposal sites in the Toledo harbor area, the spoil volume deposited in each, the selected test locations within these four sites, and the overall nature of the laboratory and field studies that were conducted.

DREDGING AND DISPOSAL CYCLE

The dredging and disposal cycle is initiated by removing sediments from the bottoms of harbors and navigation channels in order to maintain specified minimum depths of water. If these sediments are judged to be polluted or if the cost of open water disposal is inordinately high due to large travel distances, they are usually deposited within diked containment areas that may be on land, adjacent to the coast, or surrounded by water. Although a variety of techniques are available to accomplish this operation, the one employed throughout this study involves the use of a hopper dredge, whereby the spoil is dredged, transported, and pumped with large quantities of water into the containment area through a discharge pipe. Upon being ejected from the discharge pipe, the slurry is subjected to a flow-sedimentation regime wherein the large heavy particles, including rocks, gravel, and lumps of clay, settle in the vicinity of the discharge pipe, sand-size particles are carried farther from the pipe, and fines are transported to points near the overflow weir, which is normally located approximately opposite the discharge pipe.

As a result of the particle size distribution within a given containment area, both the permeability and the density decrease and the water content increases with distance from the discharge pipe. In general, the shear strength of a soil increases with an increase in dry density and a decrease in water content (test results reported by Krizek, Karadi, and Hummel (1973) indicate that dredged materials may exhibit larger variations in shear strength with relatively small variations in dry density). Accordingly, the strength of the deposits in a given landfill usually decreases with horizontal distance from the discharge pipe.

The dredging and disposal operation in a given area is normally not a continuous process, but rather occurs on a seasonal basis. The specific frequency and duration of the dredging periods depend on many factors, such as volumes of sediments to be dredged, efficiency of available dredges, capacity of disposal sites, geographic location of dredged areas, and length of freezing periods in some cases. For the most part the dredging and disposal operations in the Toledo area took place during the summer and autumn of each year, but different disposal areas were used in various years. During the periods between dredging seasons, as well as after a disposal site is filled, desiccation and consolidation of the materials take place due to evaporation, gravity drainage into the foundation soil, and transpiration due to vegetation.

McNely (1966) discussed some early experiences accumulated by placing a three-foot layer of mud at a dry density of about 350 kg/m^3 (22 lb/ft^3); as a consequence of evaporation only, the dry density doubled in about seven months. Garbe and Jeno (1968) reported the rapid drying of San Francisco Bay Mud by placing thin lifts of about one and one-half feet and using mechanical equipment to agitate the material. Nichols (1972) summarized a series of experiences with San Francisco Bay Mud and indicated that (a) although vacuum drainage has been used to accelerate consolidation, it has serious drawbacks in practical applications, and (b) drainage by evaporation from the surface is very effective. This finding has been substantiated in a field study conducted at Monroe, Michigan and reported by the Office of Dredged Material Research (1974) of the Waterways Experiment Station. The time-dependent process of desiccation and consolidation causes an increase in density, a decrease in water content, and an increase in shear strength and settlement. Field observations of the surface soils at a number of fill sites indicated the formation of tension cracks varying from a few millimeters to several centimeters in width and from several centimeters to about a meter in depth. Such cracks aid in developing a high rate of evaporation for the surface layer, since more surface area and deeper strata are exposed to the atmosphere. The rapid development of a relatively stiff crust allowed individuals to walk over the areas and perform the required field testing and sampling operations, but heavy vehicles would readily punch through this crust and become mired in the soft fill materials. The subsequent deposition of dredged materials over a previously desiccated crust causes a seasonal stratification of overconsolidated dredgings to occur in many sites.

FIELD STUDY

The field study described herein was conducted at Toledo, Ohio (a) to evaluate some of the in-situ engineering properties (such as shear strength, permeability, etc) and response characteristics (such as settlement) of the landfill materials placed in the four different disposal sites (Riverside, the Island, Penn 7, and Penn 8) shown in Figure 2-1 and (b) to obtain undisturbed and disturbed samples of materials from various locations shown in Figure 2-2 within the sites to test in a supplementary laboratory investigation. Continuous piston tube (undisturbed) samples were taken from one location at the Island in 1971, 1973, and 1974; six locations in 1971 and three locations in 1972, 1973, and 1974 at Riverside; two locations at Penn 8 in 1973 and 1974; nine locations at Penn 7 in 1974. Field vane strengths were usually measured at all sampling locations at the times when samples were taken, and an additional set of field strength data was obtained in the later summer of 1974 at some of the locations of Penn 7. Three different laboratory evaluations of shear strength were made on the undisturbed samples, and comparisons were made between values of the in-situ vane strengths and the laboratory strengths. Disturbed samples were obtained from locations in the vicinity of the discharge pipe at Riverside Site to study the particle size variation with distance from the discharge pipe. Annual surveys were conducted at Riverside Site and Penn 7 to monitor surface settlements. The dike at Penn 7 was also surveyed annually to measure its vertical and horizontal displacements.

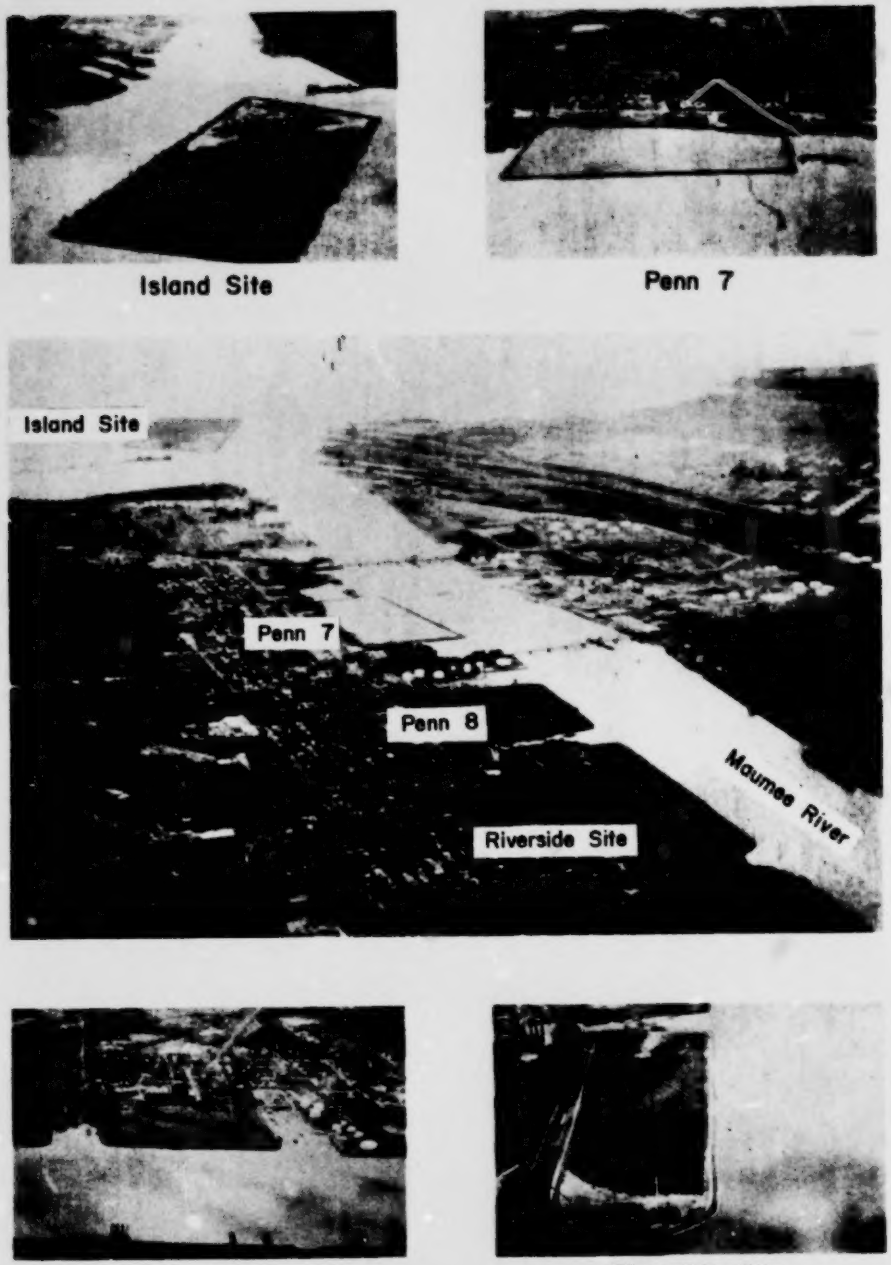

Island Site **Penn 7**

Island Site
Penn 7
Penn 8
Maumee River
Riverside Site

Penn 8 **Riverside Site**

Figure 2-1. Aerial Views of Toledo Disposal Areas

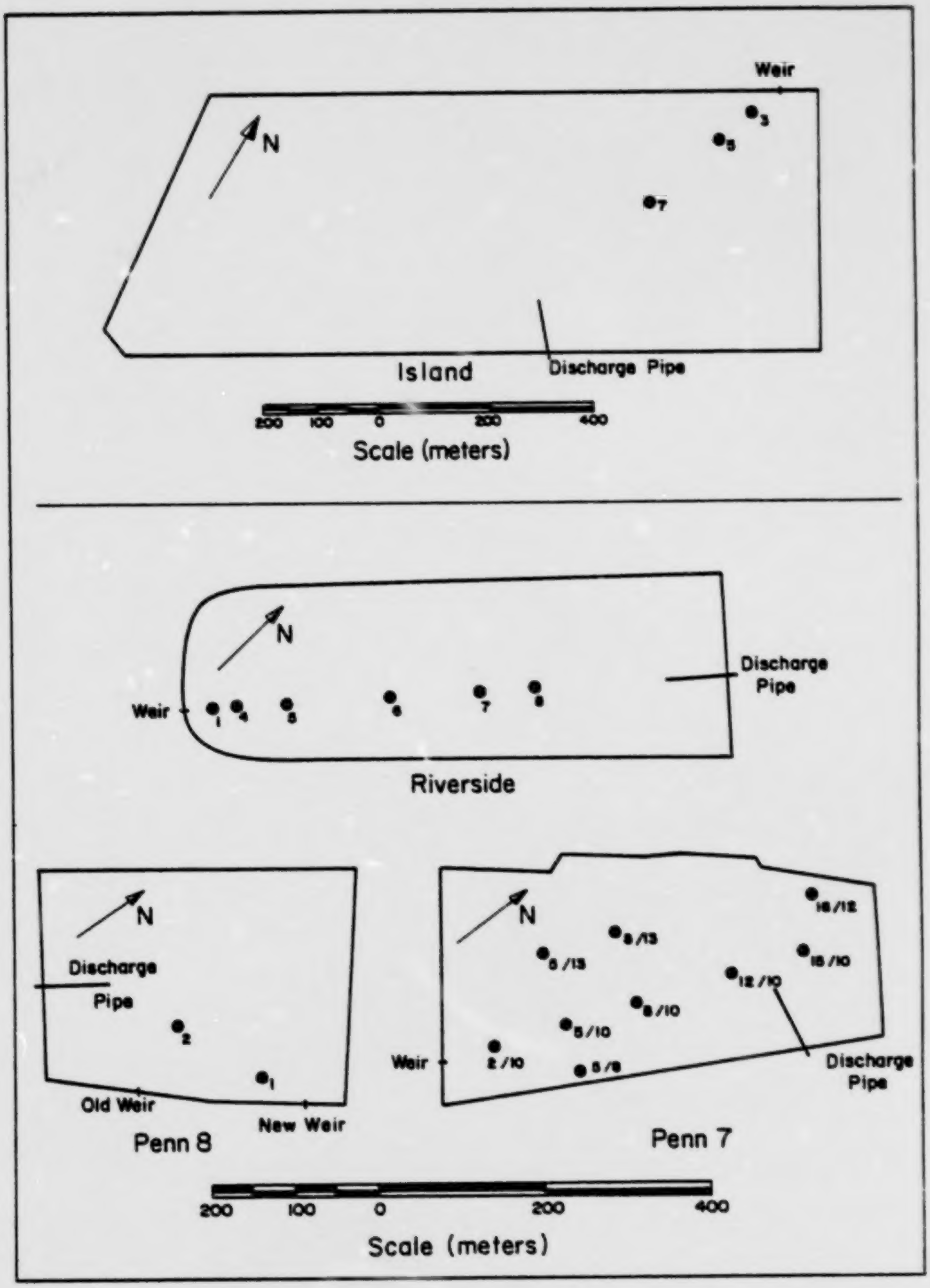
Weir
N
3
5
7
Island
Discharge Pipe
200 100 0 200 400
Scale (meters)
N
Discharge Pipe
Weir
1
4
5
6
7
8
Riverside
N
Discharge Pipe
2
1
Old Weir
New Weir
Penn 8
N
16/12
8/13
5/13
15/10
12/10
8/10
5/10
2/10
5/8
Weir
Discharge Pipe
Penn 7
200 100 0 200 400
Scale (meters)

Figure 2-2. Test Locations at Toledo Disposal Areas

Field Sites

The locations and general layout of the four field sites investigated in this study are shown in Figure 2-1. All four sites are nearly rectangular in plan and enclosed by dikes ranging from about 12 to 20 feet (4 to 6 meters) in height. The Island Site is located at the mouth of the Maumee River at the entrance to the bay; it has dimensions of approximately 3800 feet by 1800 feet (1140 meters by 540 meters) and covers about 150 acres (610,000 square meters). The other three sites are located along the north bank of the Maumee River near its mouth. Riverside Site, Penn 7, and Penn 8 have respective dimensions of approximately 2200 feet by 700 feet (660 meters by 210 meters), 1750 feet by 900 feet (530 meters by 260 meters), and 1200 feet by 900 feet (370 meters by 280 meters), and they cover areas of about 34 acres (140,000 square meters), 34 acres (140,000 square meters), and 25 acres (100,000 square meters), respectively. During the past ten years about 9 million cubic yards (7 million cubic meters) of bottom sediments were deposited in these four containment areas. As illustrated in Figure 2-3, which is based on data furnished by Boresch (1974), approximately 5 million cubic yards (4 million cubic meters) of dredged materials were placed in the Island Site during 1964, 1965, 1967, 1970, 1971, and 1973; 2 million cubic yards (1.5 million cubic meters) in Riverside Site during 1968, 1969, 1970, and 1972; 1 million cubic yards (0.75 million cubic meters) in Penn 7 during 1972 and 1973; and 1 million cubic yards (0.75 million cubic meters) in Penn 8 Site during 1966 and 1972.

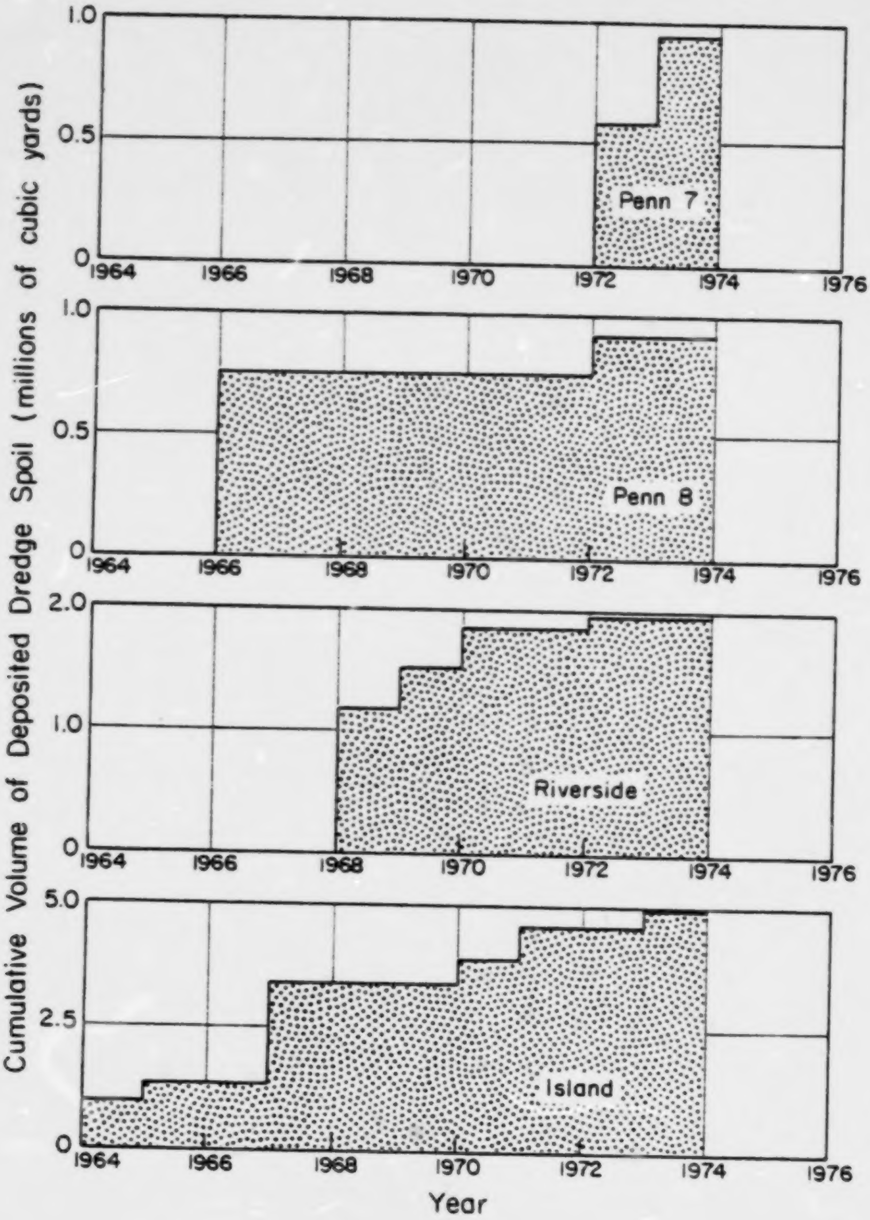

Figure 2-3. Cumulative Volume of Dredgings Deposited in Toledo Disposal Areas

Test Locations

The test locations at the Island Site, Riverside Site, and Penn 8 were selected essentially along the lines between the discharge pipe and the overflow weir; in general, these lines passed through the center of the sites and represented the full variation of material with respect to particle sizes. As indicated in Figure 2-2, the test locations were designated as 3, 5, and 7 at the Island Site; 1, 4, 5, 6, 7, and 8 at Riverside Site, and 1 and 2 at Penn 8. At Penn 7 the discharge pipe and overflow weir were not located on opposite sides of the disposal area, and a similar choice would not have produced a line that traversed the center of the site; furthermore, a more detailed study of Penn 7 was desired. Accordingly, a longitudinal base line was established between the overflow weir and the approximate geometric center of the site; specifically, the alignment was made between the overflow weir and a distant twin tower supporting electrical lines. As shown in Figure 2-4, the origin of this base line was located at the weir and designated as point 0/10, where 0 and 10 represent the longitudinal and transverse coordinates, respectively, in hundreds of feet. Five of the nine locations for piston tube sampling and in-situ strength measurement were along this base line, and the other four were at points to one side or the other. Appropriate coordinates were used to designate locations for the field settlement plate-piezometer units, and a grid was established at 100-foot (30-meter) intervals to measure surface elevations of the original ground in June of 1972 and to monitor surface settlements of the dredged material after the site was filled in August of 1973.

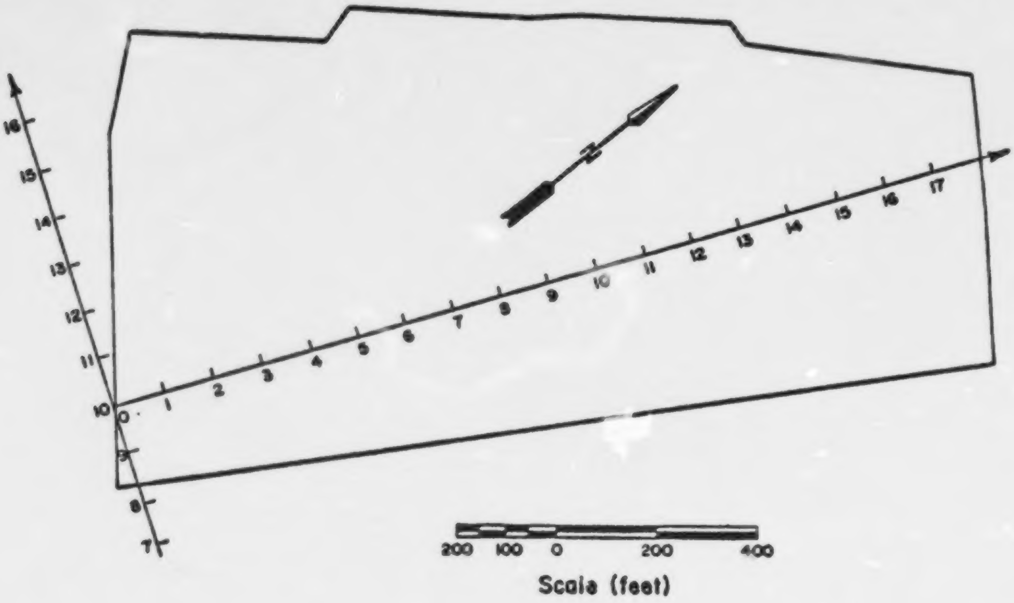

Figure 2-4. Coordinate System at Penn 7

LABORATORY STUDY

A considerable portion of the work reported in subsequent chapters is directed toward a laboratory determination of the engineering properties of dredged material. The principal parameters of interest are the index properties required for classification, consolidation and compressibility parameters, permeability and drainage characteristics and shear strength. Several slurry samples obtained during various stages of the dredging and disposal process were investigated in specially designed slurry consolidometers (Sheeran and Krizek, 1971) to determine their consolidation characteristics. Some of the consolidated slurry samples and many "undisturbed" tube samples obtained from the various sites were tested to evaluate their long-term secondary compression characteristics, as well as other engineering properties of interest. The data obtained from these studies in 1973 and 1974 are combined with those obtained in 1971 and 1972 (Krizek, Karadi, and Hummel, 1973) to establish trends in the variations of certain properties with time and with horizontal distance from the discharge pipe. In addition, the shear strengths determined by different laboratory techniques are compared with those determined in the field.

FIELD INSTRUMENTATION AT PENN 7 SITE

A detailed study of the Penn 7 disposal site was made to obtain field response data on the time-dependent variations of settlements, dry densities, and pore water pressures. The Penn 7 Site was selected for this study because it offered an opportunity to observe the complete history of a diked containment area from a time prior to the deposition of any spoil until a time about one year after it was filled. The permeability of the foundation soil at various depths was determined by different tests, and observation wells for a water quality study were installed at several locations (Figure 2-5). Settlement plate-piezometer units were installed at 10 locations (2/10, 5/8, 5/10, 5/13, 5/16, 8/10, 8/13, 12/8, 12/10, and 15/10) within the area, but vandalism, accessibility problems, and unusual weather conditions caused the final number of instrumented locations to be reduced to five (2/10, 5/8, 5/10, 5/13, and 15/10). The difficulties associated with the installation and monitoring of the wells and the settlement plate-piezometer units are explained later in this report.

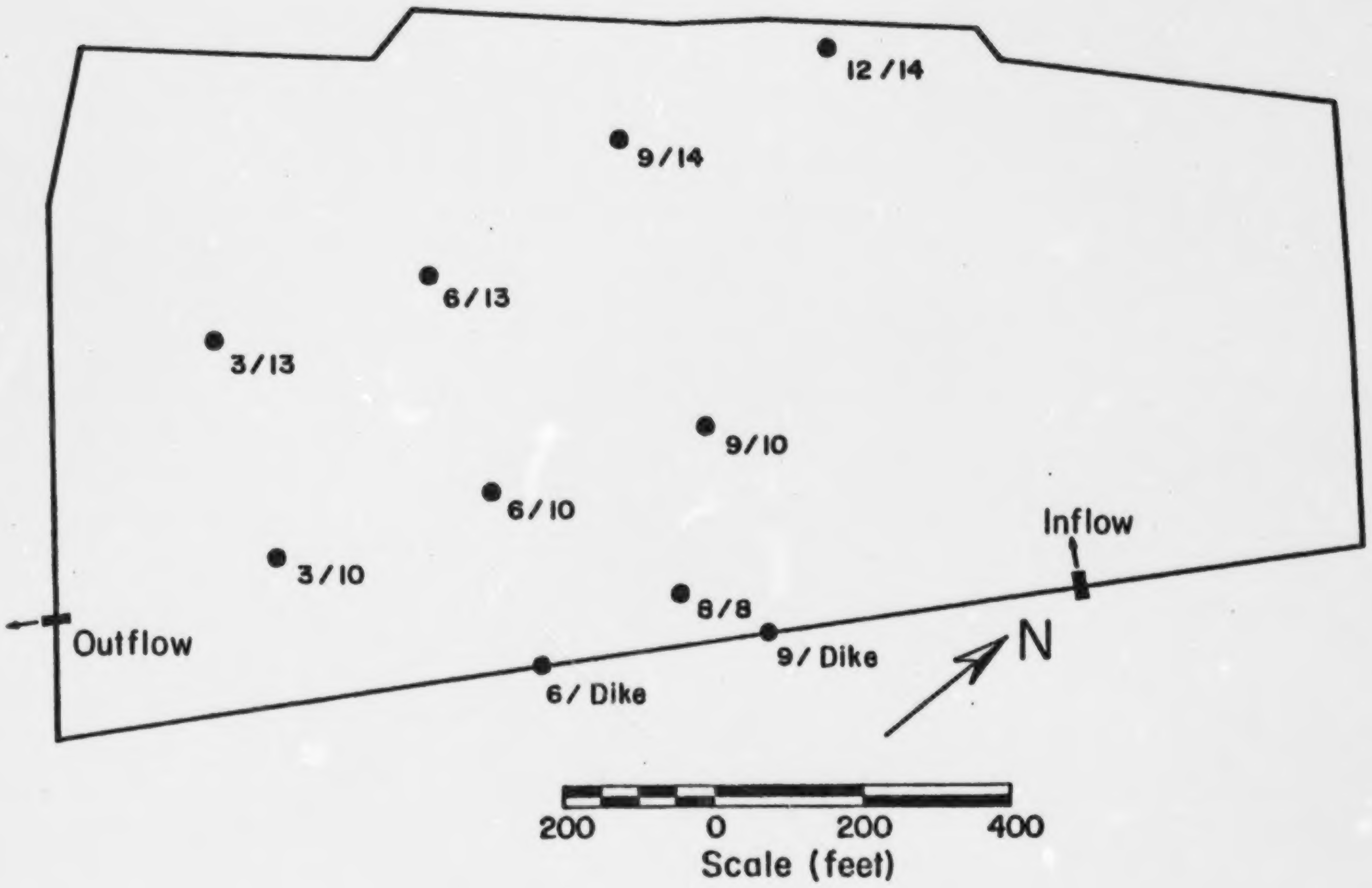
12 /14
9 /14
6 /13
3 /13
9 /10
6 / 10
3 / 10
8 / 8
9 / Dike
6 / Dike
Inflow
Outflow
N
200
0
200
400
Scale (feet)

Figure 2-5. Locations of Observation Wells and Permeability Tests

SUMMARY

Described in this chapter are a general background of (a) the dredging and disposal operation whereby bottom sediments are dredged and deposited hydraulically in diked containment areas, (b) the sedimentation process in which particles are distributed spatially according to their size, (c) the formation of a crust and shrinkage cracks at the surface of landfills composed of these materials, and (d) the variation of engineering properties with spatial position and with time. The average particle size decreases gradually with an increase in the distance from the discharge pipe, since the finer particles require more time to settle from suspension. Accordingly, desiccation and drainage occur relatively fast near the discharge pipe and becomes slower as the overflow weir is approached, and associated decreases in water content and void ratio and increases in dry density and shear strength are experienced. The engineering properties of the dredged materials in four disposal areas in the vicinity of Toledo, Ohio are studied, and one particular site was instrumented to monitor settlements and pore water pressures during and after the filling process.

CHAPTER 3

MATERIAL CHARACTERIZATION

The procedures for conducting soil characterization and classification tests (Atterberg limits, water content, dry density, grain size distribution, etc.) are fairly well standardized (Lambe, 1951), and these standard techniques were used for most of the tests conducted in this experimental program. Due to the high percentage of fines in these dredgings, hydrometer tests were performed on most of the samples for which particle size distributions were obtained; however, sieve analyses were also conducted on samples containing more than 20 percent (by weight) of particles not passing a No. 200 sieve (0.074 mm). The results of these tests are then interpreted to establish correlations among the different properties, such as liquid limit, plastic limit, plasticity index, percent clay, and activity, and the plasticity chart is used to place these dredgings in perspective with commonly encountered soils that exhibit similar behavior. The manifested correlations facilitate the interchange of one readily available property with another undetermined property, and, as described in later chapters, these easily determined characterization properties can be used to estimate major engineering response properties, such as consolidation, shear strength, and compressibility.

BACKGROUND AND DEFINITIONS

The parameters considered in this chapter can be divided into two main groups, namely, those properties related to plasticity characteristics and those dealing with grain size distribution; in addition, the activity of a soil represents the interaction between these two groups. The following sections present a brief review of the historical background and significance of the tests that are used.

Atterberg Limits

Due largely to the work of Atterberg (1911) and Casagrande (1932, 1948), the Atterberg limits and related indices have become very useful characteristics for classifying the behavior of cohesive soils. These limits are based on the concept that a fine-grained soil can exist in any of four states, depending on its water content. Accordingly, a dry soil is considered a solid, which, upon the addition of water, passes through the semi-solid and plastic states until it reaches the liquid state; the transition water contents between the foregoing states are termed the shrinkage limit, plastic limit, and liquid limit, respectively.

Many investigations have been conducted to relate the Atterberg limits to other properties of soils; however, relatively little has been done since the 1930's to clarify the meaning of the limits themselves. In one pioneering contribution to this subject, Terzaghi (1926) suggested "...before we can discuss the relative importance of these tests and the part they are called to play among the methods of soil classification, we must find out what these tests mean and what are the factors that determine their results," and he then proceeded to present a penetrating analysis of their significance and use for soil classification purposes. These concepts were supplemented by Casagrande (1932, 1948), who (a) demonstrated the relationship between the limits and the shear strength of soils, (b) presented data to show the effects of particle size and shape, soil structure, and degree of drying on the measured values, and (c) introduced the plasticity chart as a means of classifying fine-grained soils.

Liquid Limit -- Terzaghi (1926) described the liquid limit as "...the water content at which the soil grains still have a certain degree of liberty to readjust themselves under the influence of slight vibrations without changing partners freely." Moreover, he found that the liquid limit tends to increase with decreasing size of particles and with increasing amounts of scale-like particles. Casagrande (1932) showed that the liquid limit test was analogous to a shear test and that each blow of the standard device required to close the standard groove could be considered equivalent to a shear strength of approximately 1 g/cm^2 (0.1 kN/m^2). Thus, the liquid limit might alternatively be defined as the water content at which a soil has a shear strength of approximately 25 g/cm^2. However, Norman (1958) indicated somewhat lower values (on the order of 20 g/cm^2).

Measurements of the pore water tension in clay soils (Croney and Coleman, 1954) show that the negative pore water pressure at the liquid limit is on the order of 4 g/cm^2 (0.4 kN/m^2). Since the corresponding effective stress is equal in magnitude to the pore water tension, an assumed friction angle of 30° yields a shear strength of approximately 2.5 g/cm^2. Thus, the shear strength of 20 to 25 g/cm^2 at the liquid limit can probably be attributed in large part to the net attractive forces between clay particles, and not primarily the interparticle friction forces. Since the water content of a saturated soil is directly related to the void ratio, which is a measure of the average interparticle spacing, the liquid limit of a clay may be visualized as a measure of the average particle spacing at which the net attractive force is reduced to a value consistent with a shear strength of approximately 25 g/cm^2. Accordingly, the liquid limit would be expected to depend on the intensity of the net attractive forces between clay particles and thereby on the surface activity of the clay components. The greater the surface area and the intensity of the attractive surface forces, the greater will be the average spacing required to keep the strength at a value of 25 g/cm^2 and the greater will be the liquid limit. Based on the results obtained from a comprehensive experimental study, Seed, Woodward, and Lundgren (1964) showed that the liquid limit increases in a linear fashion as both the liquidity index and the percent clay increase.

Plastic Limit -- The plastic limit of a soil is determined by measuring the water content at which 1/8-inch threads of the soil begin to crumble. The physical significance of the plastic limit, other than a lower boundary of the water content range within which a soil exhibits plastic behavior, is not nearly as apparent as that of the liquid limit. Terzaghi (1926) suggested that "...for moisture contents equal to or smaller than the plastic limit, the physical properties of the water are no longer identical with those of free or ordinary water." If the clay fraction in a soil is more than sufficient to fill the voids in the non-clay fraction, cracking of a thread will occur through the clay component, and the plastic limit will be determined essentially by the characteristics of the clay fraction. It was found (Seed, Woodward, and Lundgren, 1964) that the plastic limit increases linearly with an increase in the clay fraction when the latter was sufficient to fill the voids in the non-clay fraction; in other words, there is a lower value of clay content below which the above mentioned linear relationship between plastic limit and clay fraction does not hold true. However, an inverse proportionality between these parameters exists for virtually all soils.

Shrinkage Limit -- Given a saturated mass of a cohesive soil subjected to appropriate environmental conditions, water evaporates from the surface and capillary forces develop at the air-water interfaces (or menisci) between surface particles. As a consequence of the resulting pore water tension, the soil mass experiences an effective compressive stress, and consolidation occurs until the soil mass reaches its minimum volume for all practical purposes. When this minimum volume is attained, continued evaporation results in a desaturation of the soil mass, since the water evaporates from the void spaces within the mass. This process is known as shrinkage, and the shrinkage limit is defined as that water content which is just sufficient to fill the voids when the soil mass is at its minimum volume. Although no standard shrinkage limit tests were conducted in this experimental program, numerous field observations and evaporation tests indicate that the shrinkage limit for most of these dredged materials is on the order of 24 percent.

Plasticity Chart -- To assist in utilizing the Atterberg limits in the classification of soils for engineering purposes, the plasticity chart, which represents a plot of plasticity index (liquid limit minus plastic limit) versus liquid limit, was devised by Casagrande (1948). Despite the extreme simplicity of this chart, it has been found most useful for identifying the anticipated behavior of cohesive soils, since certain regions of the chart are related directly to soil types described in the Unified Classification System. In general, there are reasonably definitive relationships between the position of a soil on the plasticity chart and its compressibility, permeability, clay content, and organic content.

Particle Size and Gradation

The particle size distribution of an assemblage of soil particles is usually expressed as a plot of percent finer (by weight) versus equivalent particle diameter, where the terminology D_P is used to designate the equivalent diameter for which P percent (by weight) of the soil is finer. The uniformity coefficient is defined as the ratio of D_{60} to D_{10}, and it characterizes the nature of the particle size distribution. A soil with a uniformity coefficient less than about 2 is considered uniform, and a well-graded soil has a uniformity coefficient of 5 to 10.

There are many reasons, both practical and theoretical, why the measured particle size distribution of a soil is only an approximation of the actual particle size distribution. For example, the definition of particle size is different for coarse particles and fine particles, with the accuracy of the distribution curves for fine-grained soils being more questionable than that for coarse soils. In addition, the chemical and mechanical treatments given to natural soils prior to performing a particle size analysis (especially a hydrometer test) may cause the measured effective particle sizes to be quite different than those existing in the natural soil. Although the behavior of a cohesionless soil can often be related to its particle size distribution, the behavior of a cohesive soil usually depends much more on geological history and structure than on particle size. Despite these limitations, particle size distributions for fine-grained soils are commonly obtained by mechanical sieving and/or hydrometer tests and used as a guide to assist in classifying the soil.

Activity

Notwithstanding the widespread use of the Atterberg limits, it was not until 1953 that any further work was done to advance our understanding of the relationships between these limits and the nature of the clay particles present in a soil. Skempton (1953) suggested that, since the plasticity of a soil was mainly attributed to its clay-size particles, the activity of these clay-size particles should logically be defined as

$$\text{Activity} = \frac{\text{Plasticity Index}}{\text{Percent Clay}}\ , \tag{3-1}$$

and he showed that, for any given clay with activity values ranging from about 0.4 for kaolinite to about 5 for montmorillonite, an approximately linear relationship existed between the plasticity index and the percent clay. This term has subsequently proven extremely useful for classifying the nature of the clay components of different soils. About a decade later, Seed, Woodward, and Lundgren (1964) found a linear relationship between the plasticity index and the percent clay for kaolinite/bentonite and illite/bentonite clay mixtures, but they observed that the plasticity index became zero at a clay content of about 9 percent. Accordingly, the definition for the activity of these artificial soils was modified to be

$$\text{Activity} = \frac{\text{Plasticity Index}}{\text{Percent Clay-9}}\ . \tag{3-2}$$

Organic Content

Organic soils are usually formed in situ either by the growth and subsequent decay of plants or by the accumulation and degradation of skeletons or shells of organisms. Sometimes the term organic soil refers to a transported soil consisting of the products of rock weathering and a conspicuous admixture of decayed vegetable matter. On the other hand, the organic matter in dredged materials may assume several other forms, including sanitary sewage with varying degrees of treatment, industrial wastes containing various amounts of petroleum products and other hydrocarbon compounds, and agricultural wastes and other plant and animal matter which are transported with the run-off of a given watershed. In addition, once the spoil is placed in a diked containment area for a brief period of time, a variety of dense vegetation grows rapidly. When a new dredging season begins, the newly placed spoil floods the fill area, partially or totally covering the previous growth of vegetation and thereby incorporating a considerable amount of fibrous material in the landfill at rather distinct levels. The testing procedures for determining organic content are not standardized, and results are very dependent on the testing technique; one fairly comprehensive comparative study of organic content determinations in dredgings has been reported by Krizek and Katz (1974).

Mineralogy and Chemistry

Experimental evidence indicates that large variations in the mineralogy and chemical composition of dredged materials may occur among harbors and at different locations within a given harbor; these characteristics are governed in large part by the urban and industrial wastes that are discharged into the harbor and the erosion potential of the surrounding watershed. Most harbor sediments contain various petroleum products and other hydrocarbons that interact in complex ways with the mineral particles to influence both the engineering properties of the material and the test procedures used to determine these properties. Based on various mineralogical analyses reported in the literature, most dredgings apparently contain substantial portions of illite and kaolinite, and extensive chemical analyses have been reported by Krizek, Karadi, and Hummel (1973) and Krizek, Gallagher, and Karadi (1974).

MATERIALS TESTED AND TEST PROCEDURES

Most of the dredgings samples tested in this program were obtained by piston tube sampler from the four diked disposal areas (namely, the Island, Riverside, Penn [illegible], and Penn 8) near Toledo, Ohio. The engineering properties of principal interest were strength, compressibility, consolidation, and permeability, but the water content, Atterberg limits, dry density, grain size parameters, organic content, mineralogy, and chemical characteristics were found for many of the samples. Most of the results that were determined in 1970, 1971, and 1972 have been reported by Krizek, Karadi, and Hummel (1973), and the results determined in 1973 and 1974, together with appropriate summaries of the foregoing findings, are presented herein.

As explained by Krizek, Karadi, and Hummel (1973), the samples were identified by a letter (C or D for slurries, depending on their estimated consistency immediately after sampling, and E for tube samples), a chronological number, and the first letters of the city and state from which the sample was obtained (TO for Toledo, Ohio, in the case of most samples discussed herein). The letter C designates a slurry that has the consistency of muddy water (solids content between about 10% and 25% by weight); the letter D represents a sample with a consistency of thick mud (solids content greater than 25% by weight); and the letter E identifies a sample of solid material capable of maintaining a given shape. The numbers in the sample designation simply indicate a chronological ordering of the samples within a given consistency group. The data analyzed in this study were obtained either from tests on samples of C, D, or E materials reported by Krizek, Karadi, and Hummel (1973) or from tests on samples of E materials listed in Appendix A; however, most of the investigation was concerned with the samples of E material taken from landfills. Ninety-five samples of E material are included in this experimental program; of these 16 were obtained from Riverside Site in 1972, two sets of 24 each were obtained from the Island, Penn 8, and Riverside Sites in 1973 and 1974 (one set each year), and 31 were taken from Penn 7 in 1974.

As mentioned previously, most tests were performed according to the standard procedures outlined by Lambe (1951). However, a minor modification was made in the standard method for the hydrometer test in order to reduce the time needed to test the large number of samples (over 80); this modification involved omitting the step of oven-drying the fines passing the No. 200 sieve. Based on experience, a wet weight of 80 to 100 grams of material was washed on a No. 200 sieve (0.074 mm) and the fines were used immediately for the hydrometer test without oven-drying. Hence, the actual weight of dredgings used in the hydrometer test was 50 ± 7 grams instead of 50 grams, but this variation has little practical significance in the interpretation of the test results. In cases where the actual weight of dredgings was found to lie outside the indicated range, the test was repeated. When it was difficult to estimate the dredgings passing the No. 200 sieve, the step of oven-drying was introduced to enable the use of the specified weight of 50 grams according to the standard procedure. The methods of testing for organic content and chemical constituents are explained and discussed by Krizek, Karadi, and Hummel (1973).

RESULTS AND ANALYSIS

The results presented and discussed in the following sections are summarized in Tables 3-1 through 3-4. Table 3-1 gives a list of the samples tested, their depth and location, and their natural water content, Atterberg limits, dry density, and clay content. A summary of the average values obtained from grain size analyses on samples taken from different sites and an overall average of the same parameters (percent clay, percent silt, percent sand, mean size (D_{50}), effective size (D_{10}), and uniformity coefficient) for all samples is given in Table 3-2. Results of organic

Table 3-1

Index Properties of Tested Samples

Sample	Bore Hole	Depth (m)	Water Content w_n (%)	Liquid Limit w_L (%)	Plastic Limit w_P (%)	Dry Density γ_d (kg/m^3)	Percent Clay
E117TO	10	1.60	65	78	35	960	40
E118TO	10	2.60	70	75	30	910	45
E119TO	10	3.35	60	76	36	970	50
E120TO	10	3.80	61	75	32	960	48
E122TO	11	1.20	54	68	40	1070	32
E123TO	11	1.90	56	74	32	1040	43
E125TO	14	1.20	53	64	33	1080	35
E127TO	14	2.70	66	75	29	940	42
E131TO	15	1.70	61	67	34	960	40
E133TO	15	2.80	62	68	36	950	42
E135TO	16	0.90	52	76	31	1090	47
E137TO	16	2.40	55	68	37	1060	49
E142TO	17	1.80	63	70	23	930	47
E144TO	17	3.10	66	72	27	940	36
E148TO	18	1.60	45	53	34	1180	28
E151TO	18	3.00	61	66	37	960	35
E162TO	21	1.30	57	77	27	1010	48
E164TO	21	2.00	59	68	33	960	44
E166TO	21	2.60	63			850	49
E169TO	21	3.50	56			960	
E170TO	26	0.80	57	65	35	1090	33
E172TO	26	1.30	65	75	43	940	28
E175TO	26	2.30	73	78	51	850	34
E177TO	26	2.90	68	80	49	890	
E180TO	28	1.30	47	53	43	1140	18
E181TO	28	1.80	60	76	24	940	
E182TO	28	2.30	62			880	
E184TO	28	2.90	63	70	44	860	40
E186TO	23	0.80	55	74	46	980	37
E190TO	23	2.00	55	73	21	1020	
E194TO	23	3.20	54	56	30	1120	31
E196TO	23	3.80				1080	
E240TO	21	0.45	74	78	45	900	28

Table 3-1 (continued)

Index Properties of Tested Samples

Sample	Bore Hole	Depth (m)	Water Content w_n (%)	Liquid Limit w_L (%)	Plastic Limit w_P (%)	Dry Density γ_d (kg/m^3)	Percent Clay
E242TO	21	1.10	73	82	45	1070	32
E244TO	21	1.70	68	72	38	830	45
E246TO	21	2.30	64	70	38	910	38
E247TO	21	2.60	64	84	40	890	43
E249TO	22	1.20	51	71	38	1060	
E250TO	22	1.80	51	58	38	1070	31
E251TO	22	2.30	61	72	26	910	35
E253TO	22	3.10	62	72	48	940	
E256TO	31	1.20	68			880	
E257TO	31	1.65	60			930	
E258TO	31	2.60	60			990	
E259TO	31	2.90	61	69	38	1000	
E261TO	36	0.90	50	61	36	1125	
E263TO	36	1.50	50			1060	
E265TO	36	2.10	65			880	
E268TO	36	3.05	64			930	
E271TO	38	1.70	42			1230	
E272TO	38	2.15	61	74	42	980	41
E274TO	38	2.85	63	70	44	1010	
E276TO	38	3.50	59	77	32	1000	36
E278TO	31	0.90	52	66	42	1090	
E280TO	31	1.65	54	65	31	1070	
E282TO	31	2.25	53	63	30	1050	38
E283TO	31	2.75	64	83	40	960	43
E284TO	32	0.90	55			1110	
E285TO	32	1.50	57	72	38	1010	31
E287TO	32	2.30	70	86	40	850	35
E289TO	32	2.75	62	73	46	990	43
E290TO	33	0.60	78	89	46	840	35
E294TO	33	1.95	55	66	33	1080	38
E296TO	33	2.60	62	62	27	1060	25
E300TO	33	3.80	43			1240	

Table 3-1 (continued)

Index Properties of Tested Samples

Sample	Bore Hole	Depth (m)	Water Content w_n (%)	Liquid Limit w_L (%)	Plastic Limit w_P (%)	Dry Density γ_d (kg/m^3)	Percent Clay
E302TO	2/10	1.10	77	76	38	870	36
E303TO	2/10	1.70	77	72	34	870	35
E304TO	5/8	0.75	86	83	33	810	40
E305TO	5/8	1.40	92	95	48	770	42
E306TO	5/8	2.00	95	83	35	750	
E307TO	5/8	2.60	81	79	30	840	37
E308TO	5/8	3.10	67	72	32	950	30
E310TO	5/10	0.75	90	84	38	780	40
E311TO	5/10	2.00	85	74	43	740	20
E312TO	5/10	2.60	77	81	32	870	
E313TO	5/13	0.60	92	94	38	770	
E314TO	5/13	1.40	97	83	40	740	
E315TO	5/13	2.00	84	73	30	820	
E316TO	5/13	2.75	76	72	31	880	
E318TO	8/10	1.40	68	59	33	910	30
E319TO	8/10	2.00	83	91	38	830	28
E320TO	8/10	2.25	73	80	27	900	
E322TO	8/13	0.75	95	82	37	750	31
E323TO	8/13	1.40	98	91	40	740	45
E324TO	8/13	2.00	94	75	36	760	30
E325TO	8/13	2.90	64	68	30	980	28
E326TO	12/10	0.75	89	87	32	790	44
E327TO	12/10	1.35	92	80	33	770	42
E328TO	12/10	1.95	82	73	40	830	40
E329TO	15/10	0.75	90	76	36	780	
E330TO	15/10	1.35	94	83	35	760	39
E331TO	15/10	1.95	81	66	30	840	43
E332TO	16/12	0.75	95	84	34	750	41
E333TO	16/12	1.35	96	90	39	750	47
E334TO	16/12	1.95	89	65	31	790	27
E335TO	16/12	3.50	78	74	38	880	41

Table 3-2

Summary of Grain Size Analysis

Site	Percent Clay	Percent Silt	Percent Sand	Mean Size D_{50} (mm)	Effective Size D_{10} (mm)	Uniformity Coefficient $U=D_{60}/D_{10}$	Number of Samples
Island	31	50	19	0.0098	0.0026	6.1	5
Penn 8	37	48	15	0.0073	0.0022	5.5	12
Riverside	40	46	14	0.0082	0.0019	5.9	26
Penn 7	36	47	17	0.0075	0.0020	7.0	23
Overall Average	37	47	16	0.0079	0.0021	6.2	66

Table 3-3

Organic Carbon and Loss on Ignition for Various Dredgings

Sample	Organic Carbon	After 5 hours at 440°C		After 24 hours at 440°C	
		Loss on Ignition	Carbon Ratio	Loss on Ignition	Carbon Ratio
C22TO	3.72	5.27	0.71	7.60	0.49
C27MM	7.55	11.89	0.63	11.93	0.63
D1DM	12.50	5.97	2.10	12.26	1.02
D2DM	8.96	11.50	0.78	12.25	0.73
D3TO	3.21	5.67	0.57	6.40	0.50
D4CO	8.21	9.00	0.92	10.00	0.82
D6TO	0.79	1.10	0.72	1.25	0.63
D8TO	4.51	7.77	0.58	8.36	0.54
D9TO	3.90	8.27	0.47	8.71	0.45
D10TO	3.69	7.29	0.51	7.93	0.46
E6TO	2.92	5.40	0.54		
E7TO	1.96	4.68	0.42	4.80	0.41
E8TO	2.14	3.90	0.55	4.40	0.48
E10TO	3.12	5.80	0.54		
E13TO	2.35	5.61	0.43	5.93	0.39
E14TO	4.09	7.08	0.58	7.43	0.55
E15TO	2.29	5.27	0.44	6.09	0.38
E16TO	3.12	6.53	0.48	6.65	0.47
E17TO	2.54	5.40	0.47	5.83	0.43
E18TO	2.78	5.70	0.49	6.39	0.43
E19TO	3.33	6.53	0.51	6.65	0.50
E20TO	3.08	6.59	0.47	6.94	0.44
E21TO	2.74	5.35	0.51	5.76	0.47
E22TO	2.17	3.54	0.62	3.84	0.57
E23TO	2.71	5.27	0.52	5.81	0.47
E24TO	2.98	6.13	0.48	6.21	0.48
E25TO	2.60	6.18	0.42	6.40	0.41
E26TO	2.41	5.91	0.41	6.00	0.40
E27TO	2.85	6.02	0.47	6.20	0.46
E28TO	2.95	6.43	0.46	6.70	0.44
E29TO	2.57	6.14	0.42	6.30	0.41
E63TO		5.20		6.20	
E71TO	2.71	5.84	0.46	6.10	0.45
E83TO	1.41	7.39	0.19	7.60	0.19

Table 3-4

Qualitative Mineralogical Analyses

Sample	Minerals Positively Present	- Minerals Possibly Present
C3TO	Mica (Illite) Kaolinite Vermiculite Carbonates Some organic matter	Quartz
C7MW	Mica (Illite) Kaolinite Quartz Dolomite Carbonates	Vermiculite
C8MW	Mica (Illite) Dolomite Carbonates Some organic matter	Seprolite Vermiculite
C9MW	Mica (Illite) Kaolinite Dolomite Quartz Carbonates Some organic matter	Vermiculite
C22TO	Mica (Illite) Kaolinite Vermiculite Dolomite Quartz Carbonates	
D4CO	Mica (Illite) Kaolinite Montmorillonite Dolomite Carbonates Organic matter	Vermiculite
D6TO	Mica (Illite) Kaolinite Vermiculite Quartz Dolomite Some carbonates	

content determinations and mineralogy are summarized in Tables 3-3 and 3-4, respectively.

Natural Water Content

Water contents ranged from 45% to 70%, 47% to 73%, and 42% to 68% for samples obtained from Riverside Site in the summers of 1972, 1973, and 1974, respectively; from 51% to 74% and 52% to 70% for Penn 8 samples and from 54% to 55% and 43% to 78% for Island samples taken in the summers of 1973 and 1974, respectively; and from 67% to 98% for Penn 7 samples taken in the summer of 1974. These values provide an appreciation for the water contents of dredgings that are left dormant in diked areas for different periods of time. Some of the variations in the water contents of samples from different sites can be explained by variations in drainage conditions, thickness of layer, relative surface levels of the different sites compared to that of the Maumee River, and the flooding that occurred due to certain abnormally high water levels of Lake Erie and the Maumee River.

Variation of Liquid Limit and Plastic Limit with Clay Content

The liquid and plastic limits are plotted in Figure 3-1 versus percent clay for 65 dredging samples (5 from the Island, 12 from Penn 8, 25 from Riverside Site, and 23 from Penn 7). Four different symbols are used in these plots to distinguish the four different field sites, but the years during which the samples were obtained are not identified. In general, no patterns can be identified to distinguish one site from another, and the data from the different sites appear to be randomly interspersed, thereby suggesting that the limits can be treated as representative of samples from one source.

The liquid limit, w_L, varies between about 50% and 100%, whereas, the clay content ranges from about 20% to 50%, and, as shown in Figure 3-1a, the

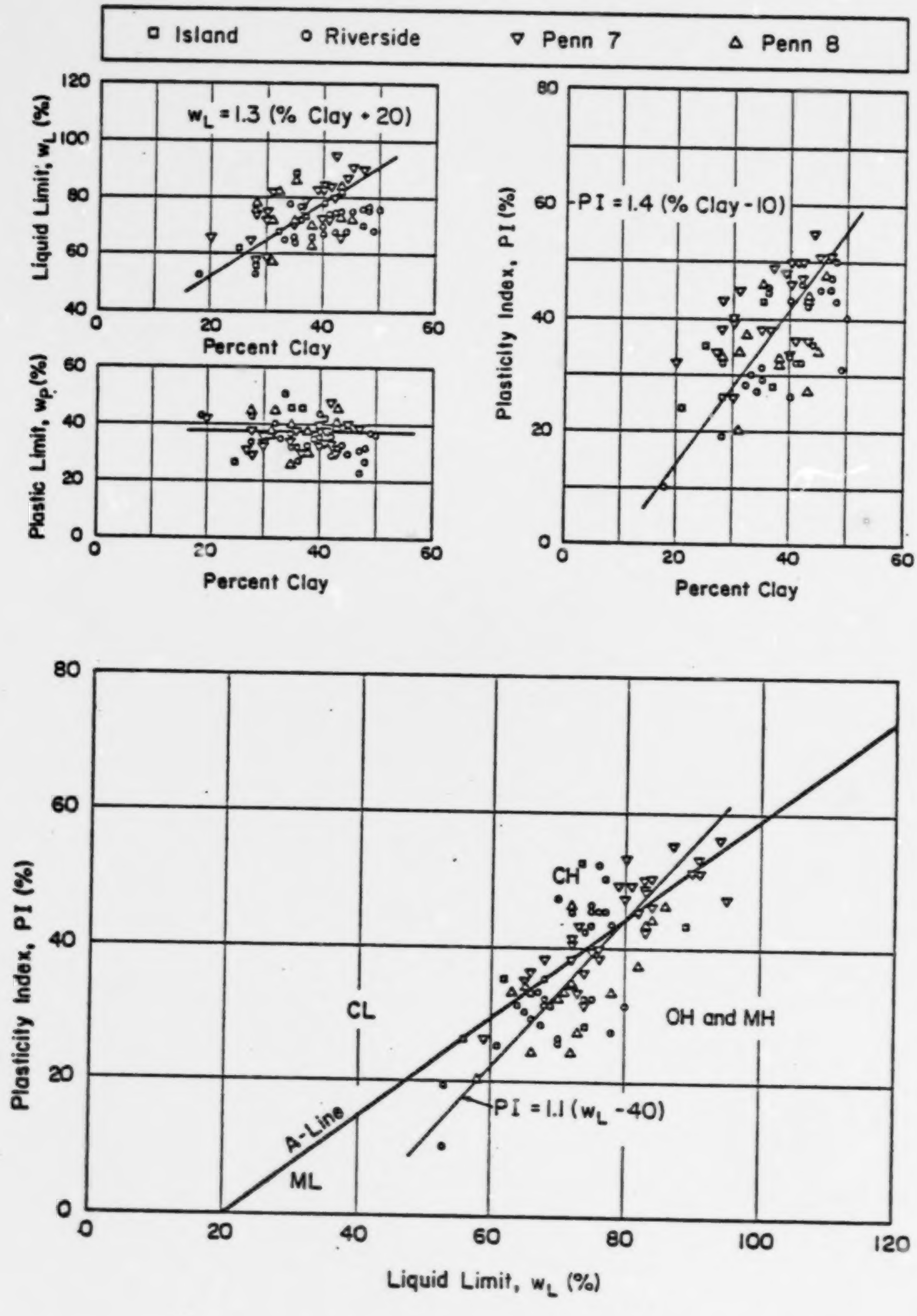

Figure 3-1. Plasticity Relationships

relationship between the two can be expressed as

$$w_L = 1.3\ (\%\ \text{Clay} + 20) \quad , \qquad (3\text{-}3)$$

in which the variables are expressed in percent. The scatter around the line represented by Equation (3-3) is about ±15% and is attributed to the variations in the bottom sediments.

The plastic limit, w_P, for the same samples is plotted in Figure 3-1b versus percent clay, but no definite trend is indicated. As mentioned earlier, Seed, Woodward, and Lundgren (1964) reported a linear increase in the plastic limit with an increase in the clay content only after the clay fraction was sufficient to fill the voids in the non-clay fraction of the soil; for the artificial clays tested, the percent clay satisfying this condition was found to vary from about 20% to 45%. Moreover, a decrease in the plastic limit with an increase in percent clay was observed for values of the clay fraction below the indicated range. Since the clay content of the dredgings studied in this program ranged from about 20% to 50%, which spans the critical range reported by Seed, Woodward, and Lundgren (1964), the lack of any clear trend in Figure 3-1b can be attributed to this condition.

Variation of Plasticity Index with Percent Clay

Of interest in any soil classification system is the relationship between plasticity index, PI, and clay content, because this has been used as the basis for defining the activity of clays (Skempton, 1953). Based on the plot in Figure 3-1c of plasticity index versus percent clay for 65 dredgings samples, a straight line relationship showing an increase in plasticity index with an increase in percent clay was found, but the most representative line did not pass through the origin. The empirical equation best representing this relationship can be written as

$$PI = 1.4\ (\%\ Clay - 10), \qquad (3\text{-}4)$$

where the variables are expressed in percent. Hence, the average value of the activity for dredged materials is found to be about 1.4.

Relationship Between Plasticity Index and Liquid Limit

The plasticity index, PI, is plotted in Figure 3-1d versus the liquid limit, w_L, on the Casagrande (1948) plasticity chart for 83 samples of dredgings (6 from the Island, 16 from Penn 8, 30 from Riverside Site, and 31 from Penn 7). All data points lie essentially within a PI range from about 20% to slightly more than 50%, and according to the plasticity chart, these dredgings can be classified as a mixture of organic clays of medium to high compressibility and inorganic clays of high plasticity, with slightly more than one-half of the samples falling into the former category. Seed, Woodward, and Lundgren (1964) reported "...in the liquid limit range 50 to 100 (percent), the analysis also indicates that organic soils may plot above the A-line. It may be noted that Casagrande also reported organic clay plotting above the A-line when he originally suggested the use of this boundary. Thus, the A-line is not a rigid boundary but recognizes some degree of overlapping in the position of organic and inorganic clays..." Because most of the data points for the dredgings samples are close to the A-line, it is difficult to decide which samples can be considered as inorganic clays, especially since it is known from organic content tests that the material, in general, is moderately organic. The relationship between plasticity index and liquid limit can be expressed as

$$PI = 1.1\ (w_L - 40). \qquad (3\text{-}5)$$

Equations (3-3) and (3-4) can be combined to give a relationship that is essentially the same as Equation (3-5). As before, the random interspersing of data from all four sites suggests an overall similarity of these materials.

Variation of Limits and Plasticity Index with Activity

The definition of activity given by Equation (3-1) implies that there is a unique value of activity for a given soil, since the plasticity index and clay content would be constant. However, this is not necessarily the case because the nature of the clay fraction may vary considerably, especially for dredged materials. It is worthwhile, therefore, to investigate the variations in the Atterberg limits and the plasticity index with changes in the activity of these dredgings, and appropriate plots are given in Figure 3-2. The liquid limit is seen to increase linearly with an increase in the activity, A, and the relationship can be written as

$$w_L = 25\ (A + 1.6)\,, \qquad (3\text{-}6)$$

which agrees with results reported by Seed, Woodward, and Lundgren (1964), who also observed that the constant of proportionality increases with an increase in the clay fraction. The plastic limit is observed to have no definite correlation with the activity, and a nonlinear increase of plasticity index is seen to occur with an increase in activity. The rate of increase of the plasticity index is high at low values of activity and decreases gradually as the latter increases. Once again, the data points from the four field sites are randomly mixed.

Particle Size Characteristics

The results of particle size distribution curves for 66 samples from the four different sites are summarized in Table 3-2. The average percentages

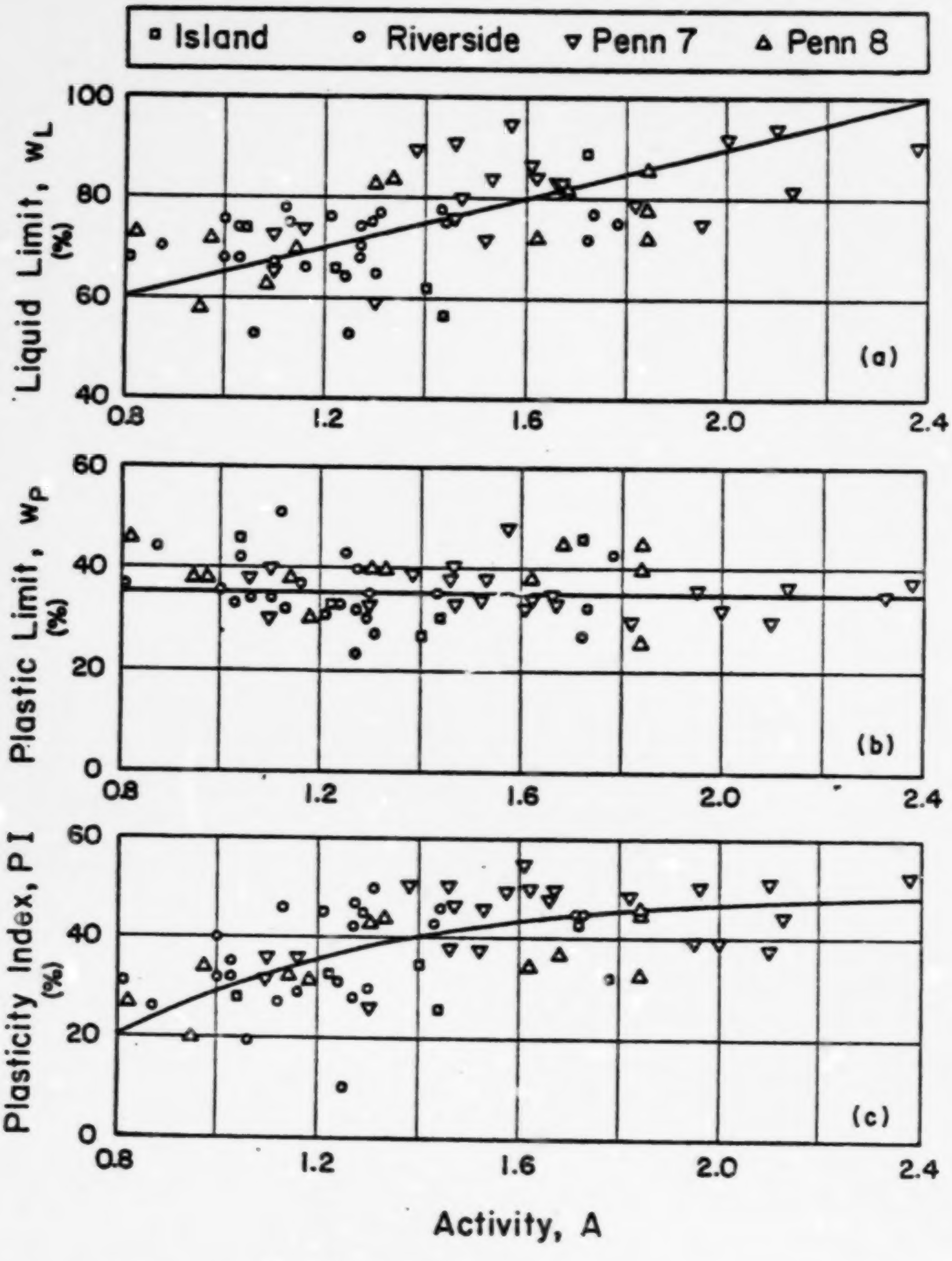

Figure 3-2. Variation of Atterberg Limits and Plasticity Index with Activity

of sand, silt, and clay fractions for the materials in each of the four sites are essentially the same, with the individual components being proportioned on approximately a 1:3:2 basis. The average values of the mean particle size, D_{50}, and the effective particle size, D_{10}, are practically the same for the materials in each of the different sites, with overall averages of 0.0079 mm and 0.0021 mm, respectively. The individual average values for the coefficient of uniformity, D_{60}/D_{10}, vary between 5.5 and 7.0 with an overall average of 6.2.

Organic Matter

The results of an extensive series of organics tests are summarized in Table 3-3 with the values obtained by wet combustion listed as organic carbon and those obtained by dry combustion listed as loss on ignition. Except for a few instances, the organic carbon of the samples tested is of the order of 2 to 4 percent. If it is accepted that organic matter consists of about 50 percent organic carbon, the organic matter content for most of the samples will vary from 4 to 8 percent. It was noticed that the samples with high organic contents (especially samples D1DM and D2DM) exhibited a strong oily odor, and the presence of hydrocarbons may account for such high organic carbon contents. Limit test data for a number of dredgings samples are plotted in Figure 3-3 as a function of the organic carbon content and the ignition loss. Although the limit values generally increase with increasing values of organic carbon content or ignition loss, the indicated relationships are not well defined; this is probably due in large part to the effects of other variables, such as gradation, percentage of fines, clay mineralogy, and type of organic material. Furthermore, since the degree of decomposition of the organic matter in the dredgings is generally very high, the existing organic compounds have probably reached

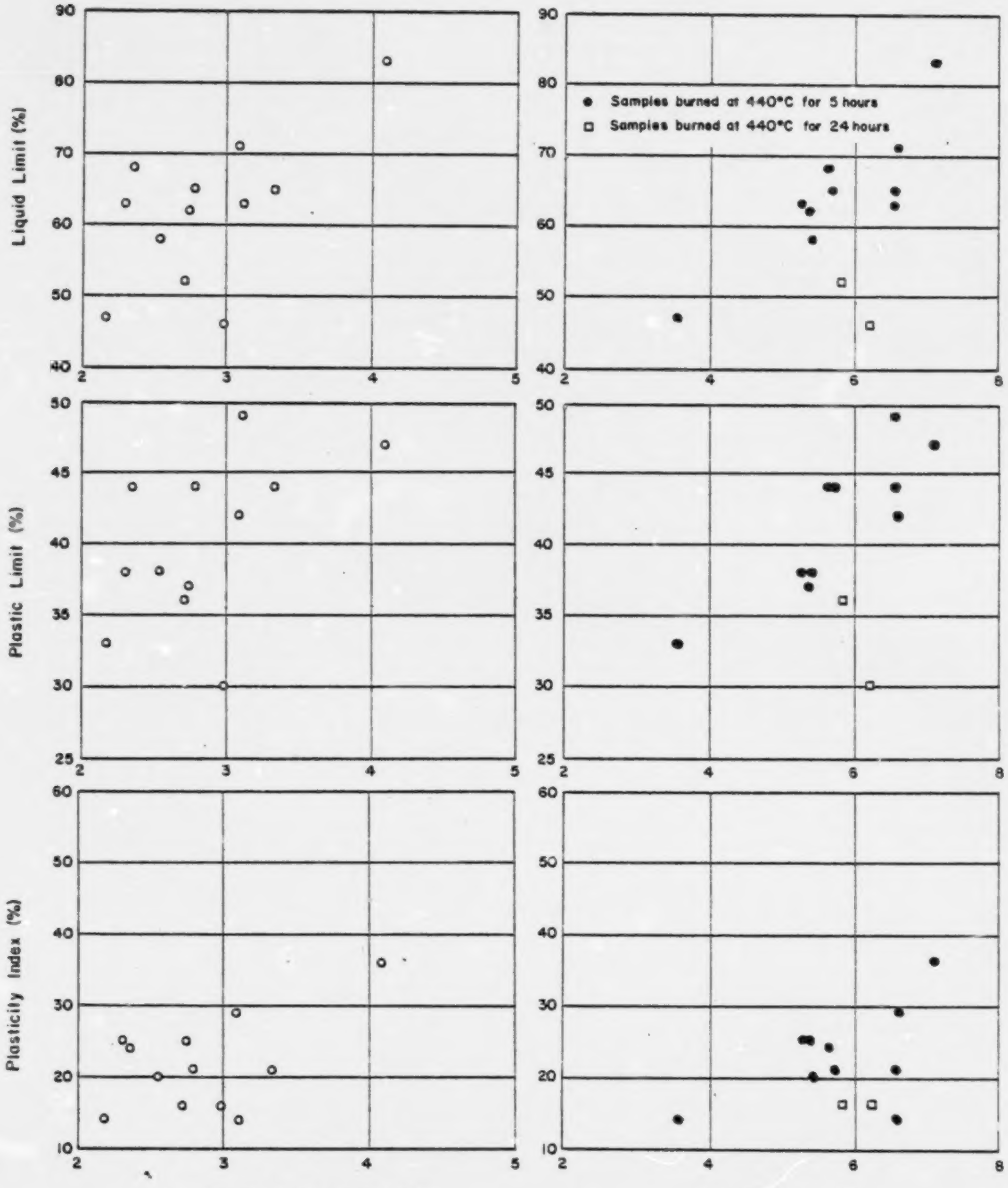

Figure 3-3. Atterberg Limits versus Organic Content for Various Dredged Materials

a chemically stable condition and do not impart to the dredged materials the same type of behavior as organic matter with a low degree of humification, such as that often found in organic soils.

Chemistry

The testing techniques and results of an extensive experimental program to analyze the chemical composition of dredged materials has been reported by Krizek, Karadi, and Hummel (1973) and Krizek, Gallagher, and Karadi (1974), and they will not be repeated herein. In general, virtually all of the dredgings tested would be classified as polluted. The degree of pollution varied considerably from harbor to harbor, from sample to sample within a harbor, and in the intensity of the various pollutants for a particular sample. The chemical composition of the water was very consistent with that expected at particular locations. For example, where sewage was emitted, the dissolved oxygen was low and the biological oxygen demand and nitrogen content were high; this was also true for bottom sediments. However, the chemical oxygen demand depended not only on organic compounds, but also on other materials (such as the nitrite and sulfide anions and the mercurous, cuprous, and ferrous cations) that are found in high concentrations in these dredgings. No definitive relationships could be established between the chemical composition of a sample and its engineering behavior, nor can any general conclusions be advanced regarding the chemical nature of maintenance dredgings, since the chemical components of a sample are so highly dependent on the localized environment from which it was taken.

Mineralogy

The results of mineralogical analyses on seven different dredgings samples are reported in Table 3-4. After being air-dried, these samples were tested for organic matter by use of hydrogen peroxide (H_2O_2) and for carbonates by use of 1N hydrochloric acid. Powder samples of the material passing the No. 200 sieve were used for X-ray analyses; the clay-size particles (less than two microns) were separated by mixing the material in a blender with a dispersing agent and then placing the mixture in a centrifuge to remove all particles larger than 2 microns. Sedimented samples were formed by allowing the decanted suspension to evaporate slowly, and three slides were prepared for each sample. One slide was X-rayed after air-drying, one after heating overnight at 500°C, and the third after treatment with glycol. Most of these dredgings were found to contain substantial amounts of the common clay minerals, such as illite and kaolinite; this is consistent with the findings reported by the Philadelphia District, Corps of Engineers (1969) and Hartzell (1968).

CONCLUSIONS

Within the framework of the characterization study reported herein, the following conclusions can be advanced:

1. Most dredgings can be classified as a mixture of organic silts and clays of medium to high plasticity (OH) and inorganic clays of high plasticity (CH), with approximately 60 percent of the materials tested lying in the first category and 40 percent in the second.

2. The organic content of most of the dredgings tested was between 4 and 8 percent, thereby enabling them to be classified as intermediate organic soils.

3. Particle size analyses indicated that sand, silt, and clay are present in these dredgings in approximate proportions of 1:3:2.

4. The liquid limit and plasticity index were found to exhibit reasonably linear relationships with the clay content, but the plastic limit apparently does not correlate with percent clay.

5. Of considerable importance to this study, the characteristics of the materials deposited in each of the four sites at Toledo, Ohio, were found to be essentially the same, thereby enabling data from all four sites to be synthesized and treated as representative of one large site spanning a time period of almost a decade.

CHAPTER 4

SLURRY CONSOLIDATION

Since dredging wastes usually contain a substantial amount of clay-like and/or organic materials and since they are frequently deposited in a containment area as a slurry with a very high water content, the effectiveness and economy of associated landfill operations are often hampered by the time-consuming process of consolidation. Accordingly, the work in this chapter is directed toward an evaluation of the consolidation characteristics of several typical dredging slurries. Special equipment is used to consolidate several typical dredging slurries that are too soft and/or too fluid to test by conventional means, and the resulting data are analyzed to develop convenient empirical relationships which may be used to estimate the compression index, coefficient of consolidation, coefficient of permeability, and various other consolidation characteristics of dredgings. Supplemental test data, such as strength, limits, organic content, and chemical constituents, are provided to place the materials into context and to assess in a broad way the effectiveness of this disposal scheme in pollution control.

MATERIALS TESTED

Dredging slurries normally consist of relatively high water content mixtures with virtually no shear strength and low permeability. Typically, a slurry pumped hydraulically from a hopper dredge into a disposal area may have a solids content of 10 to 20 percent by weight. As soon as the slurry enters the disposal site, the solids begin to settle out of suspension and the excess water passes over a weir; the height of the weir and the associated retention time of the slurry mixture is dictated to a large degree by the desired quality of the discharge from the weir. After most of the solids have settled out of suspension, the resulting slurry is somewhat thicker and has a solids content of about 30 to 40 percent by weight--essentially the same as that of the bottom sediments before they are dredged.

With one exception all dredging samples tested in this experimental program were obtained from the vicinity around Toledo, Ohio, and brief descriptions of each sample are given in Table 4-1. Although concentrated in one geographic area, the samples were taken by different methods from different locations throughout various cycles of the dredging process. The bottom sediments and materials from the hopper of the dredge were sampled by use of either a flap valve sampler or an Ekman dredge, and other procedures were employed to obtain samples from the discharge pipes and a fill area (Hummel and Krizek, 1974). Included in Table 4-2 are the results from various other tests which were conducted to characterize the dredgings. An analysis of the chemical constituents of the fluids drained from the dredgings shows a surprising uniformity in the concentrations of certain ions in the fluids during the entire consolidation process. As seen in Table 4-3, the soluble ions of sodium, potassium, and calcium were carried off in the fluid, whereas aluminum, cadmium, lead, and copper were essentially retained with the solids.

EXPERIMENTAL PROCEDURE

When a high water content slurry with virtually no shear strength is subjected to an external pressure, the water is squeezed from the voids between the solid particles; however, since the permeability of most maintenance dredgings is low, this process of consolidation usually takes considerable time. The unique problems associated with determining the consolidation

Table 4-1

Summary of Materials Tested

Sample Number	Date Obtained	Brief Description
C10TO	6/29/71	Bottom sediments from Maumee River, Toledo, Ohio
C11TO	6/29/71	Bottom sediments from Maumee River, Toledo, Ohio
C12TO	6/29/71	Bottom sediments from Maumee River, Toledo, Ohio
C13TO	6/29/71	Bottom sediments from Maumee River, Toledo, Ohio
C15TO	6/29/71	Bottom sediments from Maumee River, Toledo, Ohio
C17TO	6/29/71	Bottom sediments from Maumee River, Toledo, Ohio
C20TO	7/2/71	Material from hopper of dredge Hoffman, Toledo, Ohio
C22TO	7/2/71	Material from discharge pipe at Island disposal site, Toledo, Ohio
C27MM	11/11/71	Material from discharge pipe at disposal site, Monroe, Michigan
D3TO	12/9/70	Soft sediments from Riverside disposal site, Toledo, Ohio
D9TO	6/29/71	Bottom sediments from Maumee River, Toledo, Ohio
D10TO	6/29/71	Bottom sediments from Maumee River, Toledo, Ohio

Table 4-2

Characteristics of Materials Tested

Sample Number	Liquid Limit (%)	Plastic Limit (%)	Plasticity Index (%)	Percent Clay (< 2 microns)	Total Solids (%)	Total Volatile Solids (%)	COD	Organic Nitrogen (mg/gm)	Ammonia Nitrogen (mg/gm)	Total Phosphate (mg/gm)	Oil and Grease (mg/gm)	Hydrocarbons (mg/gm)	Total Iron (mg/gm)	Cyanide (µg/gm)	Lead (µg/gm)	Mercury (µg/gm)	Organic Carbon (%)	Loss on Ignition (%)
C10TO	61	21	40	30	18.1	14.6	185	5.3	1.4	6.5			29.4	11.8	144			
C11TO	76	48	28		14.5	14.4	114	3.4	1.7	13.9			30.0	4.1	150			
C12TO	60	32	28	34	20.2	12.1	181	3.5	1.2	11.6			28.5	3.3	161			
C13TO	65	32	33	50	18.8	10.6	47	1.8	0.4	8.4			26.5	1.1	101			
C15TO	67	39	28	48	18.1	10.1	86	2.3		7.0			26.1	1.1	81			
C17TO	71	50	21	44	12.0	10.6	80	4.1	0.8	9.7	0.8	0.2	27.9	3.4	129			
C20TO	74	36	38	53	25.7	10.2	88	4.0	0.6	14.2	11.9	6.8	31.8	2.8	105			
C22TO	75	39	36	45	17.3	9.0	116	4.1	0.9	6.4	11.5	5.7	30.9	1.2	73		3.7	7.6
C27MM	60	49	11	38	12.5	12.5							19.5		181		7.6	11.9
D3TO	66	32	34	32	43.4	7.0					2.1		0.3		50	0.4	3.2	6.4
D9TO	66	35	31		37.8	8.8		0.7	0.7	0	6.6	3.7	20.2	1.5	70		3.9	9.7
D10TO	73	25	48		38.7	8.9		0.4	0.7	0	5.4	4.1	22.3	0.8	89		3.7	7.9

Table 4-3

Chemical Analyses of Effluents

Sample	Effluent Specimen	Vertical Stress (psi)	Time (min)	Concentration in ppm					
				Pb	Cu	K	Na	Ca	Fe
C11TO	1	1	970	0	0.15	27	22	0	10
	2	4	7,416	0	0.85	27	21	8	--
	3	8	11,090	0	--	22	23	12	10
	4	16	32,603	0	--	27	26	28	--
C13TO	1	2	8,480	0	0.05	27	23	75	4.3
	2	2	11,320	0	0.03	27	21	75	12.2
	3	4	19,100	0.25	0.15	27	23	132	2.5
C15TO	1	4	1,360	0.25	0.03	18	25	95	2.7
C20TO	1	1	970	0	0.05	27	28	22	2.3
	2	9	11,090	0	--	27	--	12	2.5
	3	16	22,585	0	0	27	28	8	2.5
C22TO	1	1	970	0	6	23	30	4	--
	2	4	7,416	0	0	--	--	--	--
	3	8	11,090	0	--	27	--	50	--
	4	16	22,586	0	0	27	25	34	1
C27MM	1	2	1,460	0	0	14	27	50	2.8
	2	2	11,320	--	1	14	25	34	0.3
	3	4	19,100	0	0	14	27	75	2.8
	4	4	19,820	0	0	14	26	56	2.8
D9TO	1	2	8,480	0.25	0.01	18	22	75	2.5
	2	2	11,320	0	0.01	18	23	65	2.5
	3	4	19,100	0.25	0.03	23	23	95	80

characteristics of slurries led to the development of a slurry consolidometer apparatus (Sheeran and Krizek, 1971) which was used in this study.

Description of Equipment

The basic slurry consolidometer apparatus is shown in Figure 4-1. The fundamental unit is the cylindrical chamber into which the slurry is placed, and the supplemental equipment is used to control the conditions under which the test is conducted. After the piston is placed on top of the slurry, the load is applied by use of precisely controlled air pressure on top of the piston. The effluent emitted from the slurry is captured by means of an auxiliary tank on the back-pressure line. Back-pressure is used to enhance complete saturation of the test specimen by driving the last vestiges of gas into solution and hopefully preventing the formation of free gas bubbles during the test. Figure 4-2 shows a cross-sectional view of the consolidometer, including the drainage lines, chamber pressure lines, bleed line from between the two sealing rings on the piston, and the vent line. Porous stones are embedded in the bottom plate and in the base of the piston to transmit the effluent from the slurry to the drainage lines.

Loading Scheme

Any of several loading schemes may be used with the slurry consolidometer; these include (a) automatic loading by maintaining a constant pore pressure difference across the specimen (Lowe, Jonas, and Obrician, 1969), (b) a constant rate of strain loading (Smith and Wahls, 1969; Wissa, Christian, Davis, and Heiberg, 1971), and (c) a manually controlled load increment, which is similar to that used for conventional consolidation tests. Based on the results of a preliminary study on one sample of dredgings (D3TO), the constant-pore-pressure-difference method of loading was abandoned because the gas generating properties of dredgings precluded the use of the load

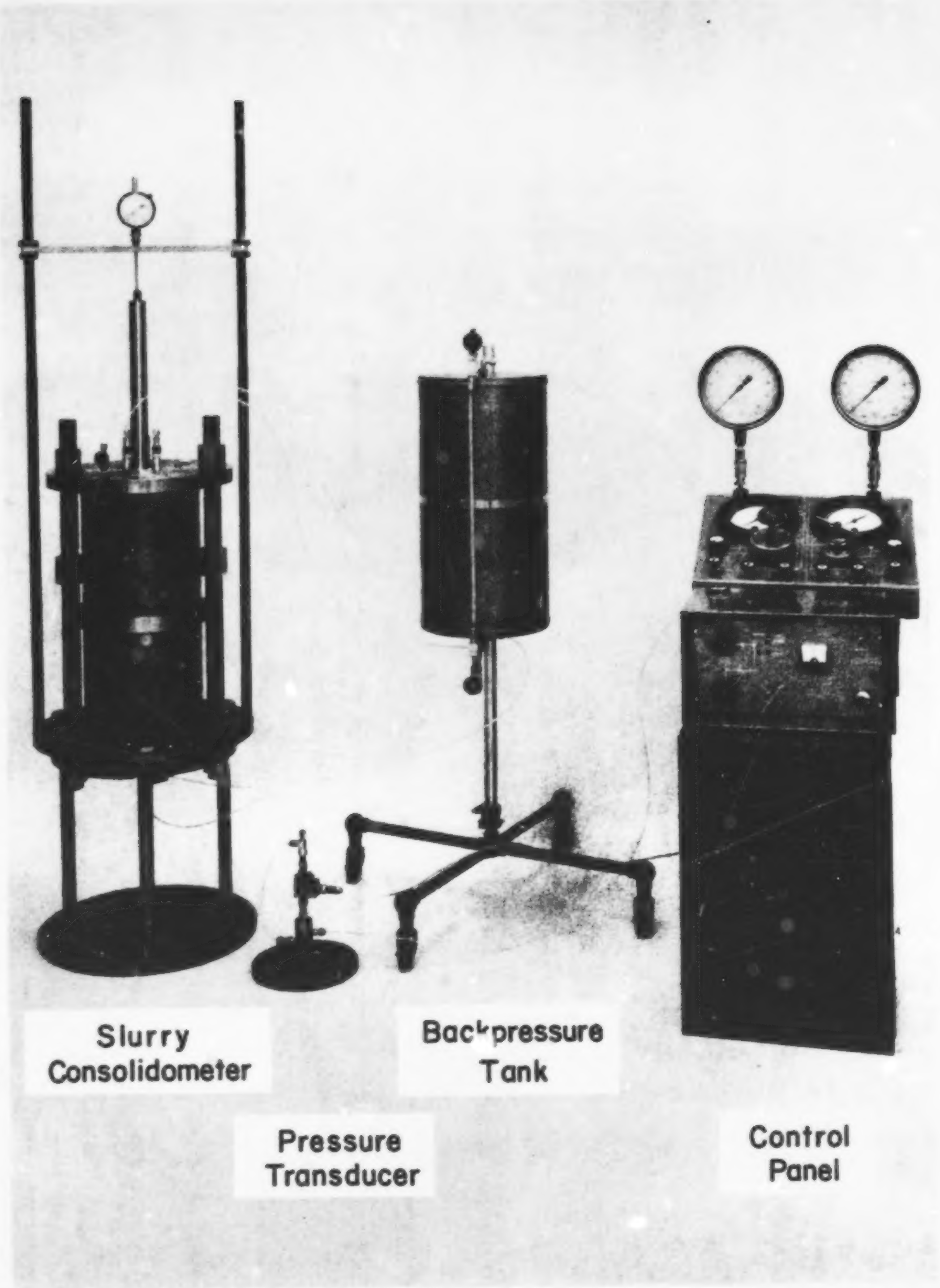
Slurry Consolidometer
Backpressure Tank
Pressure Transducer
Control Panel

Figure 4-1. Slurry Consolidation Apparatus

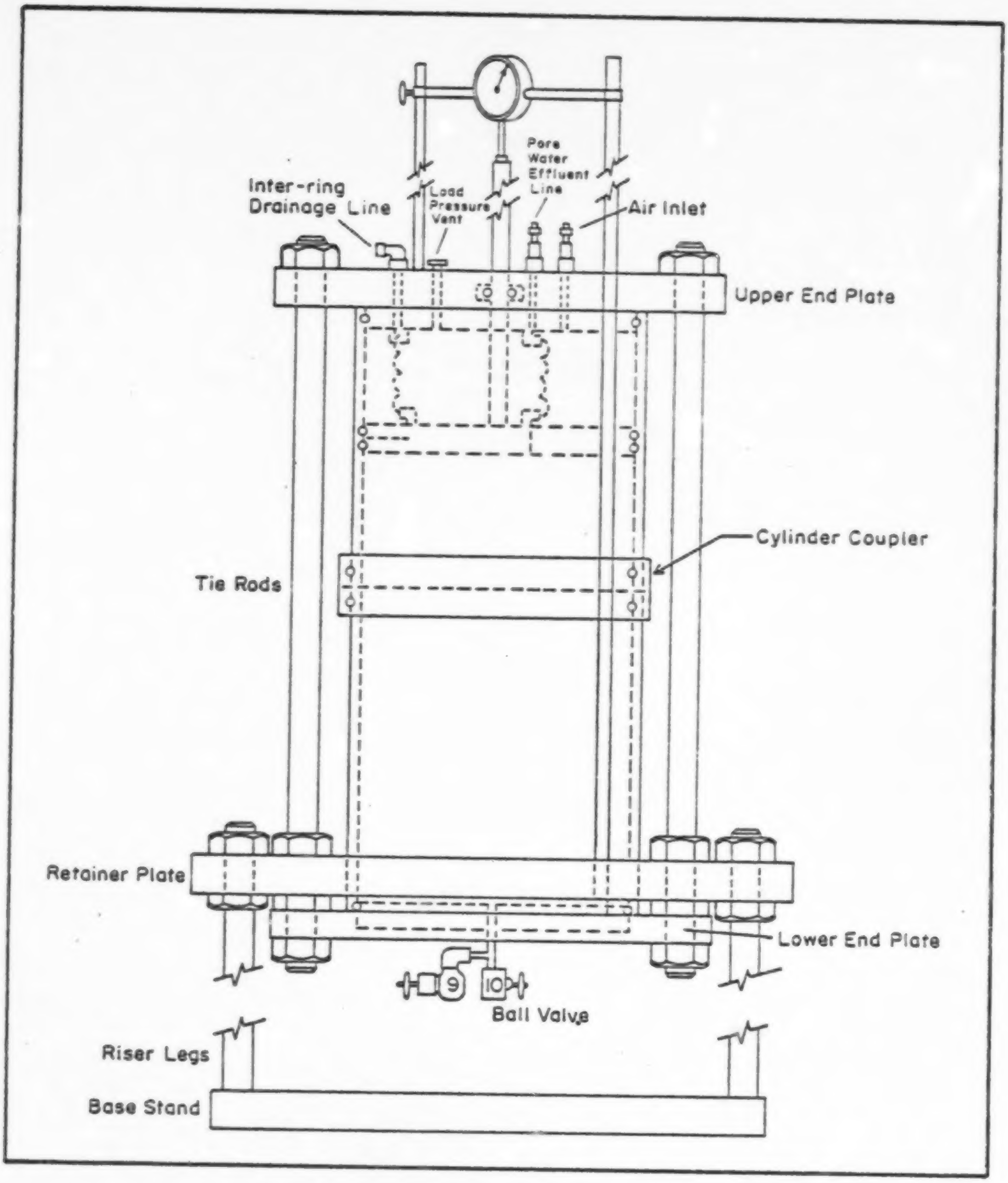
Pore Water Effluent Line
Inter-ring Drainage Line
Load Pressure Vent
Air Inlet
Upper End Plate
Cylinder Coupler
Tie Rods
Retainer Plate
Lower End Plate
9
10
Ball Valve
Riser Legs
Base Stand

Figure 4-2. Cross-section of Slurry Consolidometer

pacer. Although promising, the present state of knowledge regarding consolidation theory suggests caution in the use of a constant rate of strain loading procedure. Accordingly, the manually controlled load increment method was used for all subsequent tests on dredgings. When primary consolidation due to the final load was essentially complete, the load was removed and the block of consolidated dredgings was extracted from the bottom of the test chamber by use of a system shown in Figure 4-3. The piston was secured to the bottom test plate, and both were allowed to move downward as a unit with the sample, thereby minimizing sample disturbance. After the sample was clear of the chamber, the spacer block and nut were adjusted to hold the piston in place, and the block of dredgings was lowered and removed.

ANALYSIS OF RESULTS

As shown in Figure 4-4, typical data from a slurry consolidation test may be plotted directly as the void ratio, e, versus time, t, or the logarithm of time, log t; although the former provides a readily comprehensible demonstration of the measured response, the e-log t curves are usually preferred from an engineering point of view. The selection of one particular point (usually the last one) from each e-log t curve for a given applied stress, p, allows an e-log p curve to be plotted, and representative e-log p curves for each of the twelve samples tested are given in Figure 4-5.

Void Ratio versus Pressure

A study of the e-log p curves for these materials reveals a nearly linear plot in most cases for the last few load increments. A closer comparison of particular e-log p curves indicates considerable similarities;

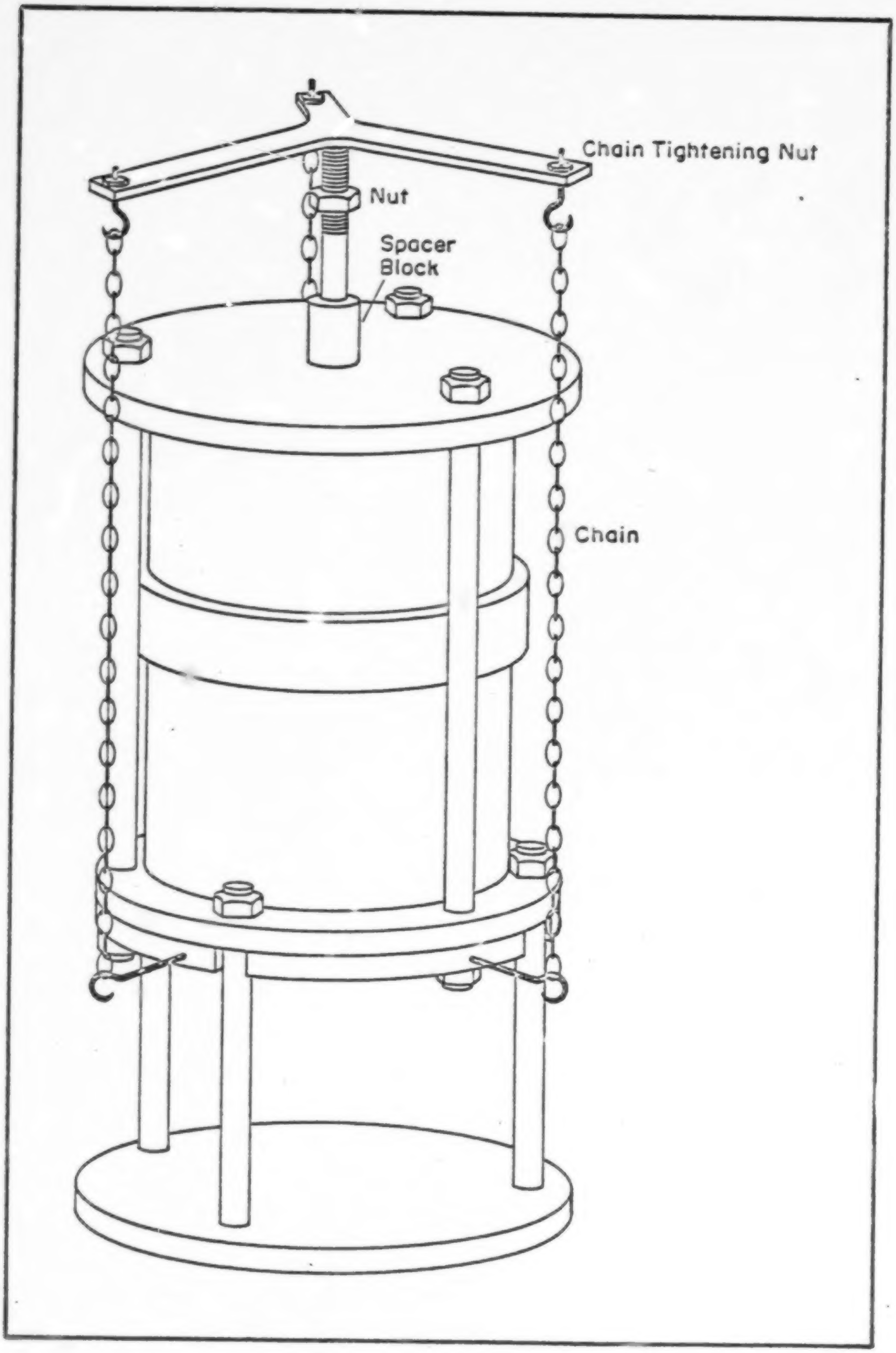
Chain Tightening Nut
Nut
Spacer Block
Chain

Figure 4-3. Slurry Consolidometer Sample Removal System

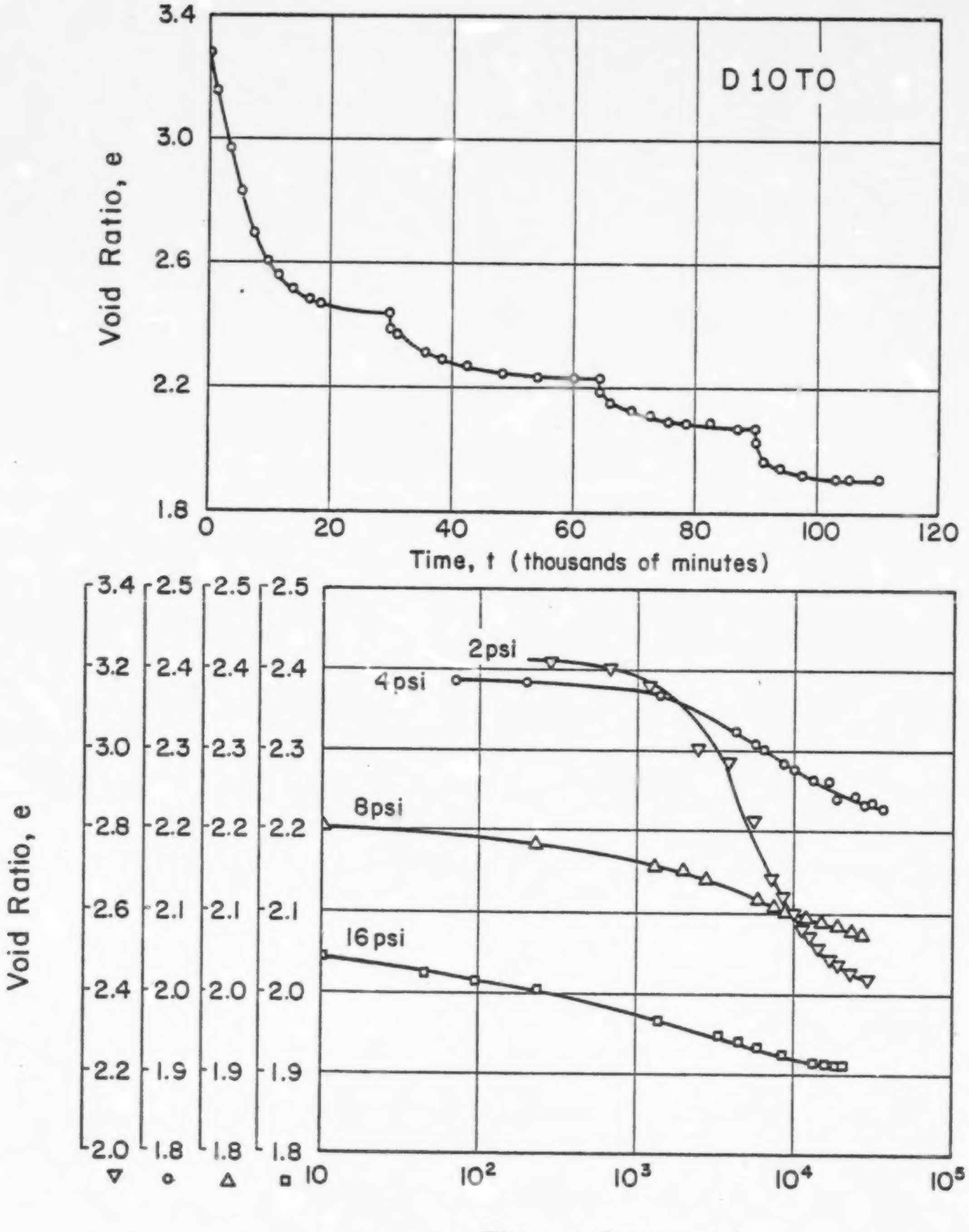

Figure 4-4. Typical Plots of Void Ratio versus Time

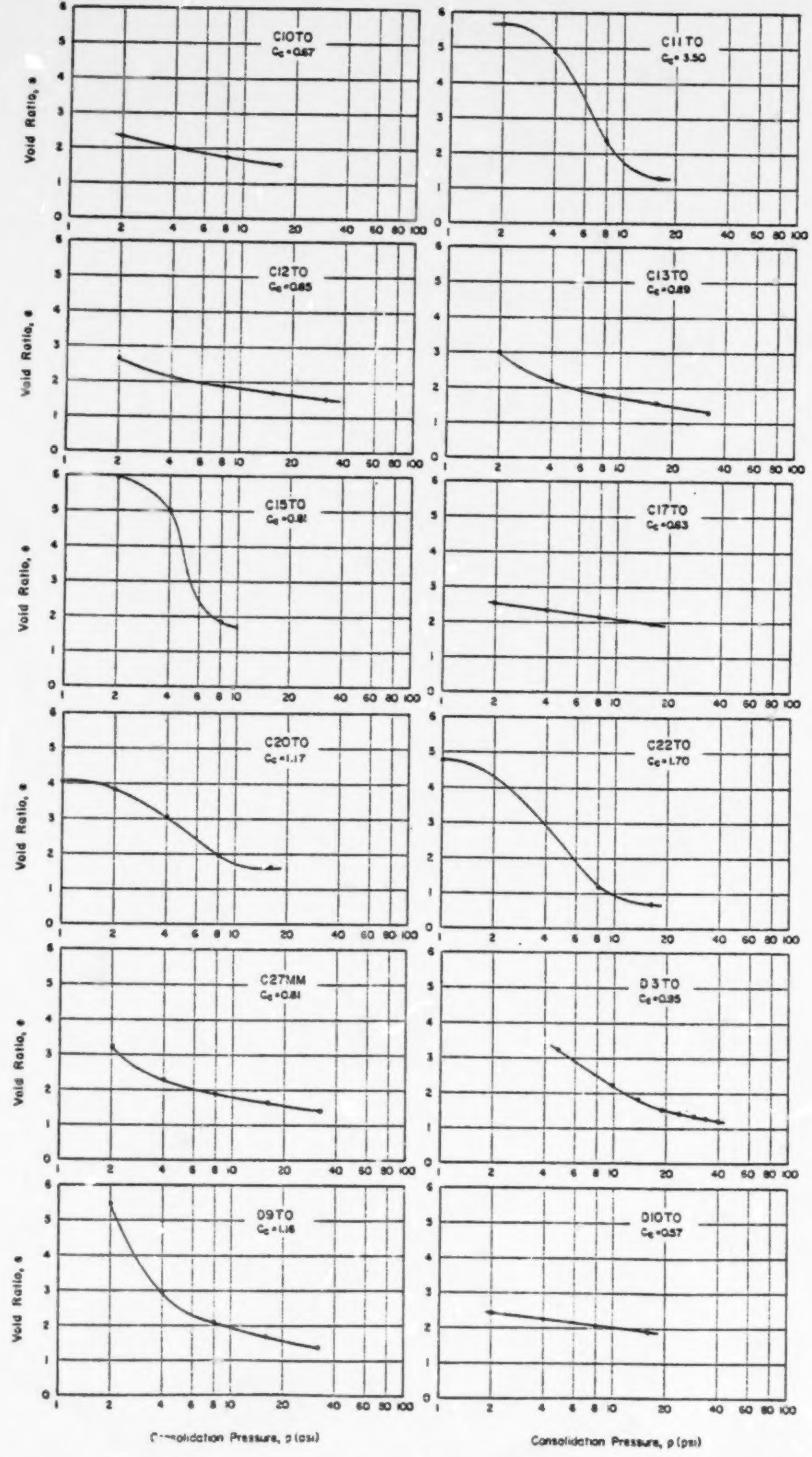

Figure 4-5. Void Ratio versus Consolidation Pressure Curves for Twelve Slurry Consolidation Tests

for example, the points for samples C15TO and C27MM are essentially coincident for the last three load increments, even though the two materials came from different cities and have quite different initial void ratios. In other cases, such as samples C13TO and C27MM or samples C17TO and D10TO, the entire curves are virtually identical. The compression index, C_c, was computed for each material by taking the slope of a "best fit" straight line through the last two or three points, and these values are included in Figure 4-5. Only two points were used in the case of samples C20TO and C22TO, since applied pressures were limited to 16 psi; in these two cases the values for C_c would probably be lower if additional load increments were applied. The analytical procedure used to interpret the data from sample D3TO differs from that employed for the other dredgings, because the load history for sample D3TO was dictated by maintaining a constant pore pressure difference across the top and bottom of the specimen, whereas all other specimens were loaded incrementally by doubling the previously applied load. In general, however, the C_c values for vitурally all the dredgings tested fall within a fairly narrow range (about 0.94 ± 0.17), even though the samples are quite diversified, as evidenced in Table 4-1.

Perhaps the most striking observations to be made from Figure 4-5 are that (a) most of the test specimens have void ratios of nearly the same magnitude over the last three load increments and (b) the values of the compression index over this loading range are quite close together, even though the initial void ratios varied over a large range. Based on experience with conventional consolidation tests on remolded soils, the compression index, as well as the void ratio at a particular load increment, usually depends on both the material itself and its initial void ratio. In keeping with this experience, these test data suggest that the observed uniformity in consolidation response is related to the relative uniformity in grain size, gradation, and general chemical composition of the different dredgings tested.

Comparisons with a Clay Soil

Although the observed e-log p curves for the slurry consolidation of dredgings do differ somewhat from those which might be expected from conventional consolidation tests on remolded soils, past experience is restricted to soils which possess a lower initial void ratio and sufficient strength and density to retain their shape and volume under a zero applied load condition. In addition, the effects of gas generation tend to cause an abnormal type of behavior. In some cases the curves for the low intensity of loading indicate an increasing void ratio with time; this behavior is attributed to the gas generation characteristics of the particular material, whereby the pressures developed by the generated gases exceed the applied pressures and cause an expansion of the sample. As one particular example of the gas generating characteristics of dredgings, a gas sample taken from D3TO was analyzed and found to contain 3.6 percent oxygen, 15.7 percent carbon dioxide, and 16.8 percent methane, with the remainder composed mostly of nitrogen. The curves become more regular at the higher loadings, thus suggesting a combined effect due in part to the inhibition of gas generation at higher loadings and in part to the decrease in gas generation with time. Some of the curves exhibit a tendency toward a flatter slope at the end of the loading period, thereby indicating the completion of primary consolidation and the beginning of secondary consolidation. Most of the loads were held constant for at least a week, and many loads were held constant for several weeks. The linear portions of the e-log p curves seem to begin at a void ratio of about 2, and this corresponds approximately to the void ratio obtained by gravity drainage in a separate series of tests on the same materials.

A comparison of the e-log p relationships for kaolinite (Sheeran and Krizek, 1971) and several dredging samples is given in Figure 4-6; the kaolinite samples were consolidated by use of the constant-pore-pressure-difference technique, the same procedure used to consolidate dredging sample D3TO. Although the qualitative behavior of all materials is quite similar, the kaolinite achieved a somewhat lower void ratio (or higher dry density) for a given consolidation pressure. This quantitative difference can be easily attributed to the variations in the mineralogical and chemical composition of the materials.

Relationship Between Compression Index and Liquid Limit

Figure 4-7 shows the values for the compression index, C_c, of the slurry-consolidated samples (obtained from Figure 4-5) plotted versus the liquid limit, w_L. Although the data exhibit considerable scatter, a clear trend, similar to that reported by Terzaghi and Peck (1968), is easily recognized and may be described by the empirical equation

$$C_c = 0.02\, w_L - 0.44, \tag{4-1}$$

where w_L is expressed as a percentage. Most observed values for C_c lie within 10 percent of the value predicted by Equation (4-1), but the range of liquid limit values is relatively small (60 to 76 percent). Similar plots of the compression index versus the plastic limit, the plasticity index, and the percent clay (< 2 microns) produced no well-defined trends.

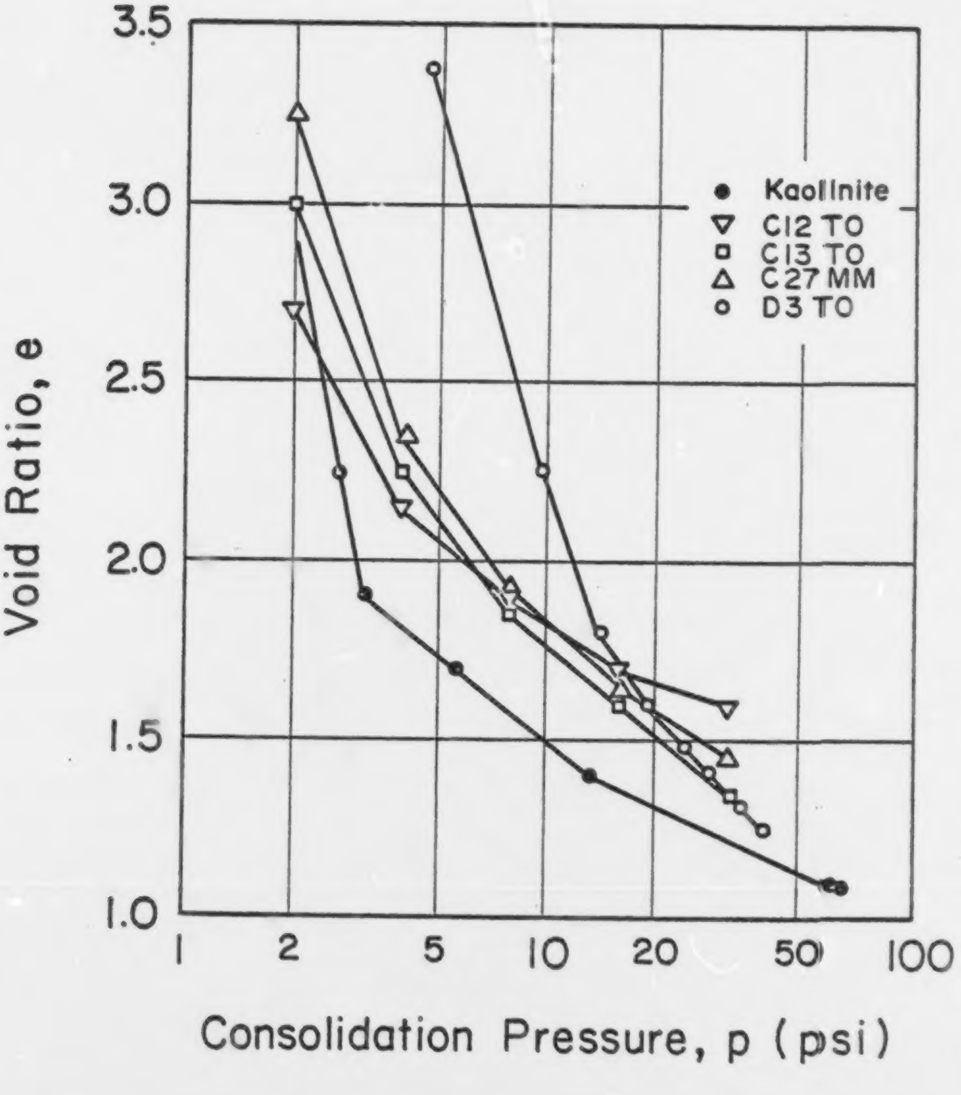

Figure 4-6. Comparison of Several Typical Curves of Void Ratio versus Consolidation Pressure

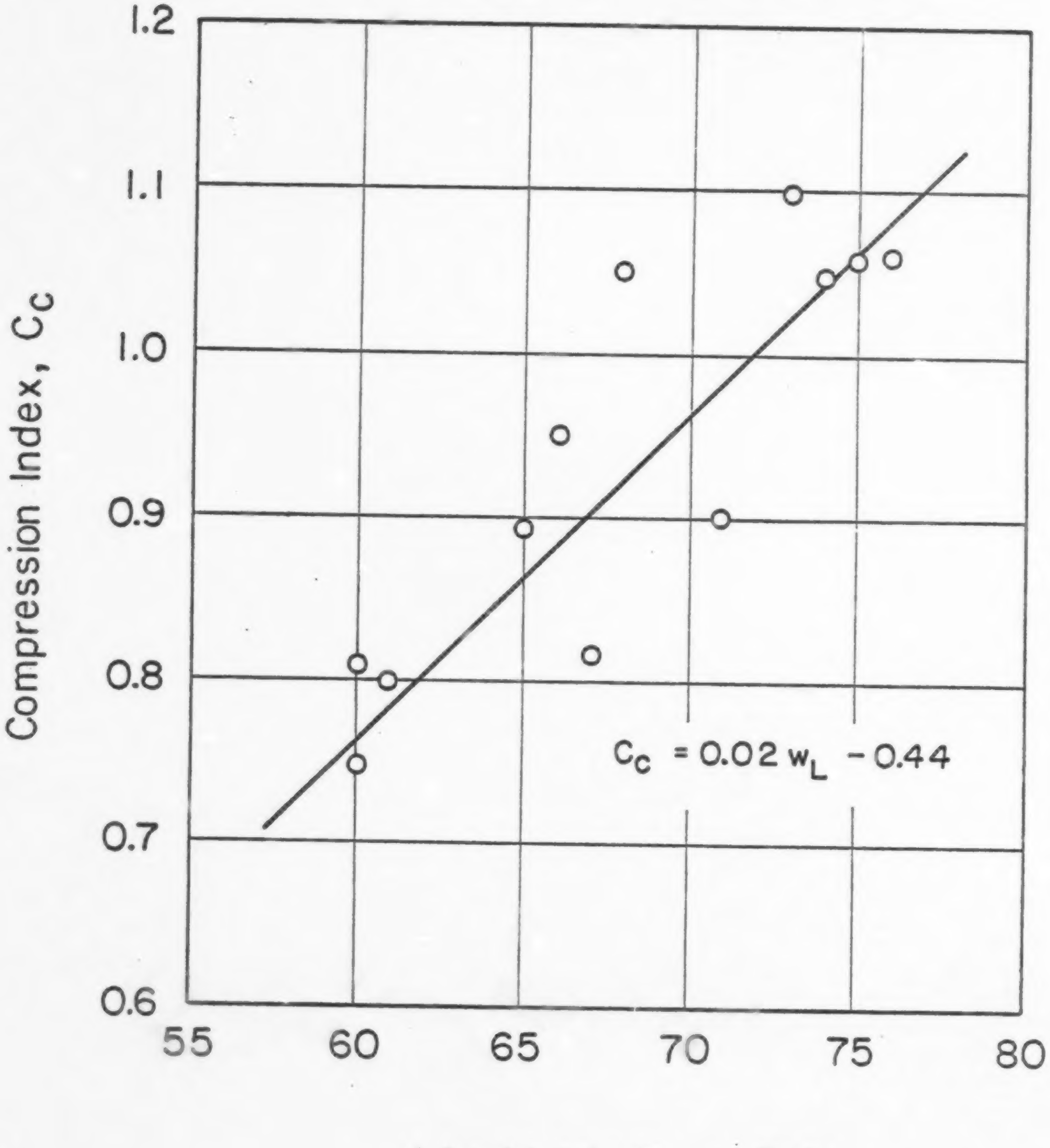

Figure 4-7. Compression Index versus Liquid Limit for Slurry Consolidation

Conventional Consolidation Tests on Consolidated Slurry Samples

In two cases conventional consolidation tests were conducted on specimens trimmed from the consolidated blocks; the reasons for conducting these tests were (a) to investigate the relationship between the compression indices, C_c, obtained from the two tests, (b) to evaluate the applicability of the well-known Cassagrande (1936) method for determining the preconsolidation pressure, p_c, and (c) to study the variation in the coefficient of permeability, k, during the process of reloading specimens with a known stress history. The first two points can be discussed in light of the data presented in Figure 4-8, and the last point will be treated later in this chapter. After samples C10T0 and C17T0 were consolidated in a slurry consolidometer, specimens were trimmed from the blocks and tested in accordance with conventional consolidation test procedures (Lambe, 1951) to a consolidation pressure of 288 psi (1984 kN/m^2). The compression indices obtained from Figure 4-8 are 0.51 and 0.55 for samples C10T0 and C17T0, respectively, and these compare with values of 0.80 and 0.90 obtained from the slurry consolidation tests. The observed reductions in the values of C_c may be attributed to the structural changes which take place during the process of unloading and reloading, but it is probably due to the fact that the virgin compression curves were not adequately defined in the slurry consolidation tests.

Using the graphical construction suggested by A. Cassagrande (1936), the preconsolidation pressures, p_c, for samples C10T0 and C17T0 were found to be 31 psi (214 kN/m^2) and 24 psi (166 kN/m^2), respectively. The deviations between these values and the known value of 32 psi (221 kN/m^2) may be due to (a) sample disturbance during trimming, (b) frictional resistance of the consolidation rings during the test, or (c) inappropriateness

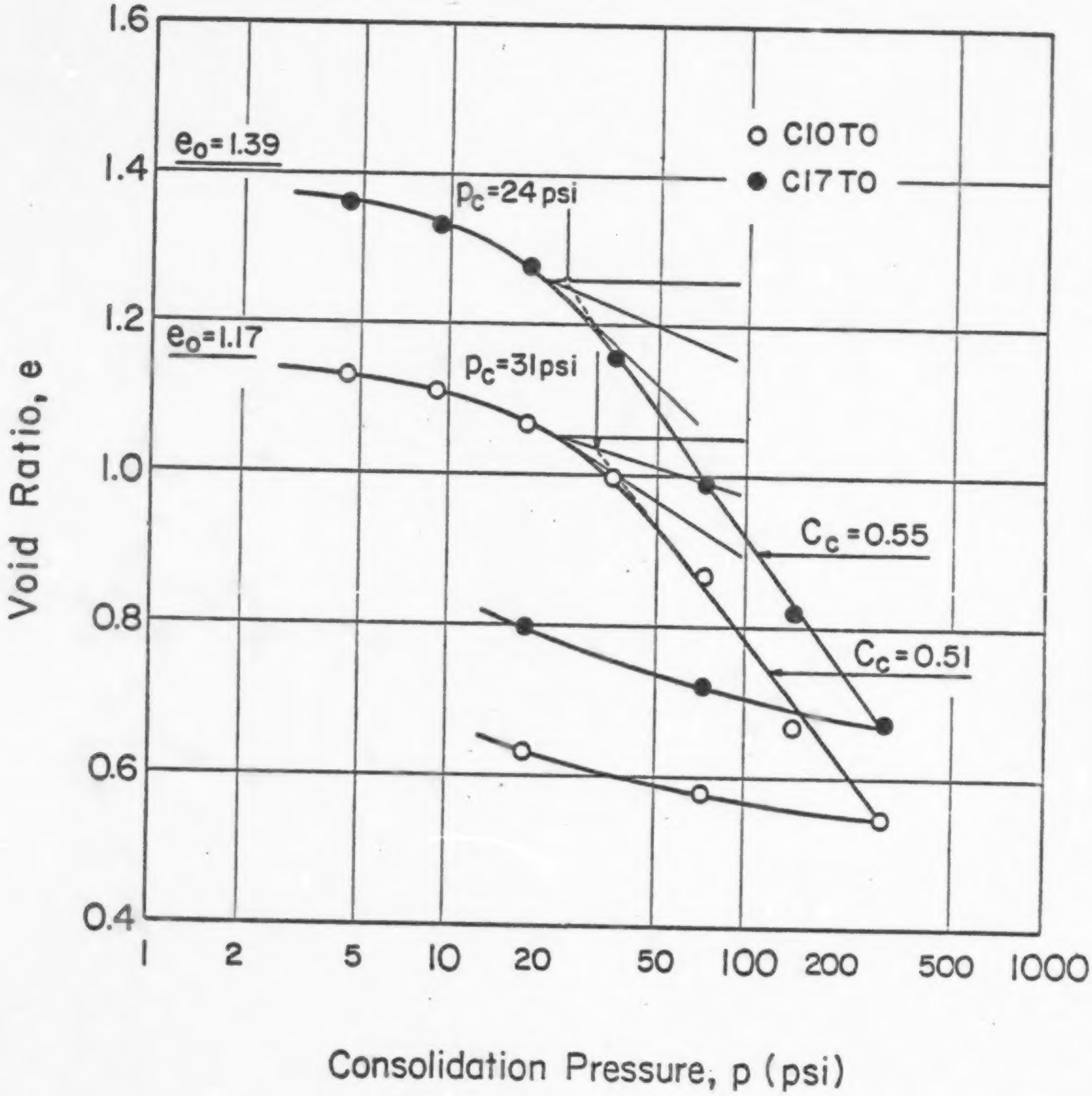

Figure 4-8. Void Ratio versus Consolidation Pressure Curves for Two Conventional Consolidation Tests

of the method. The greater discrepancy in the case of sample C17TO may be attributable to the fact that it had a high initial water content--47 percent as compared to 40.5 percent for sample C10TO.

Coefficient of Consolidation

Since eleven of the twelve slurry consolidation tests were conducted according to a procedure which is essentially the same as that used for conventional consolidation tests (Lambe, 1951; Terzaghi and Peck, 1968), the data may be analyzed in an analogous manner. Accordingly, the coefficient of consolidation, c_v, corresponding to each load increment was calculated from the relation

$$c_v = Th^2/t, \tag{4-2}$$

where t is time, h is the length of the shortest drainage path at the application of each load increment, and T is the time factor, which is a function of the degree of consolidation, U; in this study h equals one-half of the specimen thickness, because drainage took place from both the top and bottom. For the particular case where the degree of consolidation, U, equals 50 percent, the time factor, T, equals 0.197 and the associated value of time is designated as t_{50}; hence, Equation (4-2) can be written as

$$c_v = 0.197Th^2/t_{50}, \tag{4-3}$$

where t_{50} is read from the plots of void ratio, e, versus the logarithm of time, log t. For the eleven samples (excluding sample D3TO) tested the c_v values corresponding to consolidation pressures 4, 8, and 16 psi (27.5, 55, and 110 kN/m^2) vary between a high of 3.52, 3.00 and 2.66 in^2/day (22.7, 19.3, and 17.2 cm^2/day) and a low of 0.486, 0.210, and 0.280 in^2/day

(3.14, 1.35, and 1.80 cm^2/day) with average values of 1.71, 1.67, and 1.24 in^2/day (11.0, 10.8, and 8.0 cm^2/day), respectively. Only nine samples were loaded to a consolidation pressure of 32 psi (221 kN/m^2), and the corresponding value of c_v varied between 2.32 and 0.185 in^2/day (15.0 and 1.2 cm^2/day) with an average of 1.38 in^2/day (8.8 cm^2/day). The variation of the average coefficient of consolidation, $\bar{c}_v$, with consolidation pressure, p, is given in Figure 4-9 and may be described within very broad limits by the empirical equation

$$\bar{c}_v = 2.0 - 0.45 \log_{10} p, \qquad (4\text{-}4)$$

where p must be expressed in psi and $\bar{c}_v$ is determined in units of in^2/day. The observed variations in c_v for a given dredging sample are consistent with previous experience on a variety of clayey soils. A comparison between c_v values obtained from the consolidation of a slurry and from the reconsolidation of specimens trimmed from the slurry-consolidated block is given in Figure 4-10 for two dredging samples; as generally anticipated, the latter values are essentially the same as the ones associated with the higher slurry consolidation pressures.

Coefficient of Volume Compressibility

The coefficient of volume compressibility, m_v, represents the uniaxial compressive strain due to a unit increase of pressure in the axial direction and it may be expressed as

$$m_v = \frac{a_v}{1 + e}, \qquad (4\text{-}5)$$

where e is the initial void ratio corresponding to any applied pressure, p, and a_v is defined as

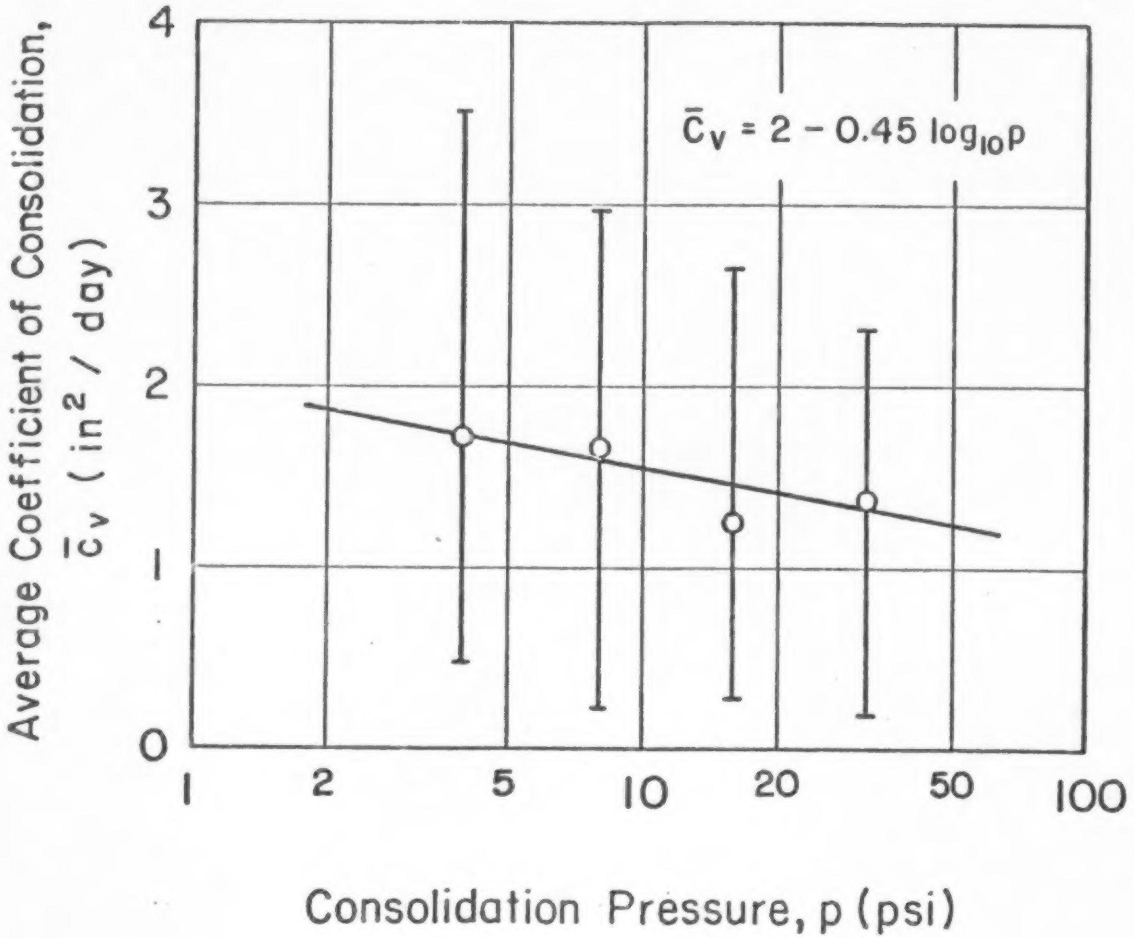

Figure 4-9. Average Coefficient of Consolidation versus Consolidation Pressure for Slurry Consolidation

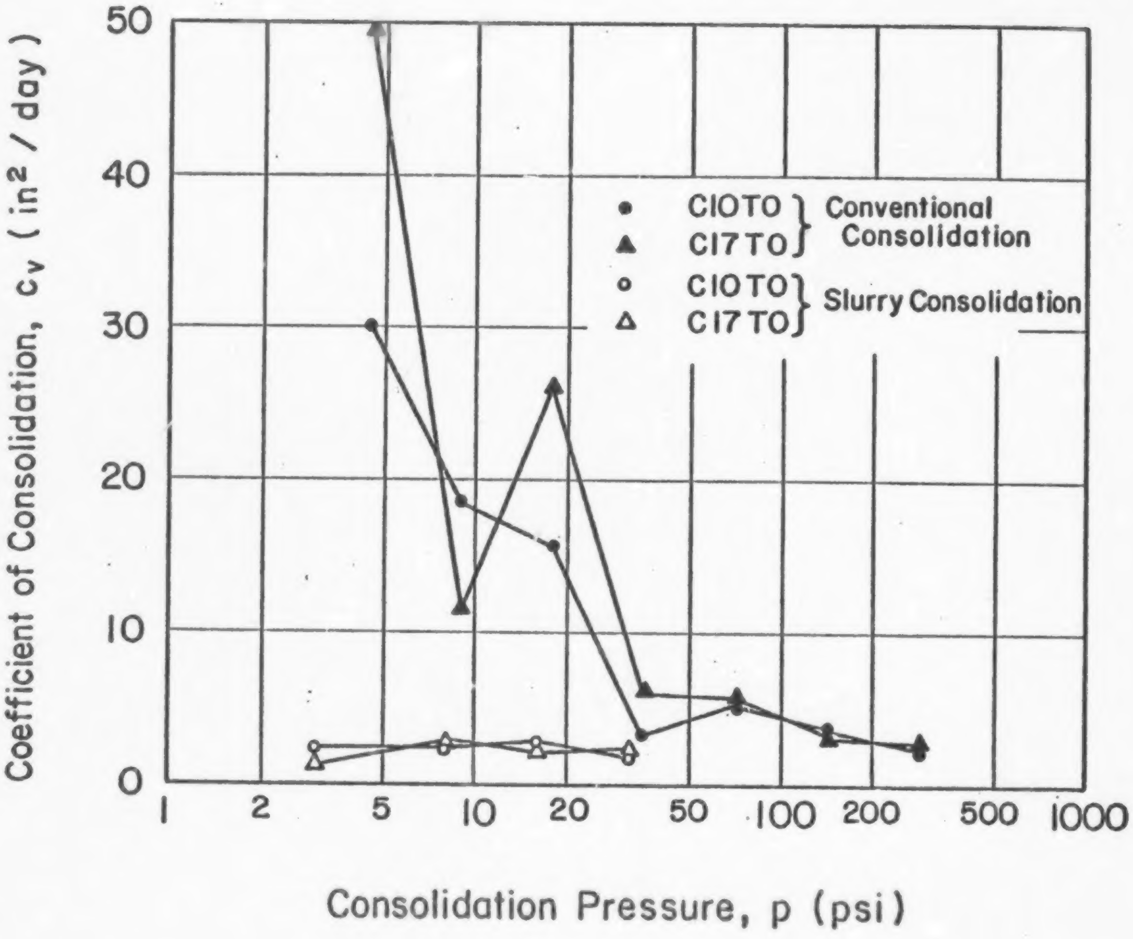

Figure 4-10. Coefficient of Consolidation versus Consolidation Pressure for Slurry and Conventional Consolidation Tests

$$a_v = \frac{\Delta e}{\Delta p} , \qquad (4\text{-}6)$$

where Δe equals the change in void ratio due to an increment of pressure, Δp. The coefficient of volume compressibility, m_v, has been calculated by use of Equation (4-5) for all eleven samples at each increment of loading, and the average values and ranges are shown in Figure 4-11. The average values, $\overline{m}_v$, can be reasonably well described by the equation

$$\overline{m}_v = 0.125 - 0.08 \log_{10} p, \qquad (4\text{-}7)$$

where p must be expressed in psi and m_v has the dimensions of $in^2/lb.$, but the range of variation is considerable (on the order of 100 percent in some cases).

Coefficient of Permeability

The coefficient of permeability, k, has been evaluated at consolidation pressures of 4, 8, 16, and 32 psi (27.5, 55, 110, and 221 kN/m^2) by use of the relationship

$$k = c_v m_v \gamma_w , \qquad (4\text{-}8)$$

where γ_w is the unit weight of water, and the average values and ranges are shown in Figure 4-12. The average values, $\overline{k}$, for the coefficient of permeability can be reasonably well described by the empirical expression

$$\overline{k} = \log_{10}^{-1} [-5.90 - 1.4 \log_{10} p], \qquad (4\text{-}9)$$

where p must be expressed in psi and $\overline{k}$ has the dimensions of cm/sec. All of the values of k for consolidation pressures of 16 or 32 psi (110 or 221 kN/m^2) were found to be less than 4×10^{-8} cm/sec; these values

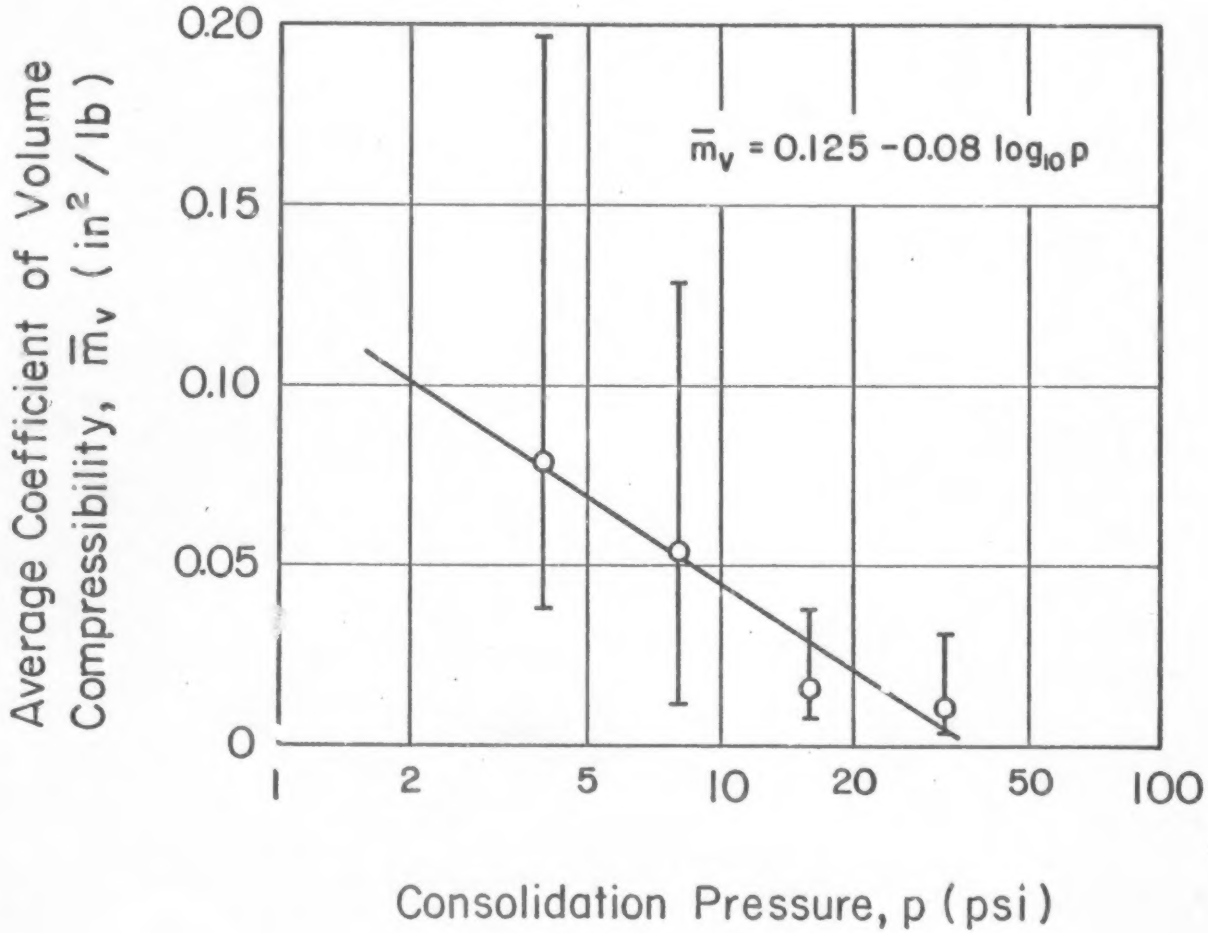

Figure 4-11. Average Coefficient of Volume Compressibility versus Consolidation Pressure for Slurry Consolidation

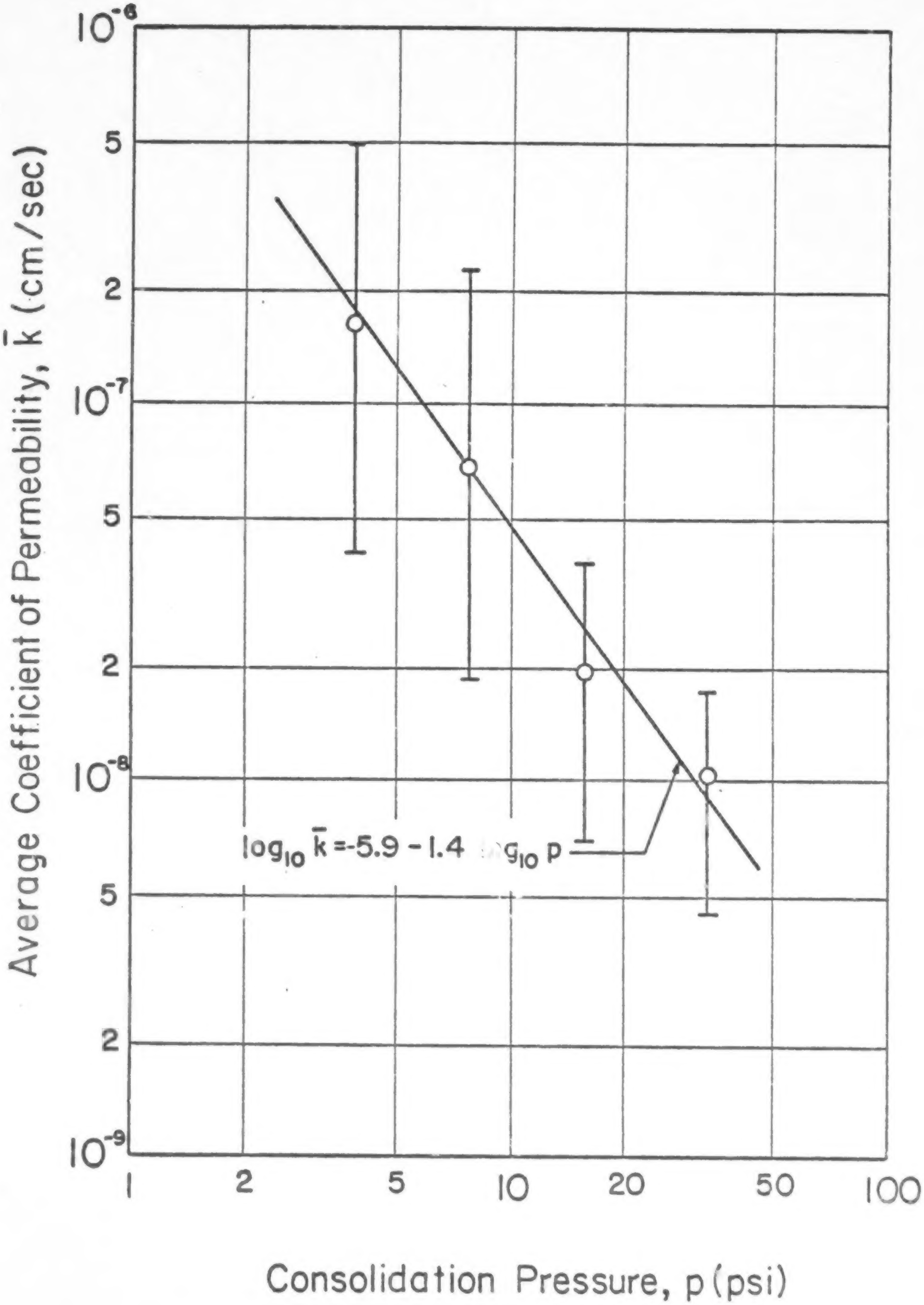

Figure 4-12. Average Coefficient of Permeability versus Consolidation Pressure for Slurry Consolidation

compare very well with values between 1.9×10^{-8} and 7.6×10^{-8} cm/sec obtained from direct permeability tests at comparable values of void ratio. Another relationship of engineering interest is given in Figure 4-13, where the average coefficient of permeability, $\bar{k}$, for all samples is plotted versus the average void ratio, $\bar{e}$, for each load increment; the resulting equation describing this relationship can be written as

$$\bar{k} = \log_{10}^{-1} [1.35\,\bar{e} - 10], \qquad (4\text{-}10)$$

where $\bar{k}$ is expressed in cm/sec. Figure 4-14 shows a comparison between the permeability values determined from slurry consolidation tests and conventional consolidation tests on the slurry-consolidated blocks for two dredging samples (C10T0 and C17T0). The particular e-log k relationships for two slurry-consolidated samples are shown in Figure 4-14 together with similar relationships deduced from conventional consolidation tests on specimens trimmed from the consolidated blocks. The higher rates of change of log k with respect to e in the conventional consolidation tests may be due to the fact that a given change in void ratio causes a greater relative change in the void ratio and consequently the permeability; however, this explanation does not seem to account for the entire phenomenon.

Shear Strength

The shear strengths, s, of the consolidated blocks were determined by either the laboratory vane or the unconfined compression test, and the results are plotted in Figure 4-15 as a function of the water content at the end of slurry consolidation. The strength tests were conducted immediately after the slurry consolidation test was completed and before any appreciable changes in water content occurred. In general, the

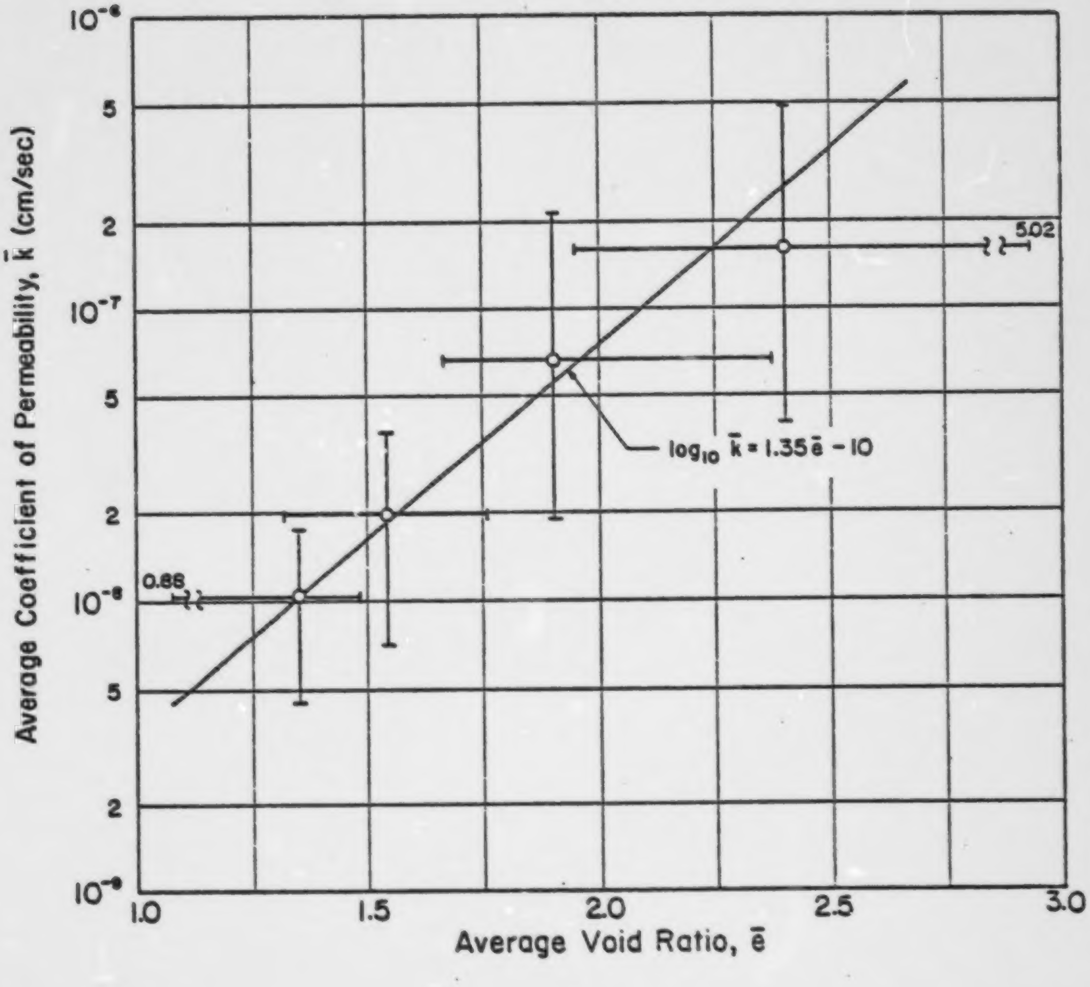

Figure 4-13. Average Coefficient of Permeability versus Average Void Ratio for Slurry Consolidation

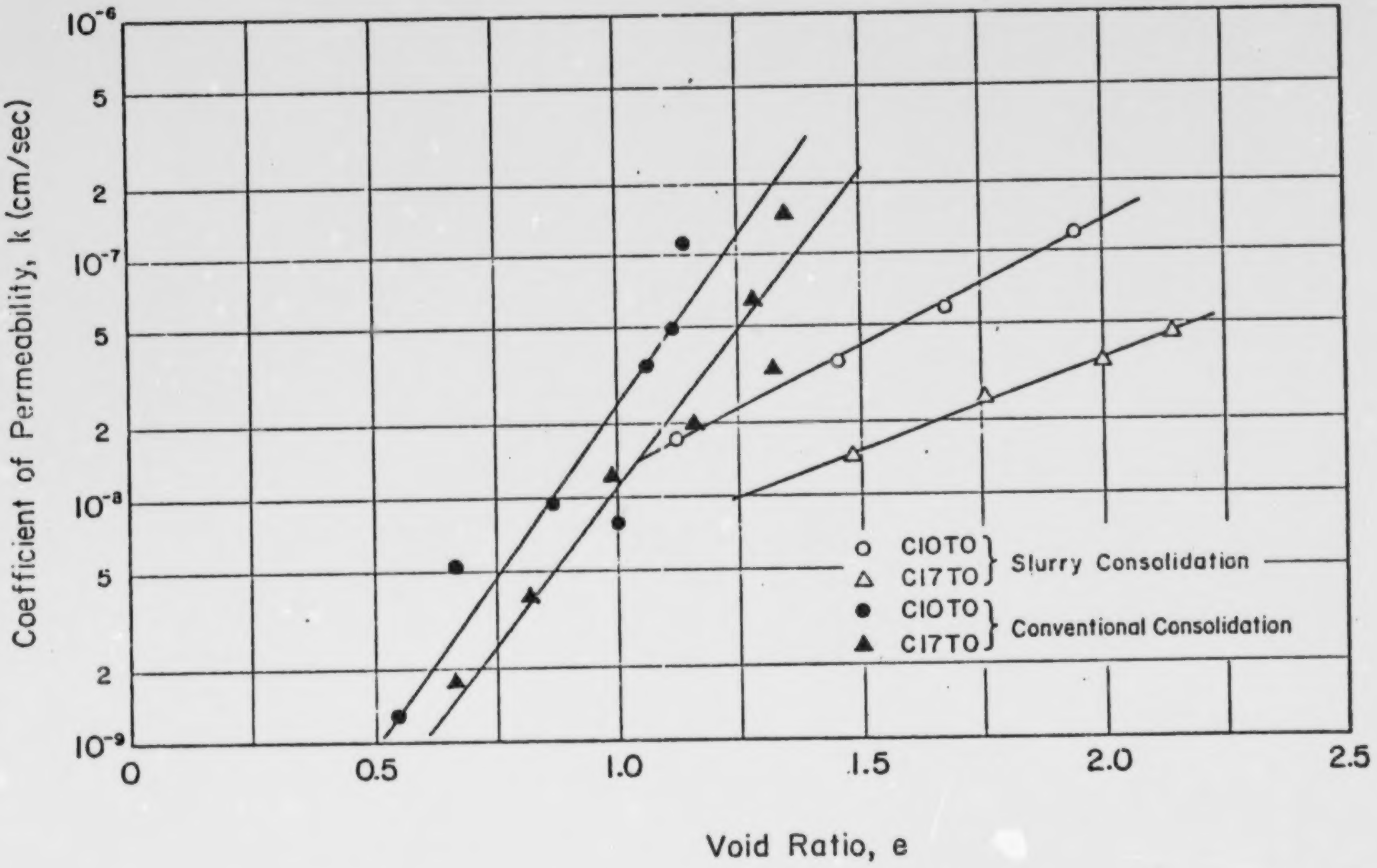

Figure 4-14. Coefficient of Permeability versus Void Ratio for Slurry and Conventional Consolidation Tests

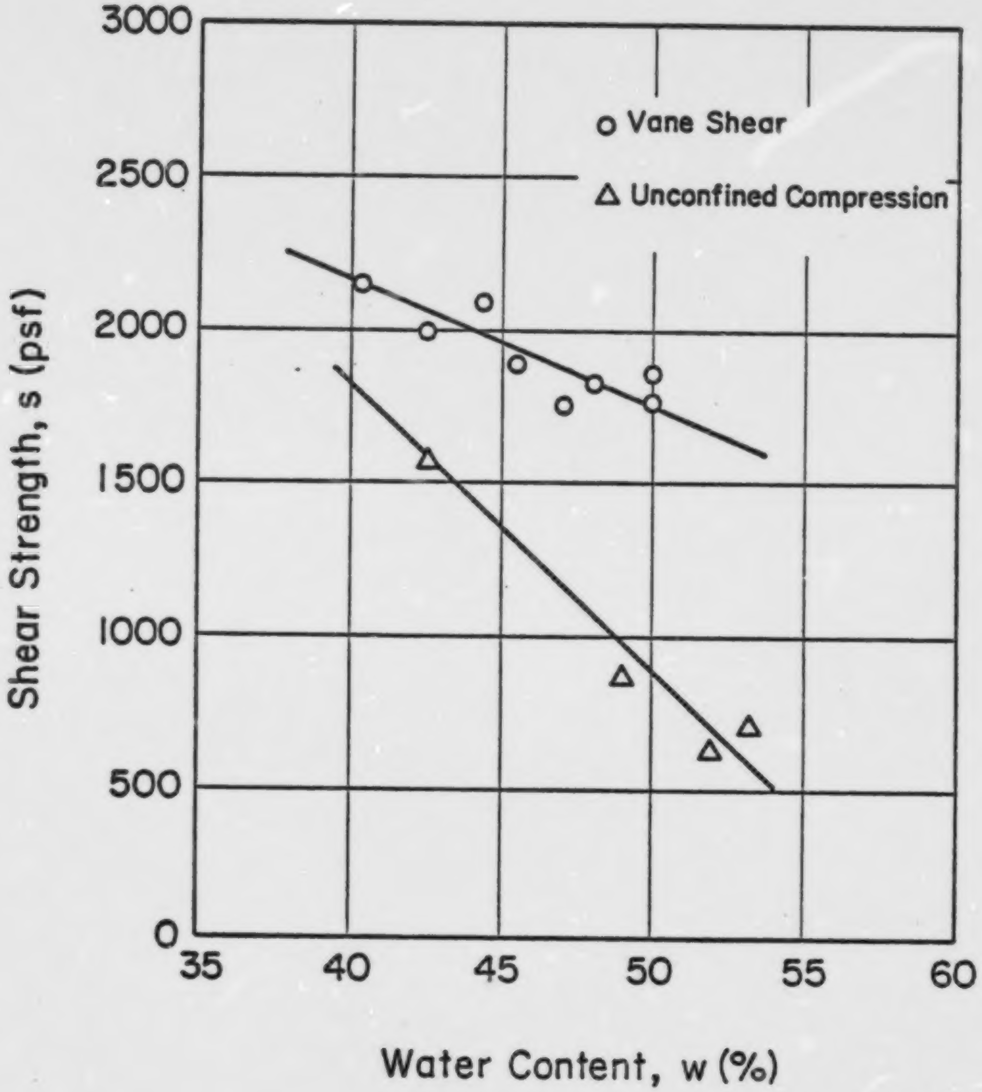

Figure 4-15. Shear Strength versus Water Content

strength values obtained from the vane test are higher than those obtained from the unconfined compression test; and the difference seems to increase as water content increases. This may be attributable to sample disturbance, which is a consequence of trimming and preparing unconfined compression test specimens from the consolidated blocks; such an effect would tend to increase as the water content of the block increases, and this is consistent with the experimental data.

SIGNIFICANCE OF RESULTS

From a practical point of view the primary significance of the foregoing data on the consolidation characteristics of dredging slurries lies in the help and guidance they will offer the engineer who is concerned with the long range behavior of landfill sites composed of these materials. For example, we may see from Figure 4-5 that a typical dredging slurry subjected to a vertical stress of 10 psi (69 kN/m^2) would consolidate to a void ratio of about 1.5. If the particular material had a liquid limit of 70% and if an additional vertical stress of 10 psi (69 kN/m^2) were applied to a 10-foot (3-meter) layer, the compression index could be obtained from Figure 4-7 as 0.96 and the expected settlement, S, would be

$$S = H \frac{C_c}{1 + e_o} \log \frac{p_o + \Delta p}{p} = 10 \frac{0.96}{1.0 + 1.5} \log \frac{10 + 10}{10} \cong 1 \text{ feet (0.3 meters)}.$$

On the basis of a typical coefficient of consolidation of 1.25 in^2/day (8 cm^2/day) obtained from Figure 4-9, 50 percent of this ultimate settlement (0.5 feet or 0.15 meters) would occur in a time, t_{50}, of about

$$t_{50} = \frac{Th^2}{c_v} = \frac{0.197(10 \times 12)^2}{1.25} = 2270 \text{ days} \cong 6\tfrac{1}{4} \text{ years}.$$

The average permeability of the dredgings at a void ratio of 1.5 would be on the order of 10^{-8} cm/sec, as determined from Figure 4-13, and the vane shear strength of the final consolidated material can be found from Figure 4-15 to be about 1800 psf (86 kN/m^2). Although dependent on other factors, the above shear strength is consistent with a bearing capacity on the order of 10,000 psf (480 kN/m^2), but the settlements under such a load would be very large. The foregoing calculations are illustrative of those which may aid the engineer or administrator in his decision regarding the potential usefulness of a dredging disposal site.

CONCLUSIONS

Based on the experimental program reported herein for slurry consolidation tests and several related tests on a variety of dredgings, the following conclusions can be advanced:

1. The slurry consolidation equipment is very useful for studying the consolidation characteristics of materials which are too soft and/or too fluid to test in the conventional manner.

2. Several very convenient empirical equations have been developed to relate the consolidation characteristics (compression index, coefficient of consolidation, coefficient of volume compressibility, and coefficient of permeability) of various dredgings to their void ratio and consolidation pressure, but these relations should be used with caution because the range of variation is often quite large for a given property.

3. Slurry consolidation tests are likely to provide more reliable values for engineering properties than those obtained from conventional consolidation tests, because larger volumes of material are tested and the samples are not subjected to sample disturbance during sampling, trimming, and testing.

CHAPTER 5

PRIMARY CONSOLIDATION AND COMPRESSIBILITY

The consolidation of saturated clays and certain other materials has traditionally been divided into primary and secondary; in a very broad sense primary consolidation is that settlement which is characterized by the classical theory of consolidation (Terzaghi, 1923), and secondary consolidation consists of all time-dependent settlement that is not described by this theory (in particular, the long-term rate of settlement usually does not decrease as rapidly as predicted by the primary consolidation theory). The factors that govern the nature and relationship between these two rather arbitrary classifications are the magnitude and history of the applied stress, thickness of the layer, compressibility, type of drainage, and permeability. Included in this chapter are the results of an extensive experimental program to investigate the primary consolidation and compressibility characteristics of dredging samples taken from various disposal sites; linear regression analyses are employed to establish useful, simple, and convenient relationships between the consolidation and compressibility parameters and various index properties of the dredgings. The long-term secondary consolidation characteristics of a limited number of samples are treated in Chapter 6.

MATERIALS TESTED

Sixty-four "undisturbed" samples of dredgings from three different landfills were tested; sixteen of these samples were obtained from Riverside Site during the summer of 1972, and the other forty-eight samples were taken during the summers of 1973 and 1974 from Riverside Site, the

Island Site, and Penn 8 Site. A three-inch diameter, light-weight, manually operated piston sampler (Hummel and Krizek, 1974) was used to obtain all samples from boreholes located along the line between the discharge pipe and the overflow weir of each site. Prior to testing, the samples were stored in a humid room while they were still inside their sampling tubes with both ends capped, wrapped with tape, and waxed. Table 3-1 summarizes the location, depth, and index properties of all samples.

EXPERIMENTAL PROCEDURE

Conventional consolidation tests (Lambe, 1951) were conducted on 3-inch (7.6-cm) diameter tube samples that were extruded and trimmed to fit 2.5-inch (6.65-cm) diameter, teflon-lined, brass consolidometer rings with a cross-sectional area 31.6 cm^2 and a height of 1.0 inch (2.5-cm). The test specimens were trimmed about 0.15 cm shorter than the height of the ring to ascertain that the loading cap fit properly into the ring, and filter paper was placed on each side of the specimen to prevent the loss of fines near the drainage faces. All specimens were submerged and loaded with a load-increment ratio, $\Delta p/p$, of unity under conditions of double drainage. For the first sixteen specimens the initial load was 31 kN/m^2 and the maximum load was 248 kN/m^2; eight specimens were rebounded incrementally to the initial load, at which point the test was terminated, while the load of 248 kN/m^2 was maintained constant for over 7 months on six samples and for 10 months on two samples to investigate their secondary compression characteristics, which are reported in Chapter 6. The load for the rest of the specimens started with 31 kN/m^2 and ended with 496 kN/m^2, after which all specimens were rebounded incrementally to 31 kN/m^2.

ANALYSIS OF RESULTS

In order to establish approximate, but practical, relationships between the consolidation and compressibility characteristics of these dredged materials and certain index properties, regression analyses with associated confidence limits (Crow, Davis, and Maxfield, 1960; Draper and Smith, 1966) were employed. Among the various multiple linear regression methods of analysis, the step-wise procedure seems to offer the most practical compromise between completeness and tractability; therefore, it was used in the analyses presented herein.

Void Ratio versus Consolidation Pressure

Each load increment was sustained for about 24 hours, and the deformation-time response was monitored continuously to ascertain the existence of sufficient data to back-calculate the time for completion of primary consolidation, t_{100}. A typical series of deformation-time response curves is illustrated in Figure 5-1. The selection of one particular point (usually the 24-hour reading) from each deformation-time curve for a given applied consolidation pressure, p, allows a deformation-load curve to be plotted. The total settlement, ΔH, in a stratum of thickness, H, due to an external applied pressure, Δp, is usually determined from the relationship

$$\Delta H = H \frac{C_c}{1 + e_o} \log \frac{p_o + \Delta p}{p_c}, \qquad (5\text{-}1)$$

where C_c is the compression index, e_o is the initial void ratio, and p_c is the preconsolidation pressure (Cassagrande, 1936). The preconsolidation pressures for all specimens tested in this experimental program varied between 20 and 90 kN/m^2; in most cases these values are higher than the estimated overburden pressures, and these deviations can be explained

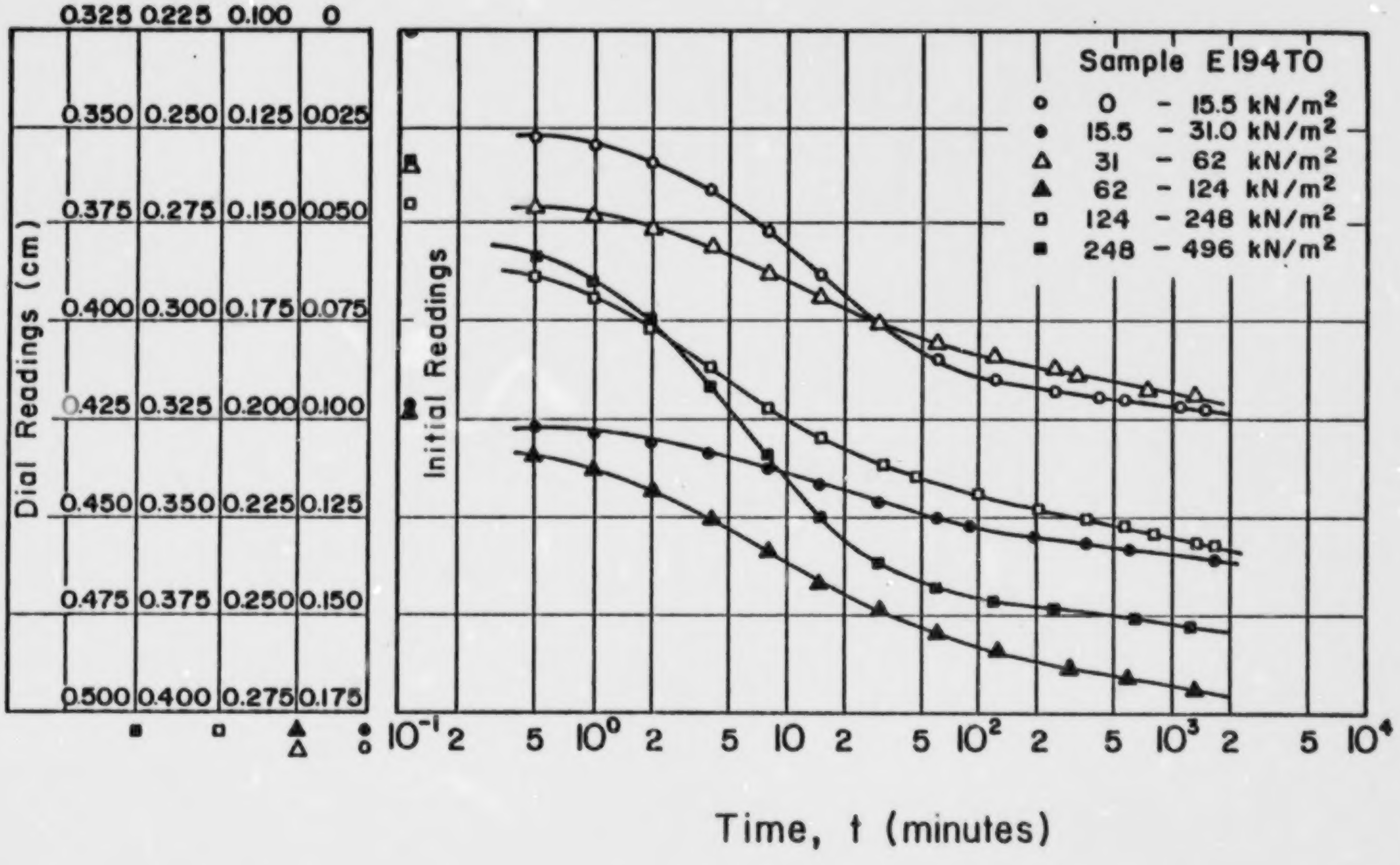

Figure 5-1. Typical Deformation-Time Response Curves

in whole or in part by (a) disturbances associated with sampling and testing and (b) desiccation that occurs during seasonal dredging cycles. The so-called virgin compression curve began at pressures between 30 kN/m^2 and 130 kN/m^2 for all specimens, and it retained its character for all pressures within the scope of this program.

Compression Index

Various empirical correlations have been advanced to enable C_c for specific classes of soils to be estimated from a knowledge of one or more soil index properties. For example, Terzaghi and Peck (1948) suggested that

$$C_c = 0.009\ (w_L - 10), \qquad (5\text{-}2)$$

where w_L is the liquid limit expressed as a percentage. Van Zelst (1948) found a straight line relationship between the initial void ratio and compression index of a lacustrine clay. Regression analyses by Cozzolino (1961) indicated that the compression indices of two Brazilian clays were related to their liquid limits and natural void ratios by means of the following empirical relations:

$$C_c = 0.0046\ (w_L - 9) \pm 0.086 \qquad (5\text{-}3a)$$

$$C_c = 0.256 + 0.43\ (e - 0.84) \pm 0.063 \qquad (5\text{-}3b)$$

for Motley clays from Sao Paulo City and

$$C_c = 0.0186\ (w_L - 30) \pm 0.41 \qquad (5\text{-}4a)$$

$$C_c = 1.21 + 1.055\ (e - 1.87) \pm 0.34 \qquad (5\text{-}4b)$$

for soft silty clays from the lowlands of Santos. The compression indices for these dredging samples varied between about 0.3 and 0.7, which lies in the lower portion of the 0.4 to 1.4 range reported by the Corps of Engineers (1969).

When C_c is plotted in Figures 5-2a and 5-2b versus the natural water content, w_n, and the liquid limit, w_L, respectively, the observed trend in both cases justifies the use of a first order linear model, and the associated equations are

$$C_c = 0.01\ (w_n - 7) \pm 0.04 \tag{5-5}$$

and

$$C_c = 0.008\ (w_L - 5) \pm 0.06, \tag{5-6}$$

where w_n and w_L are expressed as percentages; for the work reported herein, the respective ranges of validity of Equations (5-5) and (5-6) are approximately $40 < w_n < 80$ and $45 < w_L < 90$. As explained by Benjamin and Cornell (1970), the dimensionless correlation coefficient measures the goodness of fit and equals unity for perfect correlation; the plots shown in Figures 5-2a and 5-2b represent correlation coefficients of 0.89 and 0.80 for Equations (5-5) and (5-6), respectively. The dashed curves in each figure are the loci of the 90% confidence limits for the true mean value of C_c for any given value of w_n or w_L (Crow, Davis, and Maxfield, 1960); as an example, for w_n equal to 60%, one can say with 90% confidence that the corresponding true mean value of C_c, lies between 0.52 and 0.54. It is clear that the best predictions can be made in the middle of the observed range of the independent variable. The simultaneous effect of both w_n and w_L on C_c may be expressed as

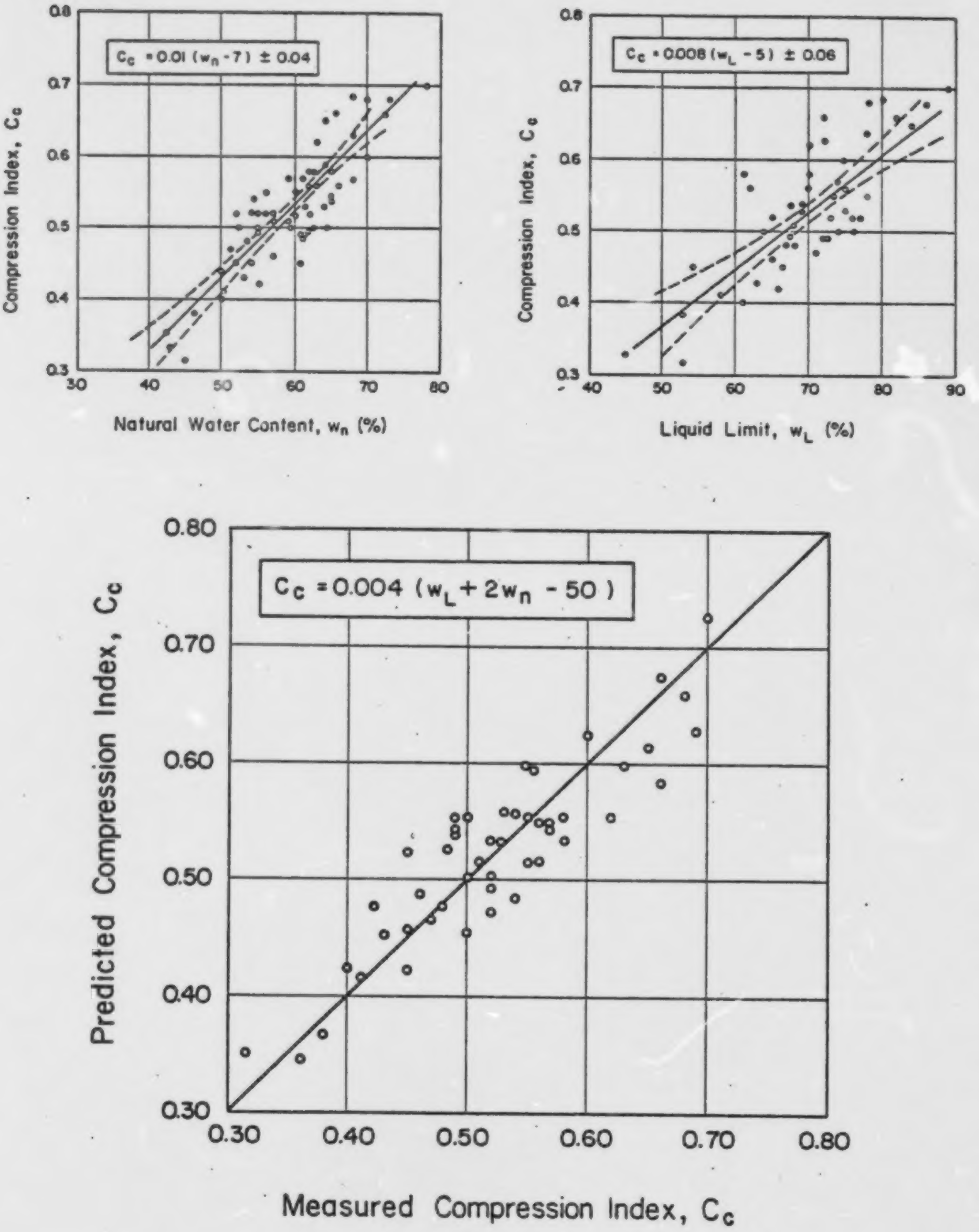

Figure 5-2. Variation of Compression Index with Natural Water Content and Liquid Limit

$$C_c = 0.04(w_L + 2\ w_n - 50) \qquad (5\text{-}7)$$

for which the computed multiple correlation coefficient is 0.88. Figure 5-2c shows the comparison between measured values of C_c and those predicted by use of Equation (5-7).

Constrained Modulus

The constrained modulus provides an alternate procedure for characterizing the compressibility of soils (Schultze and Kotzias, 1961; Janbu, 1963; Stamatopoulos and Kotzias, 1973; Salazar, 1973), and many reasons are given to suggest its preferred use; of these, the fact that the constrained modulus is more-or-less analogous to our conventional concept of modulus is perhaps the strongest argument in its favor. Based on a statistical analysis of many soils, Schultze and Kotzias (1961) found that the constrained modulus, M, could be related to the axial stress (vertical stress), p, by

$$M = B\ p^A \qquad (5\text{-}8)$$

where A and B are empirical coefficients that depend on soil type; in general, A was found to equal unity for normally consolidated clays, and B was determined to be quite dependent on the porosity, the natural water content, and the grain size (particularly for the clay-size fraction). A few years later, Janbu (1963) proposed the relationship

$$M = m\ p_a \left[\frac{p}{p_a}\right]^{1-a}, \qquad (5\text{-}9)$$

in which both the modulus number, m, and the exponent, a, are primarily functions of porosity, and p_a designates atmospheric pressure, which is introduced to normalize the axial stress, p. The coefficients m and a of

Equation (5-9) can be found by use of any two points on a given stress-strain curve. Janbu (1963) calculated the values of m and a for materials ranging from sound "elastic" rock to normally consolidated clays, and he found that a varied between one and zero, respectively, whereas m ranged from 10^5 to 10^6 for sound rock to as low as 2 to 30 for clays. Krizek, Parmelee, Kay, and Elnaggar (1971) studied the results presented by Osterberg (1952) and suggested that the constrained modulus of compacted soil may be a unique function of the dry density and the overburden pressure. Regression analyses by Salazar (1973) indicated that a modified Janbu expression yielded the highest multiple correlation coefficient for the constrained tangent modulus of compacted soils.

In order to develop compressibility relationships in terms of constrained modulus, the e-log p data were replotted in terms of axial stress, p, versus axial strain, ϵ_a. The axial strain corresponding to a particular axial stress, p, was determined by taking the ratio of the change in specimen height, ΔH, associated with a stress increment, Δp, and the initial specimen height, H, at the time of application of this load increment. Most of these plots could be reasonably well described by a parabola with its axis parallel to that of the axial stress. The constrained tangent modulus, defined as $M = \frac{dp}{d\epsilon_a}$, was evaluated at various arbitrary stress levels and some typical results are plotted in Figure 5-3, from which it is clear that M varies with p in a simple linear manner with a constant of proportionality, m, known as the modulus number; in a mathematical form we may write

$$M = m\,p, \qquad (5\text{-}10)$$

which verifies that the parameter a of Equation (5-9) equals zero, as

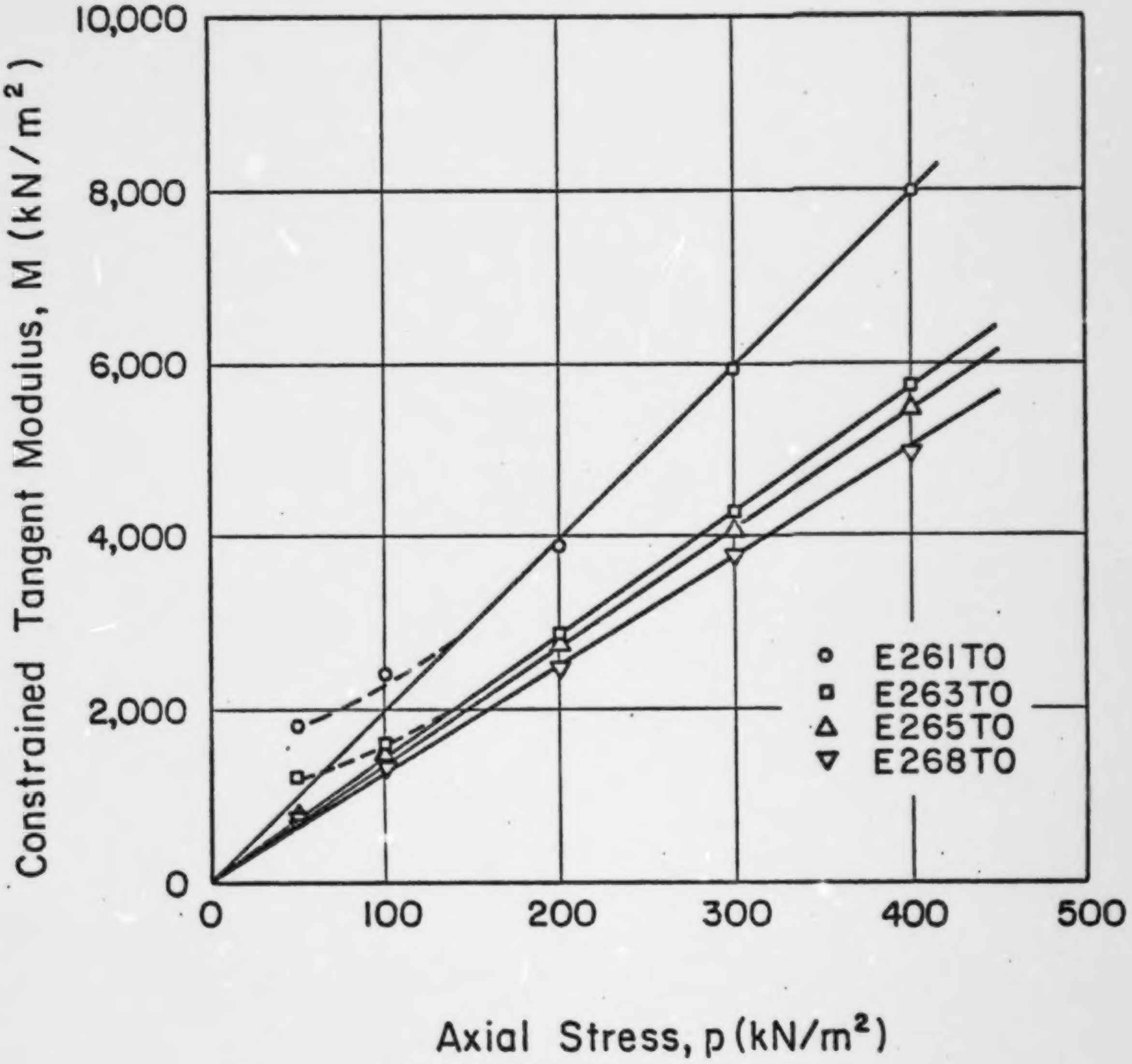

Figure 5-3. Typical Plots of Constrained Tangent Modulus versus Consolidation Stress

suggested by Janbu (1963) for normally consolidated clays. The occasional small deviations from linearity generally occur at very low values of stress; in most cases these samples probably have been slightly preconsolidated by the desiccation associated with the intermittent seasonal drying between dredging seasons.

For all samples tested the modulus number, m, in Equation (5-10) was found to lie between 8 and 20, which is within the range of 2 to 30 reported by Janbu (1963) for clays. In order to establish a quick method for estimating the expected settlement under a certain stress, m was plotted in Figures 4a, 4b, and 4c versus the dry density, γ_d, percent clay, and natural water content, w_n, respectively, and the following equations with correlation coefficients of 0.47, 0.42, and 0.67 were obtained:

$$m = 10 \frac{\gamma_d}{\gamma_w} + 1.27 \tag{5-11}$$

$$m = 17 - 0.12 \ (\% \text{ Clay}) \tag{5-12}$$

$$m = 24 - 0.2 \ w_n . \tag{5-13}$$

A more comprehensive relationship involving all three independent parameters was found to be

$$m = 1.05 \frac{\gamma_d}{\gamma_w} - 0.17 \ w_n - 0.07 \ (\% \text{ Clay}) + 24 \quad , \tag{5-14}$$

where w_n and (% Clay) are expressed as percentages and γ_w is introduced to retain the dimensionless character of the regression equation; the computed correlation coefficient is 0.71, and a comparison of the observed and predicted values of m is given in Figure 4d. Based on a step-wise regression analysis (Draper and Smith, 1966), with the independent parameters

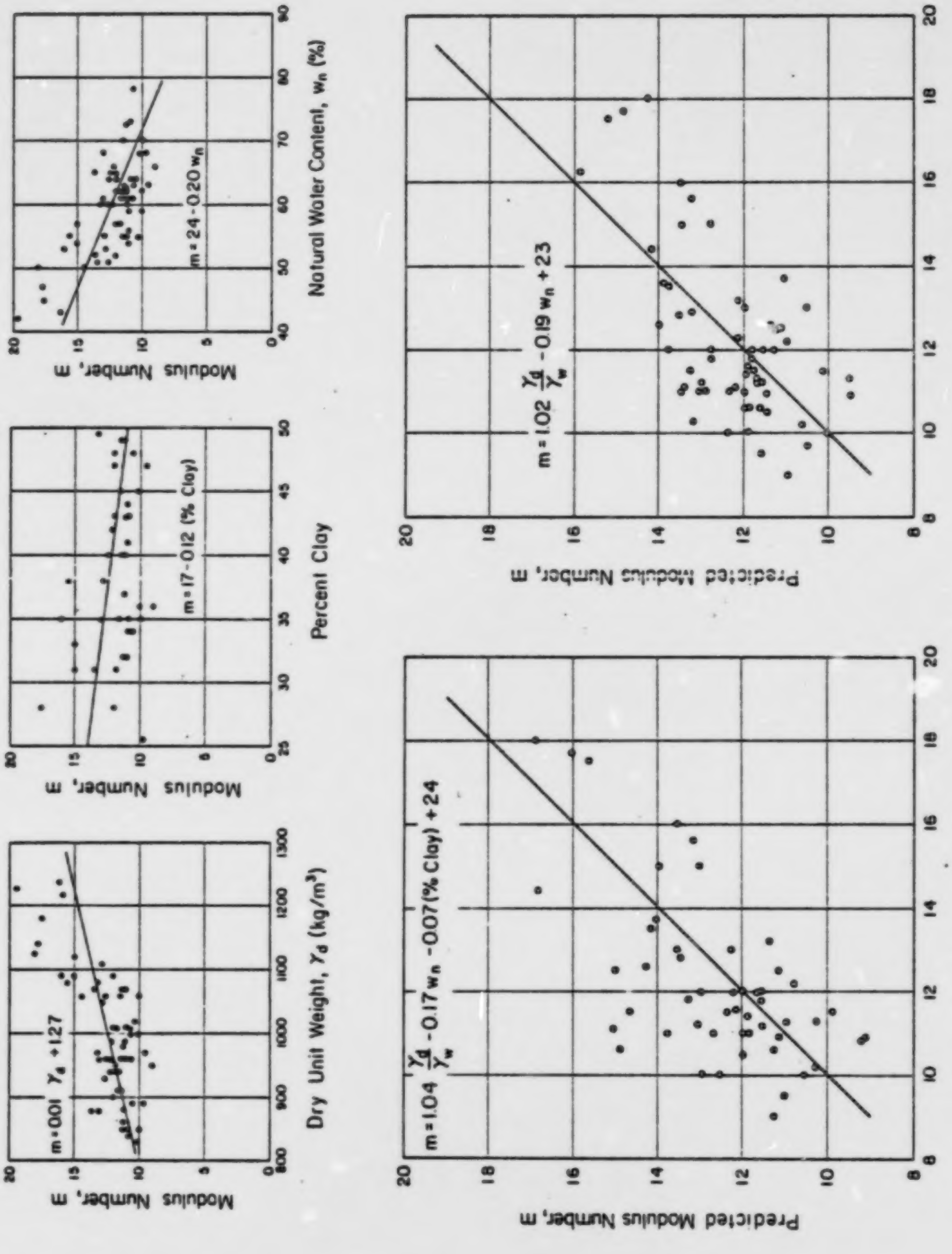

Figure 5-4. Variation of Modulus Number with Different Material Properties

in Equation (5-14) it was found that m correlated most strongly with γ_d and negligibly with (% Clay); this fact, together with the time-consuming nature of the particle size analysis required to determine the clay fraction, suggests the use of the following simplified relationship involving γ_d and w_n:

$$m = 1.02 \frac{\gamma_d}{\gamma_w} - 0.19\, w_n + 23 \qquad (5\text{-}15)$$

As can be seen from Figure 4e and the calculated correlation coefficient of 0.67, the predictive ability of Equation (5-15) is not quite as good as that of Equation (5-14).

Coefficient of Consolidation

The coefficient of consolidation, c_v, corresponding to each load increment can be calculated from

$$c_v = \frac{Th^2}{t}\,, \qquad (5\text{-}16)$$

in which t is time, h is the length of the shortest drainage path (double drainage test) at the time of application of each load increment, and T is the time factor, which is a function of the degree of consolidation, U. The logarithm of time method was used to determine the time, t_{50}, corresponding to a degree of consolidation equal to 50 percent for all consolidation pressures; since the corresponding time factor, T_{50}, equals 0.197, Equation (5-16) can be written as

$$c_v = \frac{0.197\, H^2}{4\, t_{50}}\,. \qquad (5\text{-}17)$$

The ranges of c_v values corresponding to the various consolidation pressures are shown in Figure 5-5 together with the average values and ranges

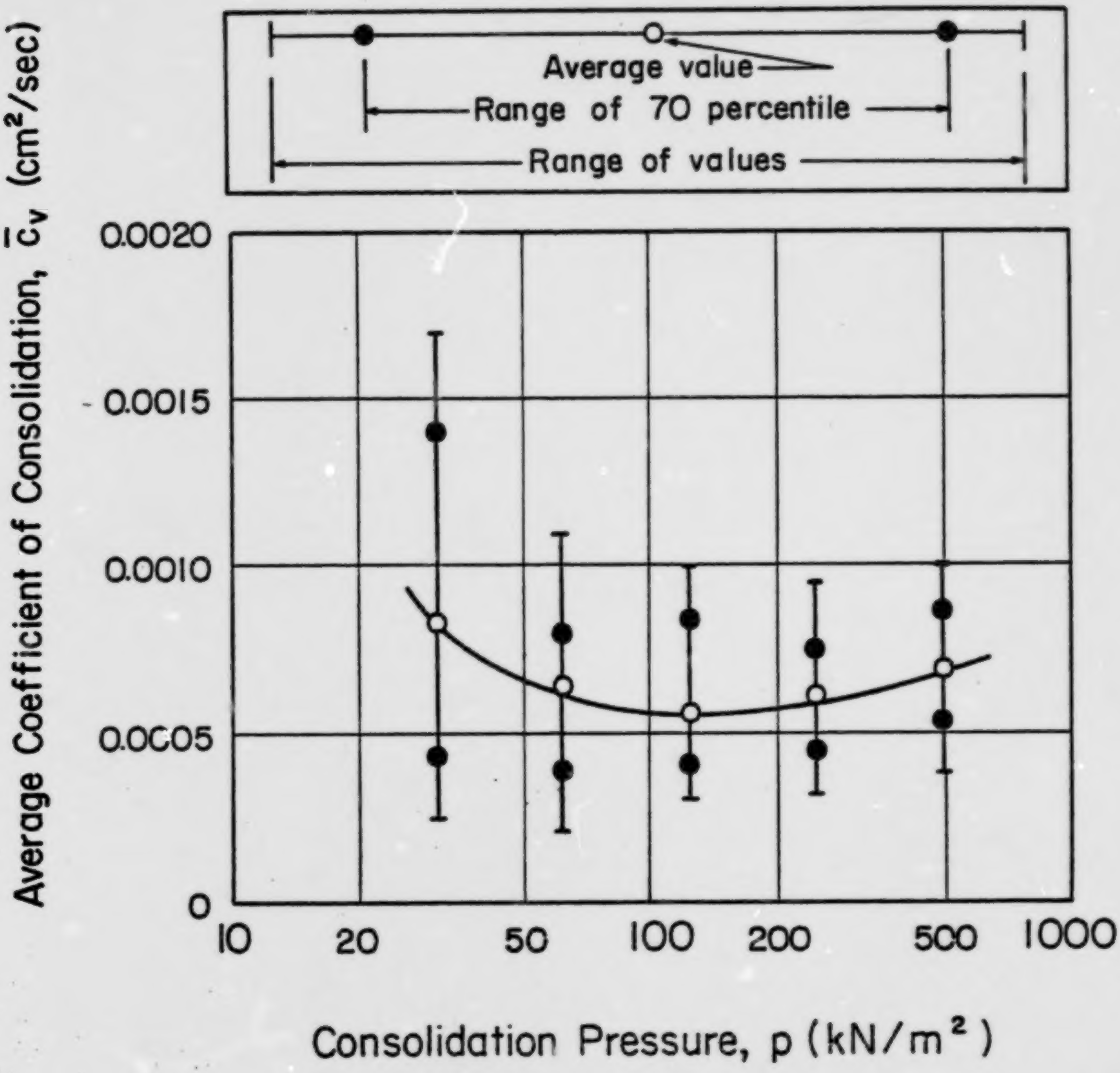

Figure 5-5. Average Coefficient of Consolidation versus Consolidation Pressure for Convention Consolidation

of the 70 percentile (70% of the values lie within this range). Although this relationship exhibits a minimum for c_v at a consolidation pressure of about 125 kN/m^2, a reasonably constant value of about 0.0006 cm^2/sec can be used to characterize the time dependency of the consolidation response of these dredgings (except for the somewhat higher c_v values at the lowest consolidation pressure, 31 kN/m^2). As can be seen, the range of c_v values at a given consolidation pressure decreases somewhat as p increases, but this effect is not particularly large. The manifested variation of $\bar{c}_v$ with p is similar to those reported by Taylor (1948) for Boston blue clay, Chicago clay, Newfoundland silt, and Newfoundland peat. The increase in c_v with consolidation pressure for p values greater than 125 kN/m^2 may be attributed to the high gradients across the sample.

Coefficient of Volume Compressibility

The coefficient of volume compressibility, m_v, represents the increment of axial strain, $\Delta\epsilon_a$, due to a unit increment of axial stress, Δp; in mathematical form m_v (which is essentially the reciprocal of the constrained tangent modulus) may be written as

$$m_v = \frac{\Delta\epsilon_a}{\Delta p} = \frac{a_v}{1 + e} , \qquad (5\text{-}18)$$

in which a_v is the coefficient of compressibility and e is the initial void ratio corresponding to any applied pressure. Figure 5-6 shows the total ranges, ranges of the 70 percentile, and the average values of m_v as a function of the consolidation pressure. It is significant in this case that the ranges for m_v decrease substantially as p increases, although the percent variations from the average values remain essentially the same. Furthermore, the average values of m_v can be represented by

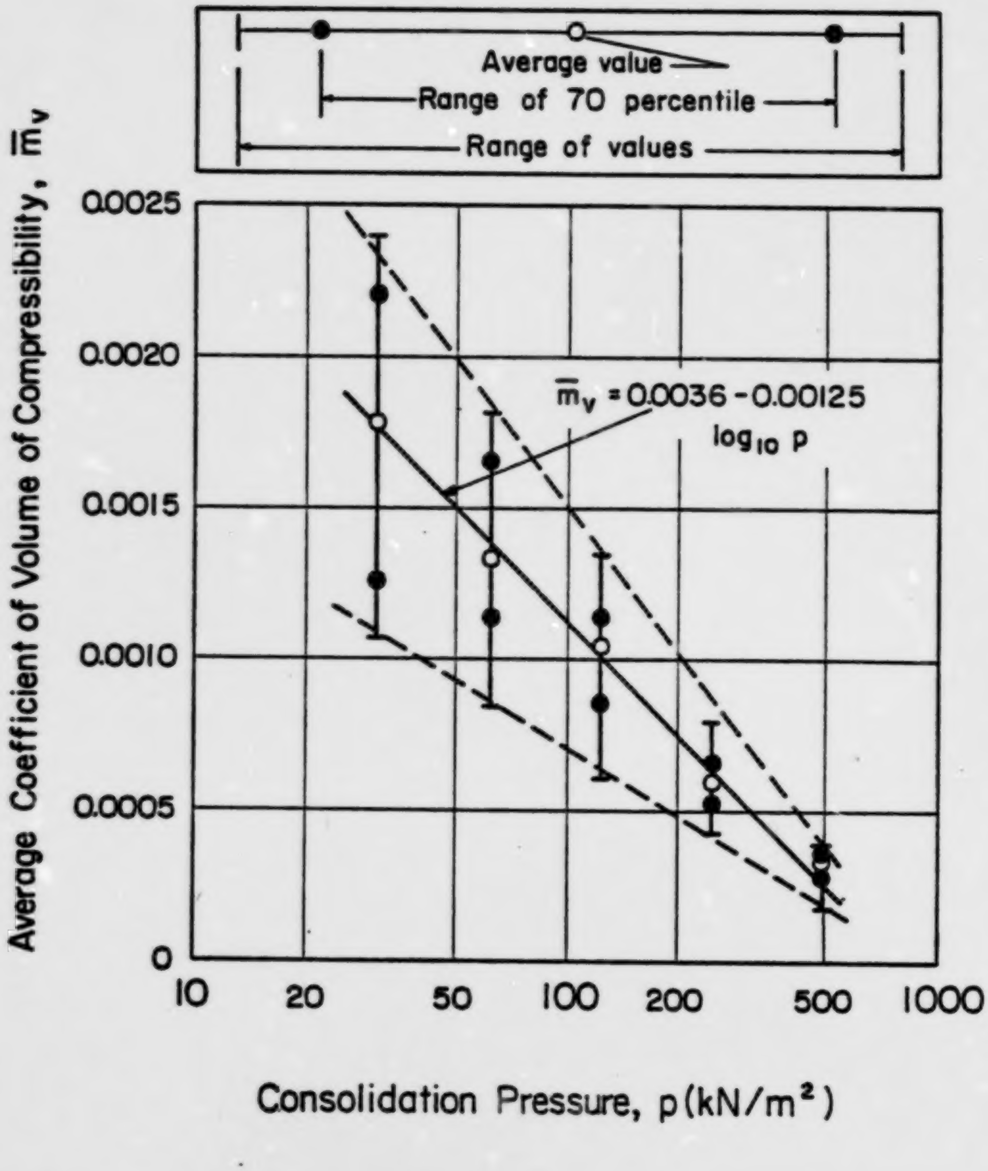

Figure 5-6. Average Coefficient of Volume Compressibility versus Consolidation Pressure for Conventional Consolidation

$$\bar{m}_v = 0.0036 - 0.00125 \log_{10} p, \tag{5-19}$$

where $\bar{m}_v$ and p are expressed in m^2/kN and kN/m^2, respectively.

Coefficient of Permeability

Permeability values determined from consolidation data have been found by Newland and Allely (1960) and others to agree well with measured permeability values. In order to evaluate this correlation for dredged materials, the coefficient of permeability, k, has been evaluated from consolidation test data at each consolidation pressure by use of

$$k = \frac{a_v \gamma_w c_v}{1 + e} = c_v m_v \gamma_w, \tag{5-20}$$

where e is the initial void ratio for each load increment; values for the initial void ratio have been calculated from a knowledge of natural water contents (measured when trimming the specimen in preparation for the test) and volume changes due to consolidation under each load increment. The change in k with e during the process of consolidation for a typical sample is shown in Figure 5-7a, and the variations of k with e for different values of p are shown in Figures 5-7b through 5-7f. The associated regression equations (based on test data from forty-eight specimens) describing each case all take the form

$$k = \log_{10}^{-1} [\alpha e - \beta], \tag{5-21}$$

where α and β are empirical coefficients. Values for these coefficients, together with the standard deviations and correlation coefficients for the respective relationships are given in Table 5-1 for the case where k is expressed in cm/sec.

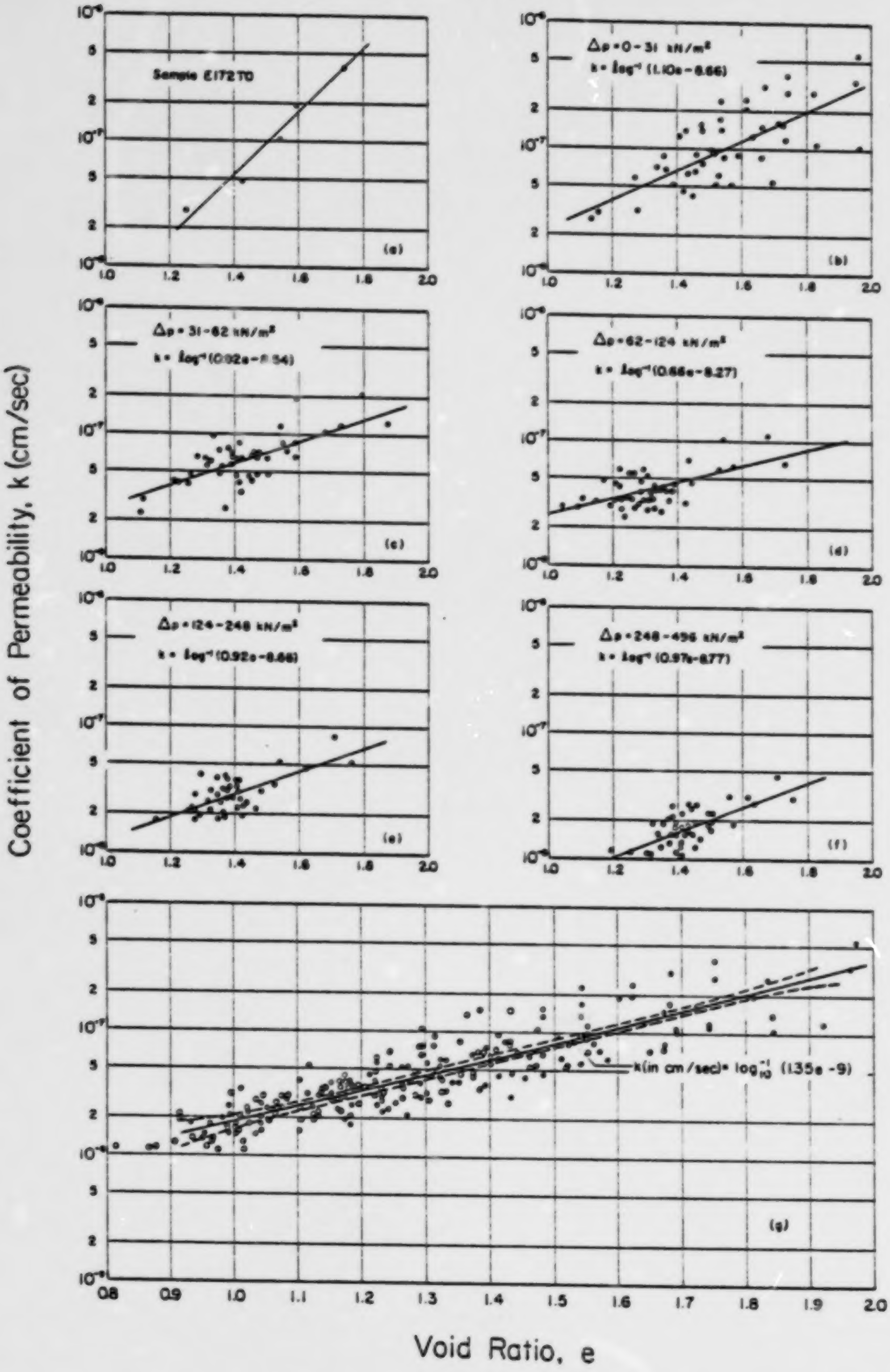

Figure 5-7. Coefficient of Permeability versus Void Ratio for Conventional Consolidation

Table 5-1

Summary of Empirical Coefficients for Permeability Relationships

Range of Consolidation Pressure	α	β	Standard Deviation	Correlation Coefficient
(kN/m^2)				
0 - 31	1.10	8.66	0.28	0.71
31 - 62	0.92	8.54	0.14	0.73
62 - 124	0.66	8.27	0.12	0.61
124 - 248	0.92	8.66	0.11	0.68
248 - 496	0.97	8.77	0.10	0.72

Although the variations of α and β in Table 5-1 suggest that k is a function of both e and p, the latter two parameters are not mutually independent; hence, it should be sufficient to relate k to either e or p. Accordingly, Figure 5-7g shows a correlation of k with e irrespective of p, and a regression analysis for k (in cm/sec) yields

$$k = \log_{10}^{-1} (1.35\, e - 9.00) \qquad (5\text{-}22)$$

with a correlation coefficient of 0.85. The dashed curves in Figure 5-7g give the 90% confidence limits for the true mean value of k for any given value of e. The average coefficient of permeability, $\bar{k}$, together with its total and 70 percentile ranges, is given in Figure 5-8 as a function of p, and the relationship can be represented by

$$\bar{k} = \log_{10}^{-1} \left[- (5.55 + \log_{10} p) \right] \qquad (5\text{-}23)$$

where p is in kN/m^2 and $\bar{k}$ in cm/sec. As can be seen from Figure 5-7, most values for k, as determined from consolidation test data, lie between

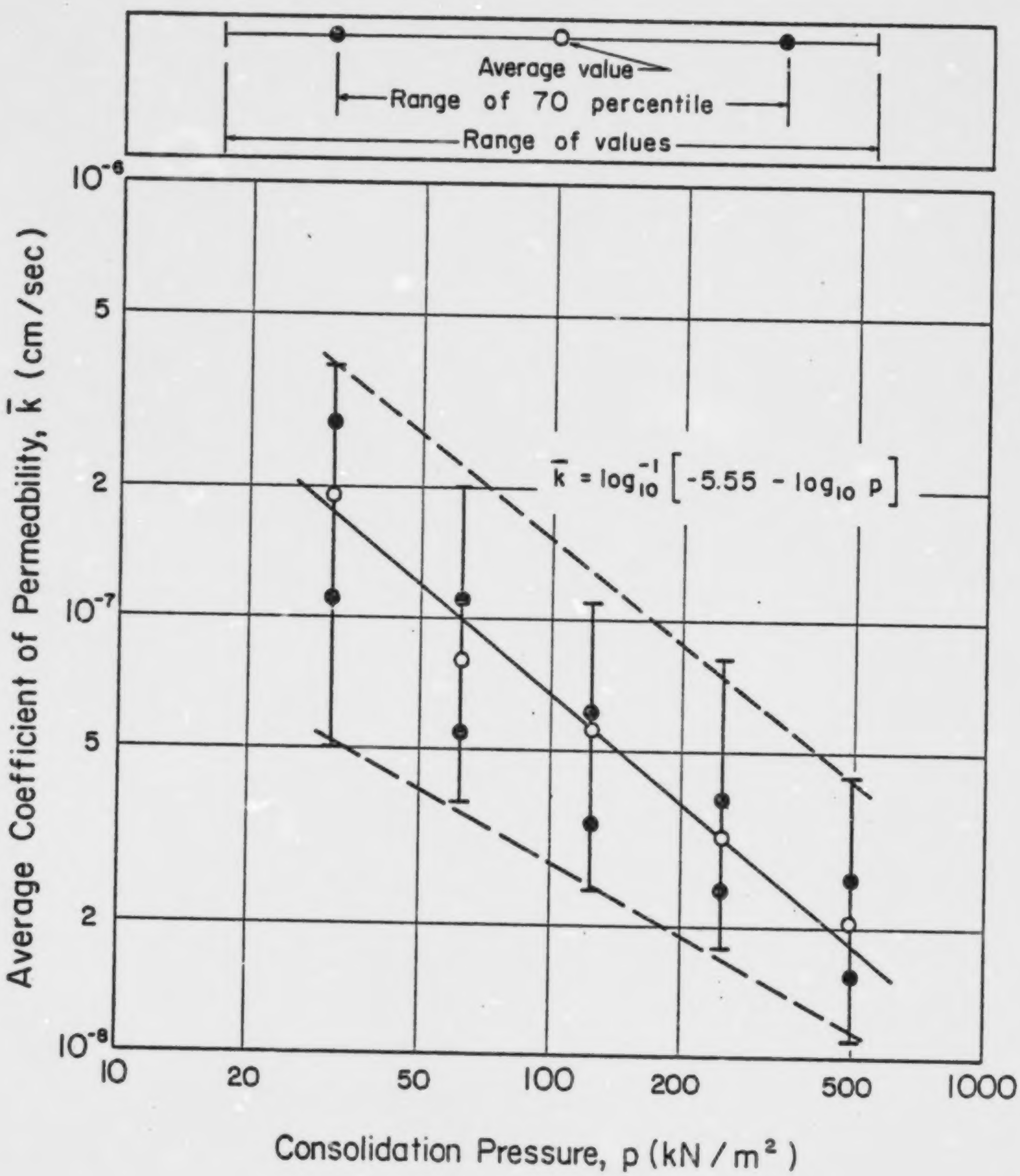

Figure 5-8. Average Coefficient of Permeability versus Consolidation Pressure for Conventional Consolidation.

10^{-6} cm/sec and 10^{-8} cm/sec with the lower values being associated with higher consolidation pressures and lower void ratios. This range of values may be compared with that found from direct permeability tests conducted in an Anteus device (Lowe, Jonas, and Obrician, 1969) on a series of six dredging samples which were similar (but not the same) to those tested in the experimental program reported in this chapter. These permeability data are placed in perspective in Chapter 7.

VARIATION OF CONSOLIDATION CHARACTERISTICS WITH DEPTH

The index properties and consolidation parameters (compression index, C_c; coefficient of consolidation, c_v; coefficient of volume compressibility, m_v; and coefficient of permeability, k) for the dredgings samples obtained from Riverside Site, the Island Site, and Penn 8 during the summers of 1973 and 1974 are plotted versus depth in Figures 5-9 through 5-14. Similar information for samples taken during the summers of 1971 and 1972 has been reported by Krizek, Karadi, and Hummel (1973). The different variations with depth for the different boreholes are due to many reasons, one of which is the intermittent or seasonal deposition of dredged material in any given site and the associated desiccation and growth of vegetation that takes place between dredging periods. Another reason for the observed variations lies in the nature and source of the deposited materials.

CONCLUSIONS

Based on various statistical analyses of data from sixty-four consolidation tests on samples of maintenance dredgings, the following conclusions can be advanced:

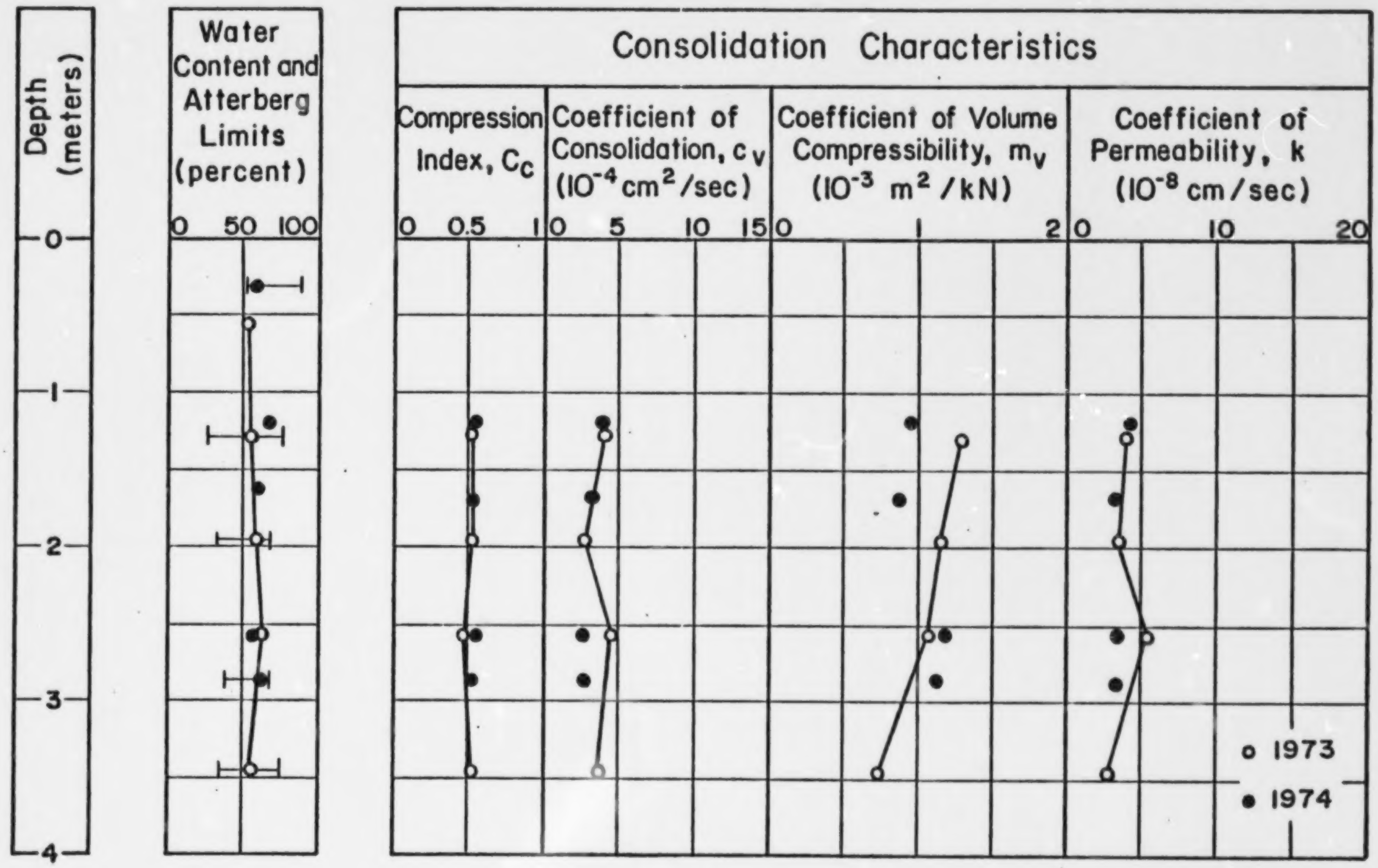

Figure 5-9. Consolidation Test Data for Samples from Location 1 at Riverside Site

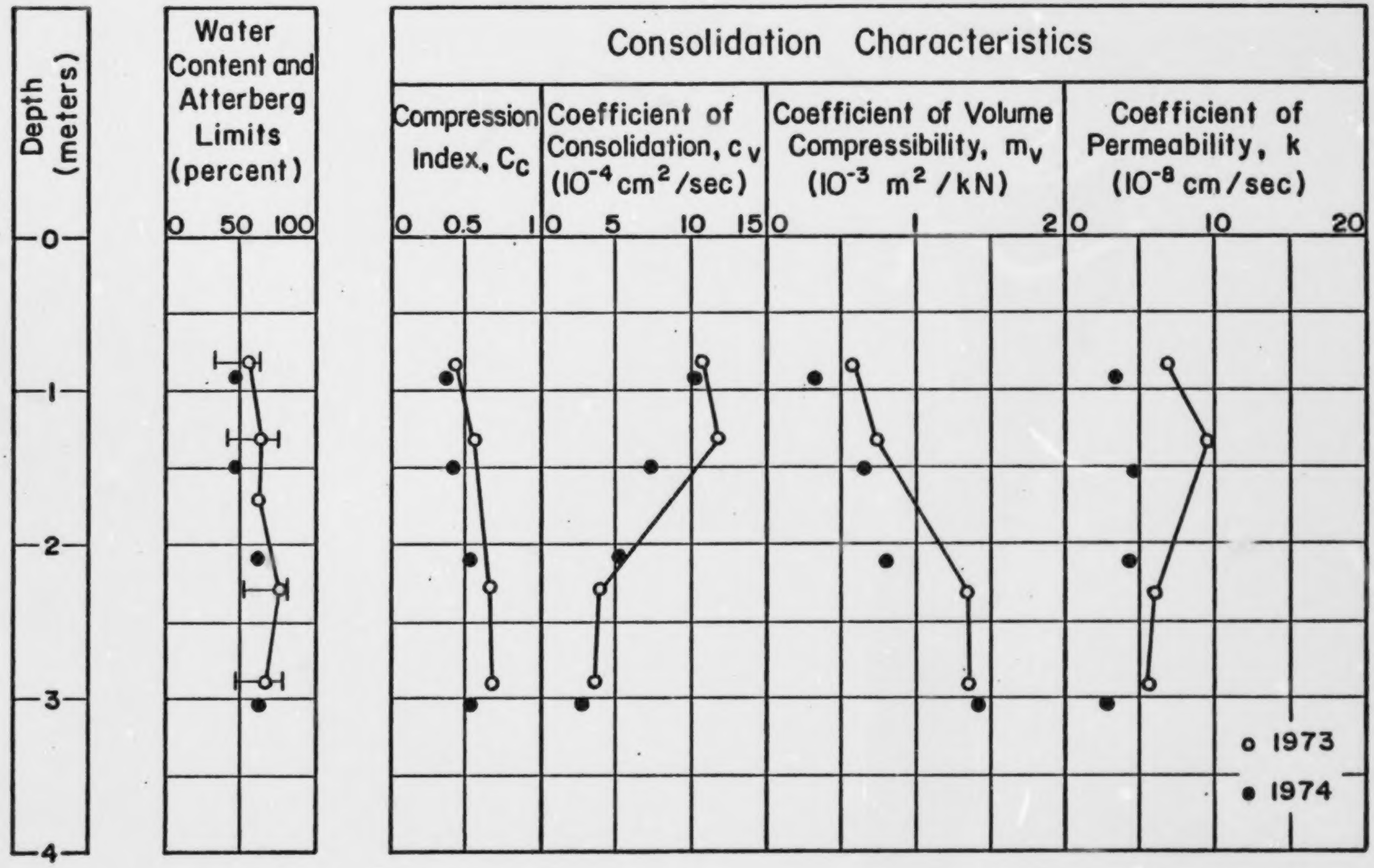

Figure 5-10. Consolidation Test Data for Samples from Location 6 at Riverside Site

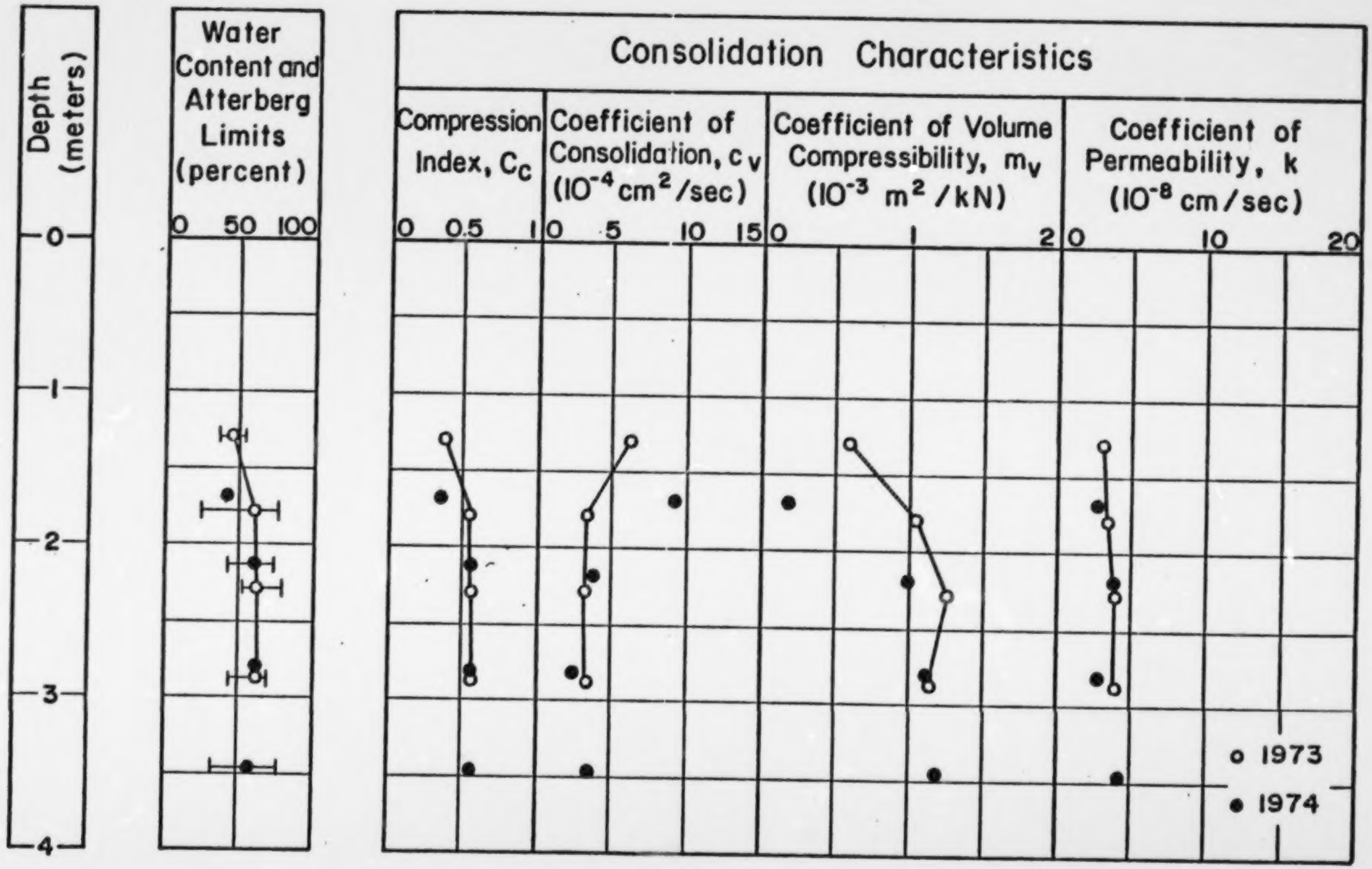

Figure 5-11. Consolidation Test Data for Samples from Location 8 at Riverside Site

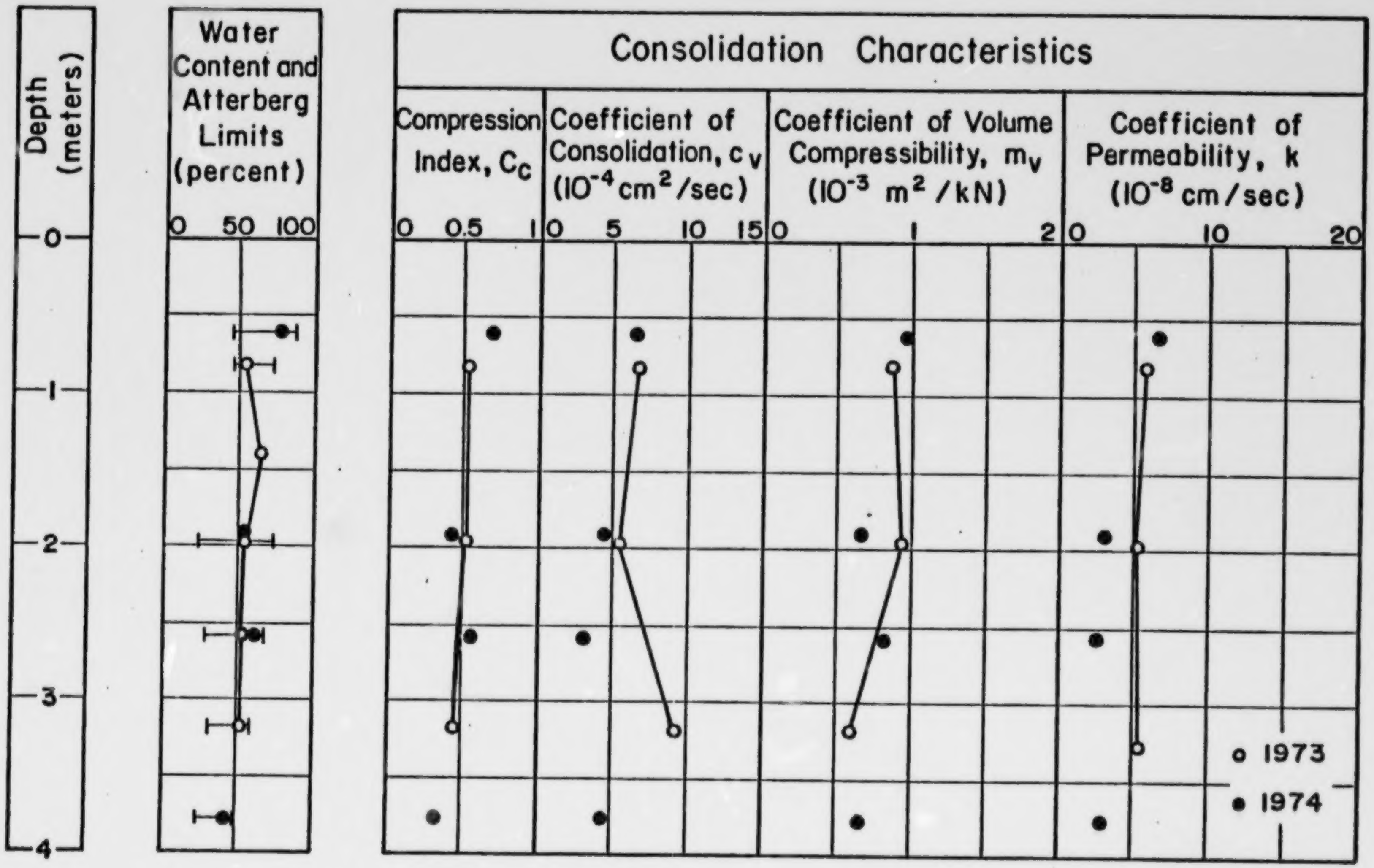

Figure 5-12. Consolidation Test Data for Samples from Location 3 at Island Site

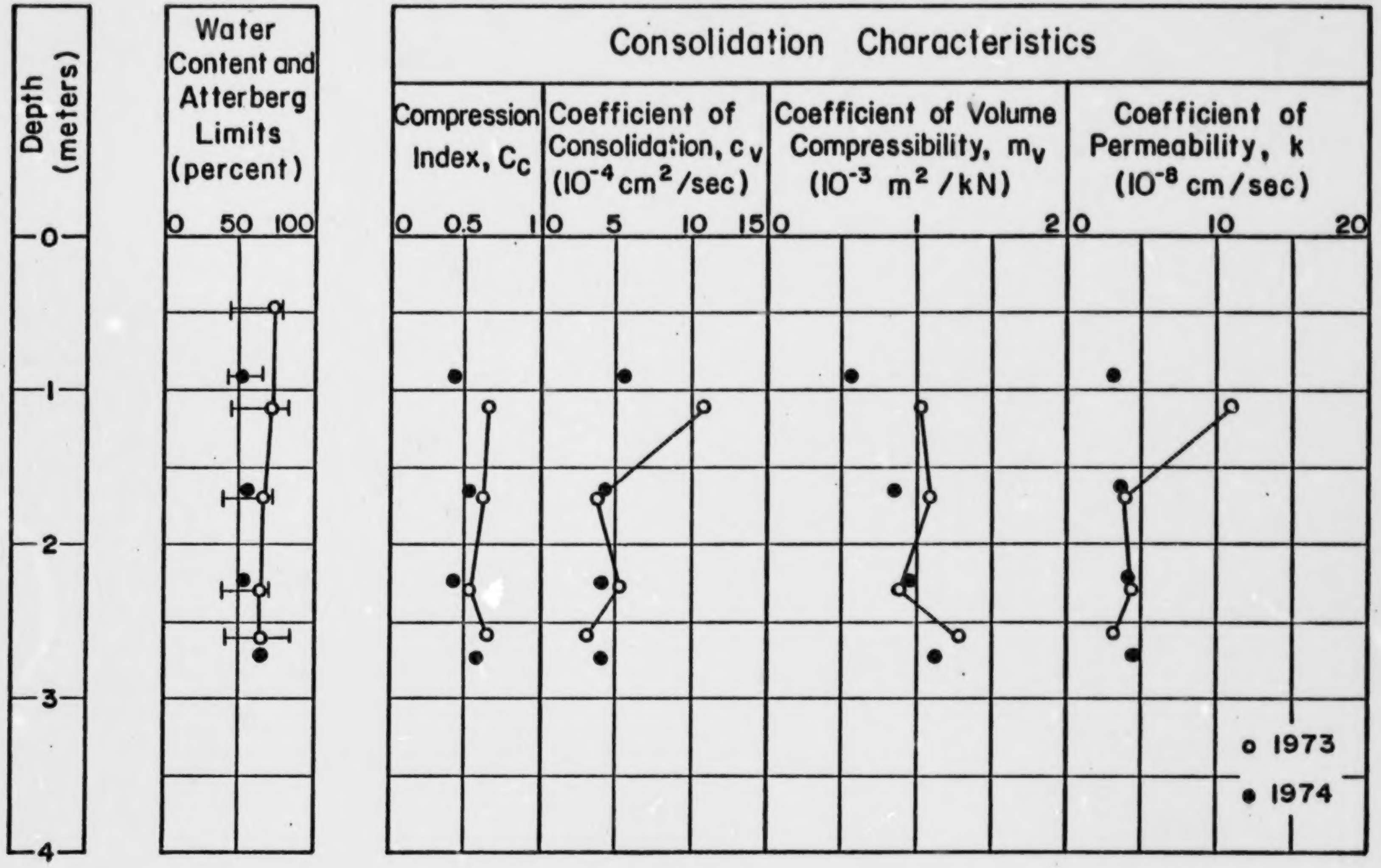

Figure 5-13. Consolidation Test Data for Samples from Location 1 at Penn 8 Site

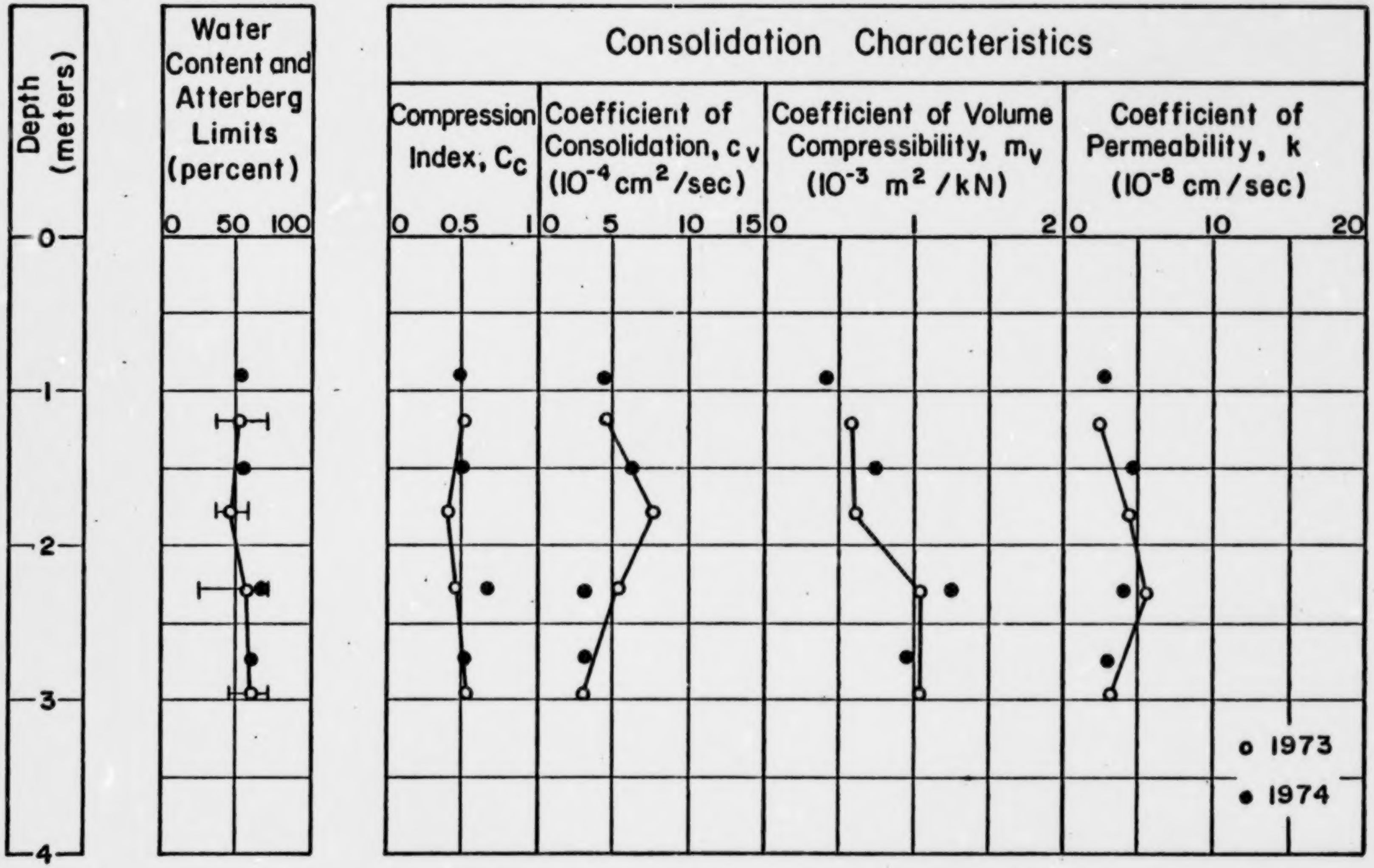

Figure 5-14. Consolidation Test Data for Samples from Location 2 at Penn 8 Site

1. Consistent with the observed response for most types of clayey soils, the compression index increases linearly with both the natural water content and the liquid limit; virtually all values lie between 0.3 and 0.7, which comprises the lower end of the range reported by other investigators.

2. The average coefficient of consolidation varies with the logarithm of the consolidation pressure in a nonlinear manner, but the degree of nonlinearity is relatively insignificant; for all practical purposes a value of 0.0006 cm^2/sec can be assumed, except possibly for very low pressures.

3. The average value of the coefficient of volume compressibility decreases linearly with an increase in the logarithm of the consolidation pressure.

4. The logarithm of the coefficient of permeability increases linearly with void ratio at all consolidation pressures, and its average value decreases with the logarithm of the consolidation pressure; values of the coefficient of permeability varied between 10^{-8} cm/sec and 10^{-6} cm/sec.

5. The constrained tangent modulus varies in a linear fashion with the stress level; the constant of proportionality, designated as the modulus number, was found to vary between 8 and 20, which lies in the range of 2 to 30 reported for a large variety of clays.

6. The modulus number varies linearly with the dry density, natural water content, and percent clay, increasing with the first and decreasing with the other two; however, its dependence on the percent clay was found to be relatively small.

CHAPTER 6

SECONDARY CONSOLIDATION

As mentioned previously, secondary consolidation consists simply of that portion of the settlement response that is not characterized by the theory of primary consolidation, and there is no implication that settlements due to secondary consolidation are of secondary or negligible magnitude. Although the relative importance of primary and secondary consolidation varies considerably with the type of soil, there are many cases where settlements due to secondary consolidation are much larger than those resulting from primary consolidation and the secondary settlements normally occur over extended periods of time. For example, Bjerrum, Jonson, and Ostenfeld (1957) observed that the abutment of the Aggersund Bridge settled about 80 cm in 15 years, and about half of the observed settlement is attributed to secondary time effects, the remainder being immediate settlement plus primary consolidation settlement. Very often secondary compressions are found to vary linearly with the logarithm of time, but this is not always the case, and several investigators (Leonards and Ramiah, 1959; Barber, 1961; Lo, 1961) have reported nonlinearity for many remolded and undisturbed peats and clays. Although the problem of secondary compression has been addressed extensively (Gibson and Lo, 1961; Lo, 1961; Barden, 1965; Mesri, 1973; and others) in an effort to develop a rational means for predicting the long-term field settlement of structures, no generally accepted theoretical solution has yet been advanced; however, several empirical or semi-empirical models are available for certain types of behavior.

Reported in this chapter are the results of several long-term tests on samples of maintenance dredgings. The coefficient of secondary compression and its variation with consolidation stress, natural water content, and compression index are investigated, and typical patterns of settlement versus the logarithm of time are shown to exhibit deviations from the well-known linear relationship; in general, there was a gradual increase in the compression rate with the logarithm of time followed by a gradual decrease, approaching a horizontal asymptote and virtually a zero rate of compression. The theory and model of Lo (1961) are used to determine the parameters needed to predict the long-term secondary compression of these maintenance dredgings, and the variations of these parameters with natural water content are given. The effect of sample thickness on the proportion of secondary to primary compression is discussed and found to shed some light on the probable error involved in using secondary compression data from laboratory tests to predict secondary settlements expected in the field.

BRIEF BACKGROUND

Based on laboratory test data, Buisman (1936) proposed a semi-empirical procedure for estimating the amount of secondary compression to be expected in a given field situation, and his relationship is

$$\Delta H = H(\alpha_p + C_a \log t)q , \qquad (6\text{-}1)$$

in which ΔH = total settlement, H = thickness of stratum, q = load intensity, α_p = coefficient of primary compressibility, and C_a = coefficient of secondary compressibility. Taylor and Merchant (1940) attempted a mathematical treatment of secondary consolidation, which, although not presented in terms of a rheological model, consisted of a Hookean element and a Kelvin element in series. Terzaghi (1941) published his general hypothesis to describe qualitatively the continuous process of primary and secondary consolidation; although rather simplified, this hypothesis is in agreement with most of the observed facts (Barden, 1965). In brief, it states, that when a pressure increment greater than the interparticle bond strength is applied, the clay passes from a solid state to a lubricated state followed by a period of consolidation. During primary consolidation the total stress is carried by the pressure in the free pore water, the plastic resistance in the highly viscous adsorbed double-layer (film bond), and the virtually solid-solid contracts between clay particles (grain bond); the film and grain bonds are considered to be components of effective stress. During secondary consolidation the pore pressure is negligible and the load increment is shared by the latter two components, namely, film bonds and grain bonds, and the transfer of stress from film to grain bond takes place gradually and is associated with a period of very slow viscous flow. As the clay particles rearrange under a given load increment, the effective viscosity increases and the adjustment proceeds at a decreasing rate until the system reaches a state of quasi-equilibrium wherein all stress is carried by grain bonds and the clay is once again in essentially a solid state.

Taylor (1942) modeled the soil skeleton as a viscoelastic material and considered secondary compression to be caused by the remolding of the structure induced by primary compression. The terms "plastic structural resistance to compression" and "structural viscosity of the clay skeleton" were introduced as an equivalent to film bond, which is a function of the rate of shear strain and the nature of the adsorbed double layer. Based on data from long-term (several years) consolidation tests on many peats and clays, Barber (1961) found that the extrapolation of short-term tests may lead to serious errors. In one particular example he showed that the S-shaped primary consolidation pattern for a Cambridge peat under the load increment from 4 to 8 kg/cm^2 was essentially complete at 0.1 day, and a linear extrapolation of the secondary compression between 0.1 day and one day considerably underestimated the consolidation at 100 days. Other tests on peats and a variety of different soils suggest that secondary compression may also be characterized by an S-shaped curve somewhat like that for primary consolidation, but extending over more cycles of time. In the early 1960's a number of investigators (Gibson and Lo, 1961; Lo, 1961; Wahls, 1962; Barden, 1965) used rheological models to characterize the secondary compression of soils, and Mesri (1973) has recently presented an excellent review of this subject.

EXPERIMENTAL PROGRAM

The materials tested in this experimental program were obtained from Riverside and Penn 7 Sites in Toledo, Ohio, and they were sampled at two different points in the dredging and disposal cycle. Slurry samples were taken from the discharge pipe of Penn 7 as the dredgings were pumped from a hopper dredge into the disposal area, and "undisturbed" samples were obtained from four different boreholes at Riverside Site, which had been filled about eighteen months before the time of sampling. A summary of all samples and their index properties is given in Table 3-1.

Sampling Procedures

The slurry sample (C80T0) was obtained from a 24-inch (61 cm) discharge pipe while it was flowing full at a velocity of at least 4.5

meters per second. Sampling was accomplished by inserting a 2-inch (5 cm) diameter tube directly into the flow stream and diverting a portion of the flow into a large container. The "undisturbed" samples of E material were taken by means of a manually operated, specially designed, piston sampler developed for this type of work. Details of the sampling procedures have been reported by Hummel and Krizek (1974).

Experimental Procedure for Slurry Consolidation Tests

A volume of dredging slurry sufficient to fill two 4-inch (10 cm) diameter slurry consolidometers to a height of 10 inches (25 cm) was mixed thoroughly at a water content of about 170 percent. The slurry consolidometers were similar to those developed by Sheeran and Krizek (1971) and used to conduct the slurry consolidation tests described in Chapter 4. The loading scheme for this test was similar to that normally used for a conventional consolidation test; a load increment ratio of unity was employed, and the load increments were 2, 4, 8, 16, and 32 psi (14, 28, 55, 110, and 220 kN/m^2). The first four load increments were applied for a period between 10 and 45 days to insure that primary consolidation was complete, and the last load increment was maintained on the two samples for 150 days.

Experimental Procedure for Conventional Consolidation Tests

Conventional consolidation tests were conducted on eight samples of E material; the samples were 2.5 inches (6.4 cm) in diameter and about 1 inch (2.5 cm) thick, and they were contained in teflon-lined, grease-coated brass rings with filter paper at the top and bottom. Drainage was permitted at both ends of the samples. Beginning with an initial load of 31 kN/m^2, all loads were doubled after 24 hours until a load of 248 kN/m^2 had been attained; this latter load was maintained on all samples for an extended period of time to study the secondary compression of dredgings. The tests on six of the eight samples were terminated after 205 days, at which time all samples manifested generally similar behavioral patterns; the load on the other two samples was maintained for approximately 100 additional days, but the general pattern did not change.

EXPERIMENTAL RESULTS

Based on experimental evidence Lo (1961) classified the settlement-time response of secondary compression into three types; these are Type (a) for which the rate of secondary compression gradually decreases with time until it becomes zero when the ultimate settlement is reached; Type (b) for which the rate of secondary compression is proportional to the logarithm of time over a considerable range of time and then decreases rapidly near the ultimate settlement, and Type (c) for which the rate of secondary compression increases with the logarithm of time and then decreases gradually until it vanishes for very large times.

Patterns from Slurry Consolidation Tests

Compression-time curves for the two tests on the dredging slurry sample (C80T0) are shown in Figure 6-1; it was intended that these two tests be identical, and the samples are therefore designated as C80T0-I and C80T0-II. Although it was not planned to study secondary compression for the load increments below 220 kN/m^2, certain of the response curves (load increments 28 to 55 and 55 to 110 kN/m^2) did manifest an unusual pattern of secondary compression wherein the rate of compression with respect to the logarithm of time increased gradually after 10 to 20 days from the application of the load increment and then decreased after 24 to 30 days, the ultimate settlement in both cases reaching approximately the

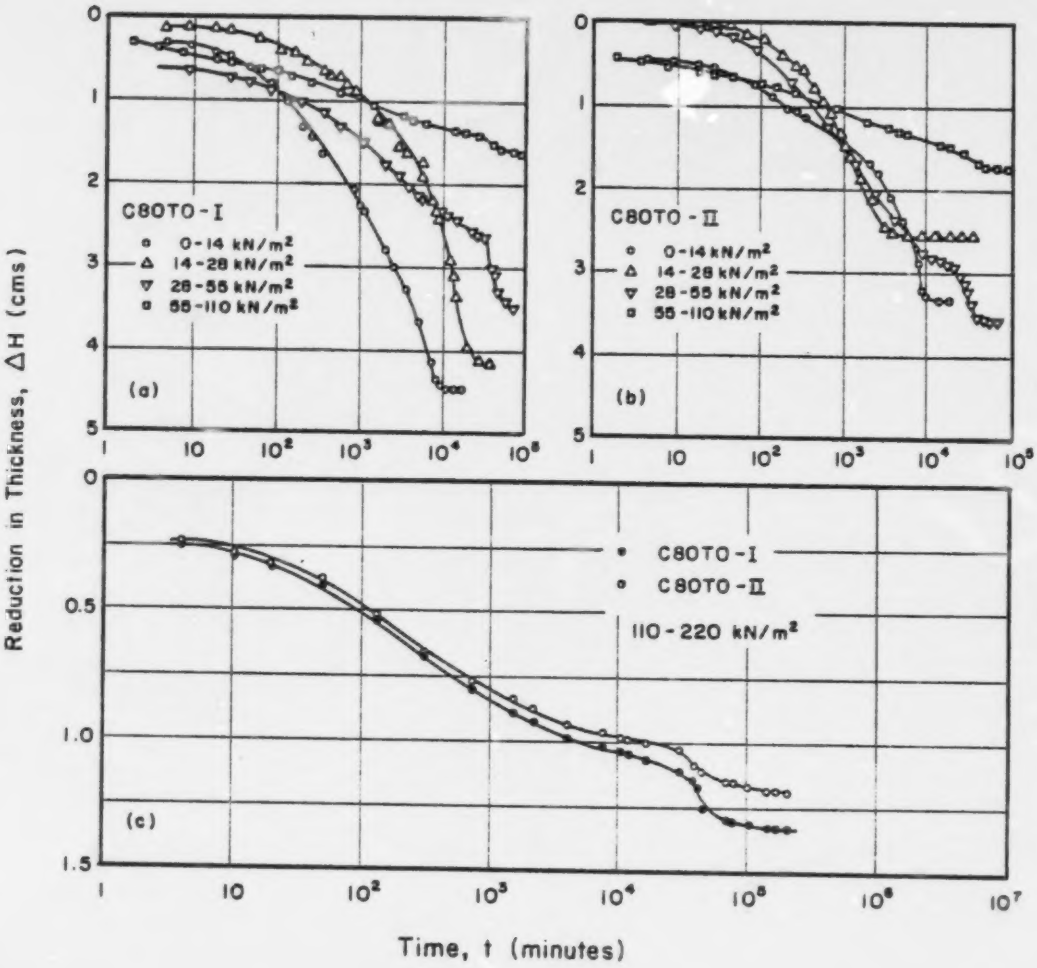

Figure 6-1. Consolidation-Time Response of Slurry Samples

same value. In general, the response curves for the first two load increments did not exhibit any appreciable secondary effects, probably due to insufficient time of loading, but the curves for the next two load increments revealed the previously explained behavioral pattern with secondary settlements ranging between 15 and 23 percent of the total settlement for each load increment.

By the time the fifth load increment was applied, the thicknesses of the two samples were only about one-half of the original thicknesses of 25 cm due to consolidation under the previous four load increments. This load increment was maintained for 150 days, and quite similar compression-log time curves [Type (c) according to Lo (1961)] for both tests are shown in Figure 6-1. The ultimate settlements attained under this last load increment were about 10 percent of the specimen thickness at the time the increment was applied, and the ratios of secondary to total settlements were about 0.25. An extension of straight lines corresponding to the early secondary compression response underestimated the observed total settlements by approximately 10 percent for both tests. The deviation from a linear compression-log time relationship began at about 15 days for both samples, and the rate of compression increased gradually for about 20 days, after which time it decreased and approached zero. This type of behavior is essentially the same as that noted for the preceding two applied consolidation stresses, and it is consistent with the behavior associated with natural deposits of soils with a loose structure and relatively high sensitivity. Particles of deposited dredgings apparently develop a kind of cementation bond due to chemical processes that occur during the time of consolidation and these developed bonds can resist compressive strains up to a certain limit, after which the structure breaks down gradually and the particles readjust their positions until a state of quasi-equilibrium is reached under the applied pressure.

Patterns from Conventional Consolidation Tests

As shown in Figure 6-2, the compression time curves obtained from conventional consolidation tests on dredgings are generally similar to those of clay soils. The time for completion of primary consolidation, t_{100}, was found by the conventional Cassagrande method to be about 100 minutes for all applied stresses. Upon completion of primary consolidation, secondary compression continued to increase linearly with the logarithm of time for about one additional log cycle of time, after which another load increment was applied. At approximately 1000 minutes the rate of compression showed a tendency to increase for the higher load increments, but this phenomenon was not noted for the first load increment. This suggests that the developed interparticle bonds are strong enough to resist structural breakdown under small consolidation stresses, although such breakdown may have occurred if the load was allowed to act for a longer time.

The final load increment (124 to 248 kN/m^2) was maintained on all specimens for more than 200 days, during which time all compression-time curves manifested the patterns shown in Figure 6-3. The normal pattern was observed for the primary consolidation stage followed by a linear increase in settlement with the logarithm of time for about 10 days, after which the rate of settlement increased substantially for about 70 days and then decreased to approach zero for longer times. The observed settlements during the final two months of the tests were practically negligible for most of the specimens, thereby indicating that the tests could be terminated with essentially no loss of significant data.

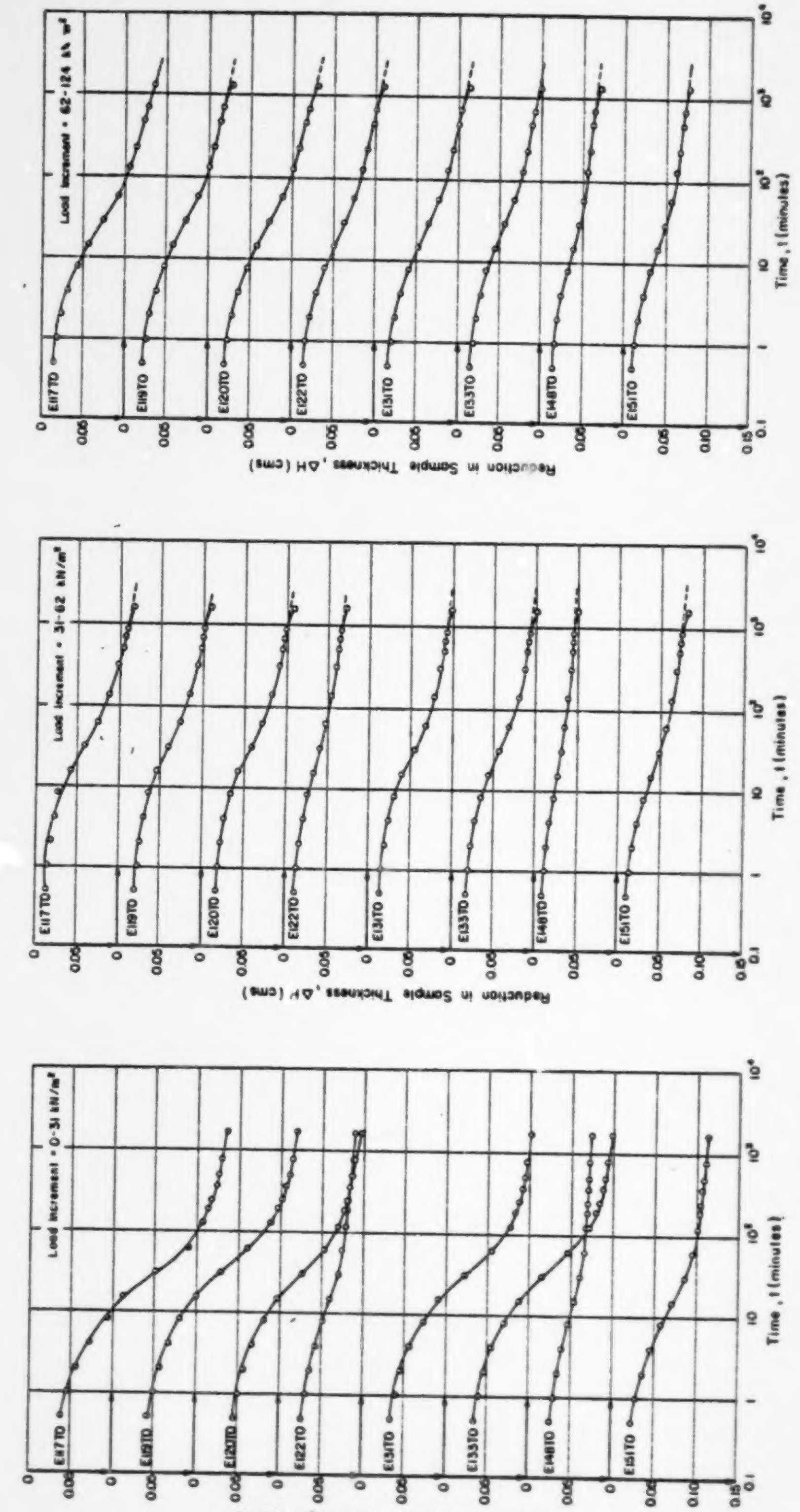

Figure 6-2. Primary Consolidation of Conventional Samples

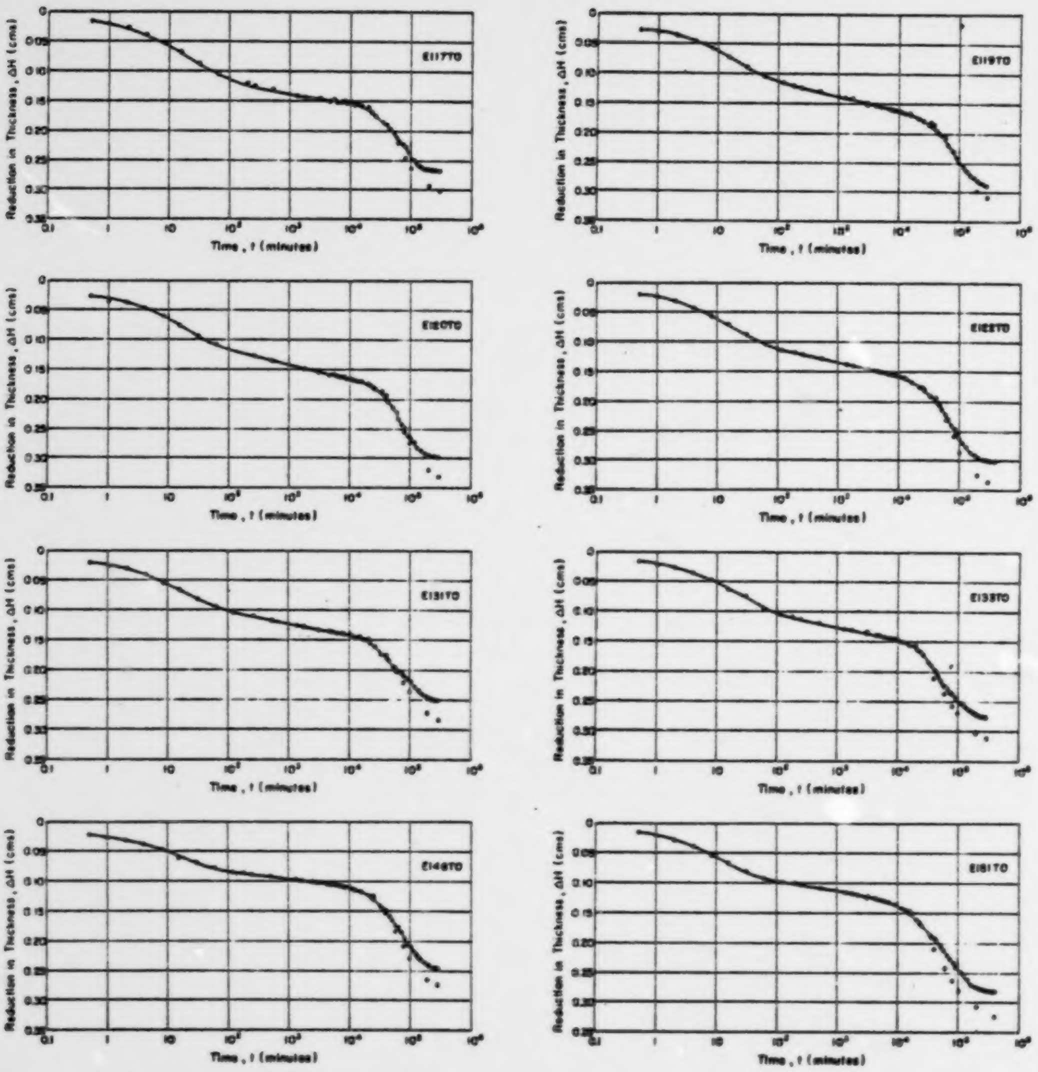

Figure 6-3. Secondary Compression of Conventional Samples

Comparison of Behavior Patterns

The unusual behavior pattern which starts at the beginning of the second S-shaped portion of the response curves for the conventional consolidation tests resembles that obtained from the slurry consolidation tests, but there are different proportions of secondary to primary compressions and the times required to reach the end of primary consolidation and ultimate settlements are different. As illustrated in Table 6-1, in the case of the slurry consolidation tests the proportion of secondary compression to total compression is about 0.25, whereas it is on the order of 0.60 for the convnetional consolidation tests for essentially the same increment of applied stress; both ratios were evaluated at long times when the rates of settlement were essentially zero. This phenomenon may be a consequence of the different thicknesses of the specimens in the two types of test; such behavior confirms the findings of Barden (1965), but is not in agreement with the nonsystematic variations reported by Hansen and Inan (1969).

The time required to reach ultimate settlements is shorter for the slurry consolidation tests than for the conventional consolidation tests, although the specimen thickness in the former is about 5 or 6 times that in the latter. Alternatively, the time required to complete primary consolidation (as determined by the conventional Cassagrande method) in the slurry consolidation tests is about 30 times of that for the conventional consolidation tests; these times are approximately proportional to the square of the specimen thicknesses, as predicted by the classical theory of consolidation (Terzaghi, 1923). These observations suggest that (a) the time required to reach ultimate settlements (including secondary compression) does not necessarily have to be longer for greater thicknesses

Table 6-1

Proportions of Compression Components

Sample	Ratio between Underestimation of Total Compression due to Linear Extrapolation of Secondary Compression Response and Observed Total Compression		Ratio between Secondary Compression and Total Compression	
	After 100 days	After 200 days	After 100 days	After 200 days
E117TO	0.31	0.30	0.55	0.55
E119TO	0.28	0.31	0.57	0.60
E120TO	0.32	0.32	0.60	0.62
E122TO	0.36	0.37	0.62	0.63
E131TO	0.29	0.31	0.55	0.59
E133TO	0.34	0.35	0.59	0.62
E148TO	0.40	0.44	0.58	0.61
E151TO	0.41	0.43	0.65	0.68
C80TO-I	0.106	0.095*	0.26	0.27*
C80TO-II	0.117	0.105*	0.20	0.22*

*Values estimated after 150 days

of material and (b) the relative amount of secondary compression that occurs in the field, where the thickness of material is normally much larger than that in the laboratory, may be considerably less than the value predicted from laboratory tests. The average ultimate settlement for the specimens in the slurry consolidation tests was about 10 percent under the final load increment (110 to 220 kN/m^2), whereas it was about 14 percent for the specimens in the conventional tests for essentially the same load increment (124 to 248 kN/m^2). A comparison of final settlements and the corresponding stresses indicates that the rates of settlement are approximately the same, despite variations in the time needed to attain such settlements and the proportions of secondary to total settlements.

As summarized in Table 6-1, average underestimations in the values of secondary compressions due to a linear extrapolation of the straight line portions of the compression-log time plots were about 45 percent and 60 percent for slurry and conventional consolidation tests, respectively, whereas average underestimations in secondary compression with respect to total compressions were about 10 percent and 35 percent for the two types of tests. These results suggest that data from the slurry consolidation tests on the thicker specimens (more than 10 cm) of dredgings may be reasonably sufficient to predict ultimate settlements, once the slope of the straight line portion of the consolidation curve is defined and the ratio between the secondary and total settlement is known, but the use of similar data from conventional consolidation tests should be used with considerably more caution.

INTERPRETATION

One common definition for the coefficient of secondary compression, C_a, is

$$C_a = \frac{\Delta H/H}{\Delta \log t} , \qquad (6\text{-}2)$$

where ΔH is the reduction in specimen thickness for a given change in time (represented by Δ log t) and H is the thickness of the specimen at the time the load increment under consideration is applied. However, as discussed previously, the compression-log time response curves for all dredging samples tested exhibited a double S-shaped pattern with a straight line portion extending over a considerable length of time between the first S-shaped curve representing the primary consolidation part of the response and the second S-shaped curve that describes the secondary compression. Nevertheless, despite variations in the proportions of secondary to primary settlements and underestimations of settlements due to linear extrapolation of the settlement-log time curves after primary consolidation, the values of the coefficient of secondary compression, C_a, from both slurry consolidation and conventional consolidation tests are practically the same, varying from 0.0072 to 0.0085 and from 0.0073 to 0.0128, respectively, for the last load increment. Accordingly, a knowledge of the relationships between this coefficient and certain other properties of dredgings, together with information concerning the relative proportions of secondary and total settlements and the settlement-time behavior for the primary portion of consolidation, will enable the engineer to estimate the extent of the expected settlements due to secondary compression.

Variation with Natural Water Content

The relationship between the coefficient of secondary compression, C_a, and natural water content, w_n, has been given by Mesri (1973) for 12 different types of clays, and these data show a reasonably linear dependence between the logarithms of both parameters (hence, the actual parameters are related by a power function); reported values of C_a for natural deposits lie between 0.001 and 0.1. As indicated in Figure 6-4, values of C_a for dredgings ranged from about 0.002 to 0.013 for a natural water content range from 45 to 65 percent, and a reasonably good straight line relationship is obtained between the logarithm of C_a and the logarithm of w_n for a given load increment.

Variation with Consolidation Pressure

As explained by Mesri (1973), the development of relationships between C_a and the consolidation pressure, p, has been complicated by the variety of ways in which C_a is defined and the different loading schemes used to reach the final consolidation pressure; accordingly, a number of conflicting relationships have been proposed, and no consensus seems to be forthcoming. Haefeli and Schaad (1948) indicated that there is no relationship between C_a and p; Newland and Allely (1960) found that C_a is independent of p; Wahls (1962) showed a decrease in C_a with p; and other workers (Adams, 1965; Keene, 1964; and Goldberg, 1964) indicated a considerable increase in C_a with p. Within the context of the foregoing definition of C_a and the described test procedures (specifically, doubling the load increment), Figure 6-5 shows that C_a increases in a reasonably linear manner with the logarithm of p for the eight dredging samples tested by use of conventional consolidation tests. In general, a different relationship is obtained for each specimen, but all straight lines are

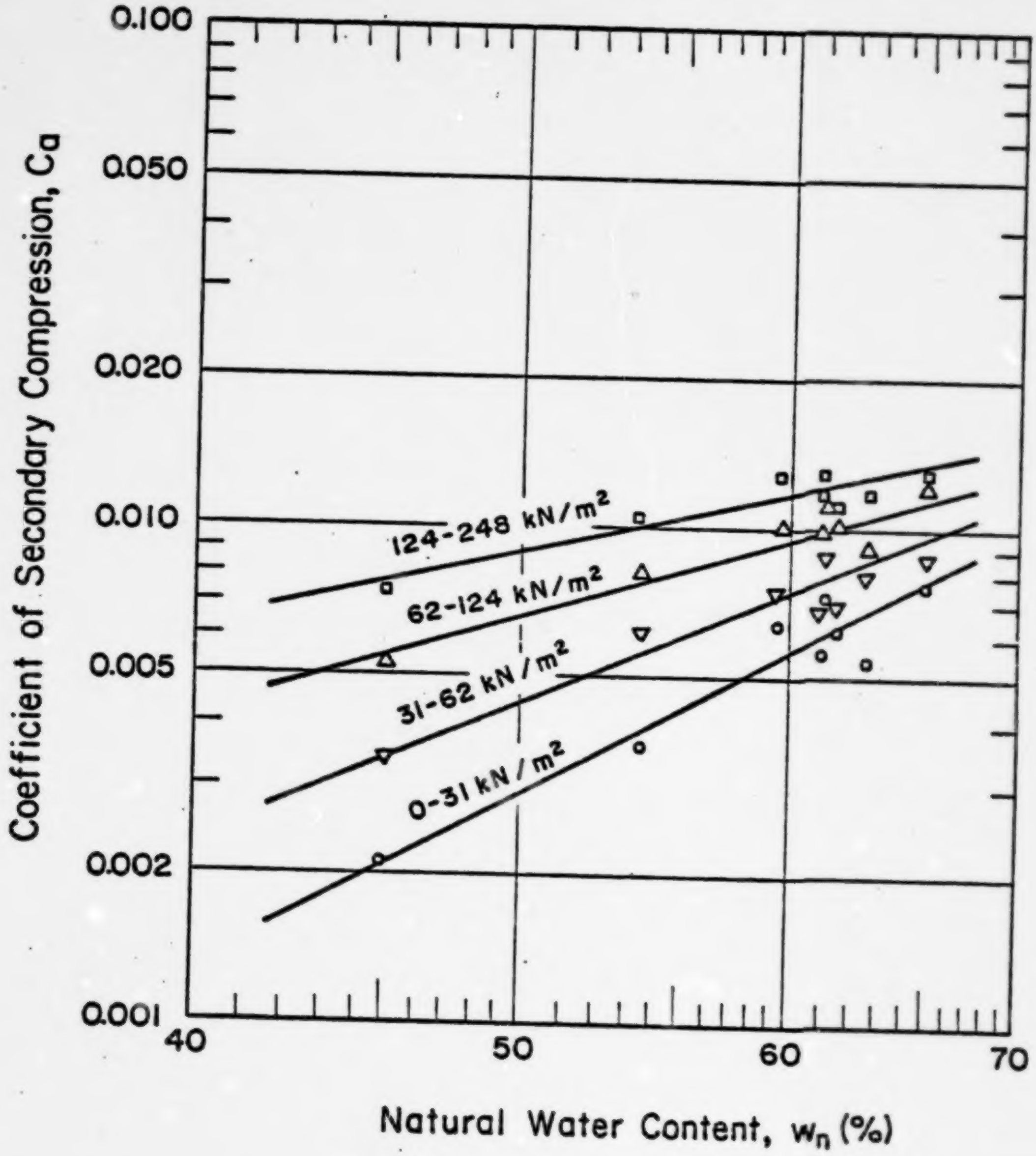

Figure 6-4. Coefficient of Secondary Compression versus Natural Water Content

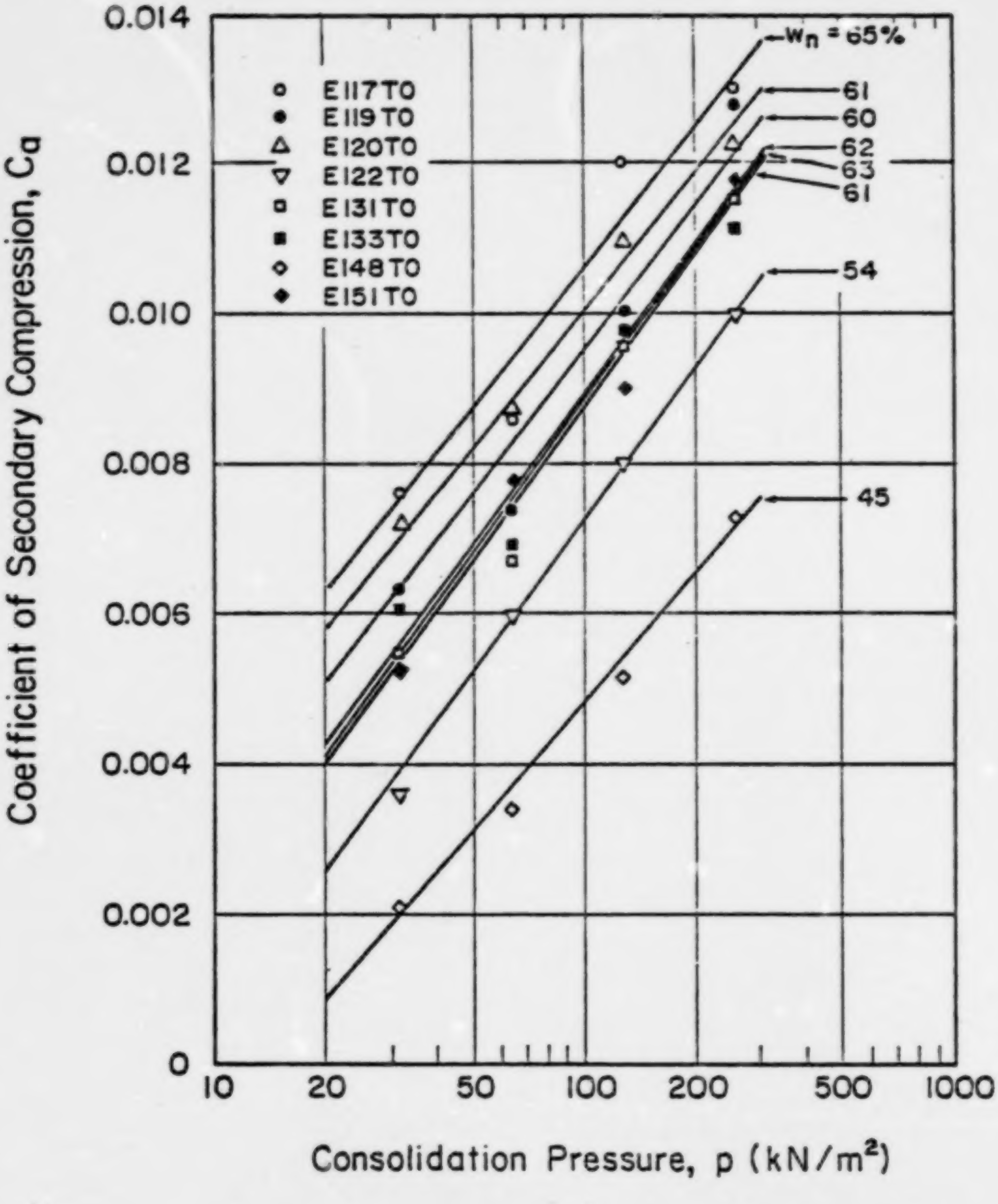

Figure 6-5. Coefficient of Secondary Compression versus Consolidation Pressure

approximately parallel with a change of about 0.006 in the value of C_a for a change in pressure from 31 kN/m^2 to 248 kN/m^2.

Variation with Compression Index

The e-log p curves for the eight samples tested by use of conventional consolidation tests are shown in Figure 6-6. The values of void ratio were estimated after about 24 hours for all pressures, including the final pressure that was maintained for a much longer period of time to study secondary effects. Values of the compression index, C_c, determined from these curves varied between 0.32 and 0.55, and, as shown in Figure 6-7, C_a showed a generally linear increase with an increase in C_c for a given load increment.

Determination of Parameters

Based on the assumption that the soil structure behaves as a rheological model, Gibson and Lo (1961) formulated a theory that is capable of describing the secondary compression of clays that may be characterized as Type (a) or Type (b), and Lo (1961) extended this theory to include the rather unusual behavior manifested by Type (c) clays and the dredgings tested in this program. If we designate as t_k the time at which a distinct increase in the observed rate of settlement occurs (due to a presumed breakdown of the structural bonds between soil particles after a certain strain has been reached), the time-dependent deformation behavior, $\varepsilon(t)$, may be characterized (Lo, 1961) by

$$\varepsilon(t) = \Delta p \left[a + b\left(1 - e^{\frac{-\lambda}{b}t}\right) + b_1\left(1 - e^{\frac{-\lambda_1}{b_1}(t - t_k)}\right)\right]; \quad t > t_a, \qquad (6\text{-}3)$$

where Δp is the pressure increment for the loading step in question and a, b, b_1, λ, and λ_1 are empirical parameters to be determined from the test data according to procedures outlined in Figure 6-8. For times

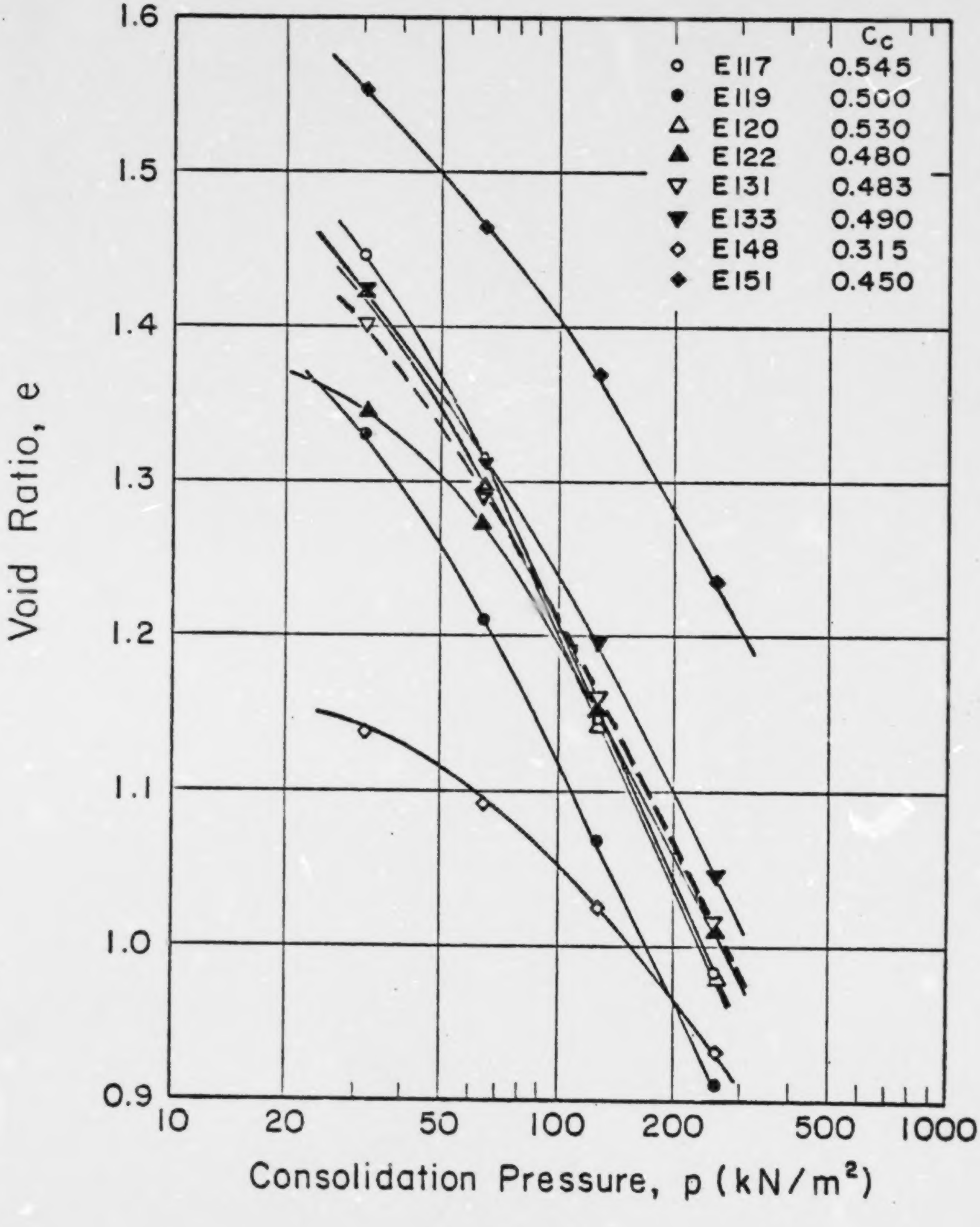

Figure 6-6. Relationships Between Void Ratio and Consolidation Pressure

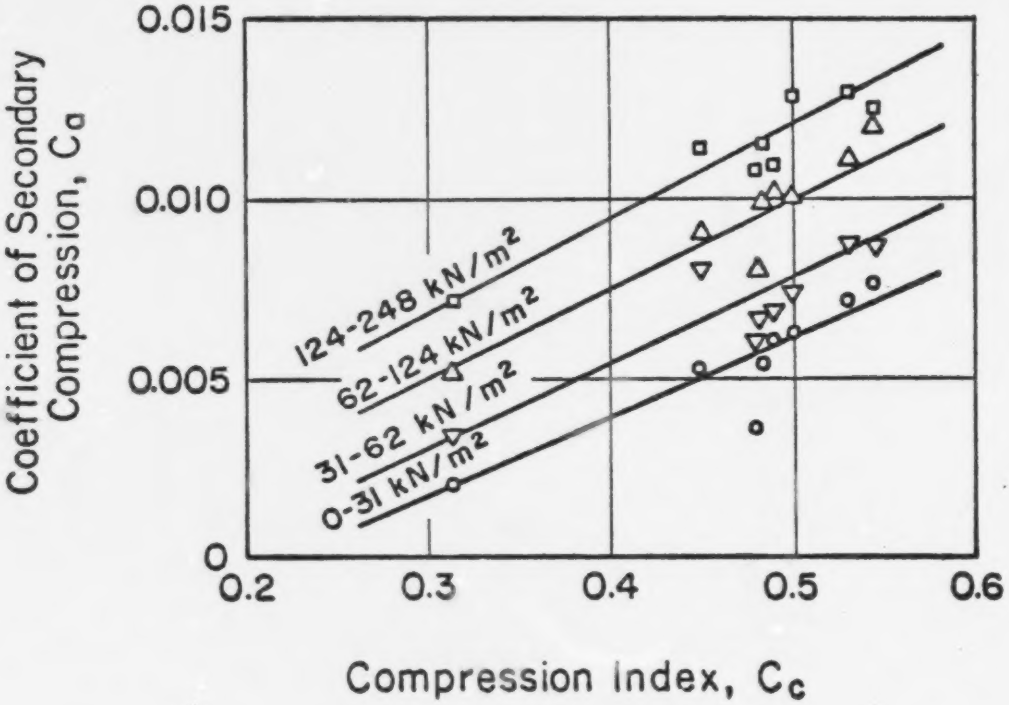

Figure 6-7. Coefficient of Secondary Compression versus Compression Index

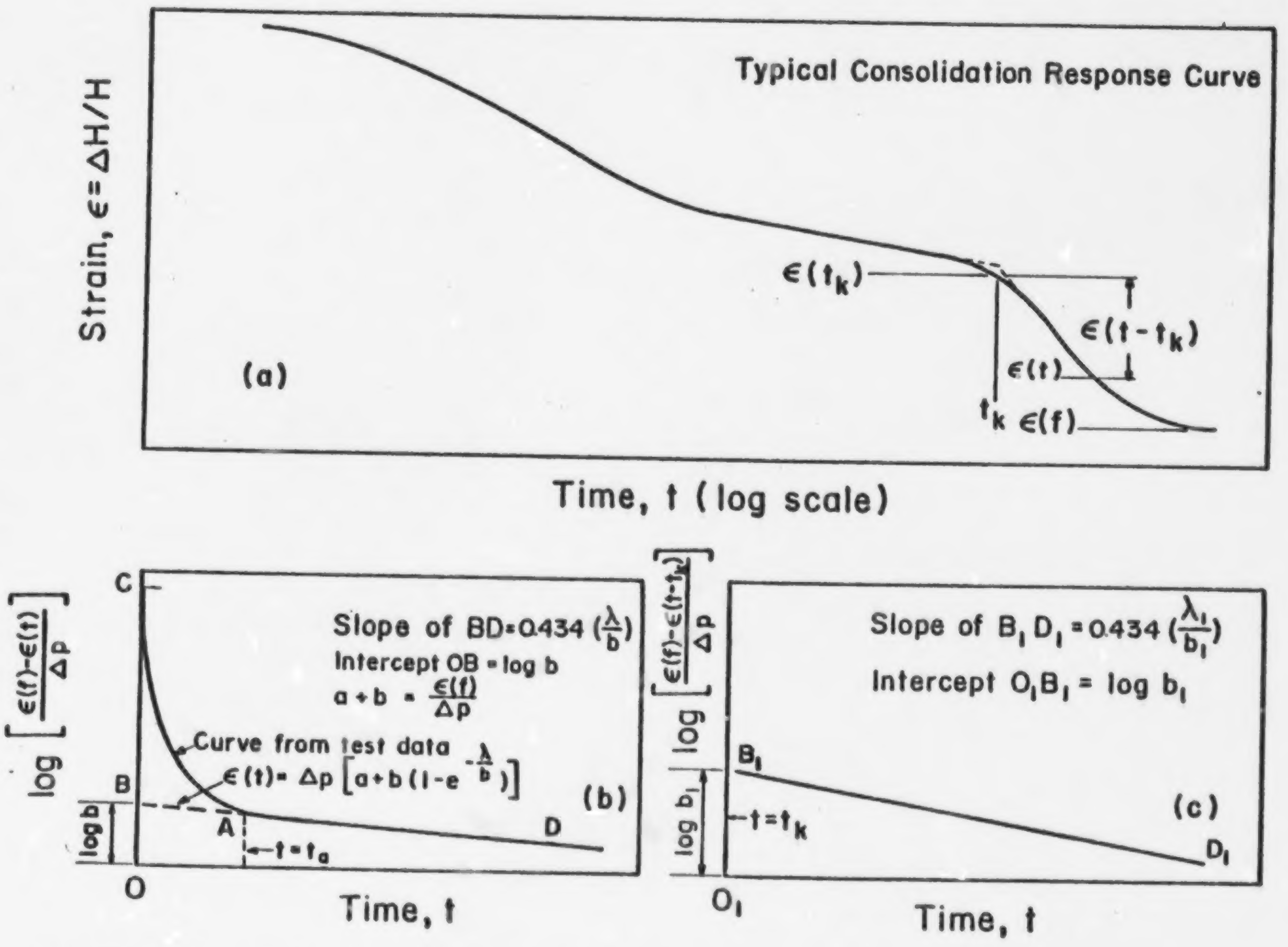

Figure 6-8. Method for Determining Parameters from Typical Consolidation Curves

greater than t_a but less than t_k (where the determination of t_a is illustrated in Figure 6-8), only the first term within the brackets in Equation (6-3) is needed to describe the response. Figure 6-8a shows a typical consolidation curve for dredgings and explains how values can be deduced from it to plot Figures 6-8b and 6-8c, from which the parameters can be determined. Plots similar to those described in Figures 6-8b and 6-8c are given in Figure 6-9 for the eight dredging samples subjected to conventional consolidation tests, and the empirical parameters are summarized in each case; the left half of Figure 6-9 represents $\log\Big(\varepsilon(f)-\varepsilon(t)\Big)/\Delta p$ versus t (similar to Figure 6-8b) for $t_a \leq t \leq t_k$, and the right half depicts $\log\Big(\varepsilon(f)-\varepsilon(t-t_k)\Big)/\Delta p$ versus t (similar to Figure 6-8c) for $t \geq t_k$.

Observed and Calculated Deformations

Figure 6-3 shows the observed and calculated reduction in specimen thickness versus the logarithm of time for the eight samples subjected to conventional consolidation tests, and results are seen to be in reasonable agreement. At larger times the theoretical predictions overestimated the total settlement by about 10 percent, which is generally within the range of experimental error associated with sampling and testing procedures.

Variation of Parameters with Natural Water Content

The various empirical parameters needed to estimate the secondary compression of dredgings, both before and after t_k, are plotted in Figure 6-10 as a function of natural water content, w_n. For all practical purposes there seems to be no dependence of any of the parameters on water content within the water content range from 45% to 65%. The average values of the viscosity parameters, $1/\lambda$ and $1/\lambda_1$, are 2.0×10^8 and 1.6×10^8 kN·min/m^2, respectively. The ratio of the two components of secondary compression, b and b_1, to the primary compressibility component, a, varies from 0.85 to 1.45 and from 0.65 to 1.15, respectively,

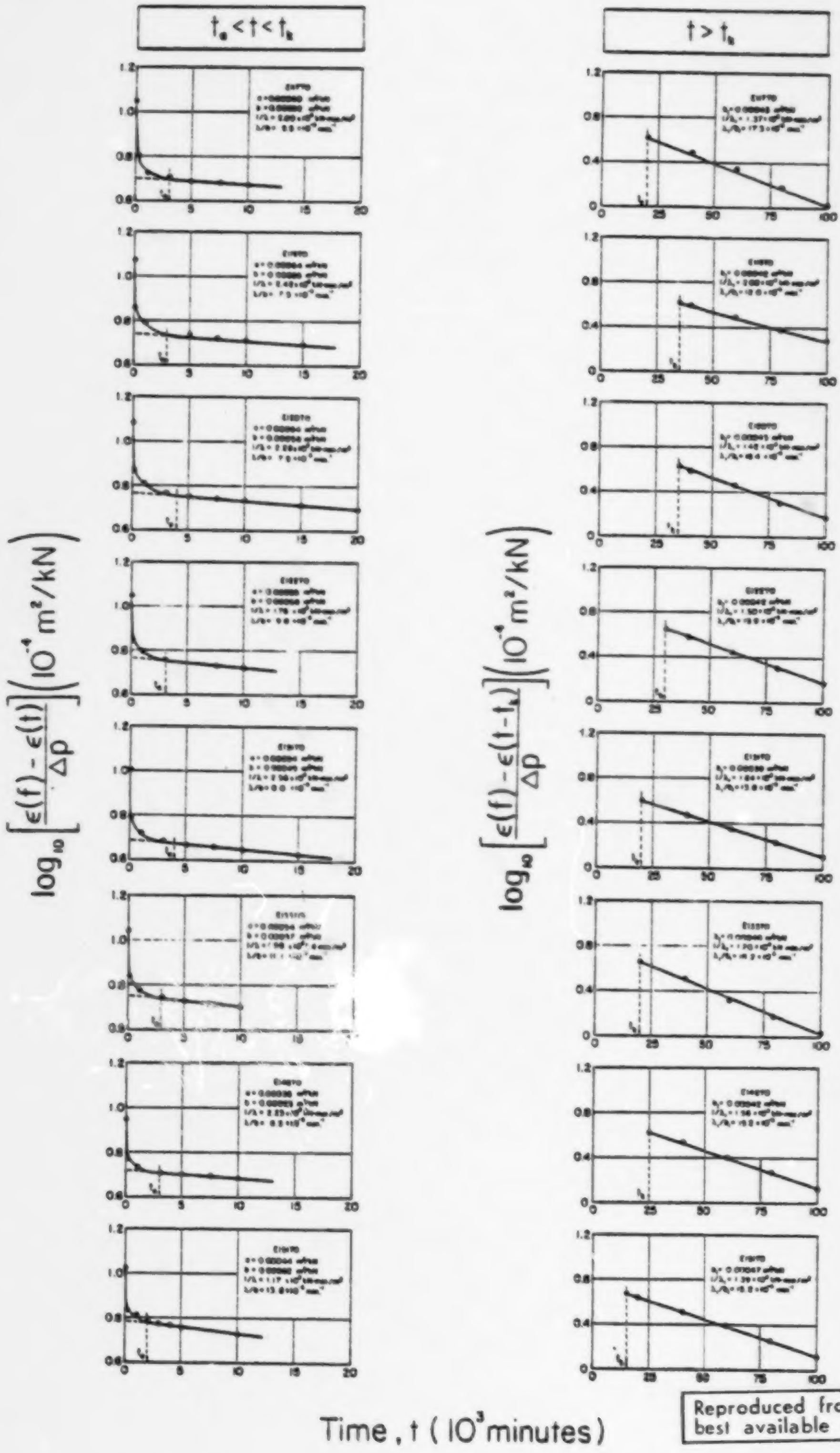

Reproduced from best available copy.

Figure 6-9. Determination of Parameters for Dredging Samples

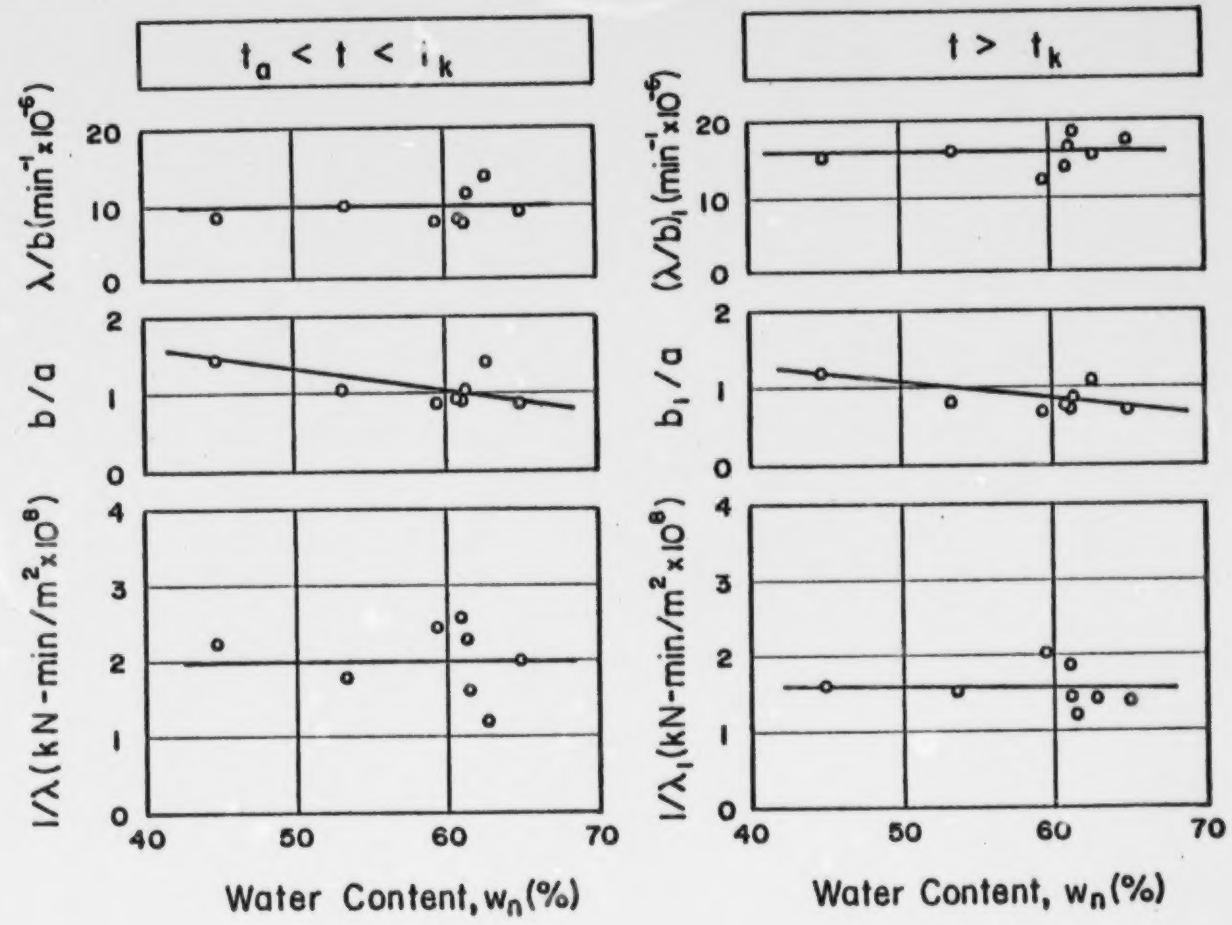

Figure 6-10. Variation of Parameters with Natural Water Content

with average values of about 1.0 and 0.8. The factors λ/b and λ_1/b_1 represent combinations of parameters which govern the rate of secondary compression, and these manifest narrow bands of scatter about average values of 10×10^{-6} and 16×10^{-6} min.$^{-1}$, respectively. Hence, these dredgings samples exhibited higher rates of secondary compression after t_k than before, and this situation prevailed for a relatively long time, after which the settlement approached its ultimate value.

Variation of t_k with Percent Clay

A linear relationship, shown in Figure 6-11, was found between t_k and the percent clay ($< 2\mu$) within the range investigated (35 to 50 percent). An increase of 15 percent in the percentage of clay in a dredging sample is seen to approximately double the value of t_k, which is described in Figure 6-8.

EXAMPLE PROBLEM

Within the range of applicability justified by the limited data presented herein, the total compression of an undisturbed sample of dredgings subjected to a long-duration consolidation test can be readily estimated, even without conducting the test, provided the natural water content and percent clay of the dredgings are known. For example, given a dredgings sample with a natural water content of 60% and a percent clay of 40% subjected to a conventional consolidation test, the total compression of a specimen 2 cm thick loaded from 100 kN/m^2 to 200 kN/m^2 at times of 50,000 and 100,000 minutes may be estimated as follows. From Figure 6-11 t_k corresponding to a 40% clay content is about 23,000 minutes, and Figure 6-10 gives $1/\lambda = 1.9 \times 10^8$ kN·min/m^2, $\lambda/b = 10 \times 10^{-6}$ min^{-1}, $1/\lambda_1 = 1.5 \times 10^8$ kN·min/m^2, $\lambda_1/b_1 = 16 \times 10^{-6}$ min^{-1}, and $b/a = 1$, where-

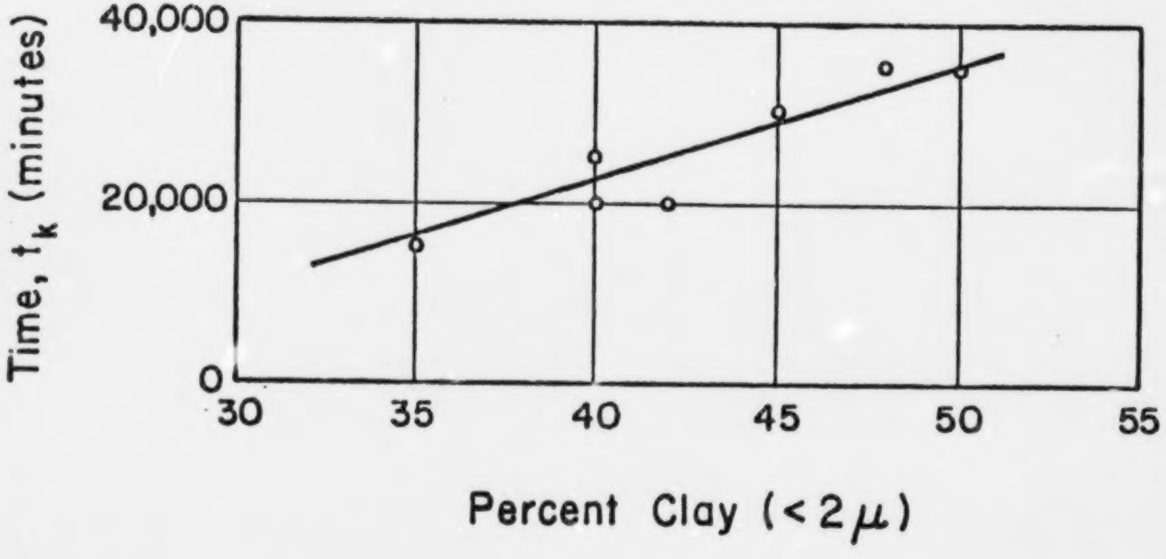

Figure 6-11. Variation of t_k with Percent Clay

upon $b = 5.56 \times 10^{-4}$ m^2/kN, $a = 5.56 \times 10^{-4}$ m^2/kN, and $b_1 = 4.17 \times 10^{-4}$ m^2/kN. Hence, the use of Equation (6-3) with the above values and Δp equal to 100 kN/m^2 yields

$$\Delta H \text{ (at 50,000 minutes)} = 0.19 \text{ cm}$$

and

$$\Delta H \text{ (at 100,000 minutes)} = 0.24 \text{ cm.}$$

Subject to the validity of extrapolating results from small scale laboratory tests to large scale field situations, a similar procedure can be employed to estimate field settlements due to secondary compression.

CONCLUSIONS

Based on this investigation of the secondary compression of various polluted maintenance dredgings subjected to long-term conventional consolidation tests and slurry consolidation tests, the following conclusions can be advanced:

1. After primary consolidation was complete, the secondary compression of all samples tended to increase in essentially a linear manner with the logarithm of time for a considerable period of time, after which the rate of secondary compression increased significantly, reaching a maximum and then decreasing to zero at large times. This type of behavior suggests that a structural break-down of interparticle bonds occurs at some value of strain for each particular load increment.

2. Although the ratio of secondary to total settlement from the slurry consolidation test is much less than that from the conventional consolidation test, the total settlement per unit height associated with corresponding load increments is approximately the same for both types of test.

3. The times necessary to reach ultimate settlements are shorter for the slurry consolidation tests than for the conventional consolidation tests, despite the fact that the thicknesses of the former specimens were about 5 or 6 times those of the latter; this suggests that the times required to obtain ultimate

settlements in the field may be much shorter than those predicted from conventional consolidation test results, but it likewise emphasizes the need for further investigation into the effect of sample thickness and test procedure on the results.

4. The coefficients of secondary compression from both types of test are practically the same for corresponding ranges of load, irrespective of the method of testing and the ratios of secondary to total settlements from each test, and values ranged between 0.002 and 0.013 for a natural water content range from 45 to 65 percent, increasing as a power function for a given load increment. In addition, the coefficient of secondary compression increased exponentially with the consolidation stress for a given natural water content and linearly with the compression index for a given load increment.

5. The theory advanced by Lo (1961) was used to describe the observed response, and the parameters involved were evaluated quantitatively and correlated with the natural water content and percent clay of the dredgings to facilitate a rapid estimate for anticipated settlements.

CHAPTER 7

PERMEABILITY AND DRAINAGE

The potential usefulness of landfills composed of dredged materials depends to a large extent on their ability to be dewatered, and this is related directly to their permeability and drainage characteristics. Accordingly, the work described in this chapter was undertaken to enhance our understanding of these important properties and to provide quantitative data for use in subsequent evaluations. Since the bulk of the maintenance dredgings under consideration are fine-grained, the major emphasis is directed toward a study of these materials. Several series of laboratory and field tests have been conducted on undisturbed and remolded samples of dredged material, and, insofar as possible, correlations are deduced among the various dependent and independent variables.

EXPERIMENTAL PROGRAM

Included in this experimental program are tests involving gravity drainage, vacuum drainage, electro-osmosis, direct permeability, conventional consolidation, slurry consolidation, and field infiltration. The samples were taken from several harbors around the Great Lakes, but the majority of them came from the vicinity of Toledo, Ohio; in virtually all cases the materials were taken directly from fill areas or from the discharge pipes through which the materials were pumped in slurry form. Chapter 3 presents a characterization of these materials in terms of their mineralogy, organic content, Atterberg limits, and grain size parameters. The materials were tested over a broad range of water contents, depending on the stage of the disposal-sedimentation-consolidation process at which the sample was taken. Since the grain size characteristics of soils play such an important role in permeability determinations, it is instructive to study the gradation curves shown in Figure 7-1 for four typical samples, each with and without the addition of Calgon; the significant differences in the particle size distribution curves obtained from tests with and without the addition of Calgon reflect the flocculating effect of the Calgon on the so-called "equivalent particle diameter." Based on gradation tests from over 30 additional samples, the effective grain size, D_{10}, was approximately 0.00045 ± 0.00010 mm and the coefficient of uniformity, C_u, was about 20 ± 10 with a few values around 40. Hence, most of the dredgings tested were found to be relatively well-graded, fine-grained materials, and their permeability and drainage characteristics, as deduced from a variety of test procedures and associated interpretations, are described in the following sections.

Drainage

Three series of drainage tests were conducted to study the rate of water loss from several different dredging materials due to (a) gravity only, (b) gravity plus vacuum with the air pressure being directly applied to the surface of the dredgings, and (c) gravity plus vacuum with a membrane between the surface of the dredgings and the atmosphere. The first and second series used essentially the same equipment and procedures, with the second series incorporating several minor improvements based on the experience gained in the first series; in the third series, only gravity drainage was used.

Equipment and Procedures -- The test equipment consisted of a series of plexiglass cylinders (7½ or 15 cm in diameter and 50 or 60 cm high) with porous stones fitted into the bottom of each cylinder; the effluent was

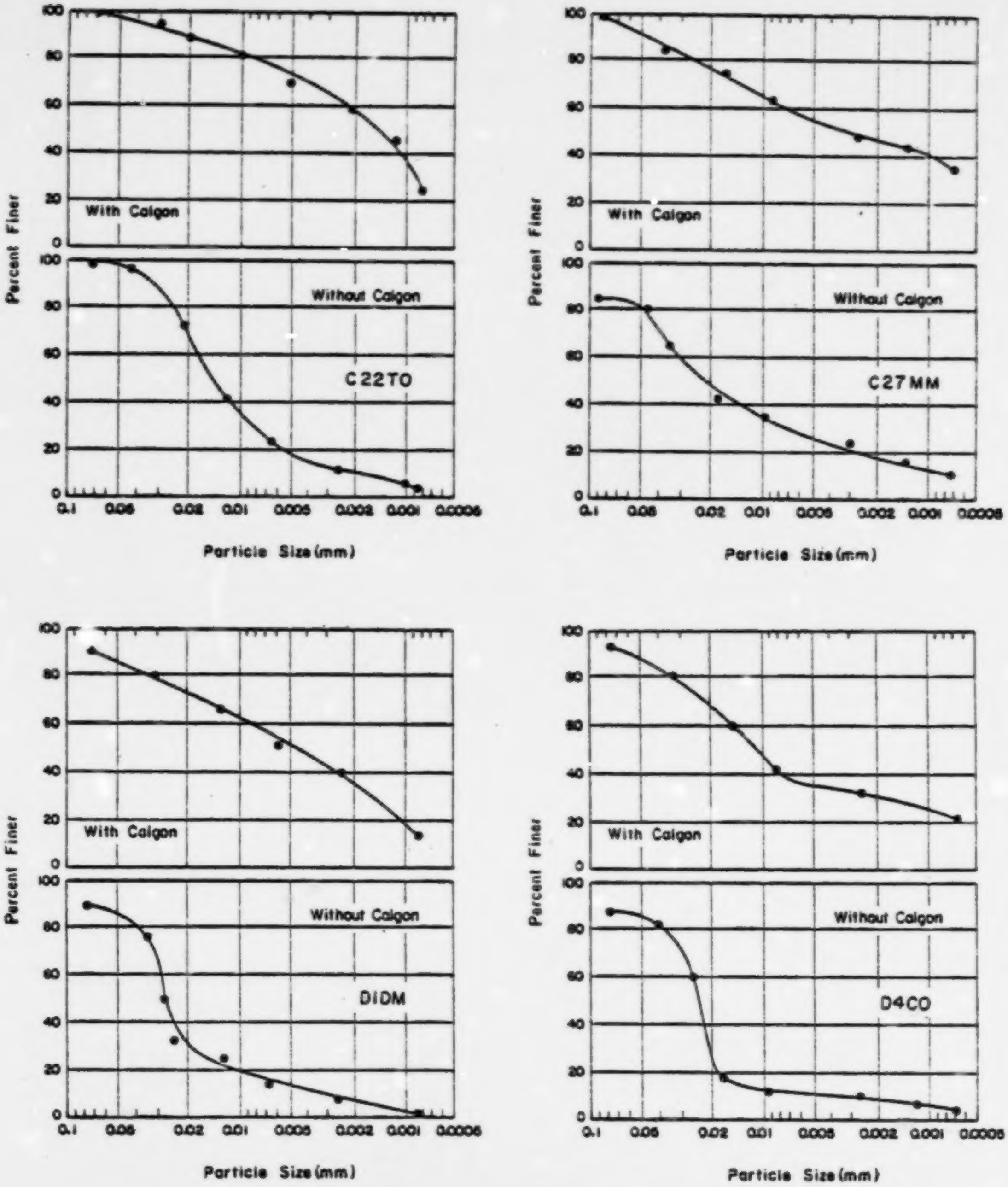

Figure 7-1. Particle Size Distribution Curves

collected in bottles, and the bottle was either vented to the atmosphere for gravity drainage or connected to a vacuum line for vacuum drainage. Two variations of vacuum drainage were used; in the first the air pressure due to the atmosphere was applied directly to the surface of the dredgings, whereas in the second a membrane was placed between the dredgings and the atmosphere. Although all tests were conducted in a humid room to minimize incidental water losses, it was found during the first test series that significant moisture was still being lost through the top surfaces; hence, one improvement in the second and third series was to use a smooth fitting plexiglass disk for the top plate. The adequacy of this arrangement was proven by showing that the water losses from a cylinder filled with only water and no drainage allowed were insignificant. The test data also revealed significant losses of water due to evaporation from the collection bottles which were under vacuum, but losses from the bottles vented to the humid room atmosphere were insignificant. Corrections were made for these losses by using the data obtained from weight changes in a bottle of water on the vacuum line, but not connected to a specimen. Samples of the drainage water were taken for chemical analysis to determine the pollutants which are translocated with the effluent.

Analysis of Results -- Figure 7-2 gives plots of the cumulative weight of the water lost as a function of time for five typical dredgings (C2DM, C5CO, D1DM, D3TO, and D4CO) drained under three different conditions; the C samples are from the first series, whereas the D samples are from the second series. The discontinuity in the drainage rates for the C samples is attributed to a continually worsening leak in the vacuum line; when fixed on the ninth day of the test, the time rate of drainage accelerated greatly for a few days. A study of the data presented in this figure

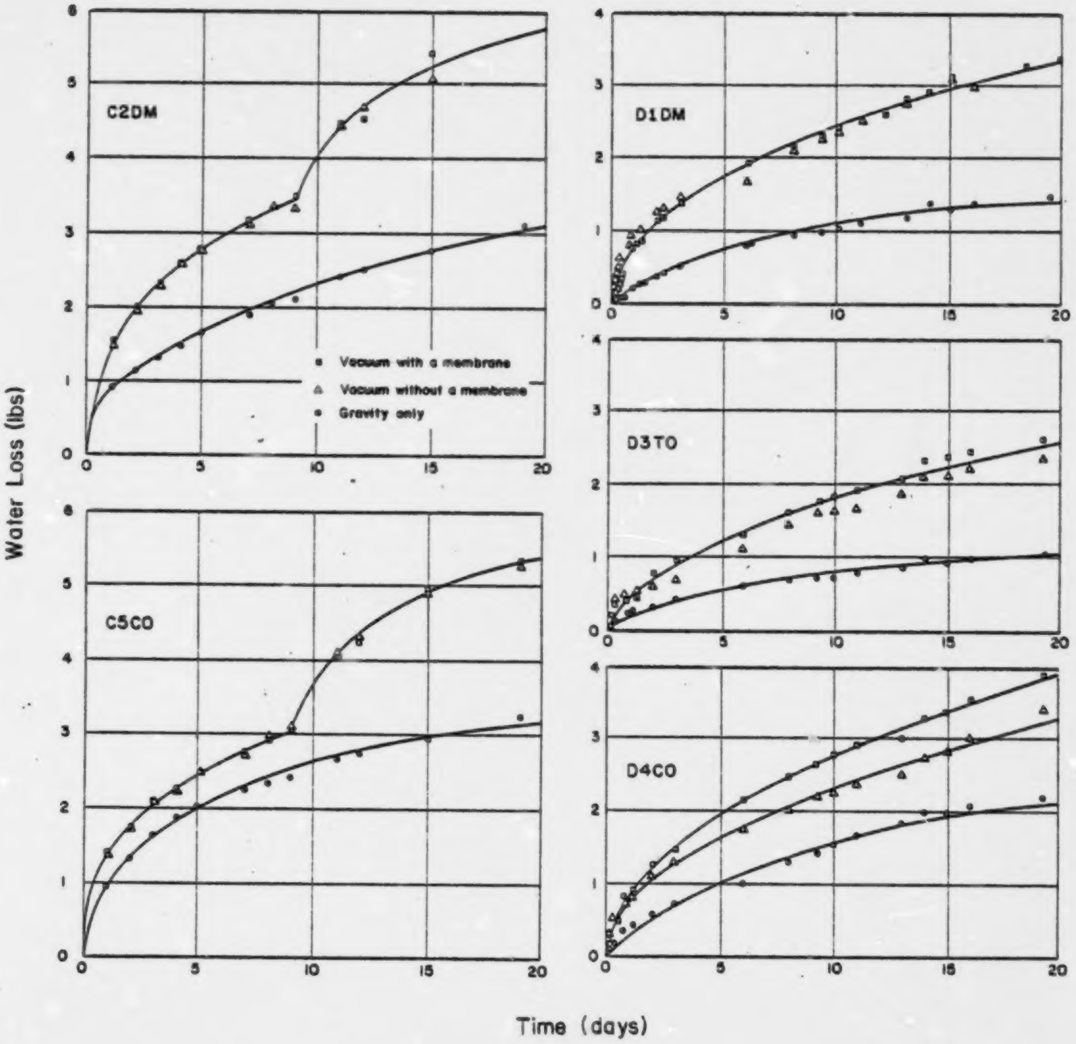

Figure 7-2. Rates of Drainage by Gravity and Vacuum Methods

indicates that (a) the use of a vacuum extracted significantly larger quantities of water from the dredgings than did gravity alone and (b) the major effect of the vacuum occurs during the initial time period. For example, the drainage amounts after one day with vacuum were from one and a half to five times the amounts obtained for gravity alone; viewed differently, the amount of drainage with vacuum during the first five hours was about the same as by gravity alone for the first day or two, while the drainage by vacuum for one day was comparable to that by gravity alone for about a week. After three weeks, the amounts of drainage by gravity alone were about one-half of those achieved by vacuum for all samples.

The results of the drainage tests for Samples D1DM, D3TO, and D4CO were used as follows to compute the coefficient of permeability, and the results are summarized in Table 7-1. The average flow rate, q, was determined from the total amount of water drained in the first 9 days; then, with a knowledge of the sample height and the height of water, the gradient, i, was calculated, and the permeability was computed by use of the expression

$$q = k\ i\ A, \tag{7-1}$$

where A is the cross-sectional area of the test specimen. In the case of the vacuum tests, the vacuum was converted to an equivalent head, and the same procedure outlined above was used. Although extracting greater quantities of water in a given time, the vacuum tests employed a greater applied head and thus generated a greater flow resistance; the head for the vacuum test was about 20 times that for the gravity test, and the flow resistance was increased by a factor of about 10, as reflected in the lower values of k for the vacuum tests.

Table 7-1

Coefficient of Permeability from Short-Term Drainage Tests

Sample	Coefficient of Permeability (cm/sec)	
	Gravity Only	With Vacuum
D1DM	3.4×10^{-6}	4.1×10^{-7}
D3TO	2.6×10^{-6}	3.5×10^{-7}
D4CO	5.1×10^{-6}	4.9×10^{-7}

Table 7-2

Coefficient of Permeability from Direct Tests

Sample	Coefficient of Permeability (cm/sec)
E78TO	9.1×10^{-8}
E80TO	1.2×10^{-8}
E64TO	1.3×10^{-8}
E70TO	2.0×10^{-8}
E59TO	6.1×10^{-7}
E62TO	2.5×10^{-8}

Table 7-3

Coefficient of Permeability from Single-Load Consolidation Tests

Sample	Coefficient of Permeability (cm/sec)
C22TO	3.2×10^{-7}
C27MM	5.5×10^{-7}
D1DM	2.9×10^{-7}
D4CO	9.0×10^{-7}

Figure 7-3 presents the results from six tests in the third series, which employed gravity drainage only; the top part of the figure describing each test gives the changing levels of the sediment and water surfaces as a function of time, and the lower part of each figure gives the weight of the water lost. An examination of the height-versus-time curves presented in this figure reveals that, shortly after the test was begun, the material settled and left a zone of relatively clear water above it. As drainage occurred, the sediment densified, and its top surface lowered initially more rapidly than the water surface. At a later stage in the drainage process, the surface of the sediment tended to stabilize as the water continued to drain from the specimen, until eventually the water surface reached the sediment surface. All four materials tested in this series had an initial thickness of about 18 inches (45 cm), but the time for drainage varied considerably for the different materials and with different concentrations of solids for a given material. The drainage times varied from about one day for sample C3TO at a water content of 2500% to periods in excess of 100 days. Several of the tests (C3TO with an initial water content of 1100% and both tests on C22TO) were concluded before all the free water had drained.

Permeability determinations were made for these samples, and the results are plotted in Figure 7-4, where it is seen that the permeability decreases rapidly with decreasing void ratio. Since these tests extended over longer periods of time, it was possible to approximate the permeability at points throughout the drainage process; an incremental flow quantity, q, was averaged over a short period of time, and this value, together with the head and length of flow path associated with that time, were used with Equation (7-1) to compute the coefficient of permeability. The steeper

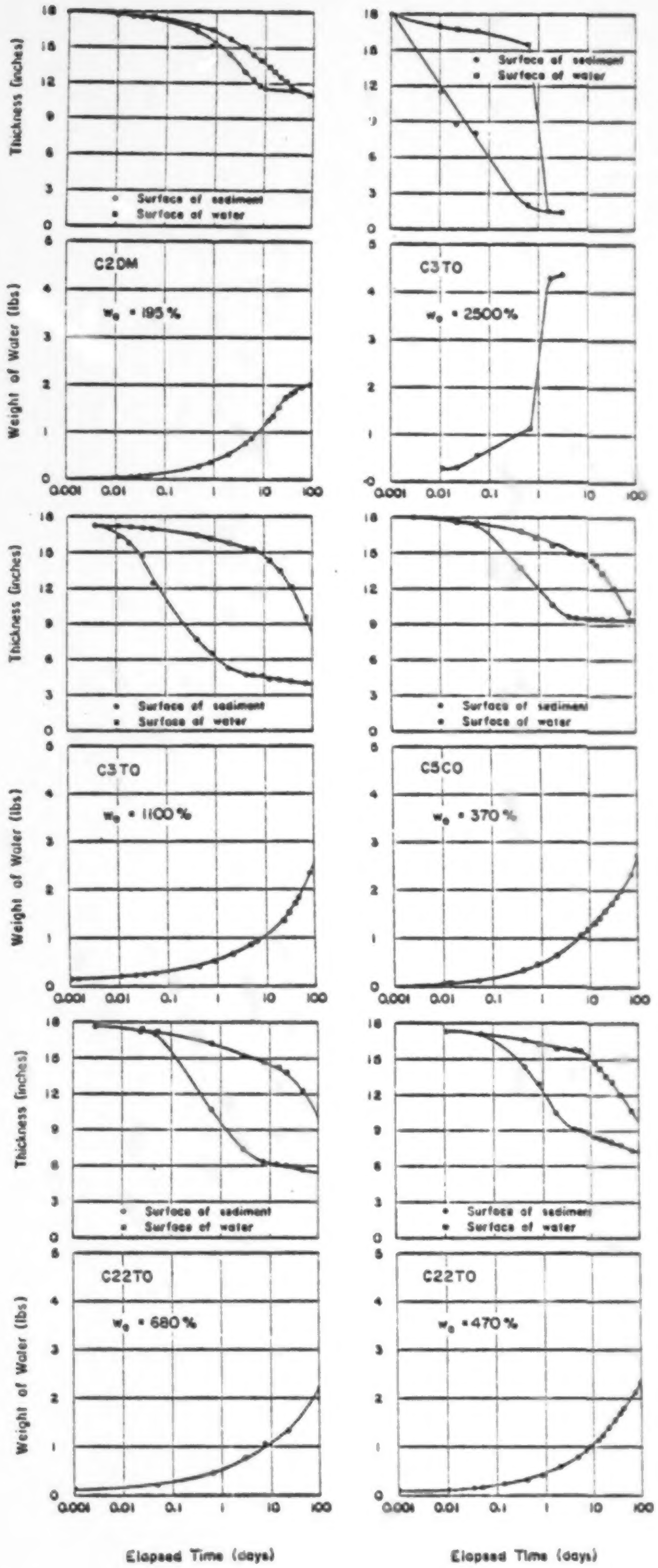

Figure 7-3. Data from Gravity Drainage Tests

Reproduced from
best available copy.

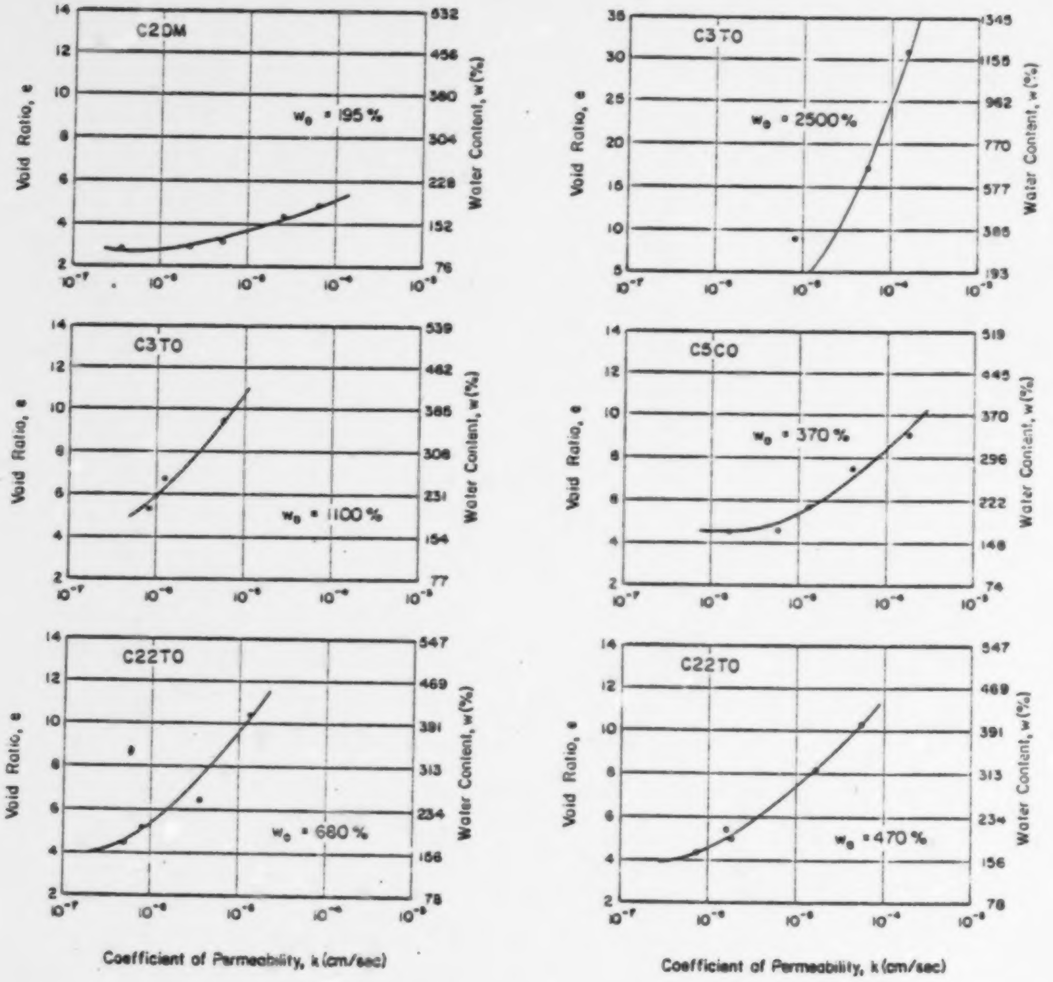

Figure 7-4. Permeability as a Function of Void Ratio or Water Content

curves are found for the samples with the lower initial concentrations of solids, thereby indicating a rapid drop in permeability with decreasing void ratio. The range of permeabilities extended from about 10^{-4} to 10^{-6} cm/sec, with the higher values being obtained at the beginning of the test and the lower values at the end. The thicker material (C2DM) had the smallest change in void ratio during the test, but it still ended with the lowest void ratio of any sample in the test series.

Direct Permeability

The Anteus consolidation device (Lowe, Jonas, and Obrician, 1969) was used to conduct direct permeability tests on six dredgings. "Undisturbed" samples were trimmed to fit the consolidometer ring, placed in the device, and subjected to 80 psi (552 kN/m^2) back-pressure to achieve a high degree of saturation. After being consolidated under a 10 psi (69 kN/m^2) stress for at least 12 hours, the samples were unloaded and tested to determine their permeability while still under the back-pressure. The test utilized falling head conditions, wherein the driving head fell as the head on the collecting burette rose. The initial head difference was chosen at about 1.5 feet (0.5 meters), and the seepage length was about one inch (2.5 cm). Accordingly, Table 7-2 gives the permeability values calculated by use of the following expression:

$$k = 0.5 \left[\ln \frac{H_1}{H_2} \right] \left[\frac{A_B}{A_S} \right] \frac{L}{\Delta t} , \qquad (7\text{-}2)$$

where H_1 is the initial height of water at t_1, H_2 is the final height of water at t_2, Δt equals $(t_2 - t_1)$, A_B is the area of the burette, L is the length, and A_S is the area of the sample.

Conventional Consolidation

The coefficient of permeability may be computed from conventional consolidation test data by use of the following relationship:

$$k = (a_v \gamma_w c_v)/(1 + e), \qquad (7\text{-}3)$$

where c_v is the coefficient of consolidation, γ_w is the unit weight of water, e is the void ratio, and a_v is the coefficient of compressibility, which is defined as $\Delta e/\Delta p$. In most cases, the permeability was determined when the stress on the specimen was 9 psi (62 kN/m^2), and a_v was taken as the change in void ratio, Δe, for the load increment from 9 to 18 psi (62 to 124 kN/m^2), in which case the stress increment, Δp, would be 9 psi (62 kN/m^2). The results of tests on over 25 undisturbed piston samples of typical dredgings from the Island Site and Riverside Site indicate that virtually all values for k lie between 2×10^{-8} and 4×10^{-8} cm/sec, and there is no apparent correlation with the effective particle size ($0.0004 \text{ mm} < D_{10} < 0.0005 \text{ mm}$), percent clay ($30 < \% \text{ clay} < 50$), coefficient of uniformity ($15 < C_u < 40$), or liquid limit ($45 < w_L < 85$). Similar calculations for the four remolded dredging materials tested in the electro-osmosis study under an applied stress 8.5 psi (59 kN/m^2), but with no electrical gradient, yield the results given in Table 7-3; these k values are approximately one order of magnitude higher than those determined from undisturbed field samples.

Slurry Consolidation

Equation (7-3) was used in conjunction with data from slurry consolidation tests on samples of twelve typical dredgings to evaluate the coefficient of permeability at consolidation pressures of 4, 8, 16, and 32 psi (27.5, 55, 110, and 220 kN/m^2). All values of k for consolidation pressures of 16 or 32 psi (110 or 220 kN/m^2) were found to be less than 4×10^{-8} cm/sec; these values compare very well with values obtained from direct permeability tests at comparable values of void ratio.

Field Tests

Since the permeability of a soil mass is greatly influenced by particle size, gradation, and density (or void ratio), it will generally vary considerably in the different zones of a dredgings landfill (Giger, Franklin, and Krizek, 1973; Krizek, Soriano, and Franklin, 1974). In addition, due to the existence of sand and silt lenses and peaty material from the annual growth of vegetation, the average permeability is probably greater in the horizontal direction than in the vertical. Thus, the fill as a whole would be expected to be heterogeneous and anisotropic with respect to permeability. For this reason the data from any and all laboratory permeability tests must be viewed with caution, because it represents only discrete points in a problem which is governed more realistically by a global response. Therefore, permeability data from laboratory tests must be regarded simply as order-of-magnitude values to aid in planning more precise laboratory and/or field permeability testing programs and to facilitate preliminary calculations for drainage schemes.

In an effort to shed some light on the insitu field permeability of a spoil area, two infiltration tests were conducted at Riverside Site. The water table was about 1.5 to 3.0 feet (0.5 to 1.0 meters) below the surface, and wells with a perforated tip surrounded by a sand filter were placed approximately 7 feet (2 meters) deep. The wells were pumped dry and the time rate of recovery was measured; data were interpreted according to the procedure outlined by Lambe and Whitman (1969; pp 284-285, Case G) with the assumption that the coefficient of permeability is isotropic, and the results indicate k values of approximately 10^{-4} cm/sec for the well located in about the middle of the disposal area and approximately 10^{-5} cm/sec for the well near the outflow weir. These values are both consistent with engineering reasoning. First, both values are significantly higher (three orders of magnitude) than those obtained from laboratory tests on samples from essentially the same locations; the probable reasons for the observed discrepancies are suggested above and probably are due in large part to the seasonal stratifications associated with dormant periods between dredging seasons. And second, the k value determined from the well near the outflow weir is about one order of magnitude smaller than that obtained from the well in the middle of the disposal area; this may be readily explained by the fact that the finer materials tend to accumulate near the overflow weir. Reasonable (within possible experimental error) modifications in the parameters used in the above described interpretation procedure (for example, the length of the filter at the well tip) were found to change the computed permeability values by a maximum of about 25 percent, and the assumption of an anisotropic coefficient of permeability increased the calculated values by about 100 percent for $k_h = 10\ k_v$; hence, the orders of magnitude for the measured permeability values are not affected by such variations in the interpretation procedure.

Electro-osmosis

A series of electro-osmosis tests with average electrical gradients of 0, ½, and 1 volt per centimeter and a pressure gradient of approximately 0.1 $kN/m^2/m$ was conducted on four dredging samples (Krizek, Karadi, and Hummel, 1973). The grain size distributions for the materials tested are given in Figure 7-1, and the average results evaluated at either 10, 20, or 40 hours after the test was begun are summarized in Table 7-4. The electro-

Table 7-4

Average Electro-osmotic Coefficient of Permeability and Flow Efficiency

Sample	Time (hours)	Electro-osmotic Coefficient of Permeability, k_e (cm^2/volt-sec)	Flow Efficiency	
			$\frac{\text{milliliters}}{\text{watt-hour x liter}}$	$\frac{\text{gallons}}{\text{watt-hour x cu. yd.}}$
C22TO	20	1.49×10^{-5}	17.9	3.62
	40	1.31×10^{-5}	17.9	3.62
C27MM	20	2.70×10^{-5}	24.6	4.97
	40	2.02×10^{-5}	23.1	4.66
D1DM	10	4.54×10^{-5}	30.4	6.14
	20	3.30×10^{-5}	27.4	5.54
D4CO	10	3.69×10^{-5}	13.0	2.62
	20	2.78×10^{-5}	12.9	2.60

osmotic coefficient of permeability, k_e, was determined from the relationship

$$k_e = q/\bar{v} A , \qquad (7\text{-}4)$$

where q is the time rate of fluid flow, A is the cross-sectional area perpendicular to the direction of flow, and $\bar{v}$ is the average voltage gradient across the sample, and the results range from about 1.5×10^{-5} to 4.5×10^{-5} cm^2/volt-sec; these values are of the same order of magnitude as those which characterize a large variety of soils, namely 5×10^{-5} cm^2/volt-sec.

By using cumulative flow quantities for the indicated times and defining the energy consumed during the associated time interval as the area under the current-time curve multiplied by the applied voltage, we can determine the effectiveness of the electro-osmotic treatment; as seen in Table 7-4, the quantity of water removed from each of the four materials varies from about 3 to 6 gallons per watt-hour per cubic yard (or 15 to 30 milliliters per watt-hour per liter) of material. However, the energy comsumption increases sharply for time periods longer than those selected; for example, Table 7-5 shows that approximately 75 to 95 percent of the total flow after 6 days occurs in the selected time periods, and additional treatment produces little additional drainage. Values are given in Table 7-5 for total flow and bottom flow because the specimens were drained at both the top and the bottom, but the electrical gradient was applied in one direction only; hence, in one half of the specimen the pressure gradient and the electrical gradient oppose each other, whereas in the other half they are additive. A good check on experimental reliability can be obtained by comparing these two flow values for the case of no

Table 7-5

Comparison of Dewatering Rates With and Without an Electrical Gradient

Sample	Time	Electrical Gradient			
		None		1 volt/cm	
		Total Flow (liters)	Flow from Bottom (liters)	Total Flow (liters)	Flow from Bottom (liters)
C22TO	6 days	0.91	0.48	1.15	0.96
	20 hours	0.50 (55%)	0.24 (50%)	0.60 (52%)	0.43 (45%)
	40 hours	0.71 (78%)	0.35 (73%)	0.89 (77%)	0.71 (73%)
C27MM	6 days	0.89	0.45	1.17	1.07
	20 hours	0.56 (63%)	0.28 (63%)	0.73 (63%)	0.64 (60%)
	40 hours	0.76 (85%)	0.38 (85%)	1.05 (90%)	0.95 (89%)
D1DM	6 days	0.59	0.31	0.94	0.80
	10 hours	0.49 (83%)	0.25 (81%)	0.67 (71%)	0.54 (67%)
	20 hours	0.57 (97%)	0.30 (97%)	0.88 (94%)	0.74 (93%)
D4CO	6 days	0.94	0.48	1.10	0.94
	10 hours	0.59 (63%)	0.29 (60%)	0.69 (63%)	0.54 (57%)
	20 hours	0.83 (88%)	0.42 (88%)	0.98 (89%)	0.82 (87%)

electrical gradient; the total flow quantities should be double the flow quantities from the bottom only, and this is approximately true.

Although certain similarities exist between fluid flow due to an electrical gradient and fluid flow due to a hydraulic pressure gradient, the physics of the situation suggests that there are substantial differences. For example, in fluid flow due to a hydraulic gradient various soluble ions may translocate with the pore fluid and leave the soil as it is drained, or they may be leached from the soil as fresh water becomes available from precipitation; however, in fluid flow due to an electrical gradient the electrical current causes the cations to migrate toward the cathode, and they carry the water with them. In the latter process the soil is depleted of its cations much more rapidly than in the former process, and the major effect is noticed quickly in a soil subjected to electro-osmotic treatment. Tests on the effluents extracted from the dredgings indicated that the electro-osmotic treatment removed substantial amounts of soluble ions from the specimen with the quantity increasing as the electrical gradient increased, but the heavy metals remained in the sediments, regardless of the degree of the electrical treatment.

POTENTIAL INFLUENCE OF ORGANIC CONTENT AND GAS GENERATION

Little is known regarding the effect of organic content on the permeability of a soil. Some evidence (Arman, 1970) indicates that, if organic matter of a fibrous nature is present in a clay or silt, the coefficient of permeability, k, increases rapidly until the organic content reaches about 40 percent, after which there is not much additional change. However, exactly the opposite happens for sands, with the coefficient of permeability stabilizing again at about 40 percent organic content. In a plot of permeability versus organic content, the curves for sand, silt, and clay converge at around 40 percent organic content to a constant value -- the sand from above and the clay and silt from below -- that seems to be the coefficient of permeability of the organic matter alone. Although the above behavior was reported for the case of fibrous organic matter, there was no data concerning the effect of finely divided organic matter on the permeability (that is, organic matter with a particle size similar to silt or clay). However, organic matter in dredgings may have a more complex influence on permeability, depending upon the degree of humification and the chemical composition of the organic matter. While fibrous peaty material may provide an open, porous, permeable soil, a fine-grained organic matter may adsorb water and swell, thereby blocking the pore passages and impeding the flow of water through the soil. In a similar fashion, fats, grease, and oil may tend to obstruct the pore passages in a fine-grained soil.

The degree of saturation is known to exert a large influence on the permeability of a given soil. Since many of these polluted dredgings are actively decomposing various organic compounds and generating gases in the process, the entrapped gases tend to block pore passages and thereby constitute a complex and influential factor in the permeability of these materials. In some cases the response for the low intensity of loading in the slurry consolidation tests show an increasing void ratio with time, thereby indicating that the pressures developed by the generated gases exceed the applied pressures and cause an expansion of the sample; however, the more regular behavior at the higher loadings suggests that gas generation may decrease with time and be suppressed at higher loadings.

SYNTHESIS OF RESULTS

As summarized in Figure 7-5, values for the coefficient of permeability were found to range from about 10^{-4} to 10^{-9} cm/sec, depending primarily on the void ratio of the specimen (which is, in turn, related to the type of test). The dredgings with the highest void ratios ($2 < e < 10$) were tested in the drainage tests, and permeability coefficients on the order of 10^{-4} to 10^{-6} cm/sec were determined; for the drainage tests in which a partial vacuum was applied (thereby consolidating the sample somewhat and decreasing the void ratio), k values on the order of 10^{-6} to 10^{-7} cm/sec were obtained. Void ratios in the slurry consolidation tests ranged from about 1.3 to 2.4, and the resulting coefficients of permeability were approximately 10^{-7} to 10^{-8} cm/sec. The direct permeability tests, the single-load consolidation tests, and the conventional consolidation tests were conducted on samples with void ratios on the order of 0.6 to 1.9, and the associated permeability values lie between 10^{-7} and 10^{-9} cm/sec with most on the order of 10^{-7} to 10^{-8} cm/sec. As expected, the insitu field tests yielded much higher values for the permeability (10^{-4} to 10^{-5} cm/sec); this was probably due in large part to the seasonal stratifications associated with dormant periods during the dredging seasons. Finally, the electro-osmotic coefficient of permeability (not plotted in Figure 7-5) was found to range from about 1.5×10^{-5} to 4.5×10^{-5} cm^2/volt-sec, and this value is consistent with that found for a large variety of soils.

CONCLUSIONS

Within the framework of the study presented in this chapter, the following conclusions may be advanced:

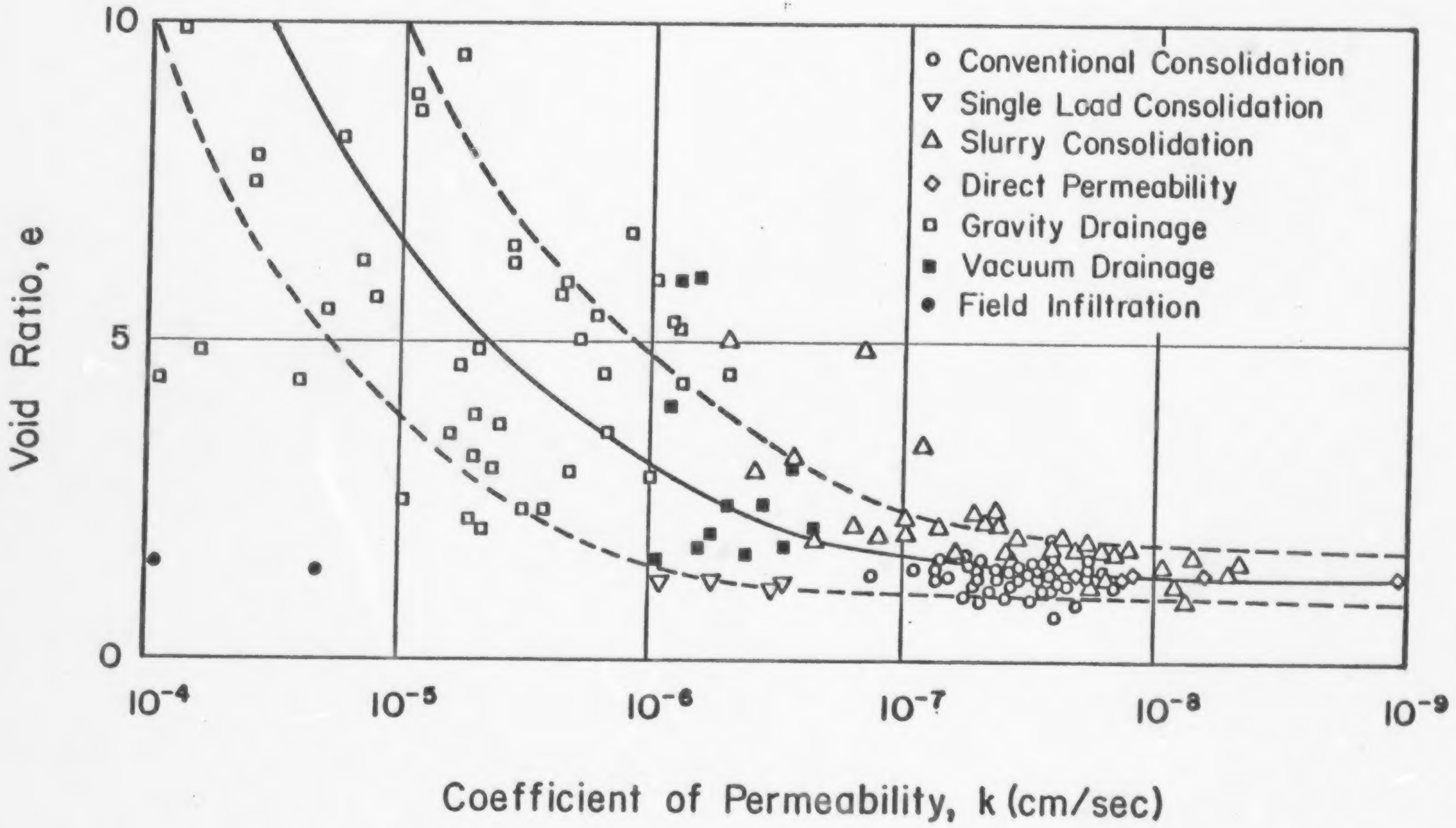

Figure 7-5. Summary of Values for Coefficient of Permeability

1. The coefficient of permeability is strongly dependent on the void ratio and decreases from about 10^{-4} to 10^{-9} cm/sec as the void ratio decreases from approximately 10 to 1. Most permeability values for the firmer materials, which had void ratios on the order of 1 to 2, were in the range of 10^{-7} to 10^{-8} cm/sec.

2. Different dredgings drain at different rates and are affected to different degrees by the application of a partial vacuum. In general, vacuum drainage was found to remove water from dredgings much faster than gravity drainage alone, and it allowed greater amounts of water to be extracted in a given period of time. However, the maximum effect of vacuum on the drainage response was achieved during the initial time period, and less significant effects were observed over longer periods of time.

3. Field infiltration tests yielded permeability coefficients approximately three orders of magnitude higher than those obtained from laboratory tests on undisturbed and remolded samples with comparable void ratios.

4. The electro-osmotic coefficient of permeability was found to be about 3×10^{-5} cm^2/volt-sec, which is approximately one-half the value determined for a large variety of soils.

CHAPTER 8

SHEAR STRENGTH

This chapter deals with an investigation of the laboratory and field shear strength characteristics of dredged material placed in four different sites near Toledo, Ohio. Field vane tests were conducted at each site and piston tube samples were taken to perform three different types of laboratory strength tests, namely, miniature vane, fall cone or penetration, and unconfined compression tests. Comparisons are made between field and laboratory values, and the time-dependent gain in strength is evaluated. Finally, in an effort to provide a quick measure for estimating the shear strength and sensitivity of dredged material in a landfill, correlations are established among shear strength, sensitivity, secant modulus, water content, dry density, and liquidity index.

TEST PROGRAM

Included in this section are descriptions of the various techniques used to measure the shear strength of dredged materials in the field and in the laboratory. Also reported in detail are data from tests conducted during 1973 and 1974; similar results for 1971 and 1972 are presented by Krizek, Karadi, and Hummel (1973).

Field Tests

The field vane test was first used as a means for measuring the undrained shear strength of deep clay strata by Carlson (1948) in Sweden. Another form of this test was developed in England to overcome the difficulty of penetrating hard layers of soil or sand or gravel strata overlying the clay (Skempton and Bishop, 1950). Also, a vane shear apparatus was developed by the Bureau of Reclamation (Gibbs, 1956) and used for extensive field work, examples of which are reported by Gibbs, Hilf, Holtz, and Walker (1960). However, most of the pioneering work on the development of this test was done in Sweden and is reported by Cadling and Odenstad (1950).

At the time of testing, the blades of the vane should be located at a depth sufficient below the casing to be reasonably sure that the clay is free from any appreciable disturbance or change in stress; also, the dimensions of the apparatus should be selected so that the corrections due to adhesion of the clay to the vane spindle and due to friction in the bearings will be only a small percentage of the measured results. The field vane is used mainly in deep beds of soft clay or silt, particularly when high sensitivity makes undisturbed sampling difficult or unreliable. Since the results of a vane test represent the shear strength which can be mobilized if the clay is brought to failure without any dissipation of pore pressures, the vane shear strength is comparable to the shear strength determined by an unconfined compression test (Andresen and Bjerrum, 1958). The vane strength, however, can not be directly related to the Coulomb strength parameters, c and ϕ, in terms of effective stresses.

The theoretical relationship between shear strength and applied torque on the vane can be established by the simple integration of moments due to resisting forces acting on the top, bottom, and curved surface of a cylinder with the dimensions of the vane; hence, the total torque, T, is given by

$$T = T_1 + 2T_2 \tag{8-1}$$

where T_1 is the resisting torque on the vertical cylindrical surface and T_2 is the resisting torque on the horizontal top and bottom surfaces. Assuming a constant unit shear strength, s, T_1 and T_2 may be expressed as

$$T_1 = (2\pi r h) r s = 2\pi s h r^2 \tag{8-2a}$$

$$T_2 = 2\pi s \int_0^r \rho^2 d\rho = 2\pi s \frac{r^3}{3} \quad , \tag{8-2b}$$

where h and r are the height and radius, respectively, of the vane. For the case where h = 4r (which is very common), we have

$$s = \frac{3T}{28\pi r^3} \quad . \tag{8-3}$$

Hence, for a given vane the shear strength is linearly related to the measured torque.

The Swedish vane borer, which was used for in situ shear strength determination reported herein, consists of four rectangular blades attached to a shaft. To conduct a strength test, the vane is pressed into the soil in the direction of the shaft until the desired position is reached; then, it is rotated slowly through a torque measuring device until a peak torque (failure) is reached. A vane rotation of six degrees per minute is suggested (Cadling and Odenstad, 1950) as a compromise between expediting the conduct of the test and minimizing the rate effects on the strength behavior, and this rate has been used throughout the field test program. The equipment was essentially identical to that described by Cadling and Odenstad (1950), and the torque measuring device (built in Norway), allows controlled measurements by means of a gear driven system in which a handle is rotated uniformly at a rate of 30 revolutions per minute, thereby causing the vane to rotate at 6 degrees per minute; a precise torque spring is used to measure the applied torque.

The test procedure does not require a borehole; the vane, which is inside a protective housing, was pressed into the layer of dredgings to the desired depth, whereupon the vane was extended about 50 cm beyond its housing to its testing position. Next, the torque head was fitted to the supporting pipe and attached to the vane shaft, using the pipe as a reaction for the torque applied to the vane. After the peak torque was reached and recorded, the vane shaft was rotated rapidly through 20 revolutions to remold the soil in the zone where the shear strength was determined. Then, the test was repeated in the usual manner to measure the remolded strength. Following this operation, the vane was retracted into its protective housing, the apparatus was advanced to a new test depth, the vane was extended, and another test was performed. This sequence was repeated until the bottom of the fill was encountered, in which case the vane could no longer be advanced manually. A calibration chart provided with the equipment gives the shear strength as a function of the number of degrees of rotation of the torque spring indicator for each size of vane used. For all field tests reported in this study a vane 6.5 cm in diameter and 13.0 cm in height was used. Several photographs of the field vane and its used are given in Figure 8-1.

Laboratory Tests

Laboratory shear strength tests (miniature vane, fall cone, and unconfined compression) were conducted on piston tube samples obtained from different locations at the four sites; in addition, other supporting tests, such as water content, dry density, Atterberg limits, and grain

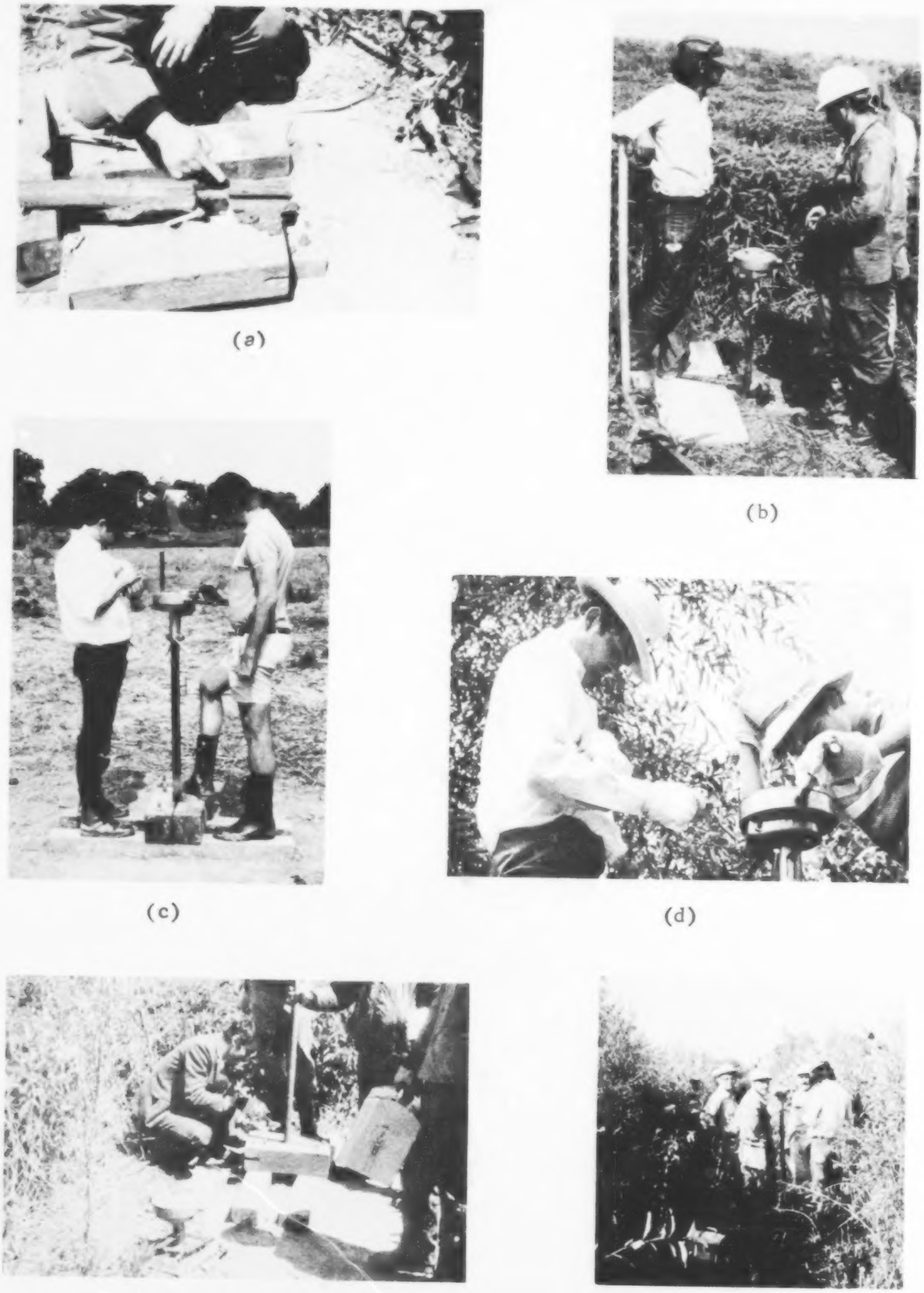

(a)

(b)

(c)

(d)

(e)

(f)

Figure 8-1. Photographs of Field Vane and Its Use

size distribution, were performed. The laboratory vane and fall cone are ideally suited for testing the soft and very soft materials that were usually encountered, whereas unconfined compression tests were performed when the samples were strong enough to extract and trim with a minimum amount of disturbance. Photographs of these three test devices are shown in Figure 8-2.

Laboratory Vane-- The theory and techniques explained for the field vane are equally applicable to the miniature laboratory vane, except that the latter has no protective housing; at the completion of each test, the vane is simply pressed from one test depth to the next. The miniature vane apparatus used for these tests was designed and manufactured in England by Leonard Farnell and Company, Limited. As with the Swedish field vane, the laboratory vane incorporates calibrated springs and a geared operation to allow control over the selected rotation rate of six degrees per minute for the vane. The dimensions of the laboratory vane that was used are 0.5 inch (1.25 cm) for both its height and diameter.

Penetration Test (Fall Cone)-- The cone penetration test is widely used in the laboratory to evaluate the consistency or shear strength of cohesive soils, especially soft ones (Skempton and Bishop, 1950). The force, P, required to cause a penetration, ρ, can be expressed as

$$P = \rho^2 K s \pi \tan^2 \beta \quad , \tag{8-4}$$

where s is the shear strength, 2β is the cone angle, and K is the cone factor. It was found, however, that the value of K varied with water content for a given clay and was strongly dependent on the type of clay (Skempton and Bishop, 1950). Accordingly, the cone test can be considered only as a rough approximation to the undrained shear strength of a clay.

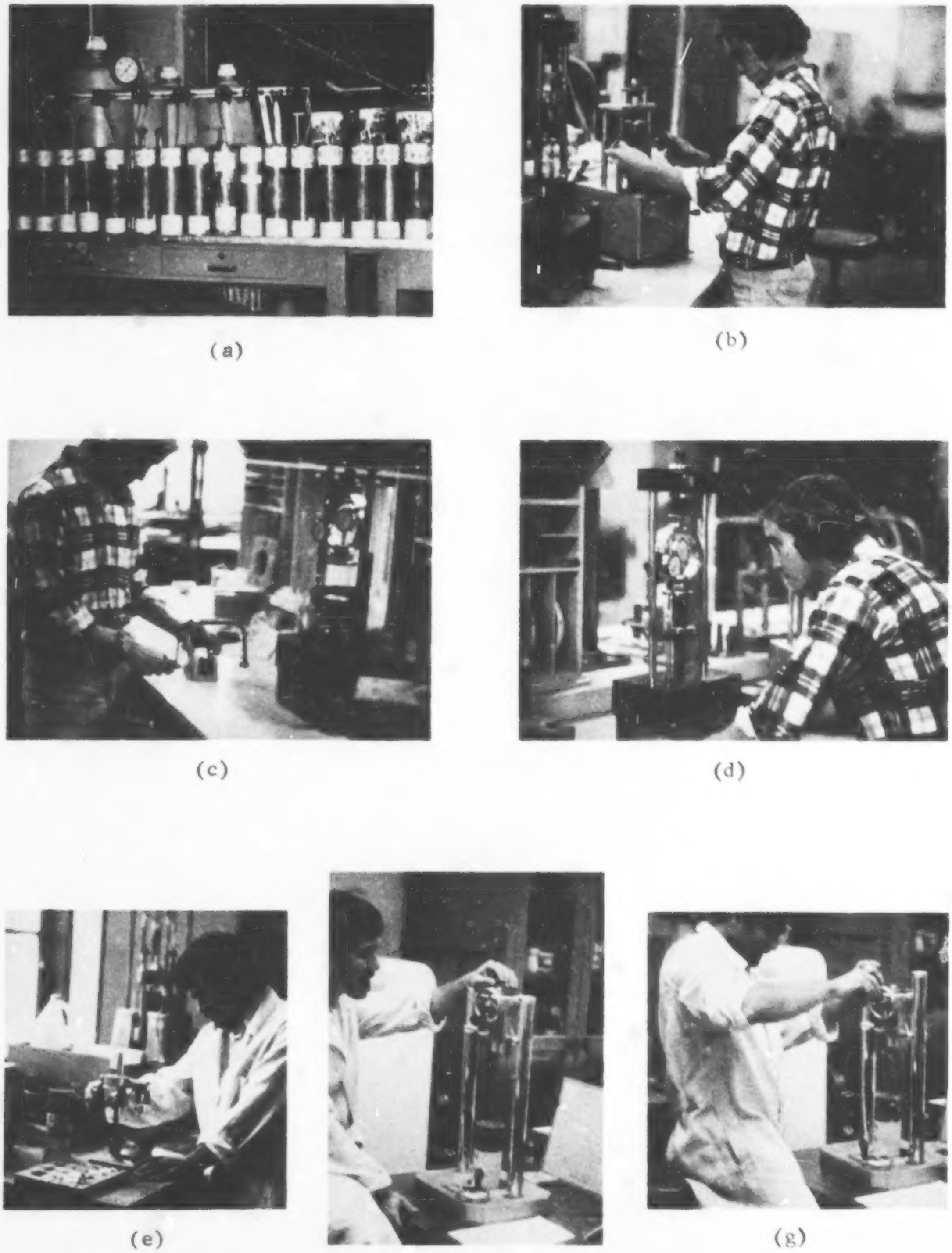

(a) (b)

(c) (d)

(e) (f) (g)

Figure 8-2. Photoghaphs of Laboratory Test Devices

Even as a measure of the sensitivity of one particular clay, the cone test can be misleading, because the cone factor (which depends on the ratio of the soil modulus to the shear strength) will generally be different for undisturbed and remolded soils.

Unconfined Compression Test-- Standard unconfined compression tests were conducted on specimens with a length-to-diameter ratio of about 2.0 to 2.5; the height of these specimens varied between 7.5 cm and 10.0 cm and the diameter varied between 3.5 cm and 4.0 cm. A constant strain rate of approximately one percent per minute was used for all tests, and the dry density and water content were determined for each specimen.

Field and Laboratory Results

The 1973 and 1974 field and laboratory shear strengths, together with sporadic values of water content, Atterberg limits, percent clay, and dry density, are plotted in Figures 8-3 through 8-8 and Figures 8-9 through 8-14, respectively, as a function of depth for locations 3 at the Island Site, 1 and 2 at Penn 8, and 1, 6, and 8 at Riverside Site (see Figure 2-2). Figures 8-15 through 8-23 give similar data for nine locations (2/10, 5/8, 5/10, 5/13, 8/10, 8/13, 12/10, 15/10, and 16/12; see Figure 2-2) at Penn 7; these data were accumulated from tests conducted in May of 1974. Miniature vane and fall cone tests were performed on 16, 21, and 53 tube samples obtained in 1972, 1973, and 1974, respectively. Unconfined compression tests were conducted on 18 samples in 1973 and 16 samples in 1974; stress-strain curves were plotted for all samples, and most exhibited behavioral patterns similar to those of soft clays. Typical plots of data from four tests on samples obtained in 1974 from location 1 at Penn 8 are given in Figure 8-24.

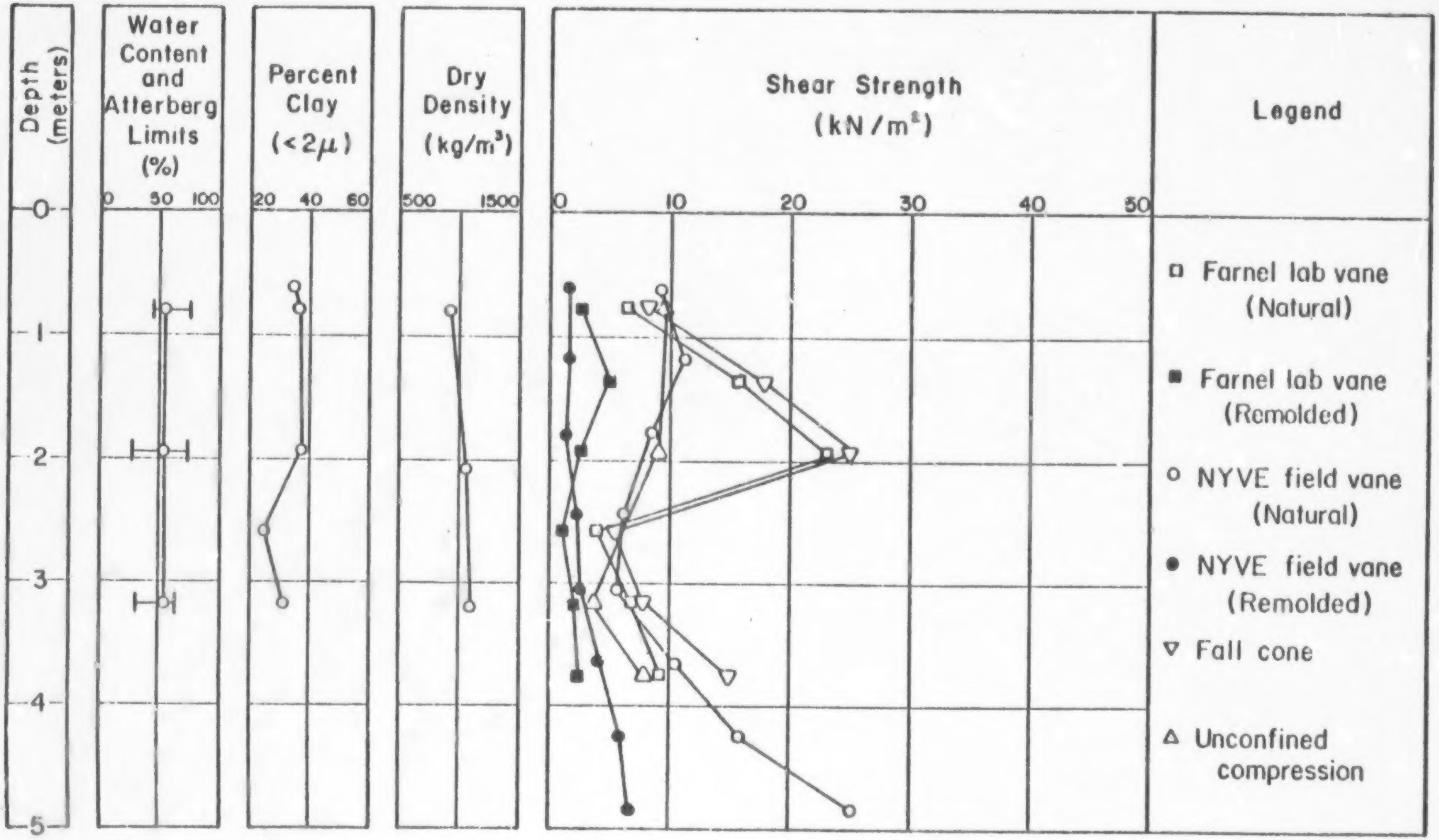

Figure 8-3. Strength Profiles at Location 3 of Island Site (1973)

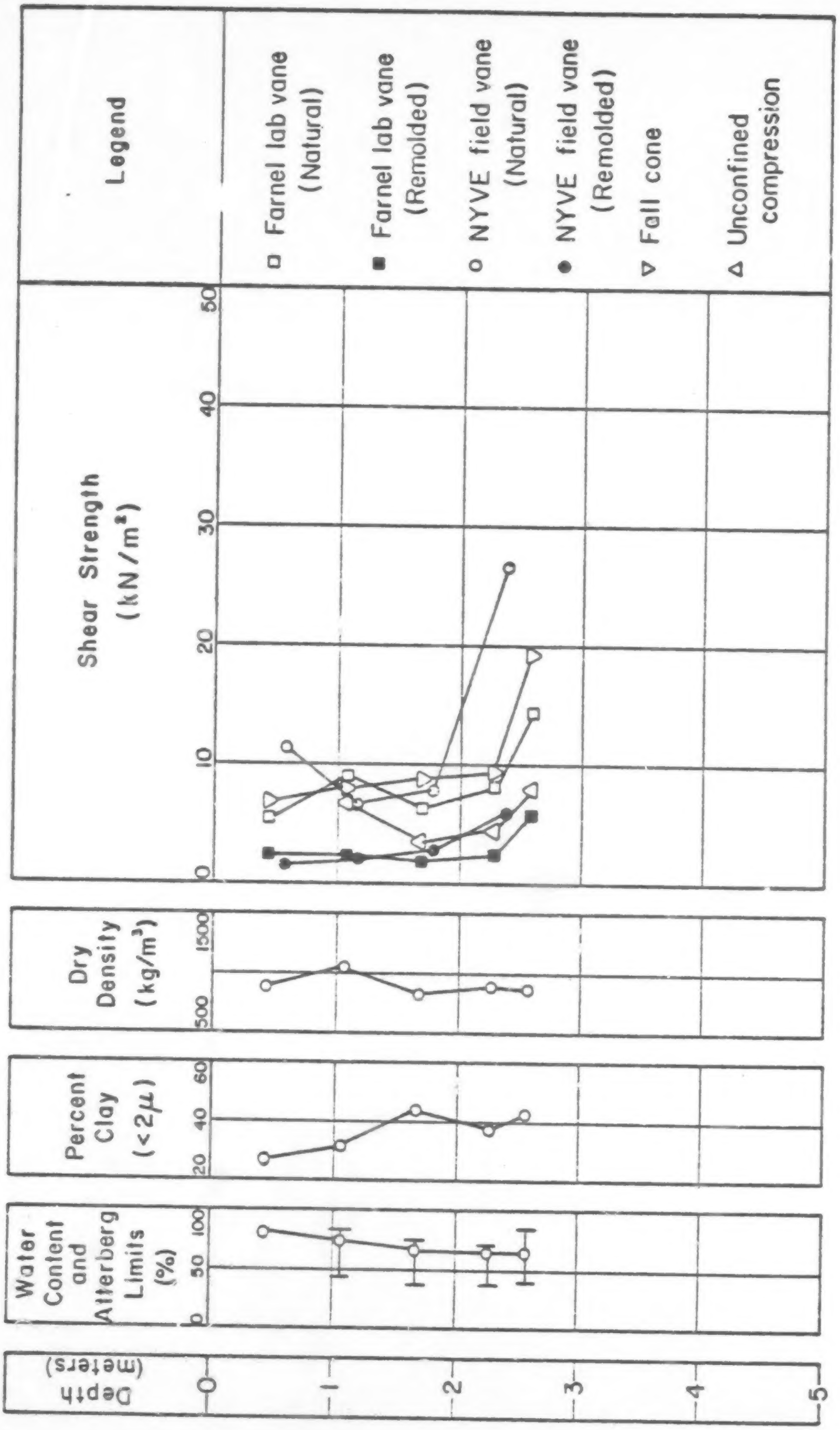

Figure 8-4. Strength Profiles at Location 1 of Penn 8 Site (1973)

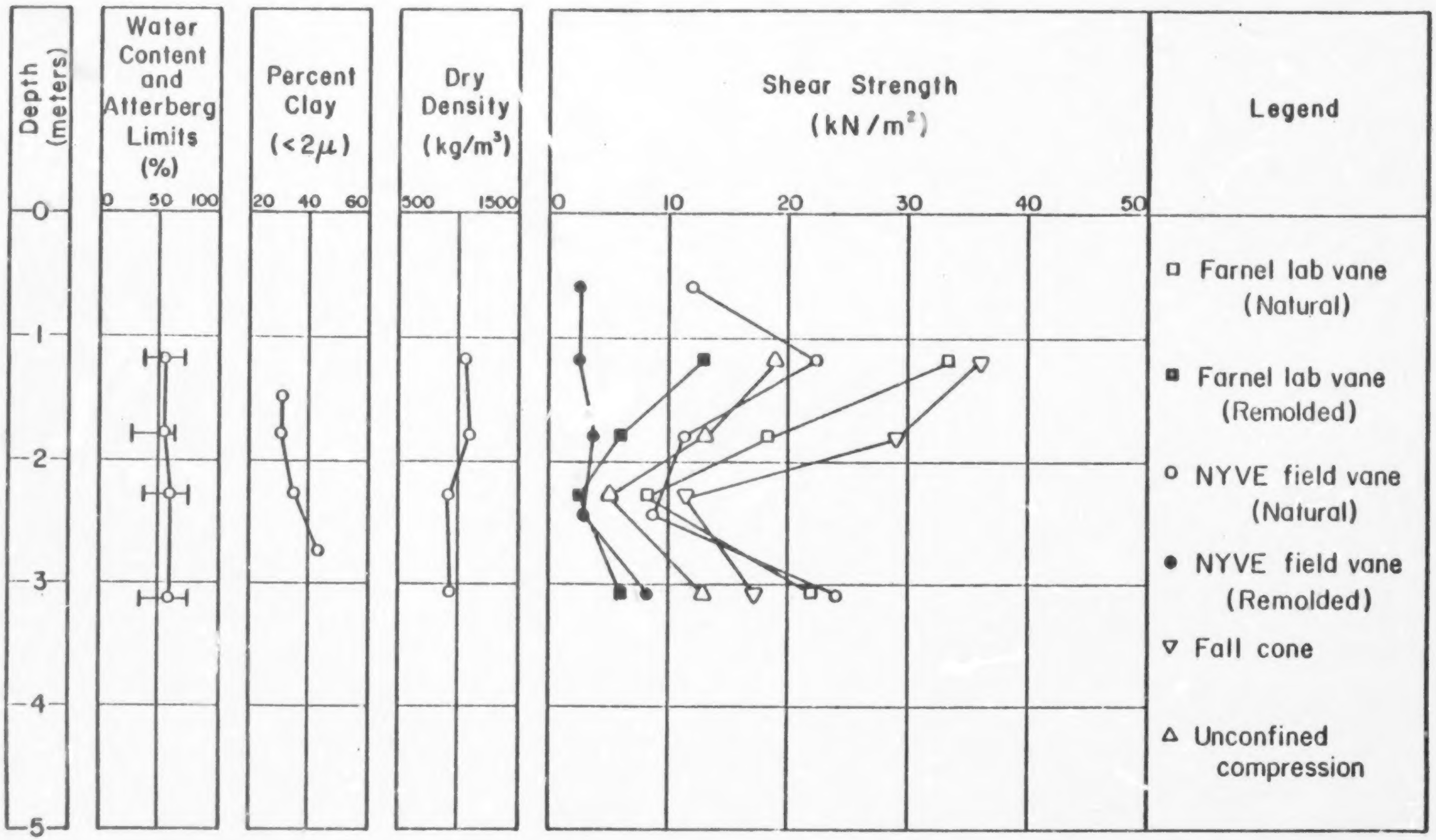

Figure 8-5. Strength Profiles at Location 2 of Penn 8 Site (1973)

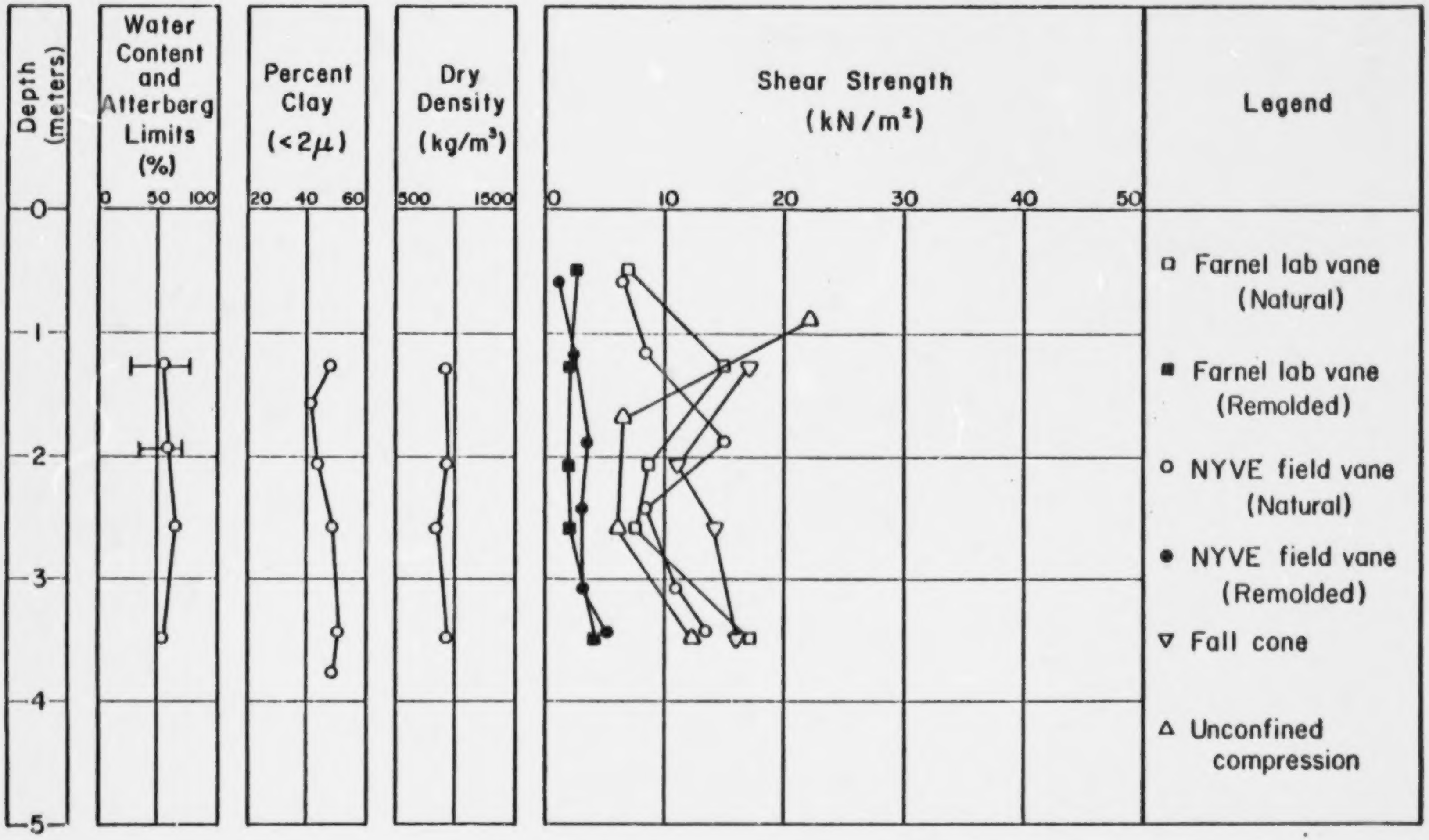

Figure 8-6. Strength Profiles at Location 1 of Riverside Site (1973)

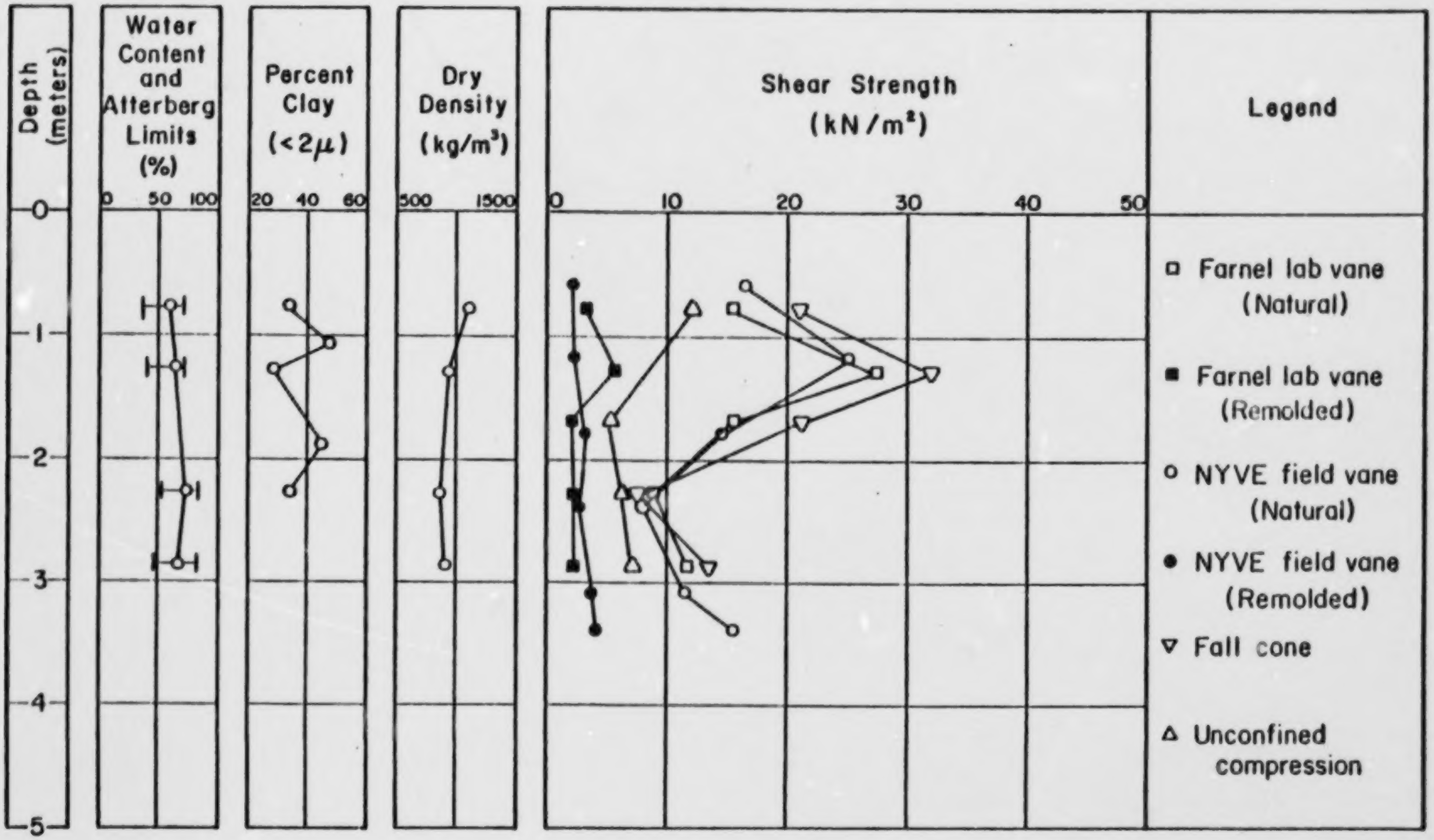

Figure 8-7. Strength Profiles at Location 6 of Riverside Site (1973)

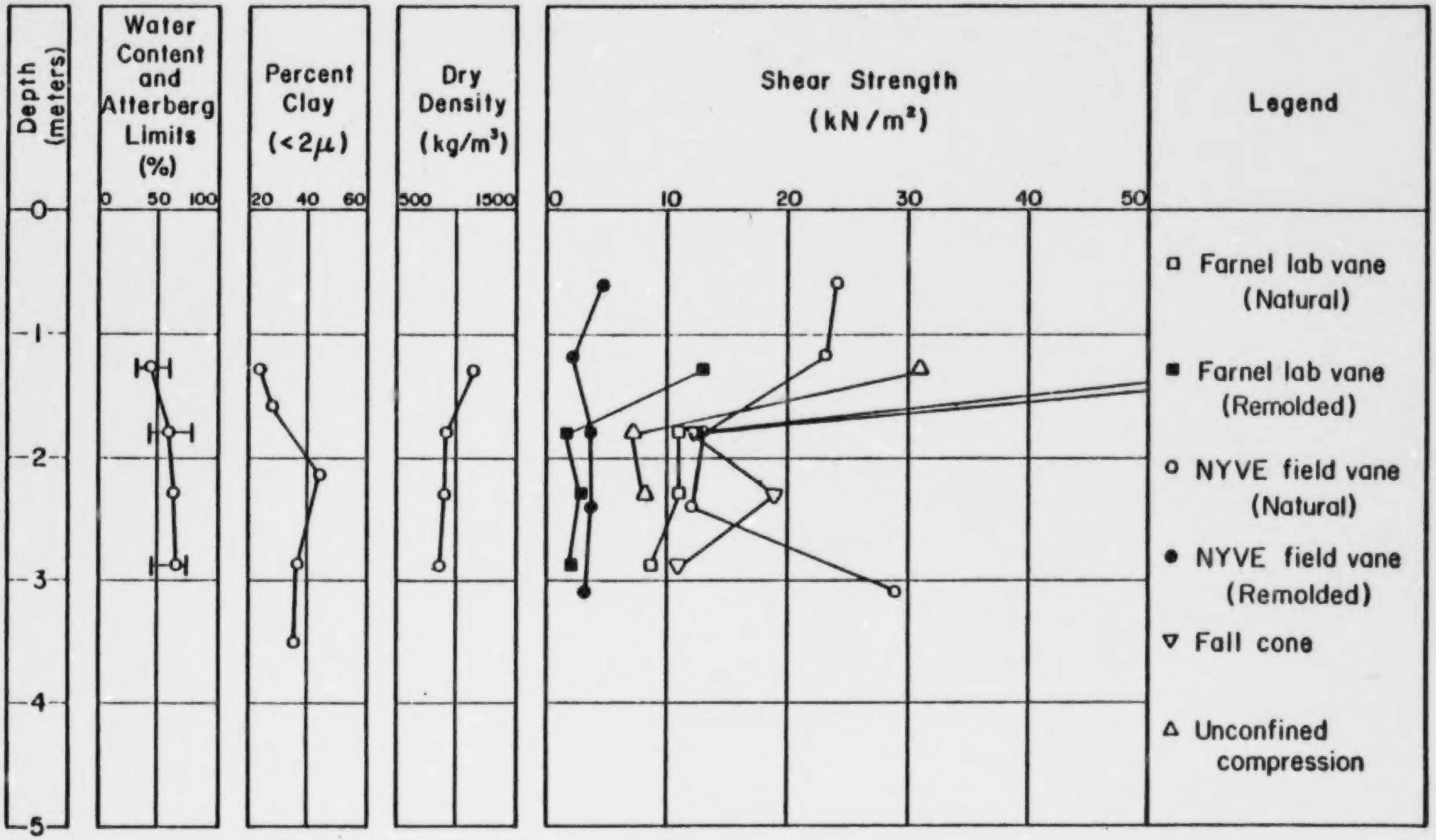

Figure 8-8. Strength Profiles at Location 8 of Riverside Site (1973)

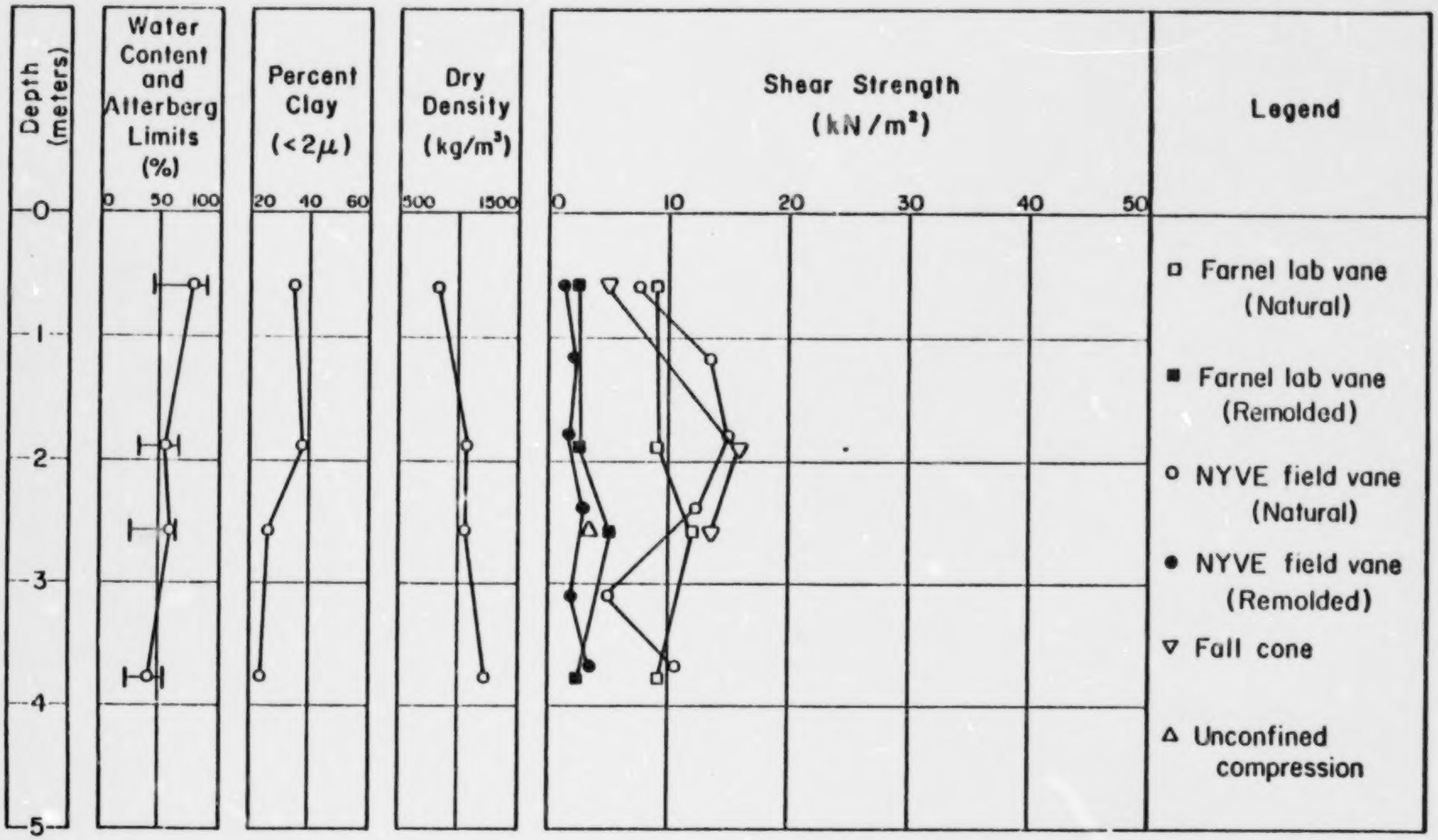

Figure 8-9. Strength Profiles at Location 3 of Island Site (1974)

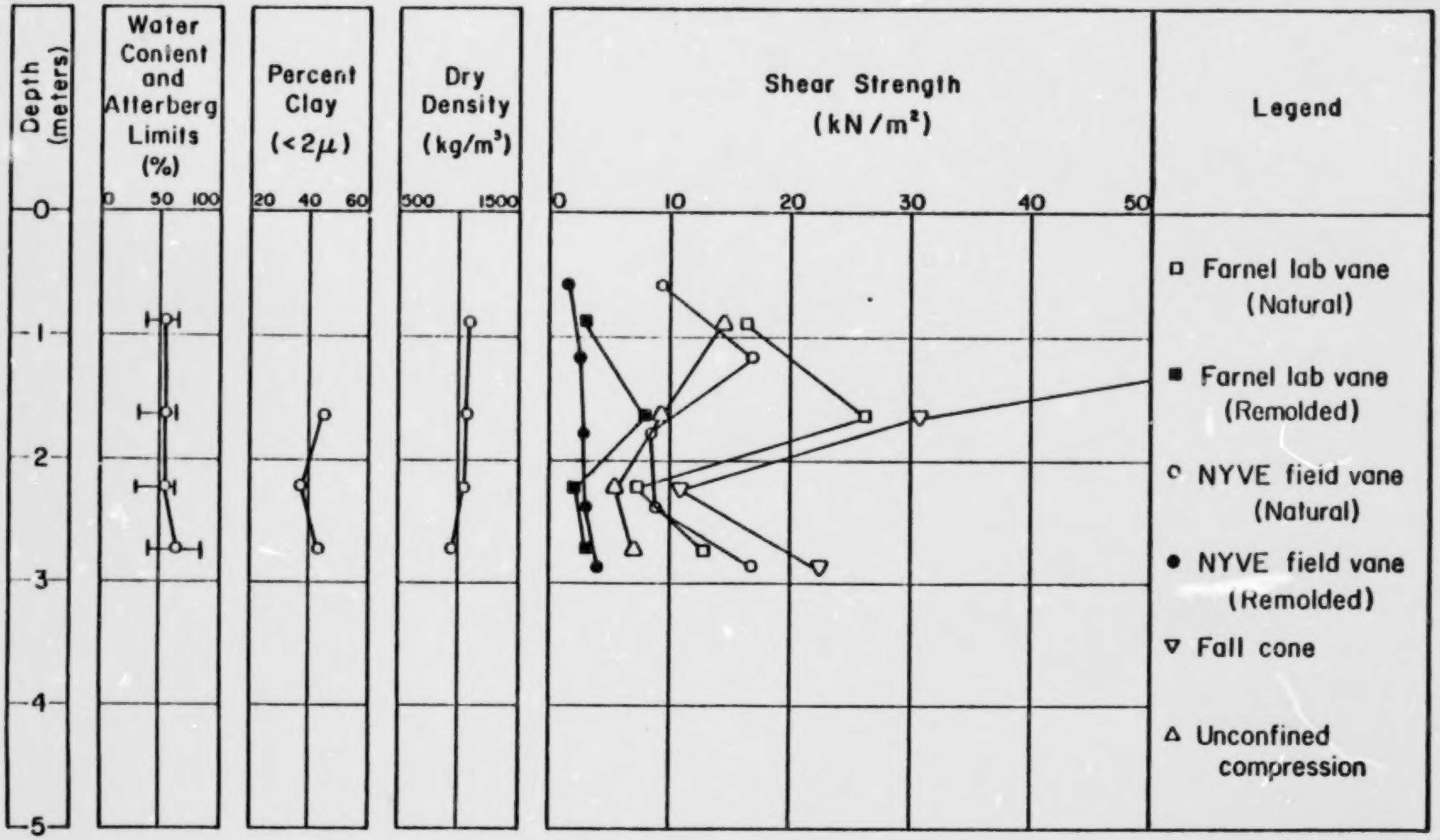

Figure 8-10. Strength Profiles at Location 1 of Penn 8 Site (1974)

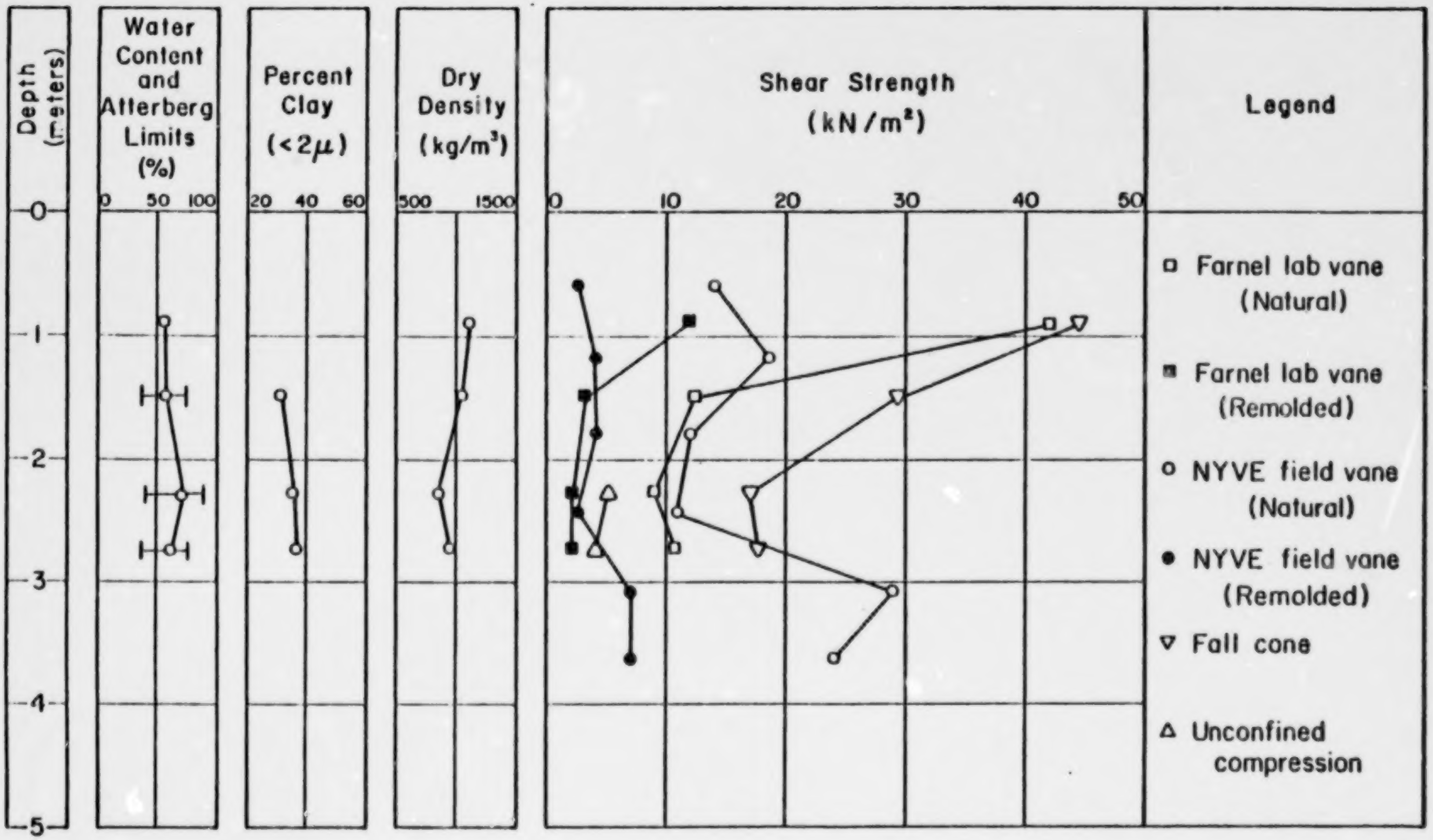

Figure 8-11. Strength Profiles at Location 2 of Penn 8 Site (1974)

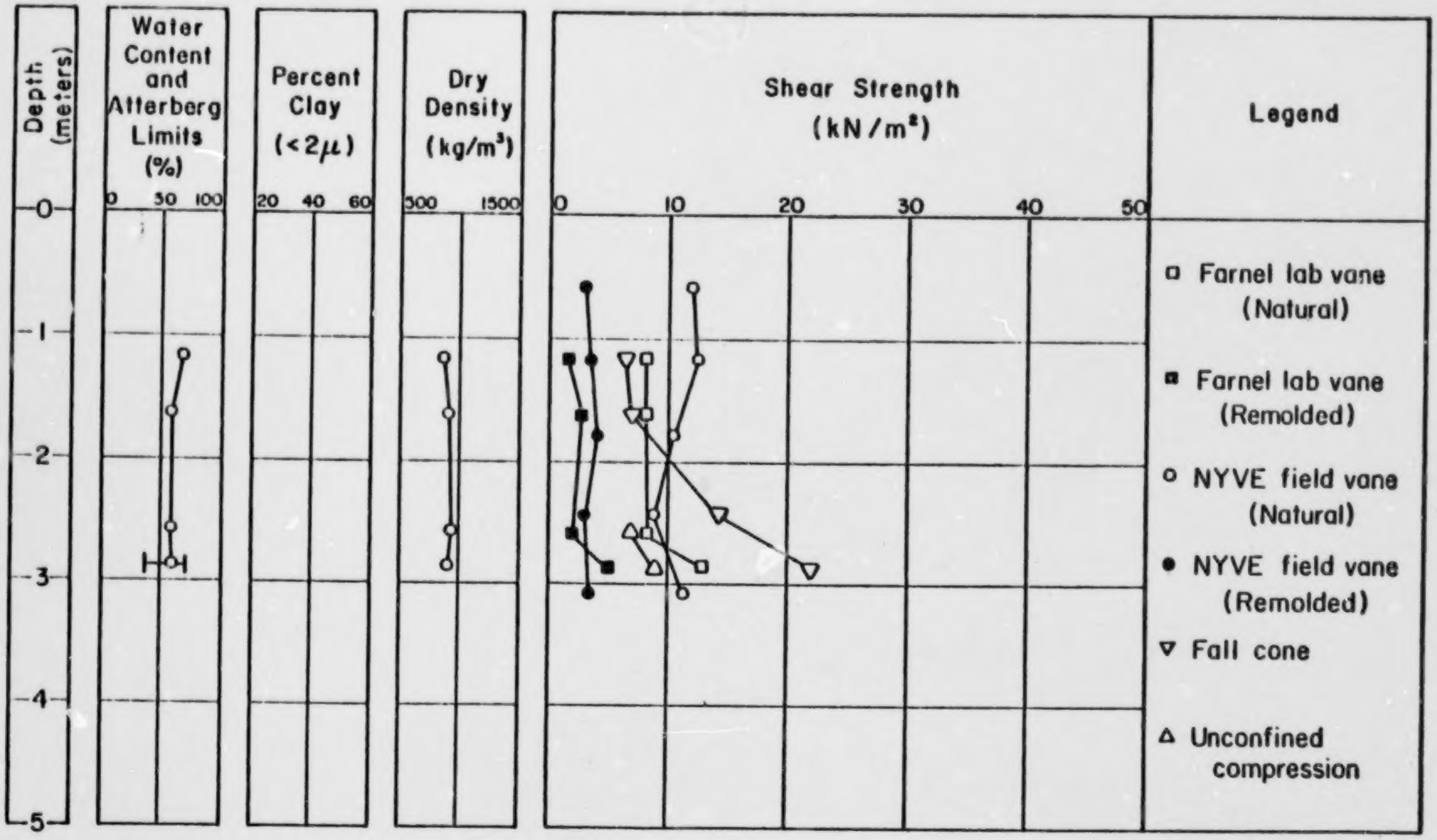

Figure 8-12. Strength Profiles at Location 1 of Riverside Site (1974)

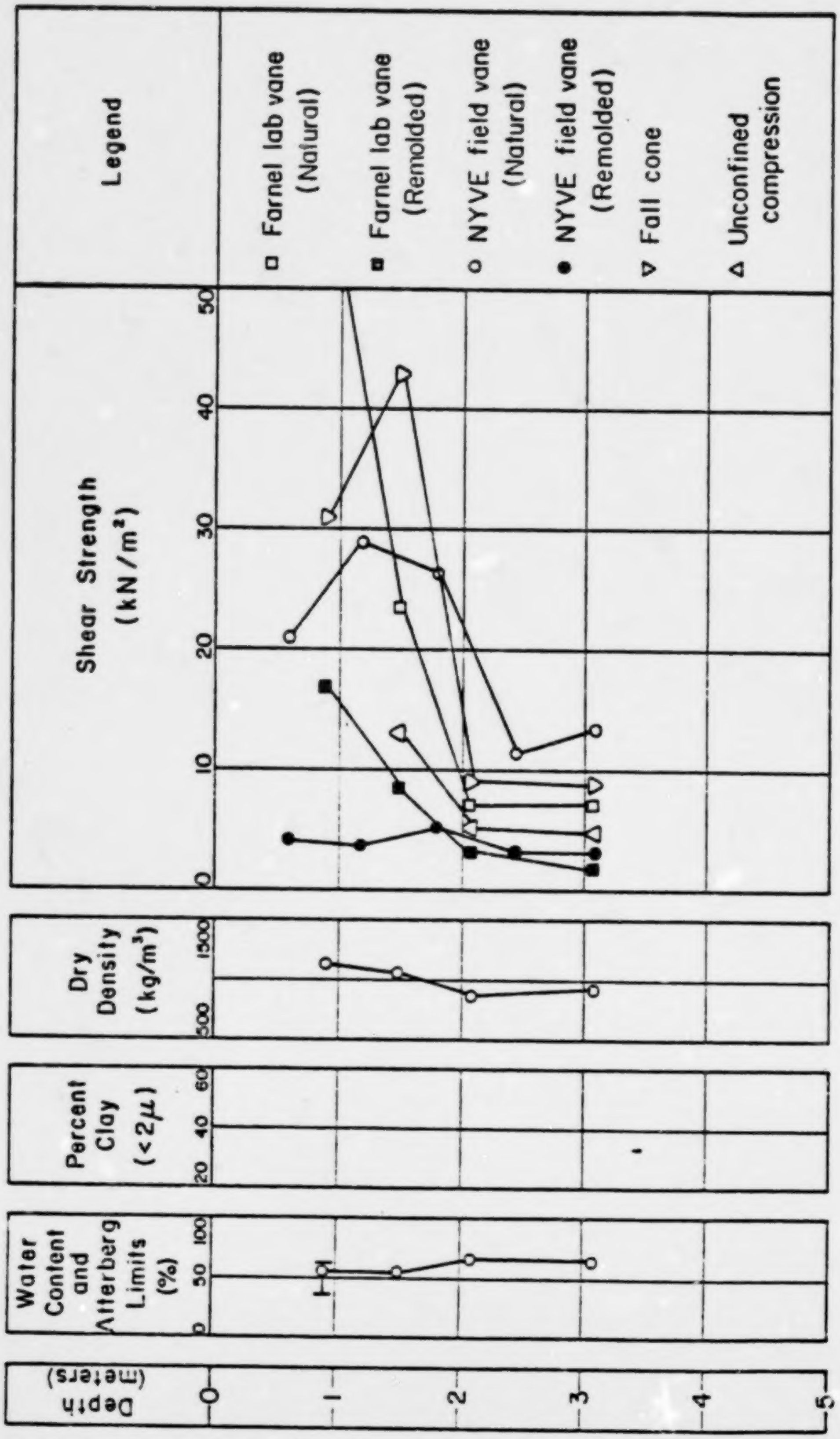

Figure 8-13. Strength Profiles at Location 6 of Riverside Site (1974)

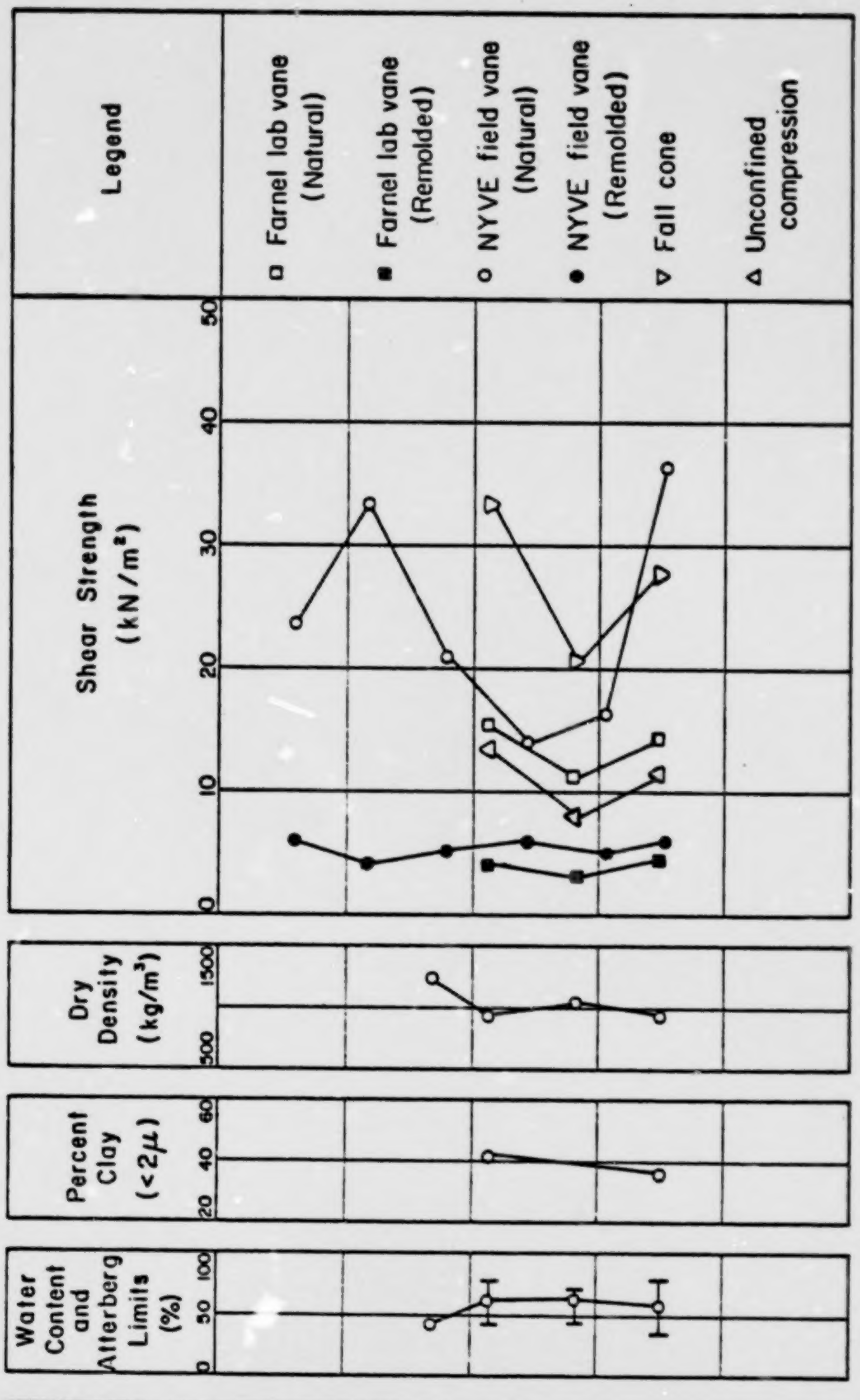

Figure 8-14. Strength Profiles at Location 8 of Riverside Site (1974)

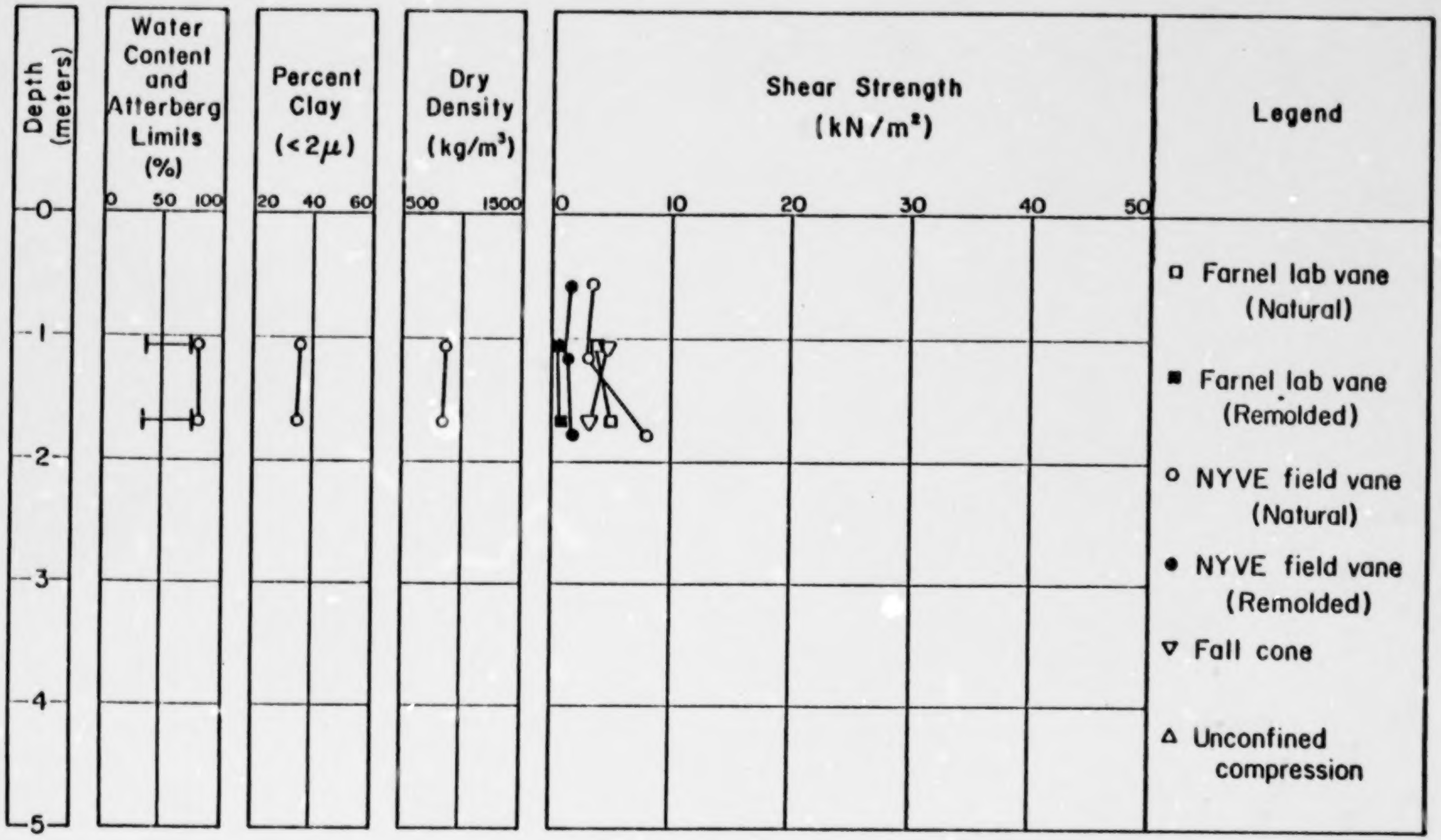

Figure 8-15. Strength Profiles at Location 2/10 of Penn 7 Site (May 1974)

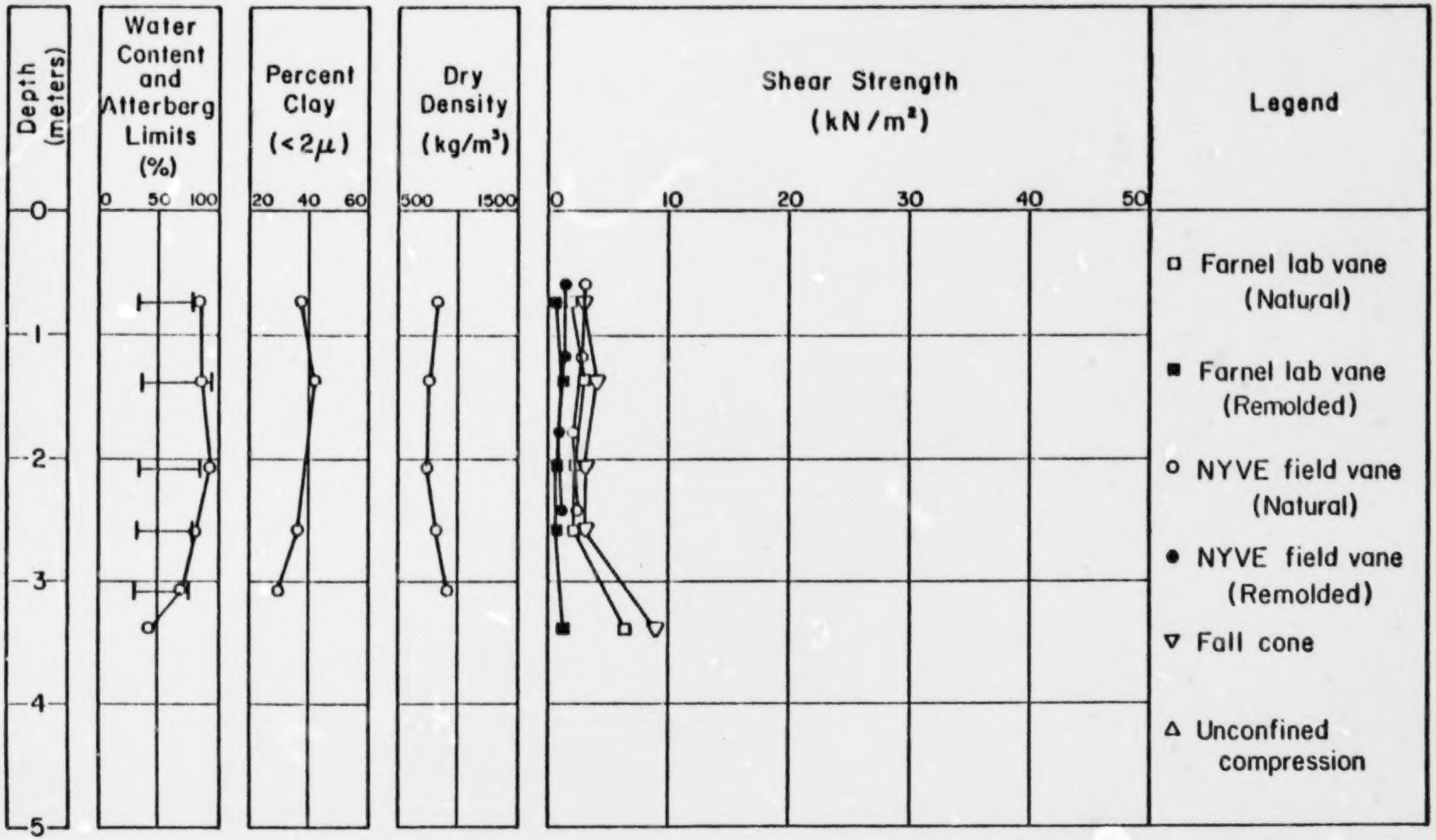

Figure 8-16. Strength Profiles at Location 5/8 of Penn 7 Site (May 1974)

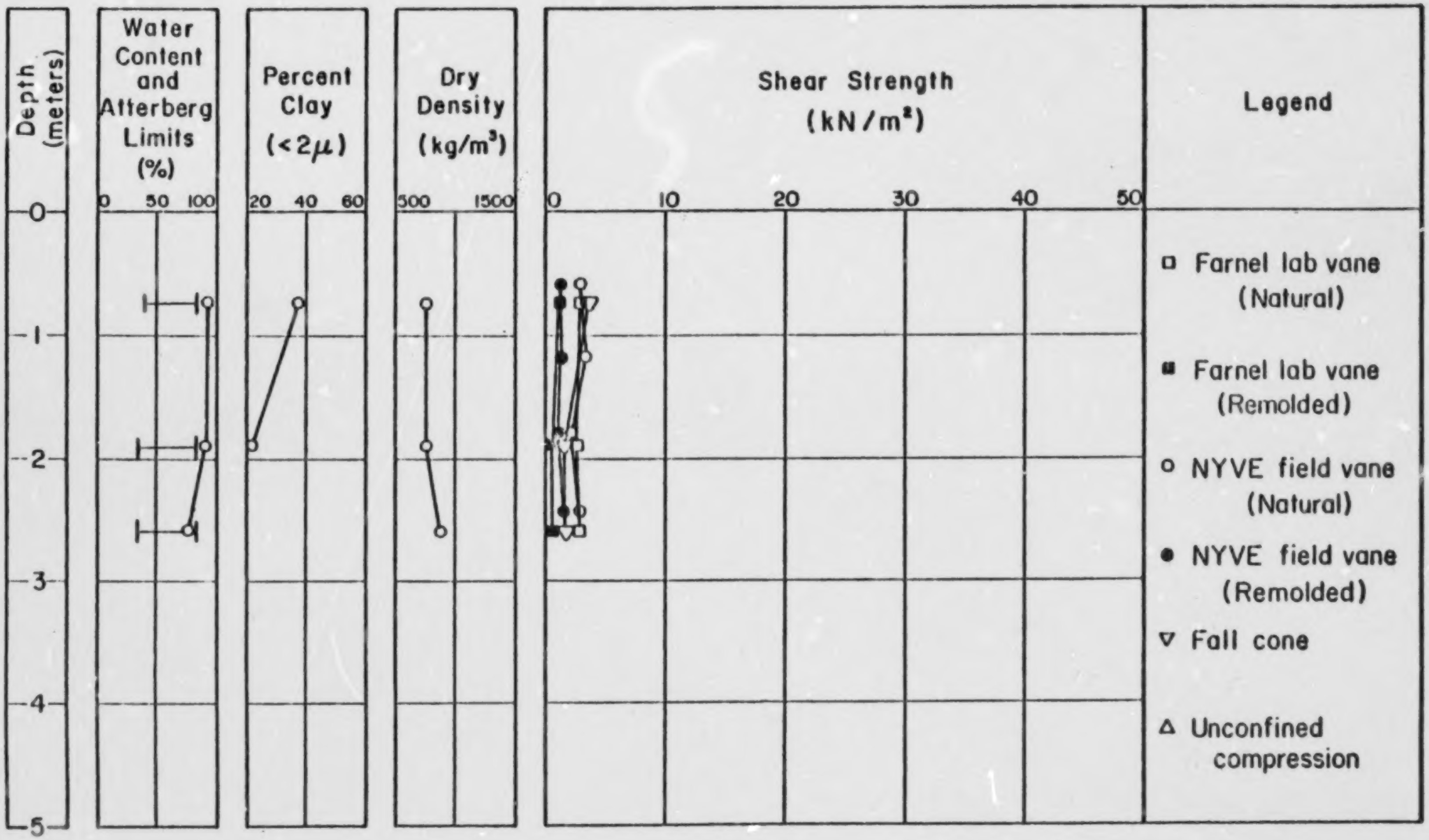

Figure 8-17. Strength Profiles at Location 5/10 of Penn 7 Site (May 1974)

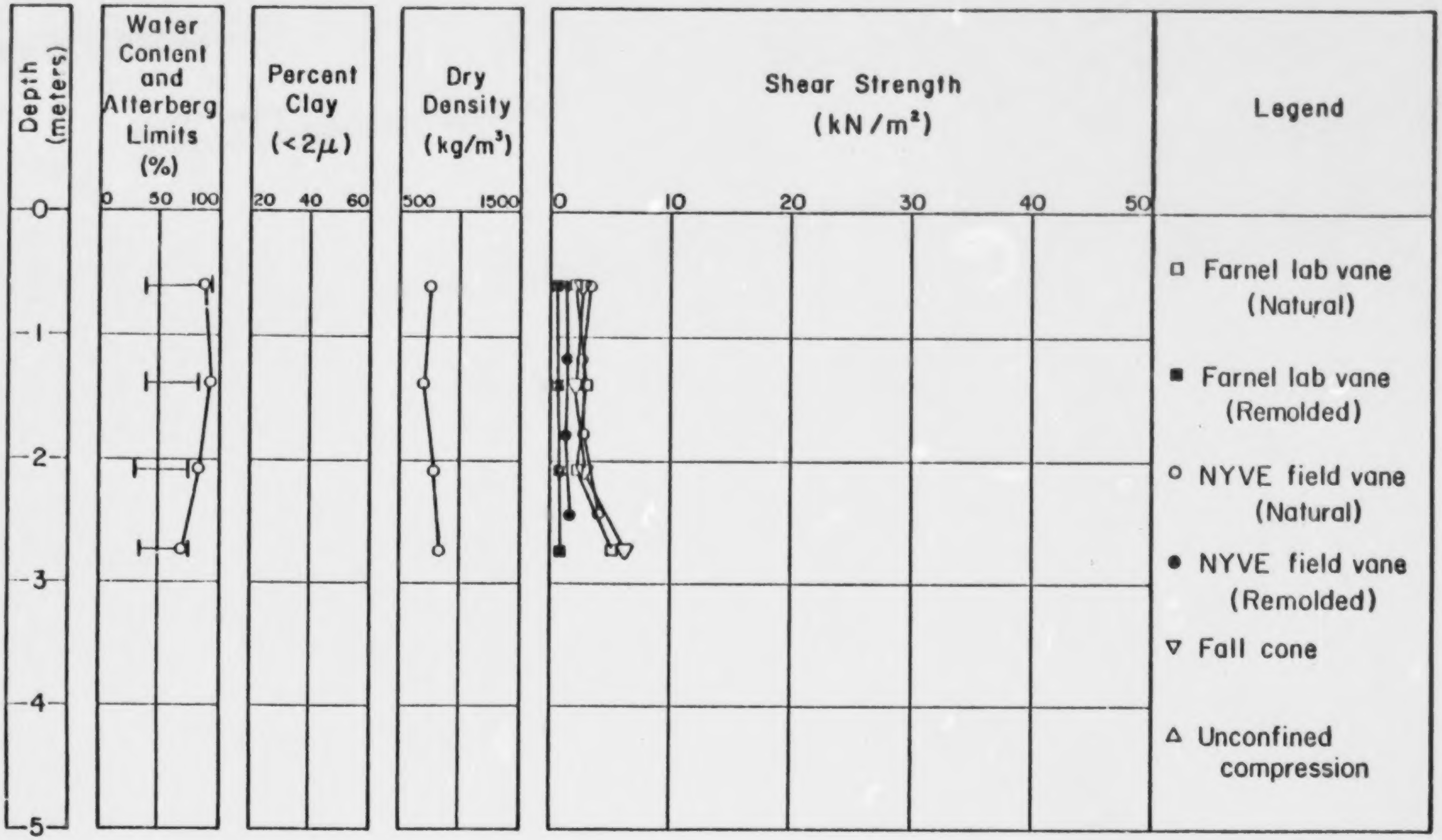

Figure 8-18. Strength Profiles at Location 5/13 of Penn 7 Site (May 1974)

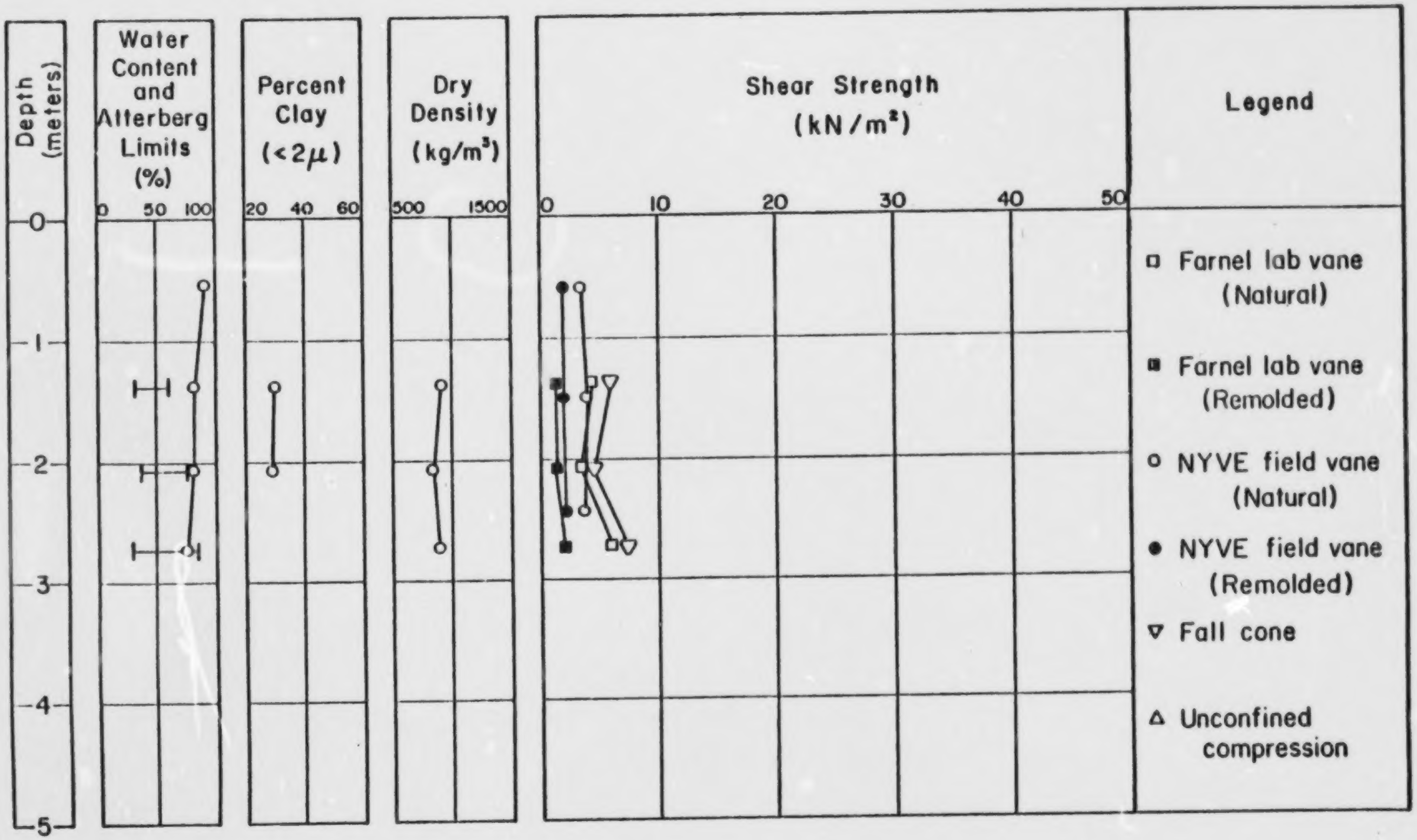

Figure 8-19. Strength Profiles at Location 8/10 of Penn 7 Site (May 1974)

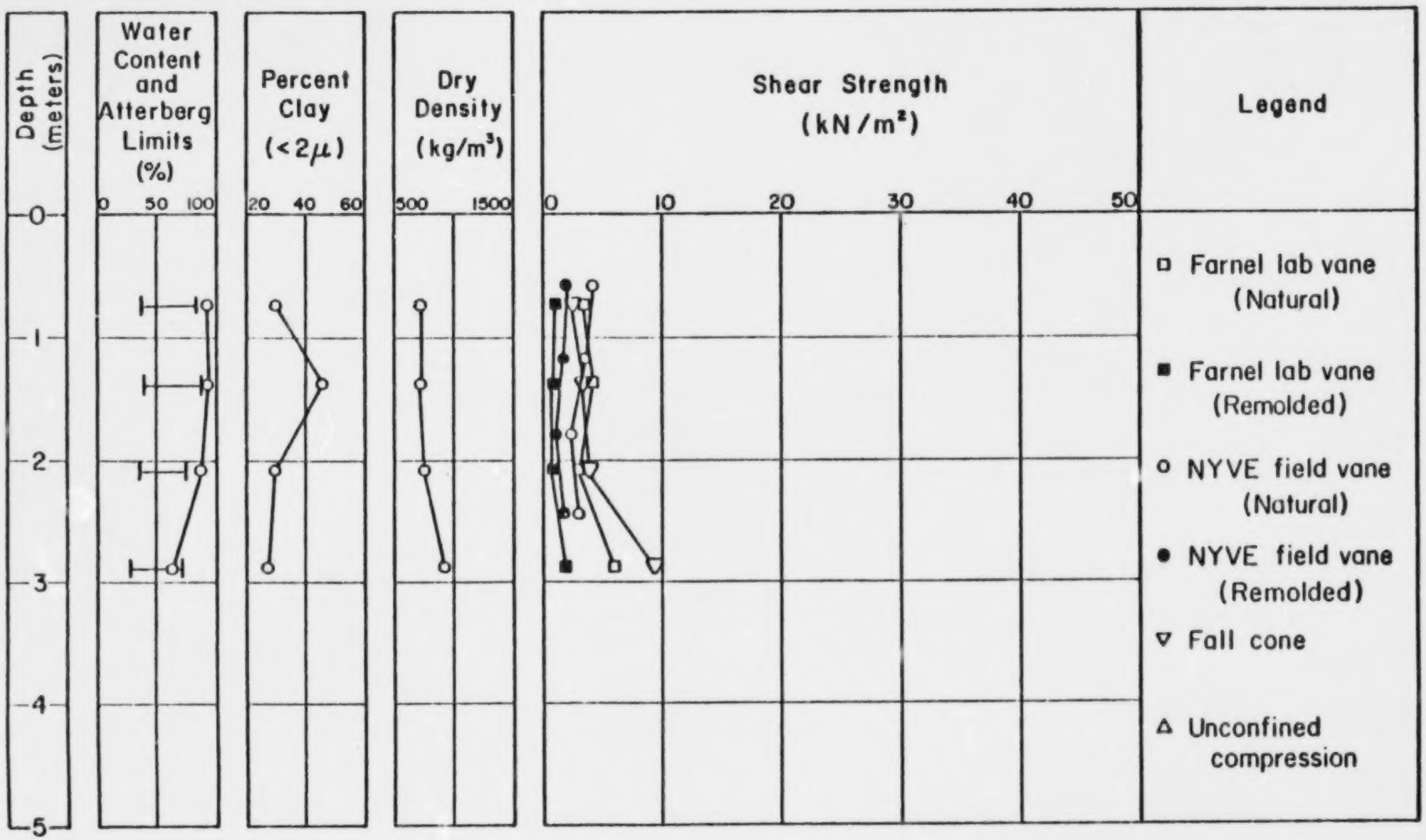

Figure 8-20. Strength Profiles at Location 8/13 of Penn 7 Site (May 1974)

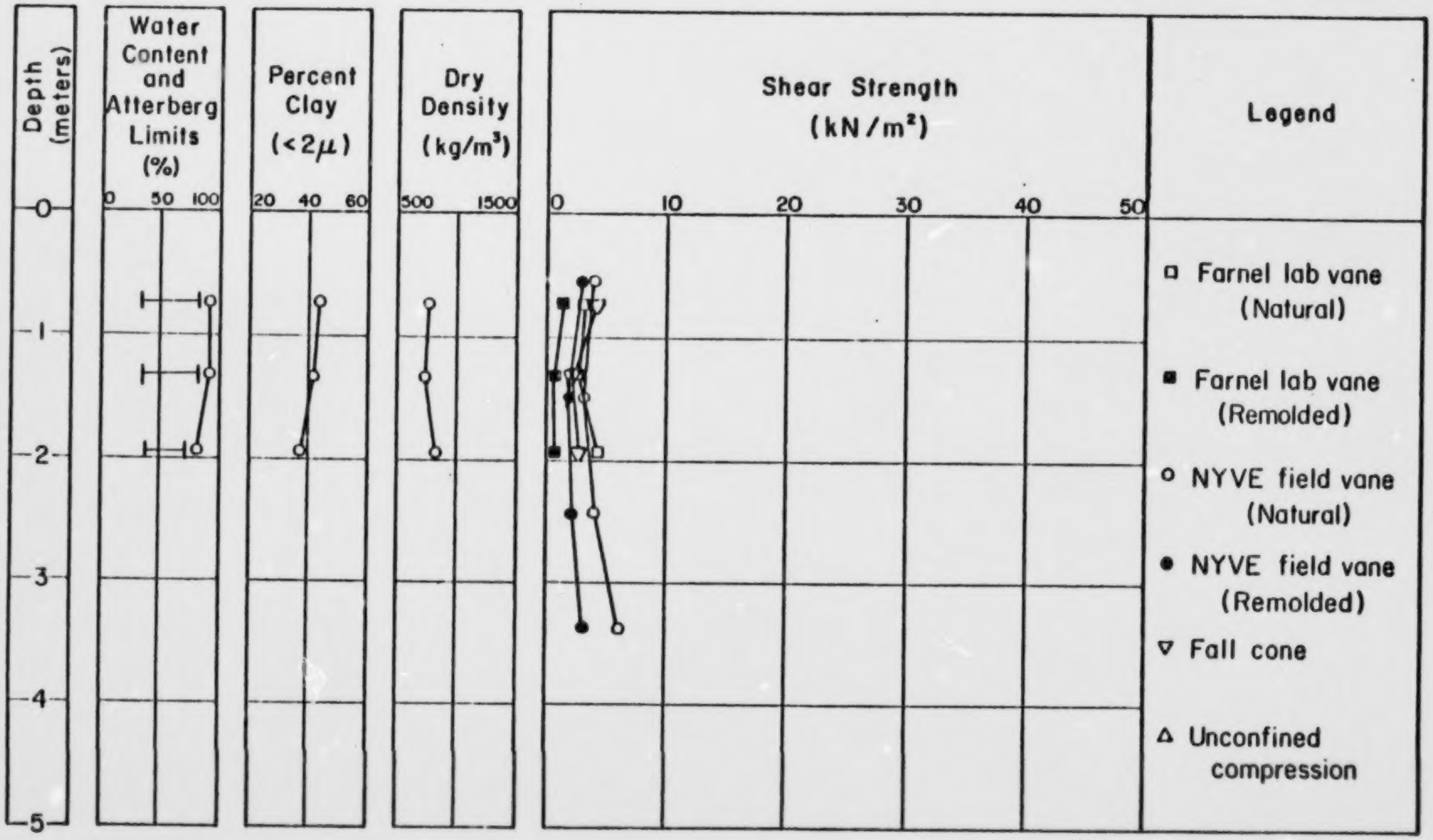

Figure 8-21. Strength Profiles at Location 12/10 of Penn 7 Site (May 1974)

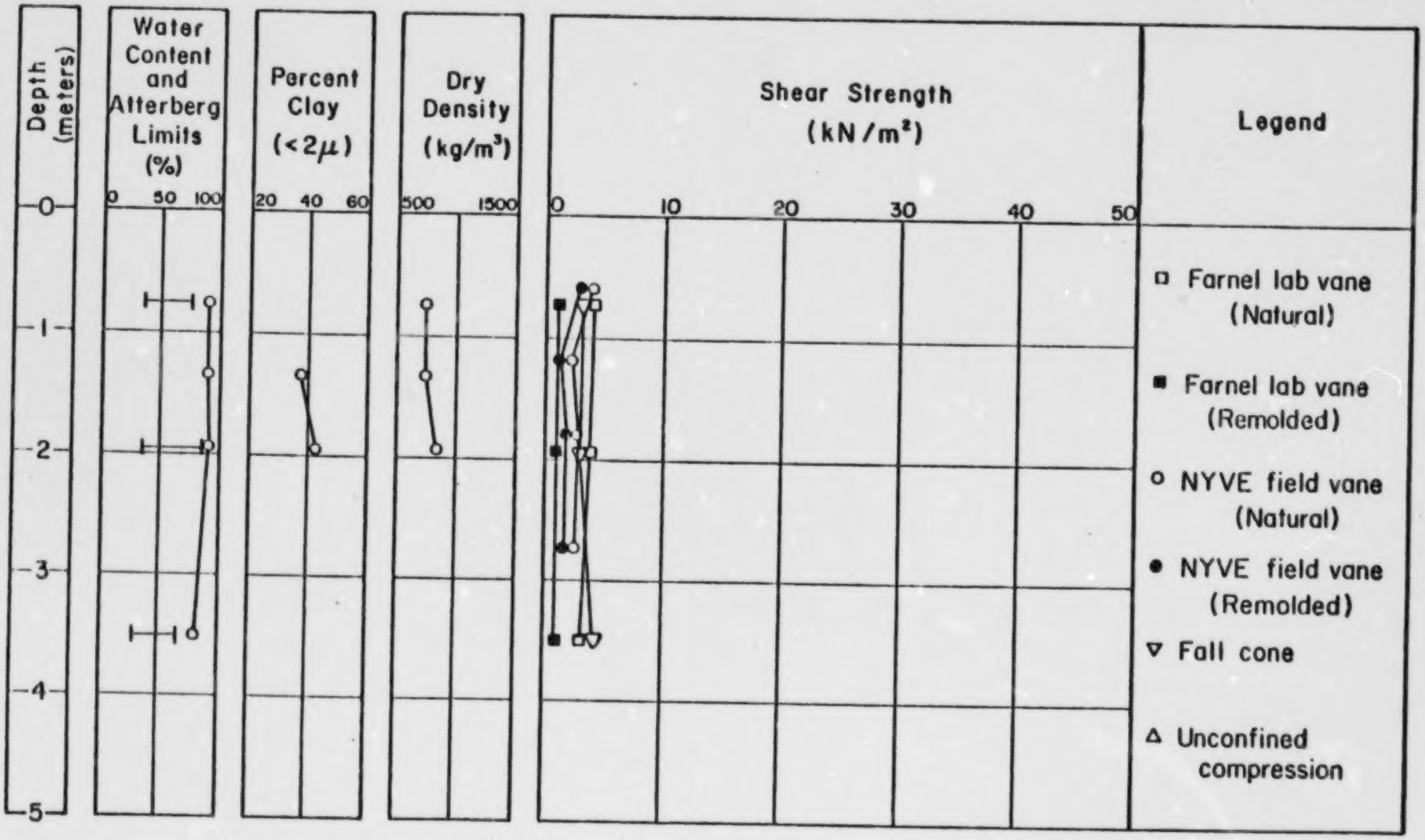

Figure 8-22. Strength Profiles at Location 15/10 of Penn 7 Site (May 1974)

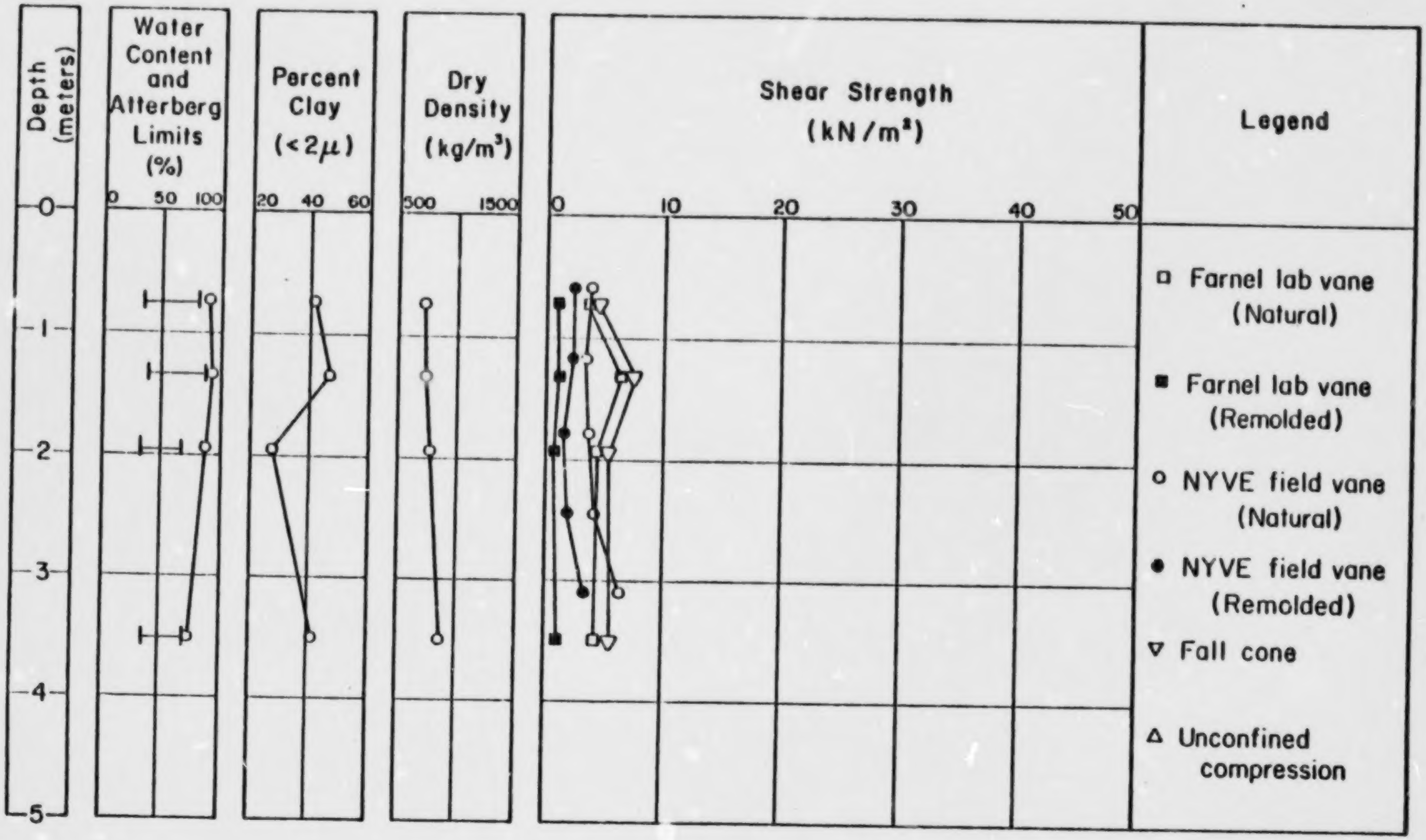

Figure 8-23. Strength Profiles at Location 16/12 of Penn 7 Site (May 1974)

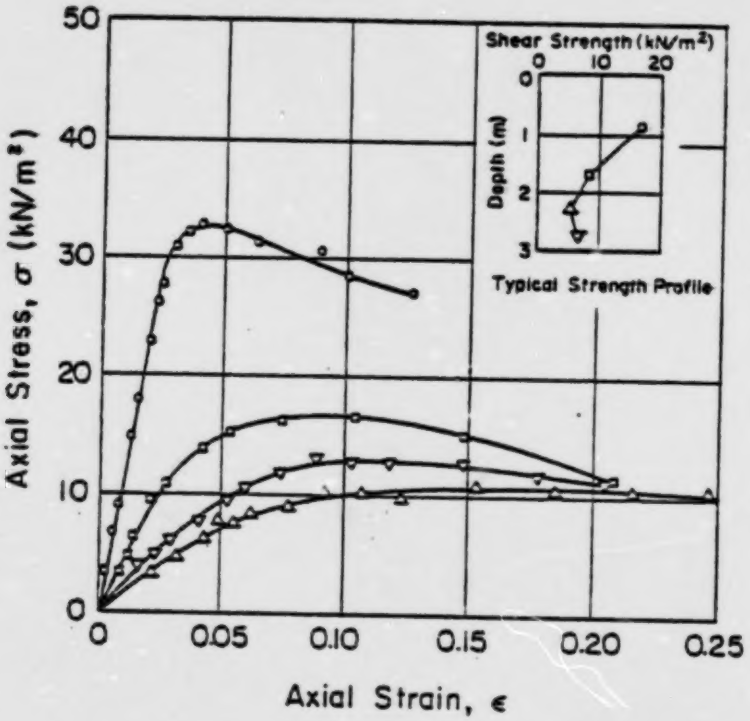

Figure 8-24. Typical Unconfined Compression Test Data from Penn 8 (1974)

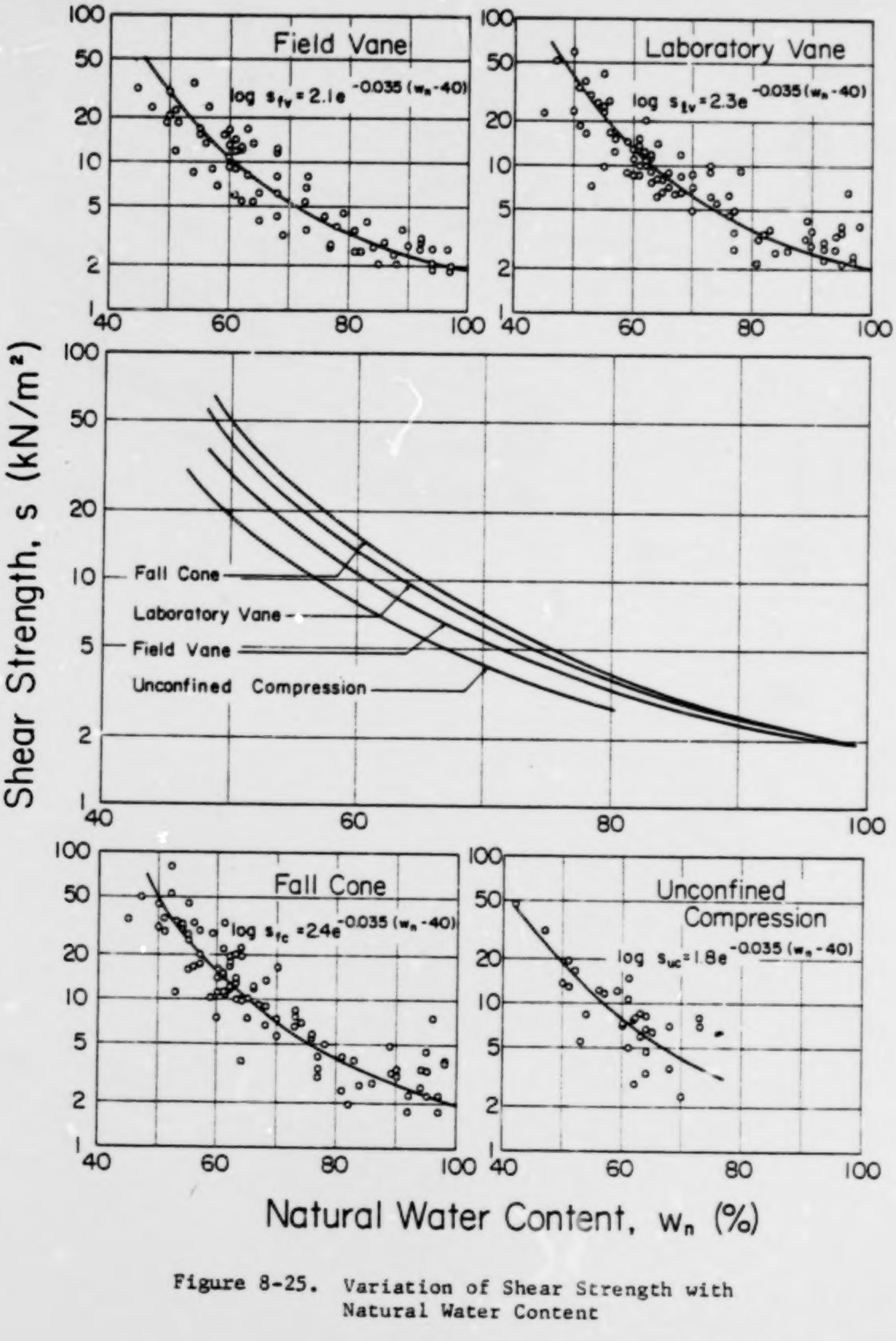

Figure 8-25. Variation of Shear Strength with Natural Water Content

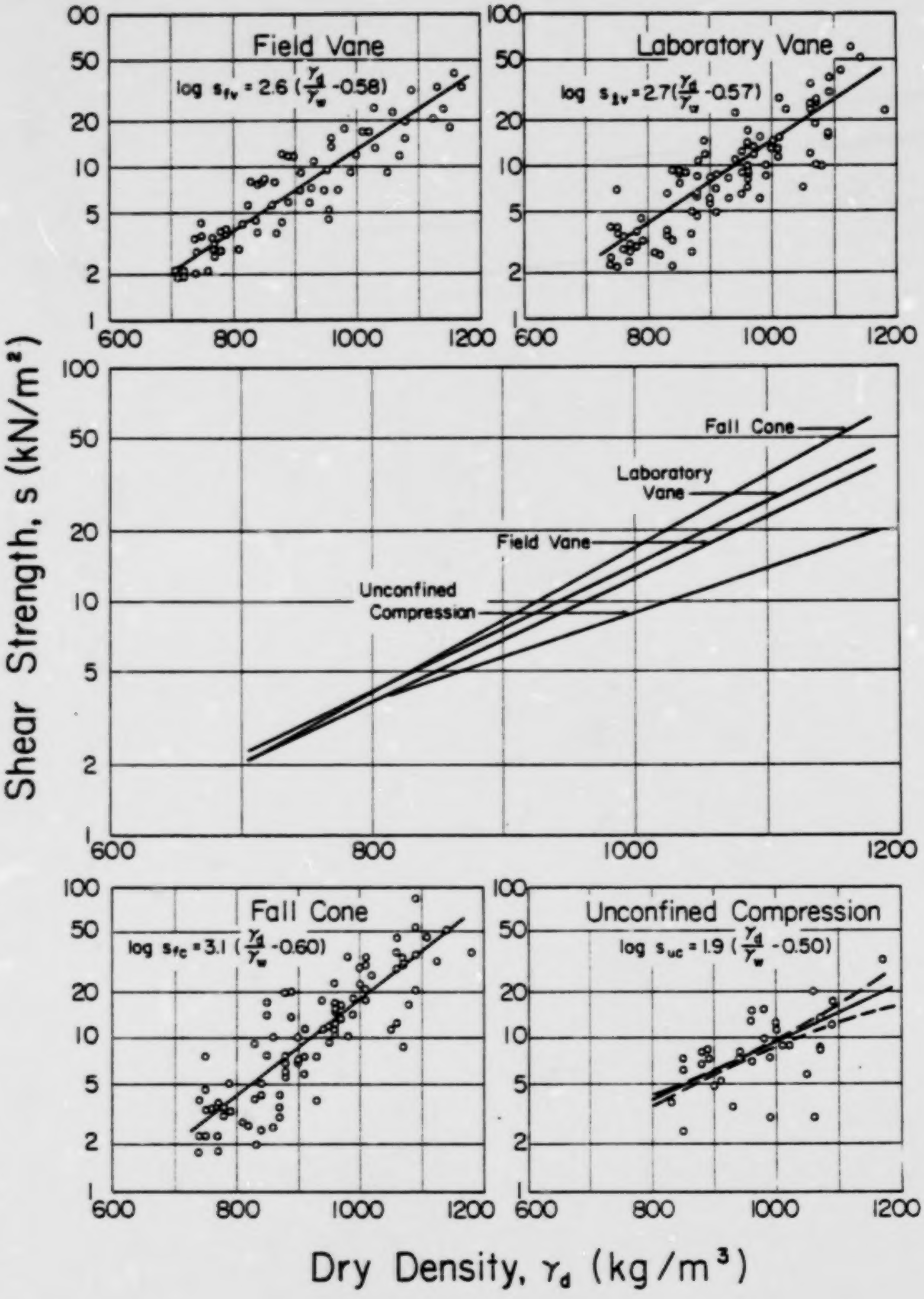

Figure 8-26. Variation of Shear Strength with Dry Density

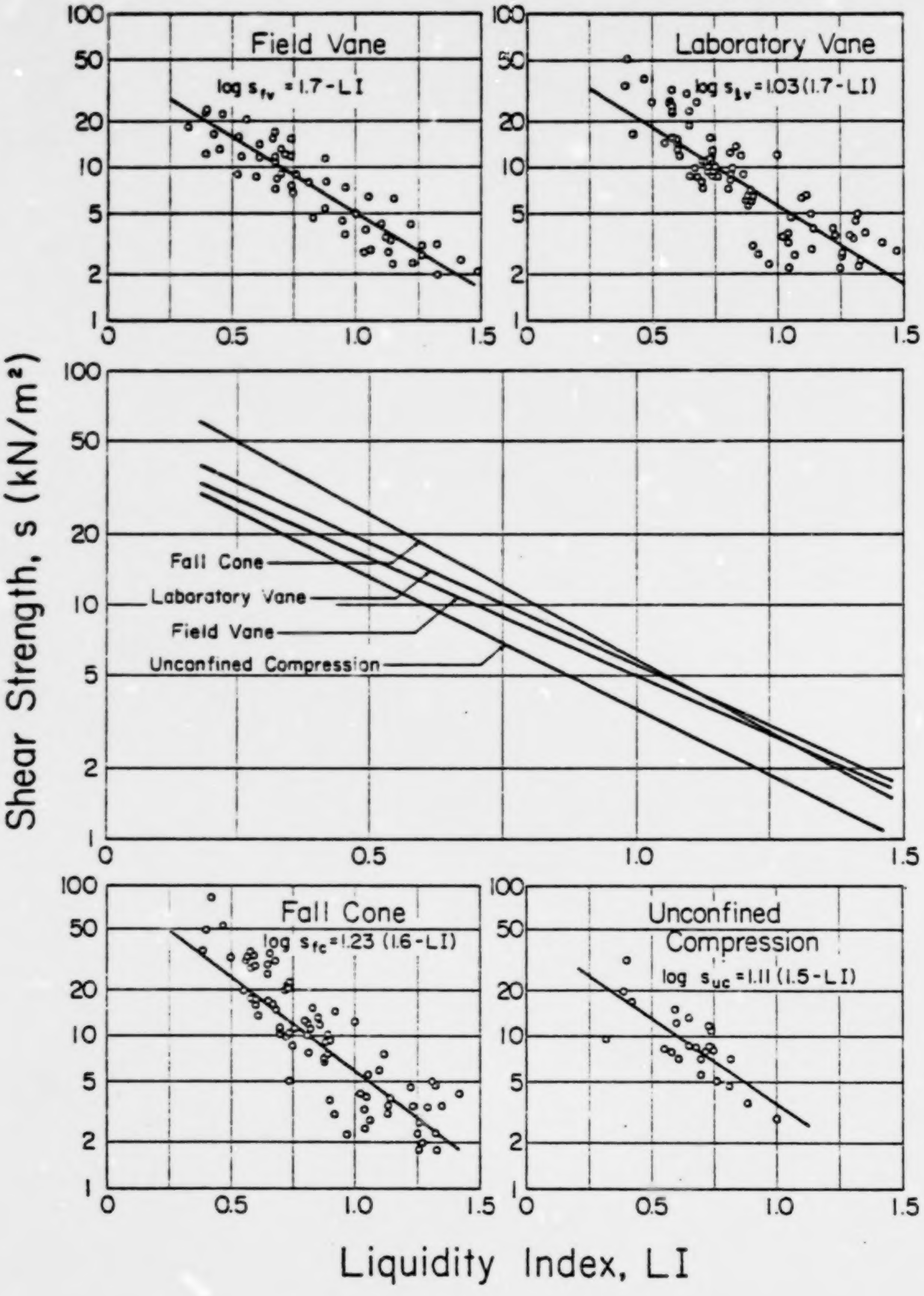

Figure 8-27. Variation of Shear Strength with Liquidity Index

Table 8-1

Values of Coefficients

Independent Variable	Type of Test	a_w	b_w
Water Content	Field Vane	2.1	0.035
	Laboratory Vane	2.3	0.035
	Fall Cone	2.4	0.035
	Unconfined Compression	1.8	0.035

Independent Variable	Type of Test	a_γ	b_γ
Dry Density	Field Vane	2.6	0.58
	Laboratory Vane	2.7	0.57
	Fall Cone	3.1	0.60
	Unconfined Compression	1.9	0.50

Independent Variable	Type of Test	a_L	b_L
Liquidity Index	Field Vane	1.00	1.7
	Laboratory Vane	1.03	1.7
	Fall Cone	1.23	1.6
	Unconfined Compression	1.11	1.5

ANALYSIS OF RESULTS

Although the strength values determined from the various field and laboratory tests should ideally be identical, substantial variations are often found in practice, and this was indeed the case in this test program. These variations may be due to a number of factors, some of which are sample disturbance, heterogeneity and anisotropy of the soil deposit, variation in density and water content, load history, and a multitude of other factors, such as particle size, particle shape, gradation, mineralogy, organic content, and chemistry. The role of certain of the more important factors will be examined in some detail to aid in evaluating and interpreting test results, but the complex interaction of many other variables allows only qualitative behavioral patterns to be established.

Correlation between Shear Strength and Index Properties

The measured field and laboratory strengths (designated as s_{fv} for the field vane, $s_{\ell v}$ for laboratory vane, s_{fc} for the fall cone, and s_{uc} for the unconfined compression tests) are correlated in Figures 8-25, 8-26, and 8-27 with the natural water content, w_n, dry density, γ_d, and liquidity index, LI, respectively. Figure 8-25 shows the correlations between the various shear strengths and the natural water content. All of these relationships can be reasonably well described by an equation of the form

$$\log s = a_w e^{-b_w(w_n - 40)} \quad , \qquad (8\text{-}5)$$

where a_w and b_w are empirical constants that depend on the type of test. To select the "best" estimate for these two constants, Equation (8-5) was transformed to a linear equation, and the stepwise regression method (Draper and Smith, 1966) tempered with engineering judgment was used to determine a_w and b_w, values for which are listed in Table 8-1. The measured strengths are plotted in Figures 8-26 and 8-27 as functions of between the strengths determined by an unconfined compression test and a fall cone test. This can be attributed in large part to the strength loss associated with sampling and trimming disturbances, which pose particularly difficult problems for soft soils, as was the case for most of the samples tested in this program. As a matter of fact, a detailed study of the profiles in Figures 8-3 through 8-23 will show that the greatest reductions in unconfined compressive strengths relative to, for example, field vane strengths occur in the middle (or softest) portion of the dredgings layer; in such cases the unconfined compressive strengths are generally about midway between the undisturbed and remolded field vane strengths. Although the probability of some disturbance of the material during the process of sampling would suggest that the laboratory vane (and fall cone) strength should be lower than the field vane strength, the contrary observation may be explained to some extent by (a) the confinement of the samples in the tubes during the laboratory tests compared to the relatively free lateral movement of the soil around the blades of the vane during a field test, and (b) the difference in the basic nature of the testing procedures (for example, size and height-to-diameter ratio of the two vanes, vane geometry versus cone geometry, etc). Remolded strengths measured by both field vane and laboratory vane are generally found to be in agreement; values obtained by the field vane are usually somewhat lower for the top crust and somewhat higher in the soft zone at depths between 1 and 2 meters. In general, the shear strength values obtained in this experimental program compare well with those reported by the Philadelphia District, Corps of Engineers (1969) for samples from four sites along the Delaware River, where shear strengths varied from the dry density and the liquidity index, respectively, and the data points in each case manifest a linear variation between the logarithm of strength and both variables; these relationships can be represented in general forms by

$$\log s = a_\gamma[(\gamma_d/\gamma_w) - b_\gamma] \tag{8-6}$$

for the dependence of s on γ_d, and by

$$\log s = a_L(b_L - LI) \tag{8-7}$$

for the dependence of s on LI. Values of the constants a_γ, b_γ, a_L, and b_L are given in Table 8-1. In all cases the correlation coefficients are on the order of 0.7 to 0.9. In the case of the latter two variables, multiple regression analyses were performed and the following equations with correlation coefficients of 0.87, 0.91, 0.92 and 0.84, respectively, were obtained:

$$\log s_{fv} = 0.07 + 1.8\ \gamma_d/\gamma_w - 0.55\ LI \tag{8-8}$$

$$\log s_{\ell v} = 0.09 + 2.0\ \gamma_d/\gamma_w - 0.63\ LI \tag{8-9}$$

$$\log s_{fc} = 0.22 + 2.0\ \gamma_d/\gamma_w - 0.80\ LI \tag{8-10}$$

$$\log s_{uc} = 0.68 + 0.9\ \gamma_d/\gamma_w - 0.96\ LI \tag{8-11}$$

Comparison between Field and Laboratory Strengths

An examination of the comparisons plotted in Figures 8-25, 8-26, and 8-27 indicates that the strength values determined by means of the four tests described are usually highest for the fall cone and decrease in the order of laboratory vane, field vane, and unconfined compression tests. In general, the strengths measured by the field vane and the laboratory vane are in reasonably good agreement, but strength values obtained from unconfined compression tests are almost always considerably lower than values obtained from any other test; very often there is a factor of two about 100 psf (5 kN/m^2) to 1000 psf (50 kN/m^2) with an average of approximately 500 psf (25 kN/m^2).

Variation of Shear Strength with Depth

Figures 8-3 through 8-23 show profiles of shear strength as a function of depth; when available, water contents, Atterberg limits, clay contents, and dry densities are also included. Physical reasoning suggests that the shear strength should be lowest in the middle of the layer (where less consolidation has occurred) and highest at the top (where desiccation and evapo-transpiration have lowered the water content considerably) and bottom (where drainage into the underlying foundation soil and some consolidation due to the overburden of dredged material have taken place); such a profile is illustrated typically in Figure 8-24, together with a set of stress-strain curves from unconfined compression tests. Although this anticipated profile was found at many locations, several other profiles were at variance; the latter profiles are probably due to the existence of preconsolidated layers at intermediate depths (caused by desiccation between dredging seasons). A summary of field vane strength profiles measured at sixteen locations over a period of four years is given in Figure 8-28; remolded strengths are included for only one year in each case (namely, 1973 for the Island Site, Riverside Site, and Penn 8, and May of 1974 for Penn 7) to place the undisturbed strengths in perspective. In order to facilitate further analysis and interpretation of the data represented in the foregoing profiles, an "average strength" at a given location is defined as the area under the strength-versus-depth curve divided by the corresponding increment of depth. Data points which were suspected to represent the foundation soil or obvious testing errors were excluded from this analysis.

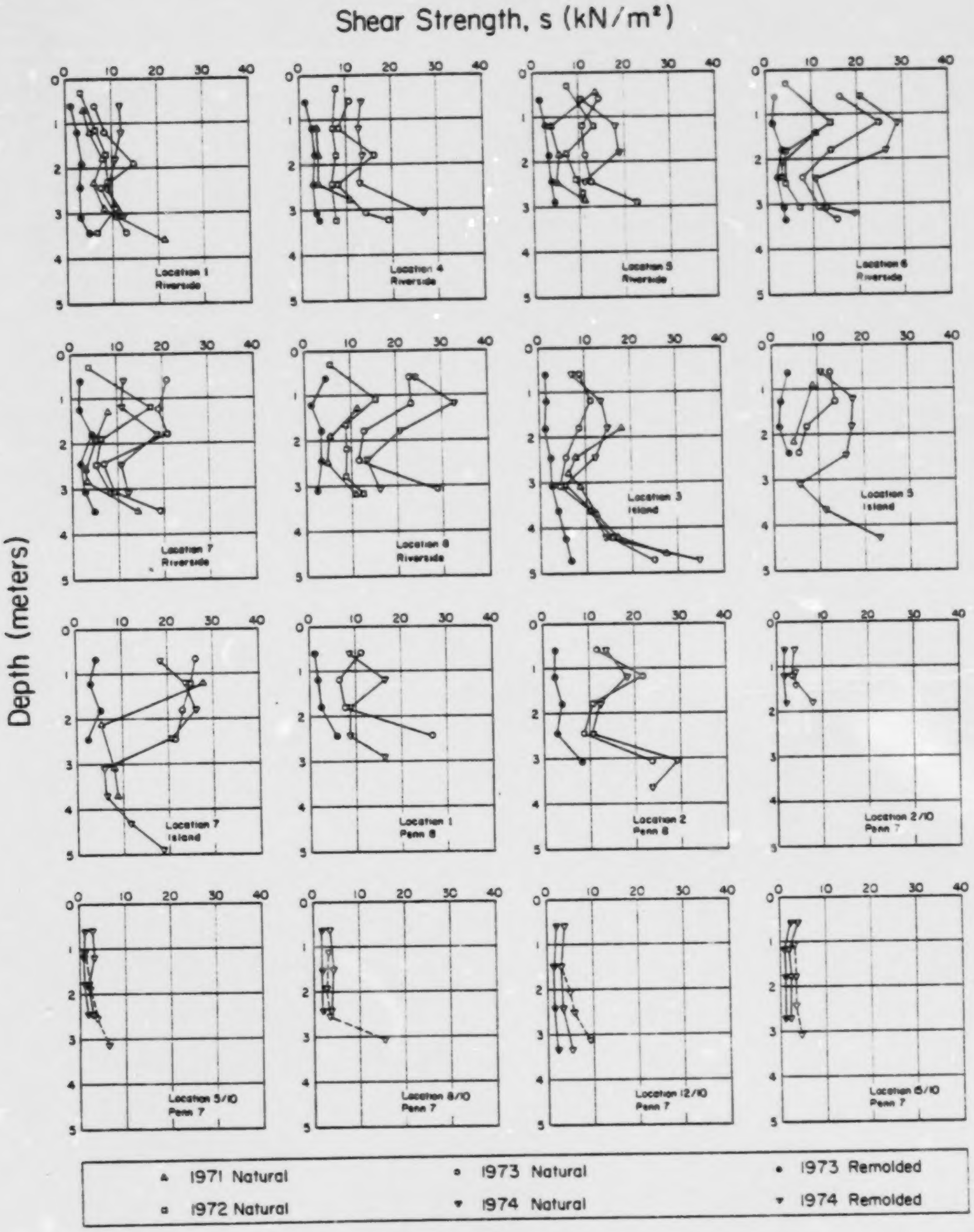

Figure 8-28. Summary of Field Vane Strength Profiles

Variation of Strength with Horizontal Distance

In general, the shear strength at a given site in a given year was found to increase with horizontal distance from the overflow weir. For example, Figures 8-6, 8-7, and 8-8 show that the 1973 field vane strengths at a depth of 0.6 meters at locations 1, 6, and 8 of Riverside Site are 7, 17, and 24 kN/m^2, respectively, and laboratory vane strengths at the same locations at a depth of 1.2 to 1.3 meters are 15, 27, and 60 kN/m^2. This variation is probably due in large part to the grain size distribution in a typical site, since the coarse particles tend to settle near the inlet pipe and the fine particles settle closer to the overflow weir; in addition to strength variations that are related directly to variations in particle sizes, the coarse material drains and consolidates faster, thereby developing greater strength in a given period of time. Since the preceding type of correlation is difficult to make at all locations and depths, the average field vane strengths for the four Toledo sites are plotted in Figure 8-29 as a function of the dimensionless distance, $\frac{x}{\ell}$, where x is the distance of the test location from the overflow weir and ℓ is the distance between the overflow weir and the inlet or discharge pipe. In general, the maximum value of $\frac{x}{\ell}$ at which the field vane test could be conducted manually varied between 0.6 and 0.7 for each of the four field sites, because the fill material became very granular and dense and the vane could not be advanced.

Variation of Strength with Time

Figure 8-28 shows time-dependent changes in the field vane strength profiles at sixteen locations in four different sites; in the case of Penn 7, only limited data are available on the time-dependent development of shear strength. The field tests were conducted during the early summer

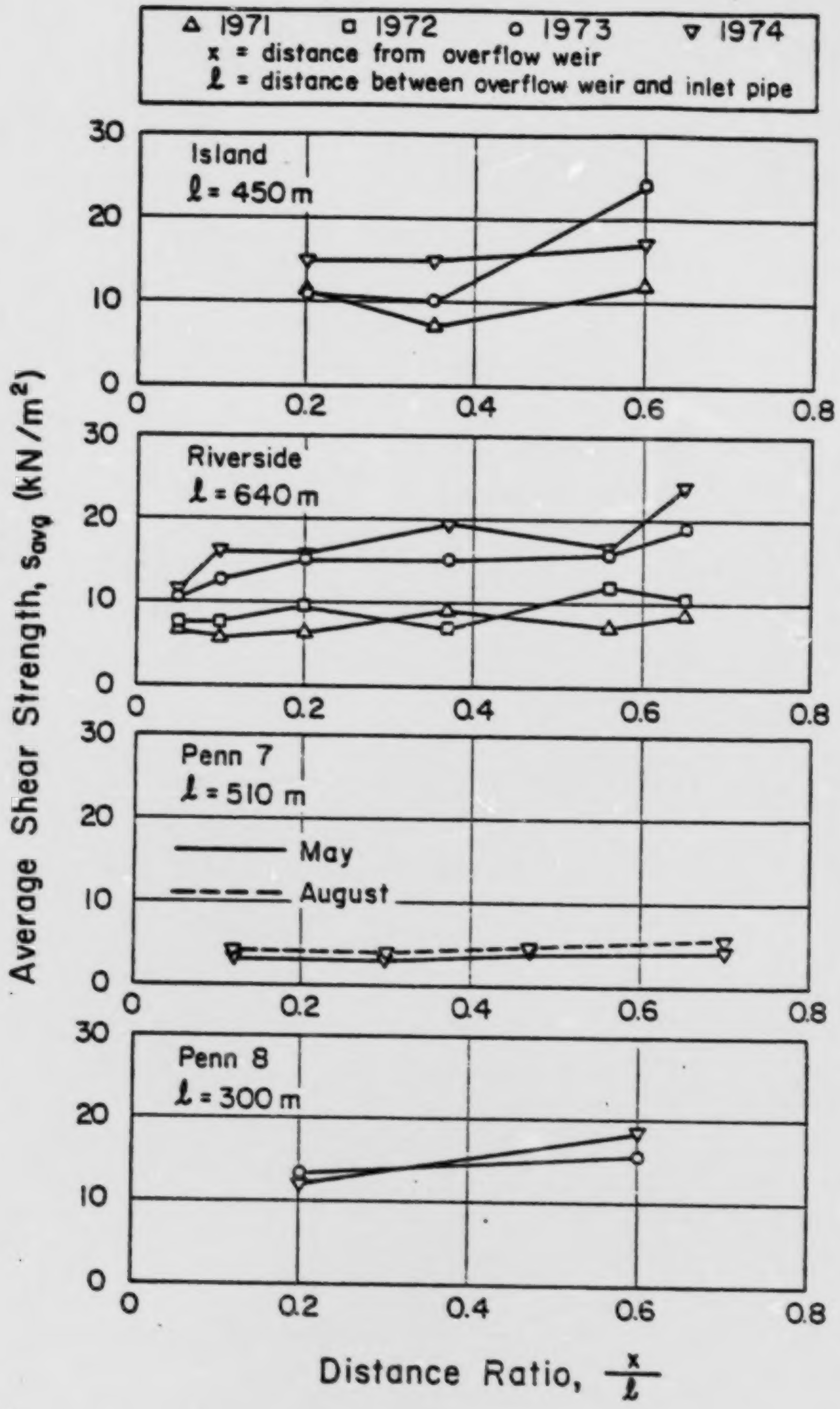

Figure 8-29. Average Field Vane Strength versus Horizontal Distance

of each year. In general, the strengths determined in any given year are somewhat greater than those measured in a preceding year, but the evidence is not entirely consistent. The reasons for the manifested inconsistencies are varied, but they seem to frequently relate to the water content of the dredged material as affected by the immediate past history of the site. For example, one inconsistency is clearly shown for location 3 near the overflow weir at the Island Site, where the 1971 strength values are higher than those of 1973; however, field records indicate that there had been an unusual rise in the water level of Lake Erie for several days during the month of April 1973, and this caused part of the Island Site close to the overflow weir to be flooded. The effect of this flooding was noticed a few months later when the field tests were conducted; the surface of the fill was very wet compared to 1971, and several pools of water were found. As a consequence, the water content of the dredged material increased from 1971 to 1973. Another condition which may have contributed to the higher water content and associated loss of strength is the fact that dredged spoil was pumped into the area for four months immediately after the 1971 field program was completed (field tests were conducted in June of 1971, and pumping was done from August to November of the same year); the amount of dredgings placed during these four months was 16 percent of the total material deposited in the years before 1971.

An average of about 30 percent increase in strength was observed at location 5 of the Island Site between 1971 and 1973, and a dramatic strength increase was recorded at location 7 (with the exception of one point at a depth of 1.2 meters); the higher strength of this latter point in 1971 is probably due to a desiccated crust that existed at that time, and the lower strength in 1973 is likely caused by the flooding that occurred in April of 1973. The rest of the profile exhibits a 1973 strength approximately triple that of 1971. Similar occurrences took place in 1974 at the Island Site and Penn 8.

In general, field vane strengths measured at location 1 of Penn 8 were higher in 1974 than in 1973, except for two points at depths of 0.6 and 2.4 meters. The approximately 15 percent reduction in the 1974 strength at the first point can be attributed to the fact that the surface layer was drier in 1973 than in 1974; although flooding of the area near the overflow weir occurred in both years, the 1974 tests were conducted sooner after the flooding. A more significant strength reduction (about 60 percent) was observed in 1974 at the second point, and this is probably due to the fact that the elevation of the foundation soil at the 1973 test location was higher than that of the 1974 test location, thereby causing the 1973 strength value at this depth to be representative of the foundation soil. At location 2 of Penn 8 the 1974 field vane strengths were higher than the 1973 strengths, except for one point at a depth of 1.2 meters; the increase at this point is likely due to the existence in 1973 of a desiccated crust that was softened in 1974 by the reoccurrence of flooding.

The first six parts of Figure 8-28 present a similar analysis for data from six locations at Riverside Site. The increase of strength with time is well established by these data, except for the fact that location 6 shows consistently lower strength values for 1972 than for 1971. Another feature of interest in Figure 8-28 is the relatively large 1972 strengths at a depth of 1.2 meters and a few other points at locations 5, 6, 7, and 8; this is likely due to the desiccation of a previous fill surface. Although this phenomenon could be explained by the presence of a layer of material with different properties, no other evidence was found to support this possibility. There are many other factors (such as the presence of roots or stems from current or previous plant growth and debris embedded in the fill) that can cause local variations of strength to occur, but these are not felt to be primarily responsible for the observed strength increases.

Since the characterization tests reported in Chapter 3 indicated that the dredged materials deposited in all four sites were generally similar, the time-dependent strength response at each of these sites can be combined and treated as one representative site which has a history covering the life spans of the four individual sites. The thickness of the fill in each site is nearly equal, and this tends to justify the elimination of this parameter (which reflects the drainage effectiveness) from the analysis. However, because the placement of dredgings into a given site took place discontinuously during several dredging seasons, the synthesis of the strength response from these four sites necessitates that an equivalent zero time or "birthdate" be established for each site. For this purpose the time corresponding to the placement of one-half of the final volume of dredgings in a site is arbitrarily assumed to be the "equivalent zero time" for that site; accordingly, as illustrated in Figure 2-3, 1967, 1968, 1972, and 1966 were taken to be the "birthdates" of the Island Site, Riverside Site, Penn 7, and Penn 8 respectively.

Within the framework of the preceding assumption, the average strength, s_{avg}, was plotted in Figure 8-30 versus the age of the landfill for $\frac{x}{l}$ values of 0.10, 0.20, 0.35, 0.55, and 0.65. The data points determined at the flooded locations in the Island Site and Penn 8 are plotted, but they are not included in the subsequent analysis to identify trends of variation. Based on the relationships illustrated in Figure 8-30, the time-dependent variation of average strength, s_{avg}, at a given point in

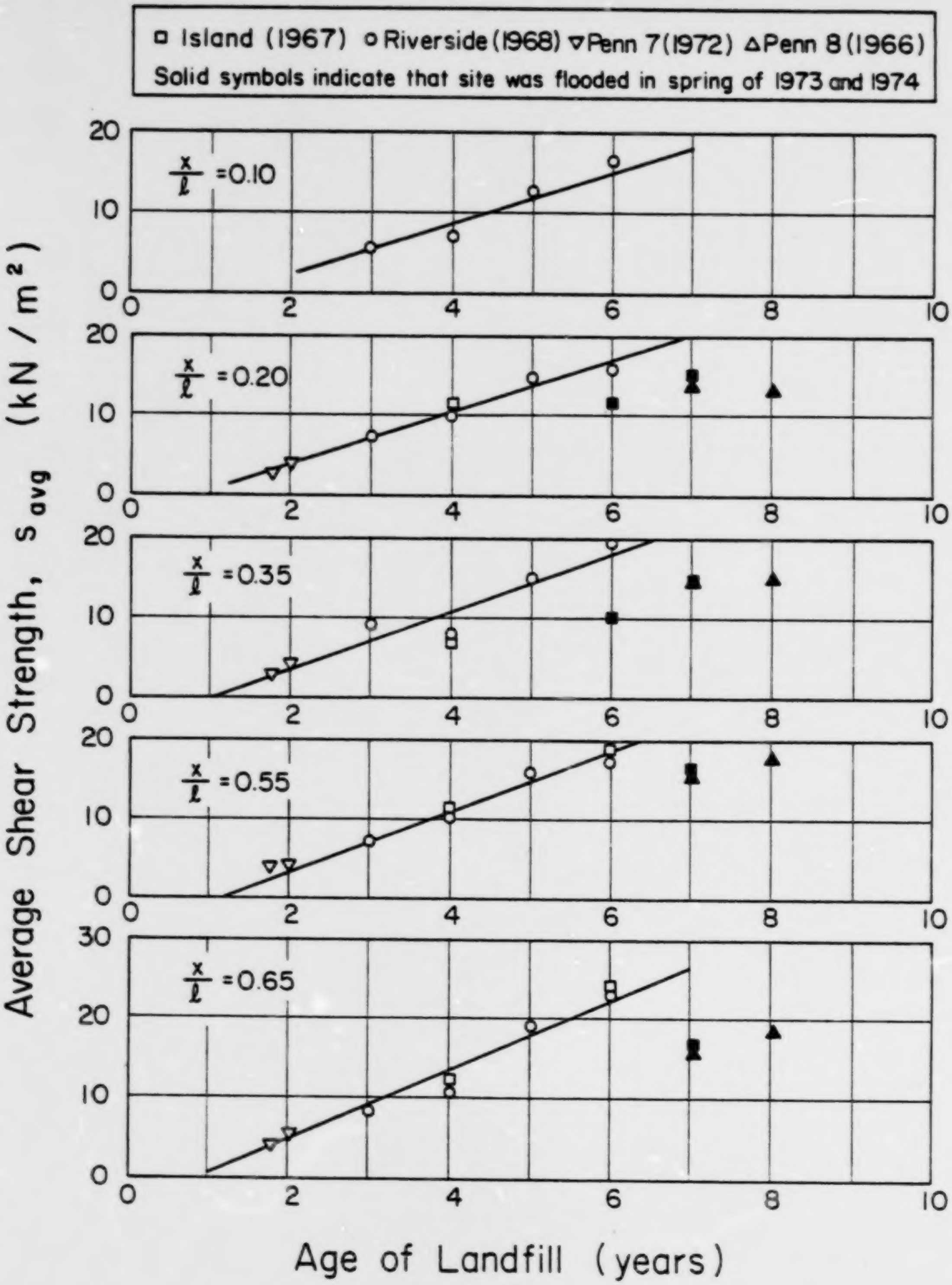

Figure 8-30 Average Field Vane Strength versus Time

a landfill can be expressed as

$$s_{avg} = \frac{\Delta s}{\Delta t} (t - t_o) \quad , \qquad (8\text{-}12)$$

where $\frac{\Delta s}{\Delta t}$ is the rate of strength change with time, t, and t_o is a reference time. According to the plots shown in Figure 8-30, t_o ranges from 0.8 to 1.3 years with an average of 1 year and, as shown in Figure 8-31, $\frac{\Delta s}{\Delta t}$ increases linearly with an increase in $\frac{x}{\ell}$, thus indicating a faster rate of strength gain for regions closer to the discharge pipe. For the specific conditions investigated herein, the particular form of Equation (8-12) becomes

$$s_{avg} = \left(2.9 + 2\frac{x}{\ell}\right) (t - 1.0) \quad , \qquad (8\text{-}13)$$

where s_{avg} and t are expressed in kN/m^2 and years, respectively. The validity of this equation for times longer than 8 or 10 years requires continued field study; simple logic suggests that it will not be valid for very large times, because the strength can not increase indefinitely at the indicated rate. Similarly, the applicability of the equation is limited somewhat by the size and geometry of the containment area considered and more significantly by the nature of the dredged materials from the Toledo area.

Sensitivity

Many normally or lightly over-consolidated clays and silts manifest a reduction in strength upon remolding. Terzaghi (1944) defined the ratio between the undisturbed strength, s, and the remolded strength, s_r, as the sensitivity, S. Values of sensitivity between 2 and 4 are commonly encountered in the types of soil described above; in clays which may be classified as "sensitive" this ratio lies between 4 and 8, and it is greater than 8 for "extra-sensitive" clays (Terzaghi and Peck, 1948). In some

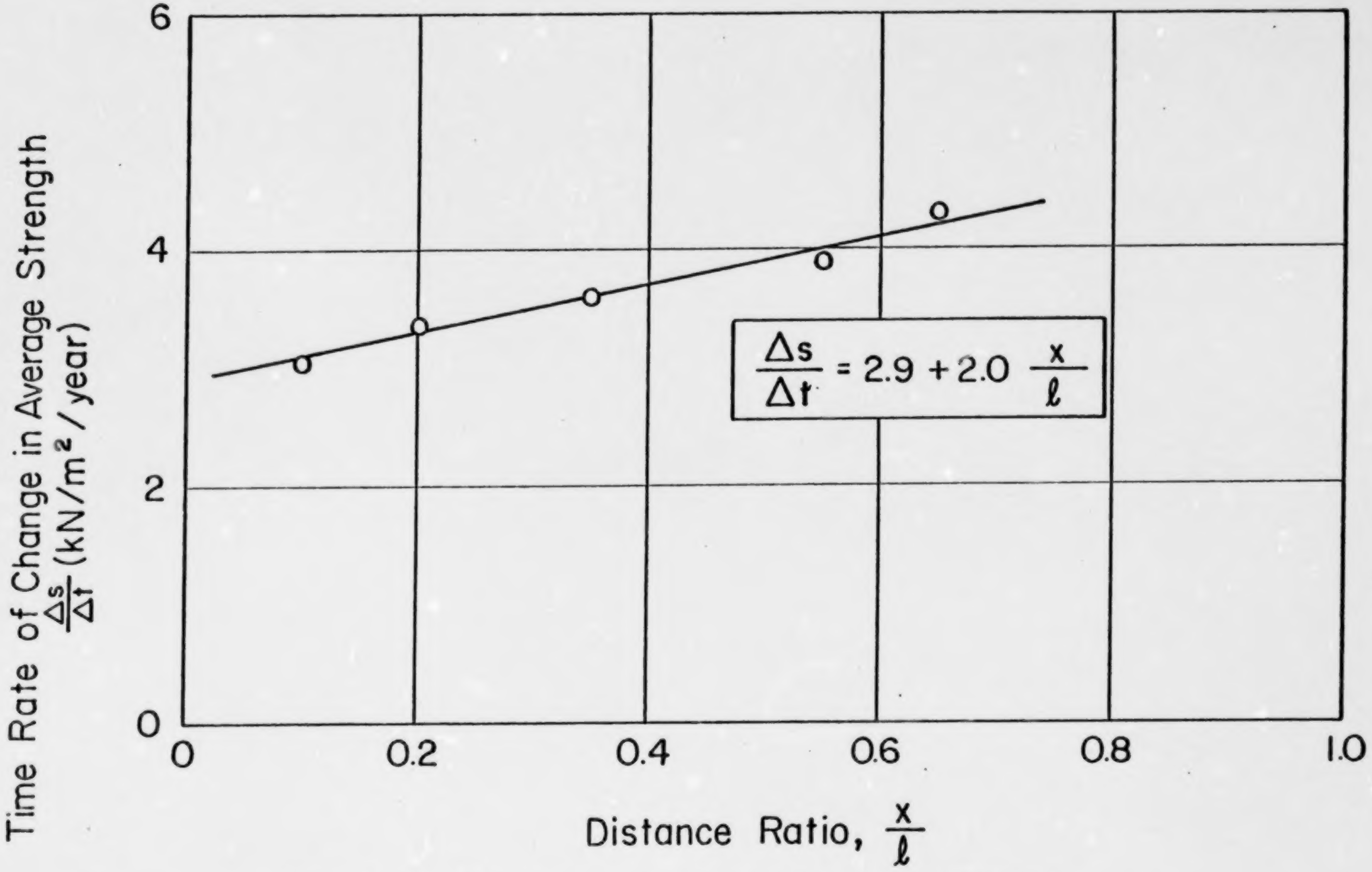

Figure 8-31. Rate of Change of Average Strength versus Distance from Discharge Pipe

problems the fact that a clay may be sensitive or extra-sensitive is as important as its undisturbed strength, and for this reason, a determination of the sensitivity is an essential part of characterizing the strength of a cohesive soil. The "remolding loss" may be defined as $(s - s_r)/s$ and, except in the case of extra-sensitive clays, it is approximately equal to the liquidity index (Skempton and Bishop, 1950). The undrained strength and sensitivity can be obtained from vane tests, and these two parameters have been found to give a very characteristic description of a clay (Andresen and Bjerrum, 1958). Based on the strength increase with depth, it is possible to determine if a clay layer is normally consolidated or over-consolidated, and the spatial variations in shear strength and sensitivity give an evaluation of the homogeneity of the deposit. A high sensitivity suggests the probability of difficulties when undertaking construction operations conducive to remolding (such as excavations and pile driving). Sensitivity is plotted versus natural water content, dry density, and liquidity index in Figures 8-32, 8-33, and 8-34, respectively, for field and laboratory vane shear tests. Values of sensitivity ranged from about 2 to 10 for the field vane tests and from about 3 to 7 for the laboratory vane tests, although considerable scatter was observed. In general, for lower values of natural water contents and liquidity index and higher values of dry density, the sensitivity measured by the field vane is higher than that measured by the laboratory vane, and it is relatively unaffected by the independent variable in the case of high values of natural water content and liquidity index and low values of dry density. The measured sensitivity values places many of these dredgings in the category of "sensitive" soils according to the classification given by Terzaghi and Peck (1948).

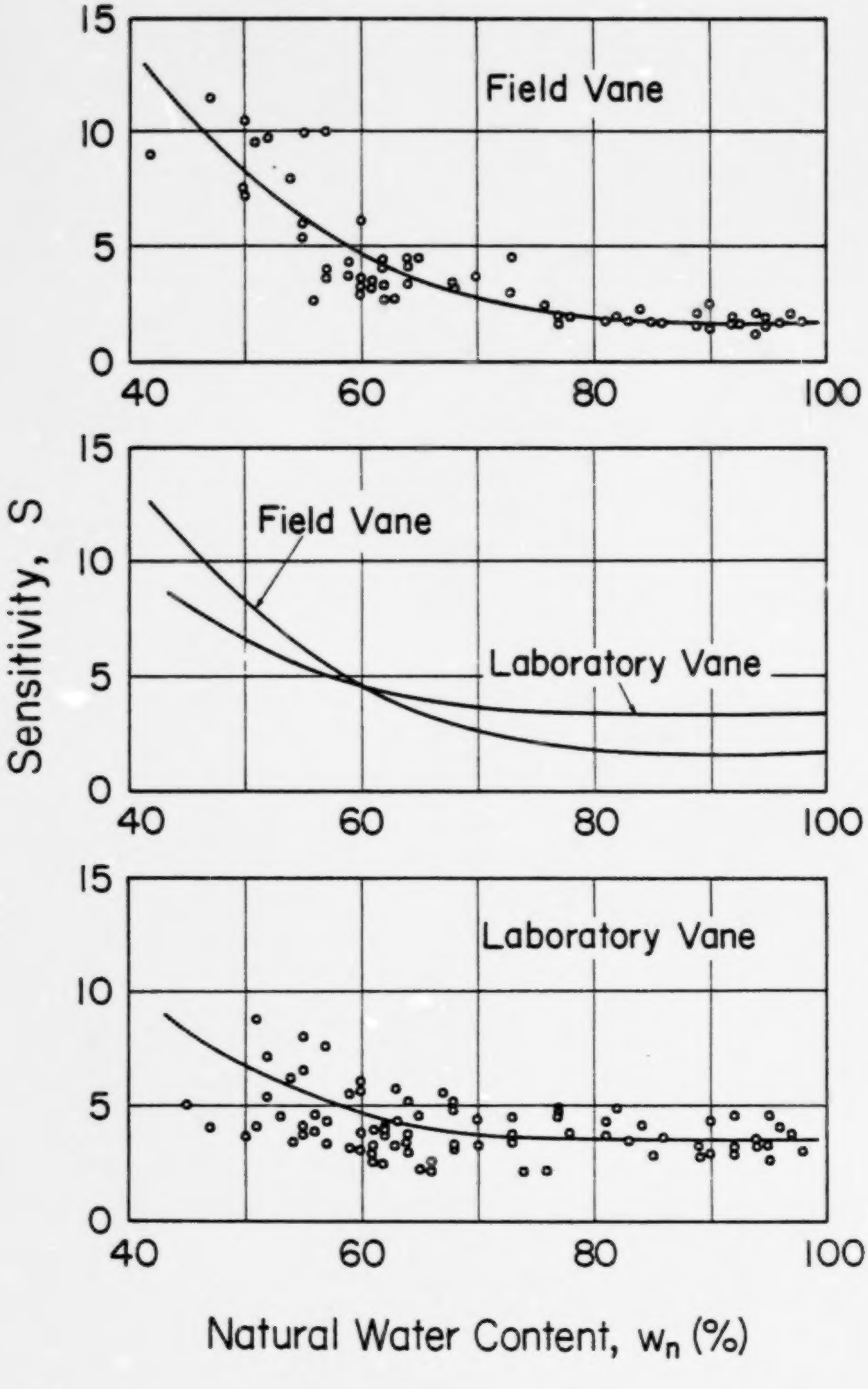

Figure 8-32 Sensitivity versus Natural Water Content

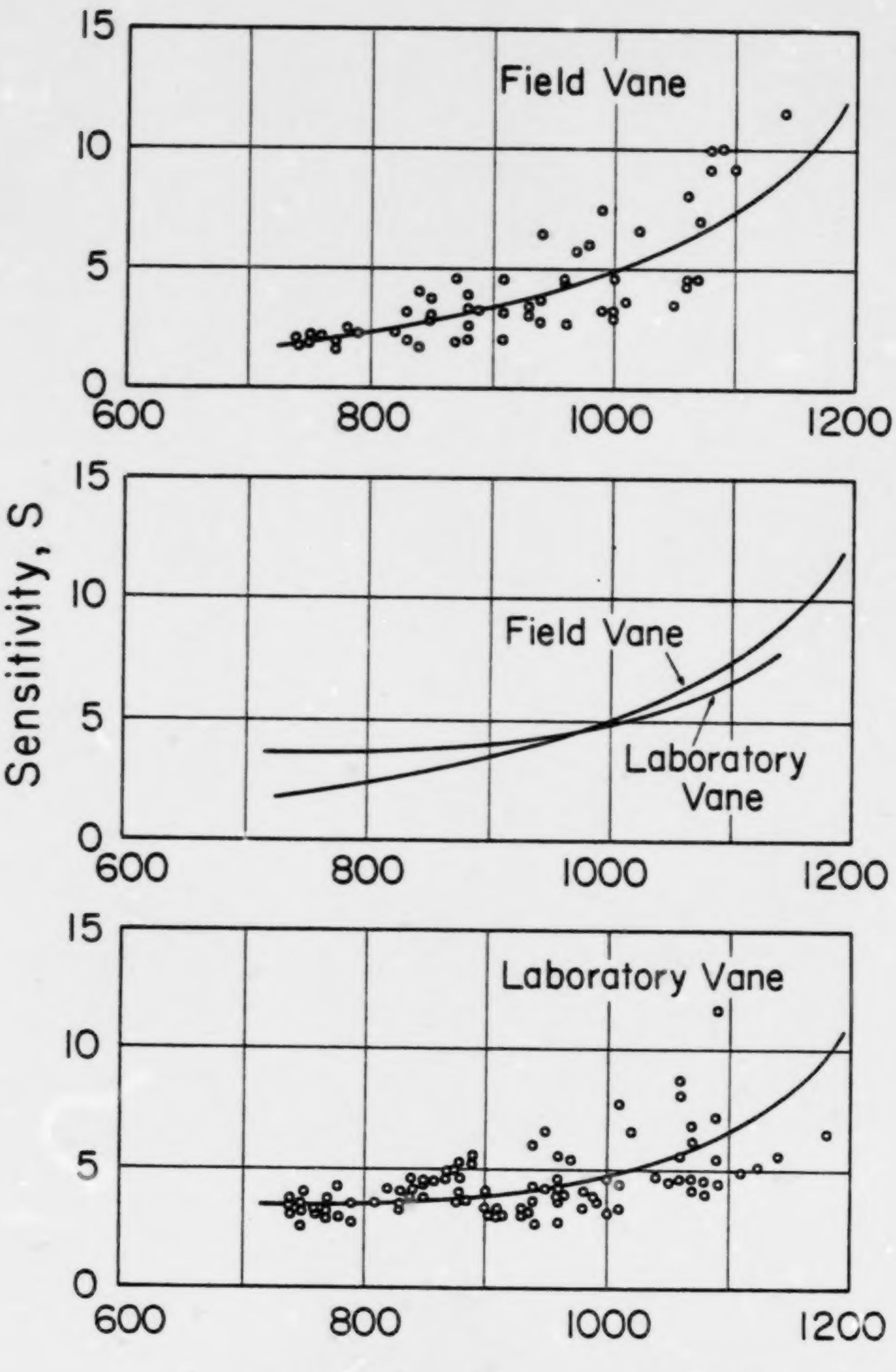

Figure 8-33 Sensitivity versus Dry Density

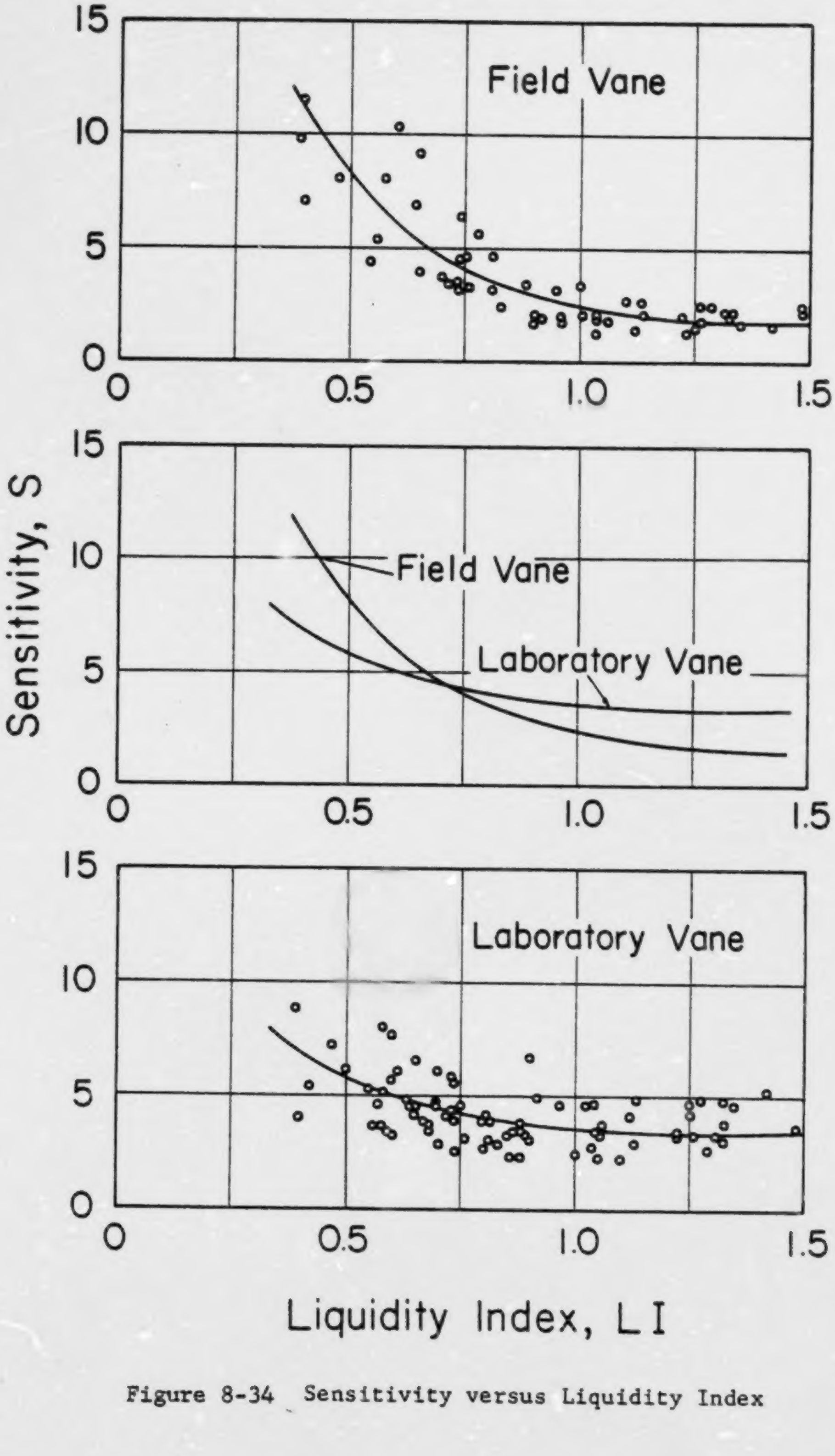

Figure 8-34 Sensitivity versus Liquidity Index

Correlations between Secant Modulus and Index Properties

Various attempts have been made in the literature to correlate the strength of a soil and some form of modulus. Plotted in Figure 8-35 is the two-percent secant modulus (slope of the straight line connecting the origin and the point on the stress-strain curve where the strain is 2 percent) versus the natural water content, dry density, and liquidity index for 33 samples tested in unconfined compression. Although considerable scatter is apparent, straight lines were found to fit the data points reasonably well; the tendency for the scatter to increase as the water content and liquidity index increase and the dry density decreases can be explained by the more erratic degree of disturbance associated with trimming the softer samples. The straight line relationships between the logarithm of the secant modulus, E_{sec}, and the natural water content, w_n, dry density, γ_d, and liquidity index, LI, can be expressed as

$$\log E_{sec} = 0.043\ (120 - w_n) \quad , \tag{8-14}$$

$$\log E_{sec} = 4(\gamma_d/\gamma_w - 0.34) \quad , \tag{8-15}$$

and

$$\log E_{sec} = 2.1(1.9 - LI) \quad , \tag{8-16}$$

respectively, where γ_w is the unit weight of water. These relationships are limited in their usage by the indicated ranges of the independent variables and by the nature of the dredged materials tested in this program.

CONCLUSIONS

Based on the results of the experimental field and laboratory program reported herein, the following conclusions can be advanced regarding the shear strength of dredged material in a landfill:

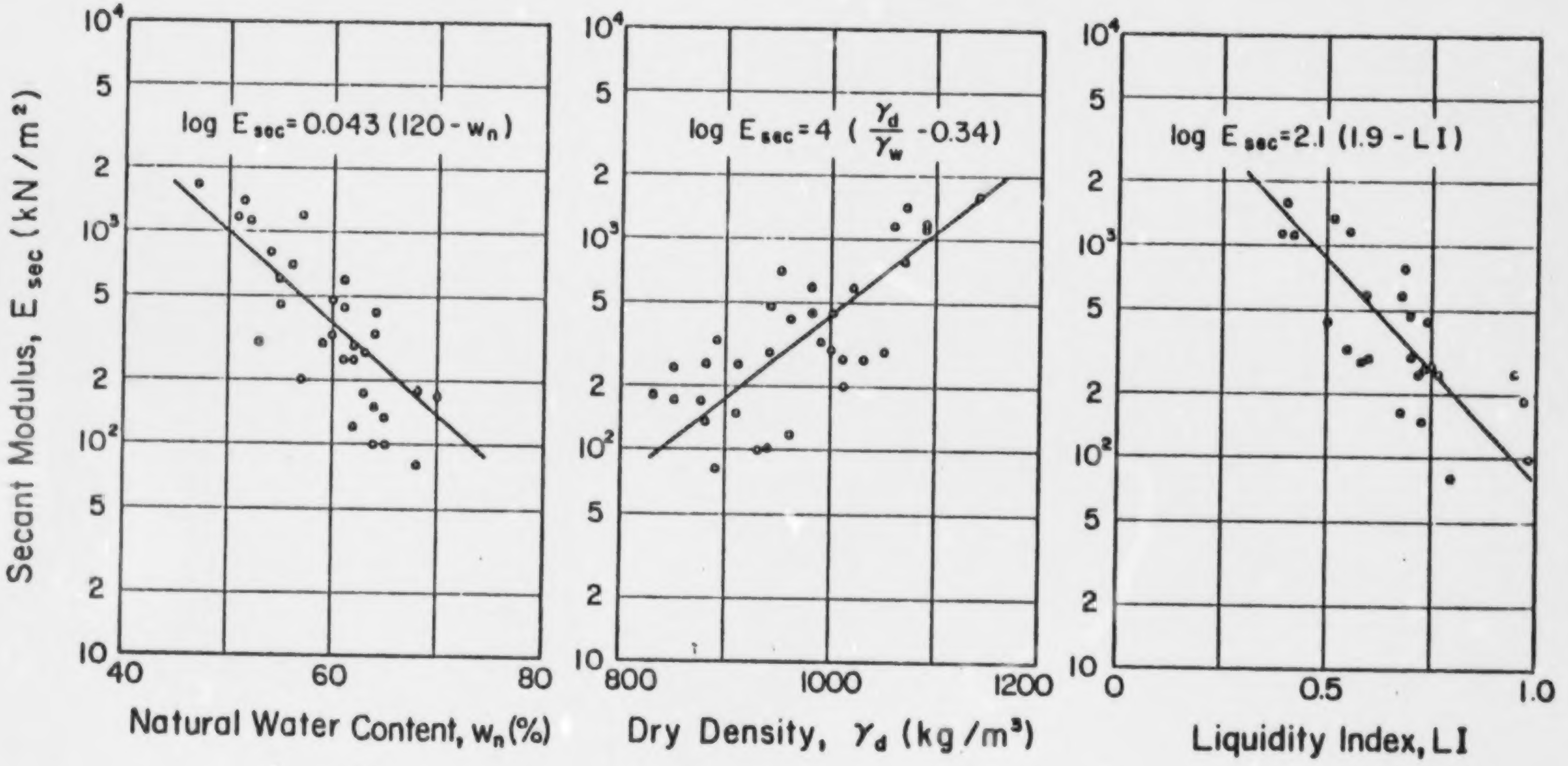

Figure 8-35. Relationships between Secant Modulus and Different Material Properties

1. The water content has a major influence on the shear strength of dredged material, and, if landfills composed of this material are inadequately drained, they will remain soft and weak for many years.

2. The shear strength of the four landfills investigated indicates that they are indeed soft and weak, as is often the case for hydraulically placed fills in the low-lying areas, but the strength appears to increase rather consistently with time.

3. The strength characteristics of dredgings are comparable to those associated with fine-grained organic soils.

4. The field vane provides a realistic way of measuring the in-place shear strength of dredged materials, because it minimizes errors due to disturbances caused by sampling, transporting, and trimming the samples; in most cases the shear strength determined from an unconfined compression test underestimated the strength values measured by means of all other tests.

5. Sensitivity values suggest that dredged materials can be classified as "sensitive" soils.

6. The logarithm of the shear strength values measured in the laboratory by the vane, cone, and unconfined compression tests varied exponentially with the natural water content for values of the latter between 40 and 100 percent and linearly with the dry density and liquidity index.

7. The logarithm of the two-percent secant modulus decreased linearly with the natural water content and liquidity index and increased linearly with the dry density.

CHAPTER 9

FIELD MEASUREMENTS

Described in this chapter are the different phases of the field monitoring program conducted at Penn 7 and the results obtained therefrom. The Penn 7 disposal area was selected for this field study because (a) a limited subsoil investigation of the site had already been completed, thus allowing a better determination of original ground conditions, (b) an opportunity was offered to observe the filling of a diked containment area and to monitor the response from the beginning, (c) the site was scheduled to be filled within a year or two, thereby enabling a logical phase of the study to be completed in a reasonable time, and (d) the material characteristics of the dredged material from the Toledo area had been quantitatively identified by means of an extensive field and laboratory test program on materials from nearby disposal areas. A limited amount of field instrumentation was installed to obtain field response data (primarily settlements and pore water pressures) to correlate with the predictions deduced from laboratory results and a mathematical model. In addition, appropriate measurements of the volume of material occupying the site at any period in time will allow the establishment of a relationship between this latter volume and the volume of dredged material (so-called bin-measure volume) pumped into the site. Movements, if any, of the dike can be determined by means of periodic level and traverse surveys around the crest of the dike during the filling operation. In a separate water quality study reported by Krizek, Gallagher, and Karadi (1974) the respective qualities of the slurry influent and the supernatent effluent waters, as well as the time-dependent quality of the groundwater, are compared.

FOUNDATION SOILS

The nature of the ground surface, its topography, and a description of the foundation soils at the Penn 7 Site prior to the deposition of any dredgings are explained in this section. Permeability values, as well as the methods used to determine them, are also described.

General Description

The Penn 7 disposal area is located on the north bank of the Maumee River upstream from the Terminal Railroad in Toledo, Ohio. The site has approximate dimensions of 800 feet by 1700 feet (240 meters by 510 meters) and is surrounded by an earth dike about 15 feet (4.5 meters) high and 8 feet (2.4 meters) wide at the crest with inner and outer side slopes of 2:1 and 3:1, respectively. About 50 percent of the area was under water prior to the deposition of any dredgings; about 80 percent of this submerged area was located at the northeast side of the site, and it had an average water depth of about 2 feet (0.6 meters) followed by about 1 to 2 feet (0.3 to 0.6 meters) of soft mud. The remaining 20 percent of the submerged area had a water depth of about 10 to 15 feet (3 to 5 meters) and was located in the northwest corner of the site. Other low areas of the site were subjected to intermittent submergence, depending on the water level of the Maumee River and weather conditions.

Topography

There was considerable variation in the topography of the foundation soil in the Penn 7 Site. Contours (given subsequently in Figure 9-13a) were interpolated from elevations taken at the nodal points of a square grid with spacings of 100 feet (30 meters) and from a level survey traversing the crest and inside toe of the dike. Elevations of the submerged areas were obtained either (a) by measuring the bottom directly with a rod resting on a flat plate for shallow depths of water (about 1 foot) or (b) by measuring the water level and the water depth at various points by use of a rubber raft for the deeper depths of water (2 to 15 feet). Maximum changes in elevation were about 17 feet (5 meters); this large variation occurred in the northwest corner of the site, where a deep excavation covering about 10 percent of the site area was made to obtain material to construct the dike. Excluding this deep hole, the change in elevation within the remaining 90 percent of the site was about 4 feet (1.2 meters). A ridge about 50 feet (15 meters) wide spanned the approximate middle of the site in the short direction; this ridge greatly facilitated the transport of materials and equipment across the area. To either side of this ridge were low areas, major portions of which were permanently under water.

Underlying Soils

In 1969, before construction of the dike, the underlying soils at Penn 7 were investigated by the Detroit District of the U. S. Army Corps of Engineers. Two boreholes were located within the area enclosed by the dike at the southwest corner of the site; according to the coordinate system explained in Chapter 2, the locations of the two boreholes are approximately 5/10 and 4/9, and the depths of the two borings are 11 feet (3.3 meters) and 50 feet (15 meters), respectively. The log of the borehole at location 5/10 (surface elevation of 579.04 feet) indicates 9.3 feet (2.8 meters) of stiff gray sandy clay followed by medium gray sandy clay to the bottom of the boring. The soil profile of the borehole location 4/9 (surface elevation of 578.60 feet) begins at the top with 2.6 feet (0.8 meters) of gray clayey silt followed by about 1 foot (0.3 meters) of very loose gray clayey silt, 3 feet (0.9 meters) of soft gray sandy clay, 1 foot (0.3 meters) of medium gray clayey sand with gravel and medium gray sand, and 5.5 feet (1.7 meters) of sandy soils with different densities and colors; the rest of the profile between depths 13.1 feet (4.0 meters) and 50 feet (15 meters) consists of 5 feet (1.5 meters) of loose to medium silty sand, 5 feet (1.5 meters) of very loose clayey silt, 7 feet (2.1 meters) of loose gray sand, 10 feet (3.0 meters) of medium sand, and 9 feet (2.7 meters) of hard sandy clay. Although the two boreholes are only 140 feet (42 meters) apart, their logs are considerably different; this variation makes it difficult to use this information to predict the nature of soil conditions over the remainder of the area.

When drilling the wells that were used to monitor the groundwater quality, split spoon samples were taken at a depth of 10 feet (3 meters) at locations 6/10, 8/8, 9/10, 9/14, and 12/14, and at a depth of 20 feet at locations 8/8, 9/10, and 12/14 (the 12/14 samples were vandalized). The grain size distribution curves for the remaining six samples were determined from seive analysis and/or hydrometer tests and are given in Figure 9-1. At the 10-foot depth the soil is mainly silty clay for the first three locations (6/10, 8/8, and 9/10) and sandy clay for the fourth location (9/14), whereas at the 20-foot depth the soil can be classified as clayey sand. However, the indicated two sources of data (Corps of Engineers boring logs and split spoon samples) show a wide range of variation in the nature of the foundation soil.

Permeability

The process of consolidation and the associated development of shear strength in a landfill of dredged material depend to a large extent on the drainage conditions at the boundaries (especially the lower boundary) of the containment area. Accordingly, the in-situ permeability of the foundation soil at Penn 7 was determined by a variety of different methods prior to the placement of dredged material.

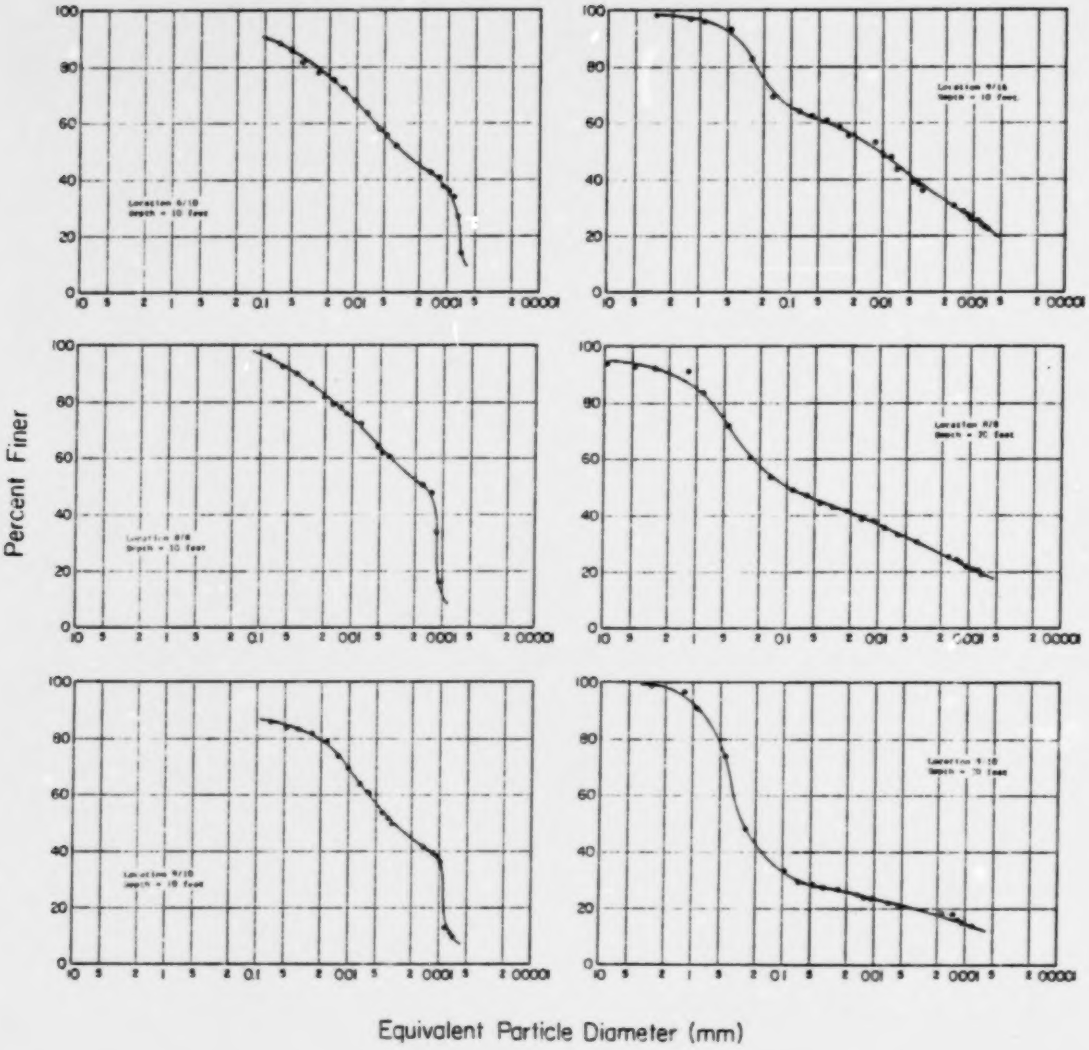

Figure 9-1. Grain Size Curves of Foundation Soils

Shallow Infiltration Tests -- Shallow infiltration tests were conducted to measure the permeability of the top layer of the foundation soil at locations 3/10, 3/13, 6/10, 6/13, 8/8, 9/10, and 9/14 (see Figure 2-5). In each case a hole about 10 inches (0.25 meters) in diameter and varying between 2 and 4 feet (0.6 and 1.2 meters) deep was dug in the ground by a hand auger, and a steel casing with an internal diameter of 5 inches (13 cm) and a length of 4 feet (1.2 meters), perforated for 8 inches (0.2 meters) above its closed bottom end, was inserted into the hole. Filter sand was placed around the perforated tip between the casing pad and the foundation soil, and the rest of the space above this filter was plugged to the ground surface with a soil-bentonite mixture and saturated with water to ensure a good seal above the filter sand. The casing was then filled with water, which was allowed to seep into the foundation soil while the level was recorded as a function of time (considering zero time when the water level was at the top of the casing). After completion of the test, the casing was recovered and the procedure was repeated at another location.

Deep Well Tests -- Holes with a diameter of 4 inches (10 cm) and a depth of 10 feet (3 meters) or 20 feet (6 meters) were drilled at several locations either by a truck-mounted drilling rig (locations 6/10, 8/8, 9/10, 9/14, and 12/14) or a hand-operated power auger (locations 3/10, 3/13, and 6/13), depending on accessibility. Although these holes were drilled mainly to install wells for obtaining samples of groundwater before and during the deposition of polluted dredged spoil into the site, they served the dual purpose of providing opportunities for field permeability determinations for the foundation soil at depths of 10 feet (3 meters) and 20 feet (6 meters). PVC pipes with a diameter of 2 inches (5 cm) and a perforated tip of 2.5 feet (0.75 meters) above the closed bottom ends were inserted in these holes, and a filter sand was placed around and above the perforated tip to a depth of about 4 feet (1.2 meters); then, a bentonite seal was installed above the filter, and the remaining annular space was filled with local soil. In most cases an outer 4-inch (10 cm) diameter casing was used temporarily to prevent the caving of surrounding soils into the drilled hole; this casing was retracted after placement of the well pipe, the filter, and the seal.

Pumping tests were attempted for all wells, but in most cases the wells did not flow sufficiently fast to attain a continuous discharge. At locations where the wells did supply water continuously, a steady-state was not attained; however, the flow quantity and corresponding times were measured. In all cases the rates at which the water level in the wells approached the ambient water level were recorded, and associated in-situ permeabilities were determined. At a few locations where the flow into the well was slow, the well was filled with water and an infiltration test was conducted in a manner similar to that used for the shallow infiltration tests. Figure 9-2 shows several photographs in the conduct of the field permeability tests. At location 6/10, where the ground surface and consequently the top of the well was lower than the water level in the northeast corner of the site, the 20-foot (6-meters) well exhibited an artesian flow condition, and the water flowed freely from the well. When the height of the well casing was extended, the water level reached equilibrium at a height of about 32 inches (0.8 meters) above the top of the ground surface; this water level was about the same as that of the water in the northeast corner of the site.

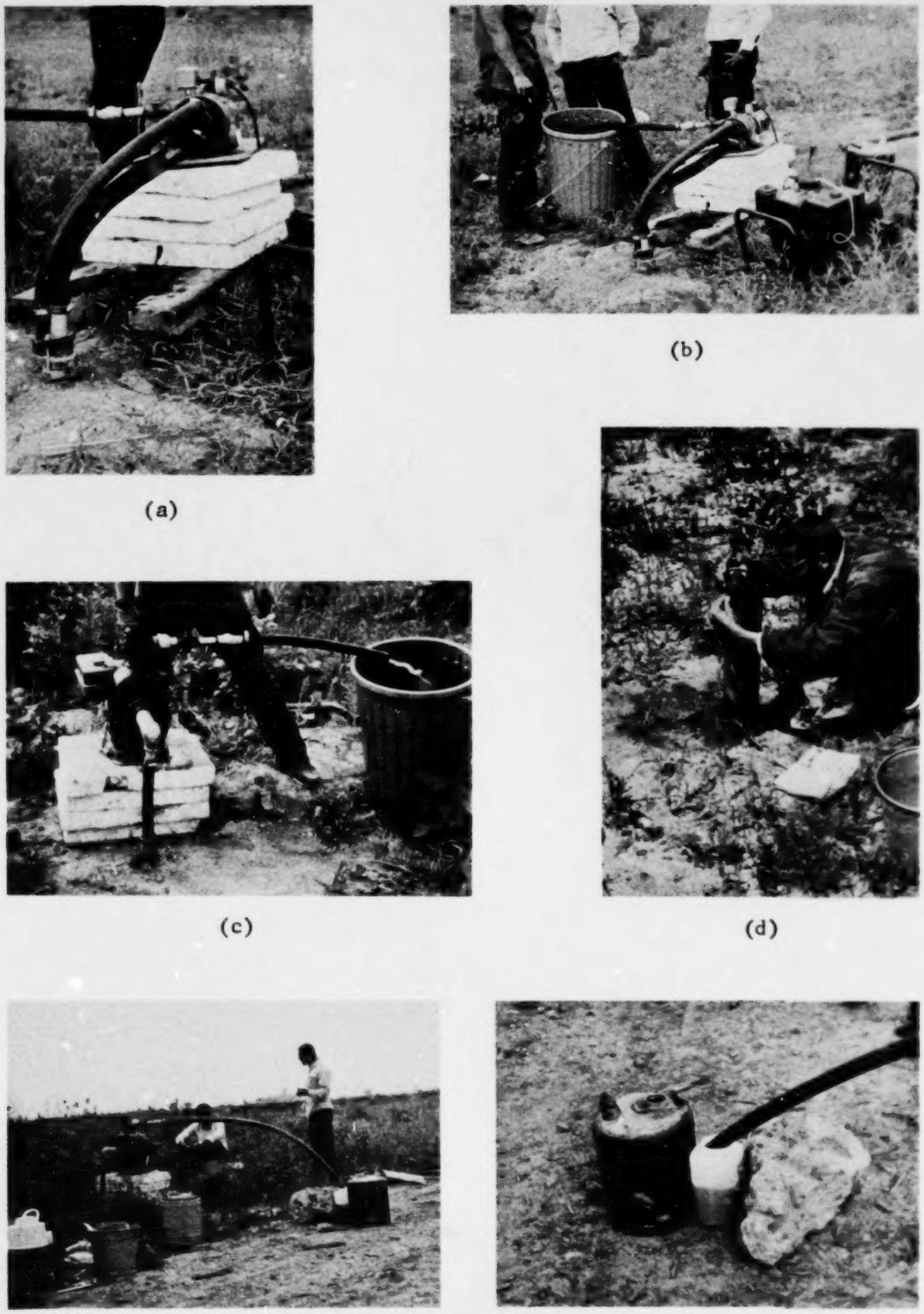
(a)
(b)
(c)
(d)
(e)
(f)

Figure 9-2. Photographs of Field Permeability Tests

Results -- Appropriate formulae compiled by Lambe and Whitman (1969) and Hvorslev (1949) were used to interpret these data, and permeability values were calculated on the assumption that the vertical and horizontal permeabilities are equal. A summary of the ranges for permeability coefficients at different locations and various depths is given in Table 9-1.

Table 9-1

Coefficient of Permeability for Foundation Soil

Location	Ranges for Coefficient of Permeability, k (cm/sec)		
	Shallow Infiltration Test	Three-meter Well	Six-meter Well
3/10	1.4×10^{-3} to 6.7×10^{-3}	9.0×10^{-5} to 2.8×10^{-4}	
3/13	1.0×10^{-4} to 3.0×10^{-4}		
6/10	1.6×10^{-5} to 8.0×10^{-5}	4.0×10^{-6} to 1.0×10^{-4}	1.8×10^{-3} to 2.3×10^{-2}
6/13	4.3×10^{-6} to 9.4×10^{-5}	1.2×10^{-3} to 4.8×10^{-3}	
8/8	3.0×10^{-7} to 5.0×10^{-6}	1.5×10^{-4} to 1.3×10^{-3}	1.7×10^{-4} to 1.5×10^{-3}
9/10	1.1×10^{-4} to 2.1×10^{-4}	6.0×10^{-7} to 1.1×10^{-4}	3.4×10^{-4} to 2.8×10^{-3}
9/14	3.2×10^{-6} to 6.4×10^{-6}	2.8×10^{-5} to 4.7×10^{-4}	8.7×10^{-5} to 4.5×10^{-4}
12/14		1.4×10^{-4} to 1.7×10^{-3}	3.3×10^{-5} to 1.0×10^{-4}

SETTLEMENT PLATE-PIEZOMETER UNITS

The field measurement of settlements and pore water pressures is usually accomplished by means of settlement plates and piezometers, and the accessibility of this instrumentation is as important as its performance. For landfills composed of dredged materials the conditions that exist during the process of deposition pose a particularly difficult access and installation problem because most of the units must be placed while the fill material is in a slurry form. Presented in this section are the descriptions and locations of the settlement plates and piezometers, the methods of installation and observation, and the field data that have been obtained. These data will aid in evaluating the accuracy of predictions based on mathematical models and associated laboratory test results (compression index, coefficient of consolidation, coefficient of secondary compression, etc).

Locations

Original plans included the placement of settlement plate-piezometer units at four different elevations (original ground and 3 or 4-foot intervals during the deposition of dredged material) at each of ten locations in the Penn 7 Site, as shown in Figure 9-3; five of these locations (2/10, 5/10, 8/10, 12/10, and 15/10) lie along the base line shown in Figure 2-4, three (5/8, 5/13, and 5/16) were chosen on a perpendicular line (with location 5/10 serving as a common point on both lines), and the remaining two locations were selected to obtain some information on the behavior near the middle of the site (8/13) and near the discharge pipe (12/8). The first set of units was placed at all locations and embedded about 4 to 12 inches (10 to 30 cm) in the foundation soil. Due to various factors (weather conditions, vandalism, inaccessibility, etc) five of these units were lost or destroyed before installing others at higher levels, and they

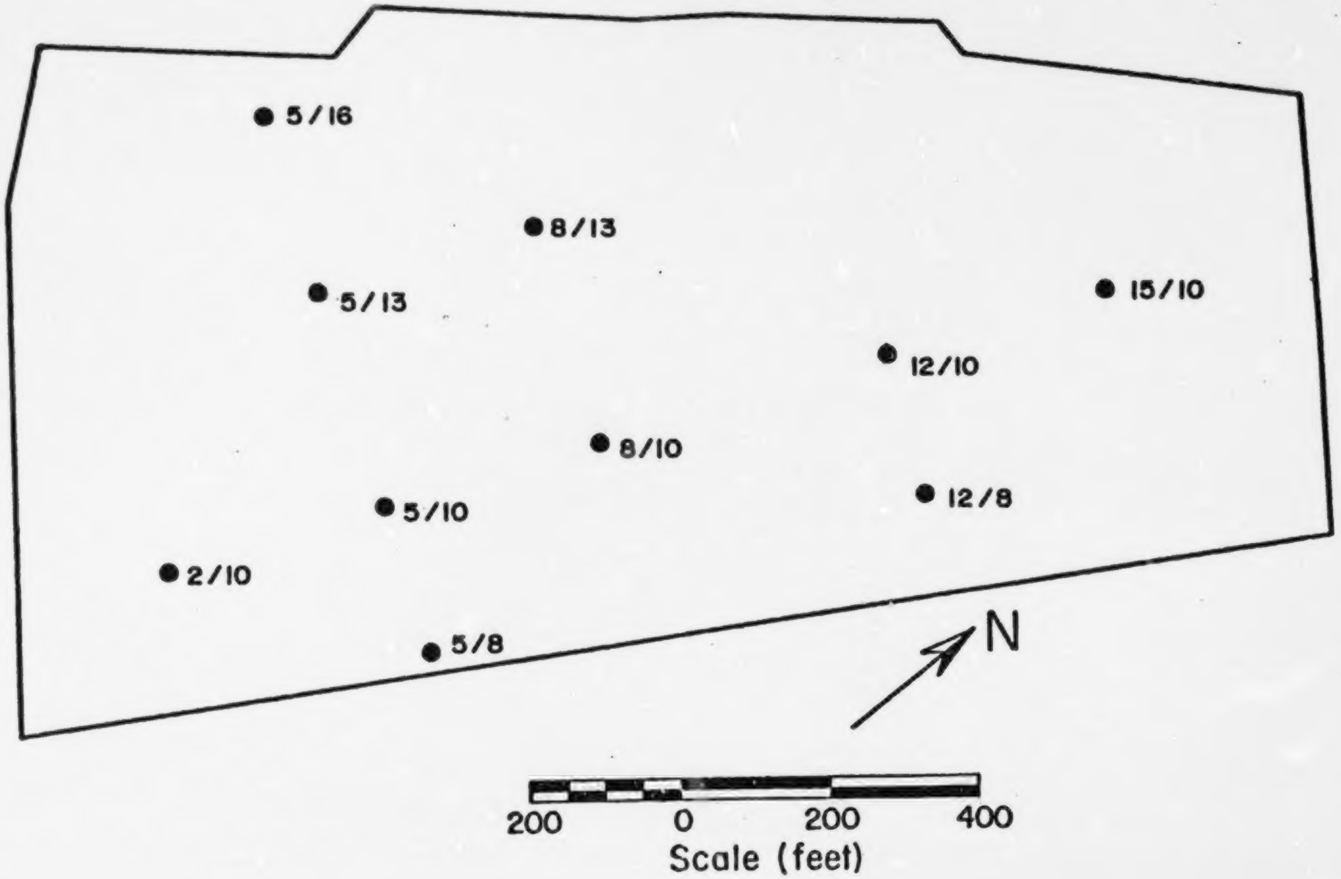
5/16
8/13
5/13
15/10
12/10
8/10
12/8
5/10
2/10
5/8
N
200
0
200
400
Scale (feet)

Figure 9-3. Locations of Settlement Plates and Piezometers

could not be replaced; subsequently, it was decided to omit all units at these locations, because the settlement of the bottom boundary could not be monitored. All other units were placed at the remaining locations at appropriate times during the dredging and disposal process, but a few of these units were lost or destroyed subsequently due to vandalism. Three units were monitored up to and including May of 1974 at each of locations 5/8, 5/10, 5/13, and 15/10; however, in August of 1974 two units at location 5/8 were missing. Also, two intermediate units at location 2/10 were monitored up to and including October of 1973 for one unit and December of 1973 for the other; the bottom unit at this location was vandalized before any measurements could be taken. The initial elevations of all units are given in Table 9-2.

Description of Unit

As shown in Figure 9-4, the settlement plate-piezometer unit is composed of a wide base plate connected to a riser with a porous collar around a perforated section of the riser. The base plates for the units installed in the foundation soil were relatively small and heavy (5/8-inch thick steel plates 18 inches square), whereas the units placed in the fill itself were much larger and lighter (two 1/8-inch thick crossed sheets of corrugated fiberglass 30 inches square) so that the weight of the entire unit is approximately that of the displaced slurry to avoid sinking. The piezometers were made by casting a mix of 20-30 Ottawa sand, epoxy, and hardener in proportions of 278:8:1 by weight in a cylindrical mold (4.5 inches (11 cm) in diameter and 8 inches (20 cm) in height) around a perforated section of 1-inch (2.5 cm) PVC riser pipe. A few reinforcing bars and keys were used to help maintain the integrity of the collar and to hold it in position along the riser pipe. Details regarding the

Table 9-2

Base Elevations of Settlement Plate Units

Location	Unit Number	Date of Installation	Base Elevation at Time of Installation (feet)	Original Elevation of Foundation Soil (feet)	Remarks
2/10	1	8-31-72	572.53	572.8	Unit lost between 1-73 and 4-73
	2	6-15-73	576.92		Unit lost between 12-73 and 4-74
	3	8-16-73	578.88		Unit lost between 10-73 and 12-73
5/8	1	8-31-72	570.54	570.9	Unit lost between 5-74 and 8-74
	2	6-13-73	577.02		Unit lost between 5-74 and 8-74
	3	8-16-73	582.24		
5/10	1	8-31-72	568.98	569.9	
	2	6-13-73	576.71		
	3	8-16-73	581.11		
5/13	1	8-31-72	570.62	571.0	
	2	6-13-73	577.23		
	3	8-16-73	580.96		Unit lost between 4-74 and 5-74
5/16	1	9-1-72	555.60	557.7	Unit lost in 6-73
8/10	1	8-31-72	571.25	571.6	Inaccessible
8/13	1	8-31-72	570.32	570.7	Unit lost in 11-72
12/8	1	8-22-72	568.10	569.0	Unit lost in 6-73
	2	10-20-72	577.30		Unit lost in 6-73
12/10	1	8-22-72	567.52	568.3	Unit lost in 11-72
	2	10-20-72	575.02		Inaccessible after 6-73
15/10	1	8-22-72	567.75	568.6	
	2	10-20-72	575.85		Unit lost between 1-73 and 4-73
	3	6-14-73	578.55		
	4	9-14-73	582.63		

1a	5/8-inch steel plate (18 inches square)
1b	Two crossed sheets of corrugated fiber glass (30 inches square)
2	5/8-inch PVC plate (12 inches square)
3	1-inch PVC flange
4	Rubber gasket
5	Steel bolts
6	1-inch PVC riser pipe
7	6-inch perforated section of PVC pipe
8	Sand-epoxy porous stone
9	Crossed reinforcing bars
10	1-inch PVC coupling
11	2-inch PVC casing

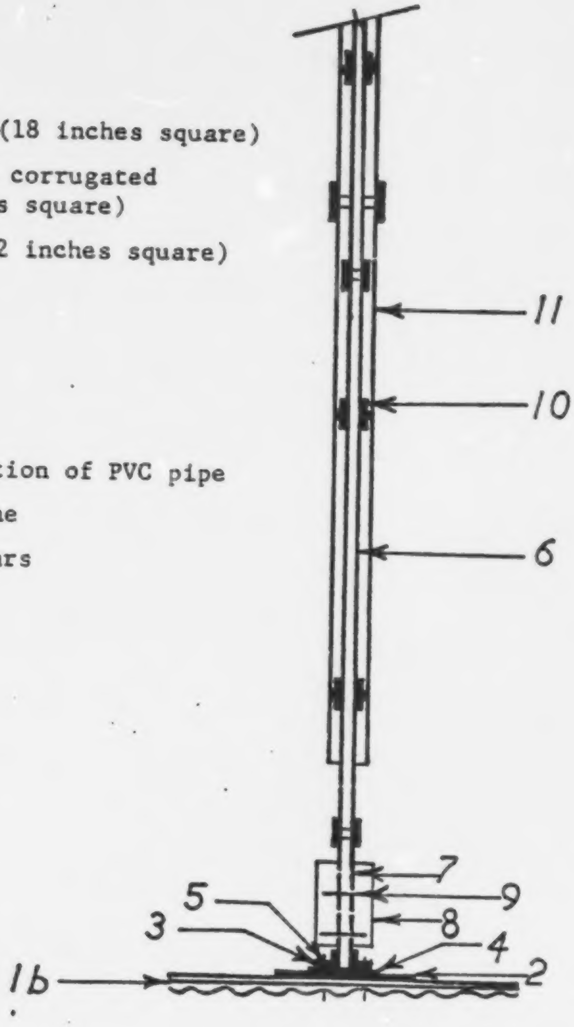

Intermediate Level Unit

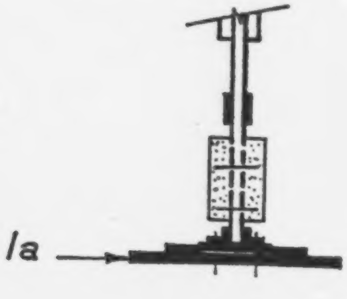

Bottom Level Unit

Figure 9-4. Construction Details of Settlement Plate-Piezometer Units

construction of these units are illustrated in Figure 9-4.

The various components of these units were transported to the field site separately and assembled at the time of installation. All PVC connections were made with a special adhesive which served very well and hardened in about 10 minutes. The riser lengths at the time of installation were about 7 to 10 feet (2 to 3 meters), and extensions were added as required to keep the risers above the fill surface.

Methods of Installation

Due to the different conditions of the soils in which the settlement plate-piezometer units were placed (the foundation soil was either relatively dry or under water of different depths, and the deposited dredgings were primarily in a slurry form covered with less than one meter of water), various methods of installation were used. These methods and the techniques used to establish the elevations of the units at the time of placement are explained briefly in the following sections.

Dry Foundation Soil -- At locations 2/10, 5/8, 5/10, 5/13, 8/8, and 8/13, the foundation soil was relatively dry. In these cases the ground surface was excavated to a depth of about 4 to 12 inches (10 to 30 cm) and leveled horizontally. Then, the steel base plates and piezometers were installed, and the elevations of the tops of the riser pipes were determined by conventional level-and-rod techniques. Well-graded sand was placed around the porous collars to afford extra protection against plugging by the dredging slurry.

Submerged Foundation Soil -- At locations 12/10, 15/10, 12/8, and 5/16, the foundation soil was submerged under a depth of water ranging from about 2 feet (0.6 meters) at the first three locations to 14 feet (4.2 meters) at the fourth location. In these cases a rubber raft was used to transport and install the assembled units and the filter sand. The top 1 to 1.5 feet (0.3 to 0.5 meters) of the foundation soil was a thick mud, and the steel base plates were seated in this mud and leveled horizontally. The elevations of the base plates were obtained by an appropriate combination of the elevation of the water surface, the total length of the riser pipe, and the portion of the riser pipe above the water surface. Sufficient sand was poured around the riser to cover the porous collar at locations 12/10, 12/8, and 15/10; at location 5/16 several large stones and buckets of sand and gravel were gently released around the riser to stabilize the base plate and cover the piezometer.

Dredging Slurry -- A rubber raft was used to install the units at predetermined points in the soft slurry of hydraulically placed dredged material. The relatively deep layer of water above the slurry at some locations made it relatively easy to maneuver the raft and place the units at their proper locations, but in most cases the layer of water above the mud surface was too shallow (only a few centimeters) to permit adequate maneuverability by paddling only; therefore, a rope was extended across the site near the desired locations to afford some assistance in moving the raft. Although this procedure was very difficult, tiring, and time consuming, it served the purpose and seemed reasonably practical for the existing conditions.

Extensions to the risers of previously installed units were also placed by this method. Figure 9-5 shows several photographs of the procedures followed during the installation of settlement plate-piezometer units on the mud surface. In two cases it was possible to walk on the surface to place new units and to extend the risers of existing units while the dredging and disposal process continued. The first of these

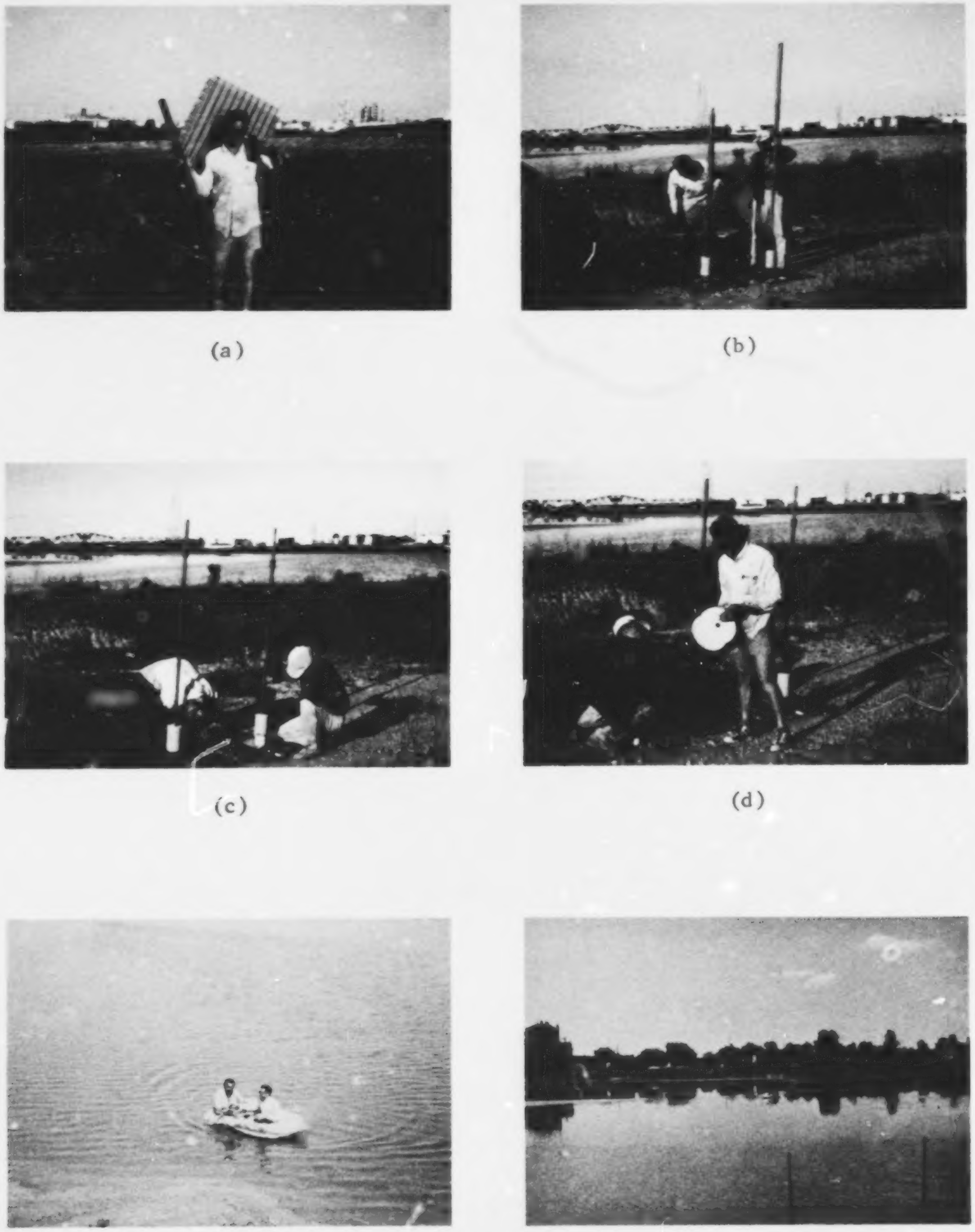

(a)

(b)

(c)

(d)

(e)

(f)

Figure 9-5. Photographs of Settlement Plate Installation

was at location 15/10 several days after the second dredging season started (June 1973), and the second was at location 12/10, which was close to the major channel of mud flow from the discharge pipe; in this latter case it was possible to walk on the relatively firm bottom of the channel in about 2 feet (0.6 meters) of slurry.

Some of the settlement plate units tilted by as much as 30 degrees from the vertical; this was caused during the first winter primarily by strong winds and ice floes acting on the risers while the plates were embedded in very soft materials. When the units became accessible in the spring, considerable vertical realignment was achieved by using large stones as anchors and attaching tension ropes to the risers.

Methods of Monitoring

Depending on the accessibility of the settlement plate locations, different methods of monitoring were used. Up to a certain stage, the risers were accessible by means of the rubber raft; this stage was followed by a period of time during which the units were virtually inaccessible; still later the units could be reached by using plywood "mudshoes" to walk on the mud surface; and finally, the dredged material desiccated sufficiently to afford a reasonably solid surface capable of supporting an individual. The various methods of monitoring that were used are explained in the following sections.

Measurement of Risers Above Water Surface -- During the early stages of slurry deposition, a sufficiently deep layer of water existed over most of the site to afford a relatively effective use of the rubber raft, as explained previously. The plate elevations were established by subtracting the length of the riser below the water surface from the elevation of the water surface.

Measurement of Calibrated Risers -- As the site filled, the elevation of the mud surface was very close to that of the water surface, and the units were virtually inaccessible. At this time 5-foot (1.5-meter) sections of 1-inch (2.5-cm) riser pipes were calibrated and affixed to all existing risers. Subsequently, these calibrated risers were monitored by use of a level located on the top of the dike, and the base plate elevations were established in a straight-forward manner.

Conventional Level Measurements -- After the fill surface desiccated sufficiently to allow a person to walk on it (either with or without "mudshoes"), the units were monitored directly by conventional leveling techniques (that is, measuring the elevation of the top of the riser and subtracting the length of the riser to obtain the plate elevation). Riser lengths in excess of 1 to 2 feet (0.3 to 0.6 meters) above the fill surface were cut and measured, and the remaining riser lengths were calculated.

Piezometric Heads -- The piezometric water levels were measured by lowering an electrode in the pipe, measuring the length of the electrode cord necessary to close a circuit, and subtracting this length from the elevation of the top of the riser.

Results

Figures 9-6 through 9-10 show the measured settlements and piezometric heads above the mid-height of the porous stones for two units at location 2/10 and three units at each of locations 5/8, 5/10, 5/13, and 15/10 (no water heads were measured at location 2/10). The latest installed units near the surface of the fill were dry throughout the period of observation; hence, records of piezometric heads are given only for the deeper units. The initial elevations of the base plates at each location are given in Table 9-2. The monitoring of settlements started about 280

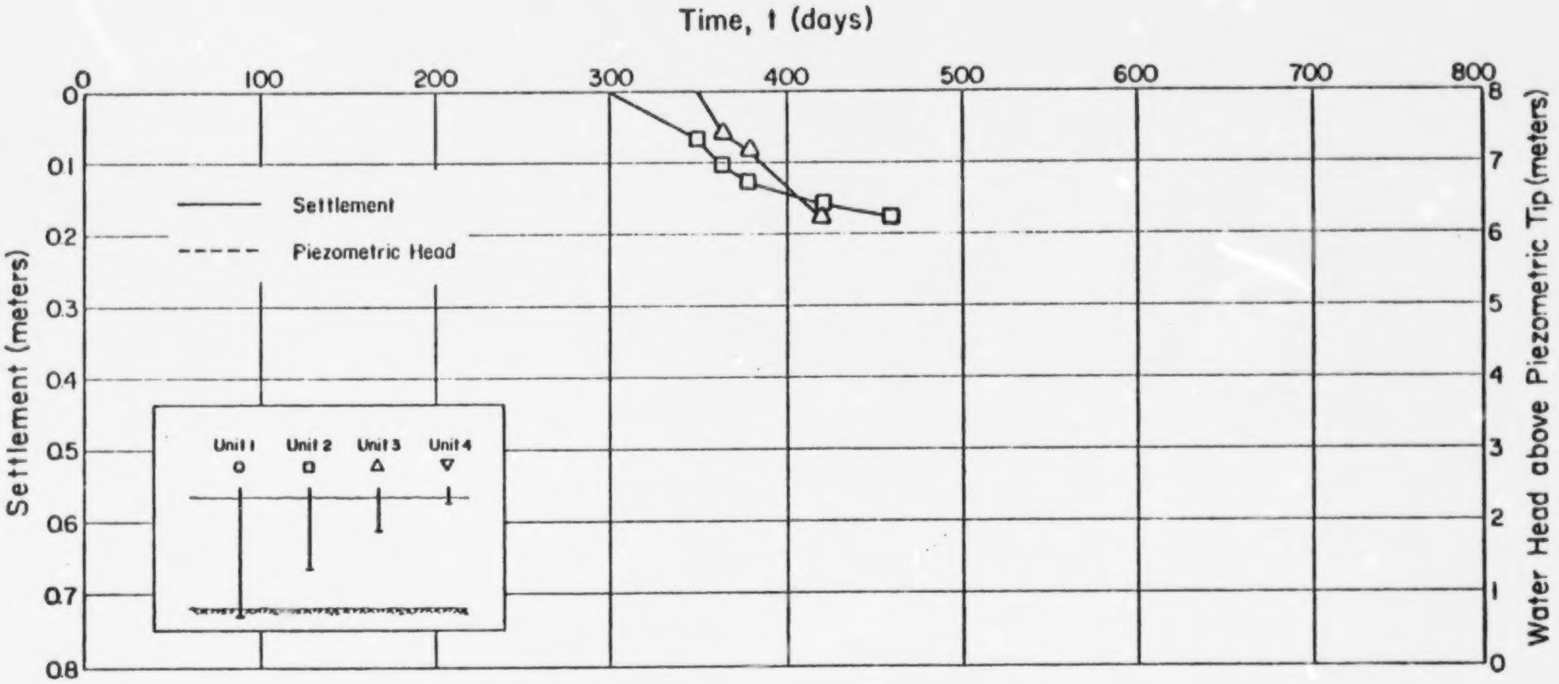

Figure 9-6. Settlement and Piezometric Head versus Time at Location 2/10

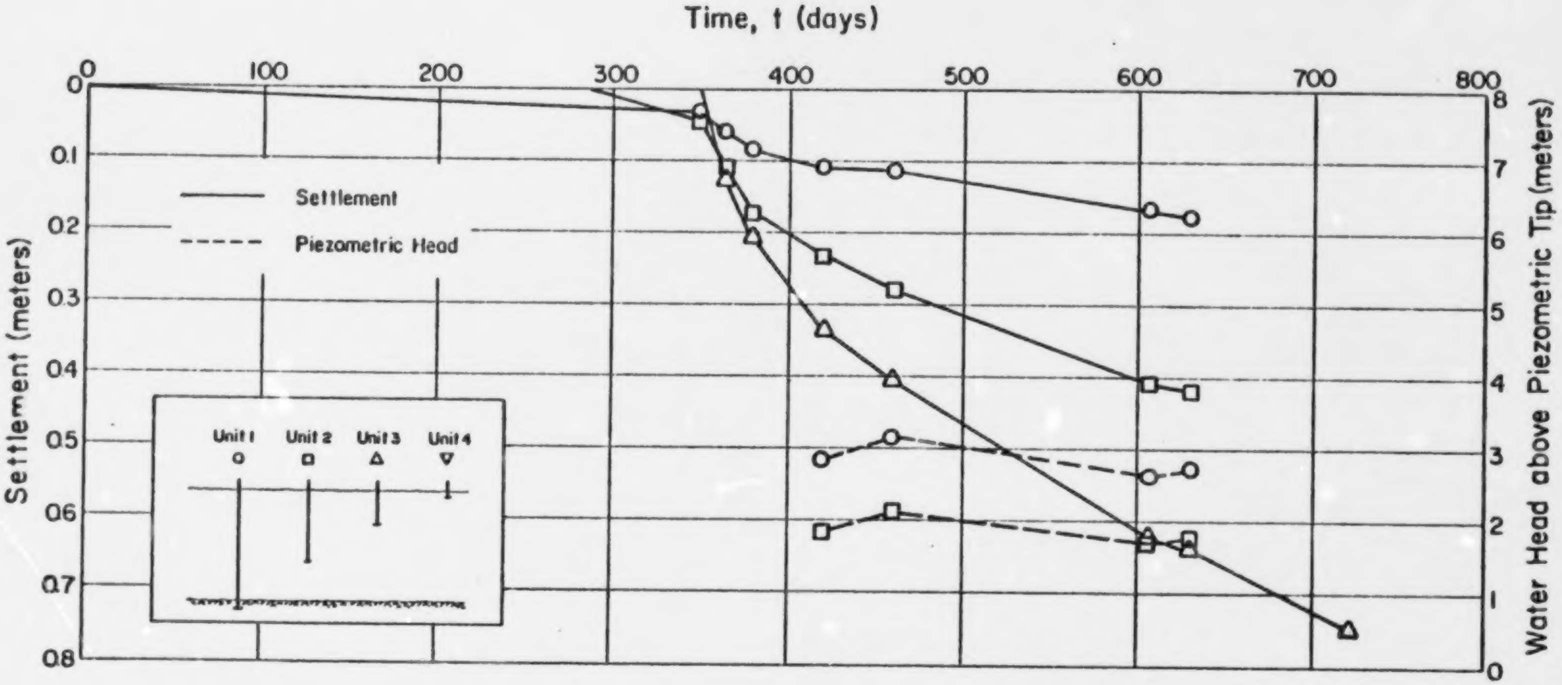

Figure 9-7. Settlement and Piezometric Head versus Time at Location 5/8

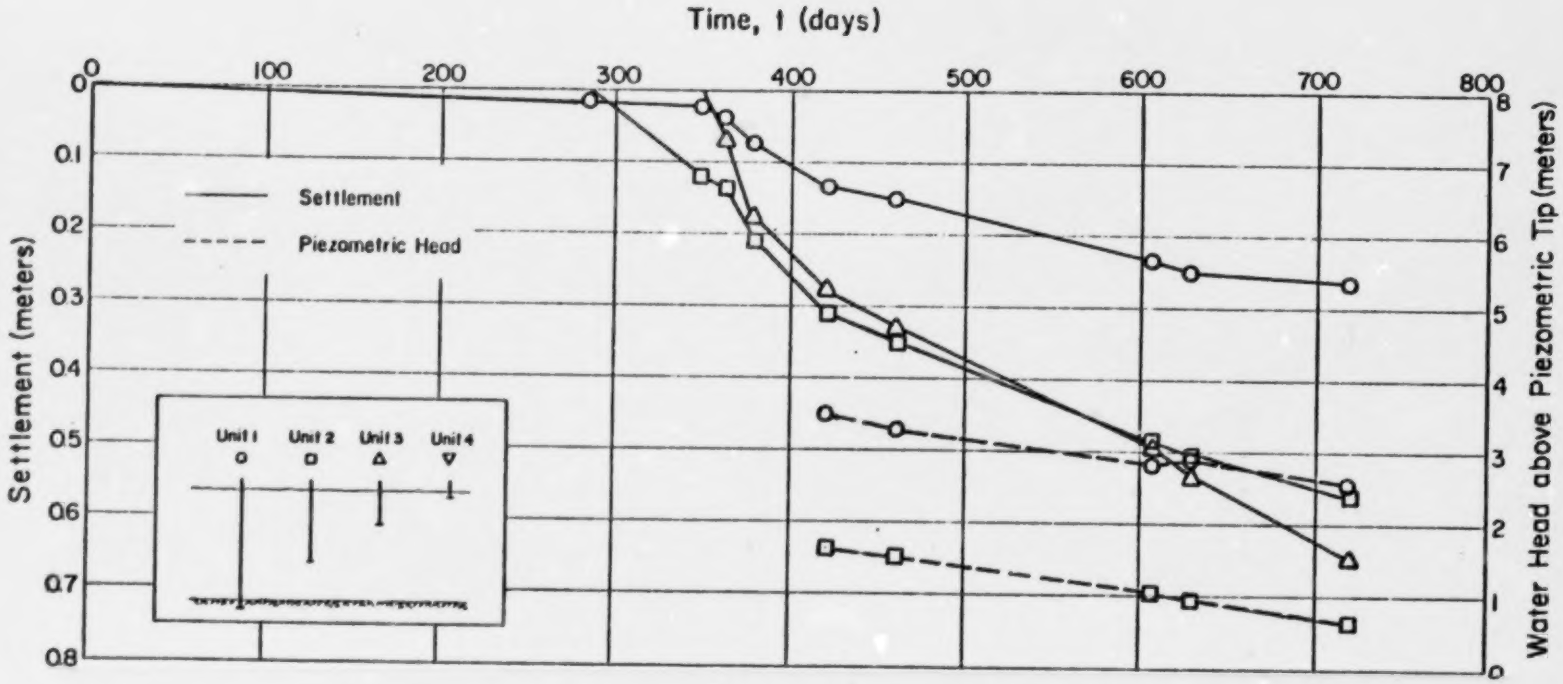

Figure 9-8. Settlement and Piezometric Head versus Time at Location 5/10

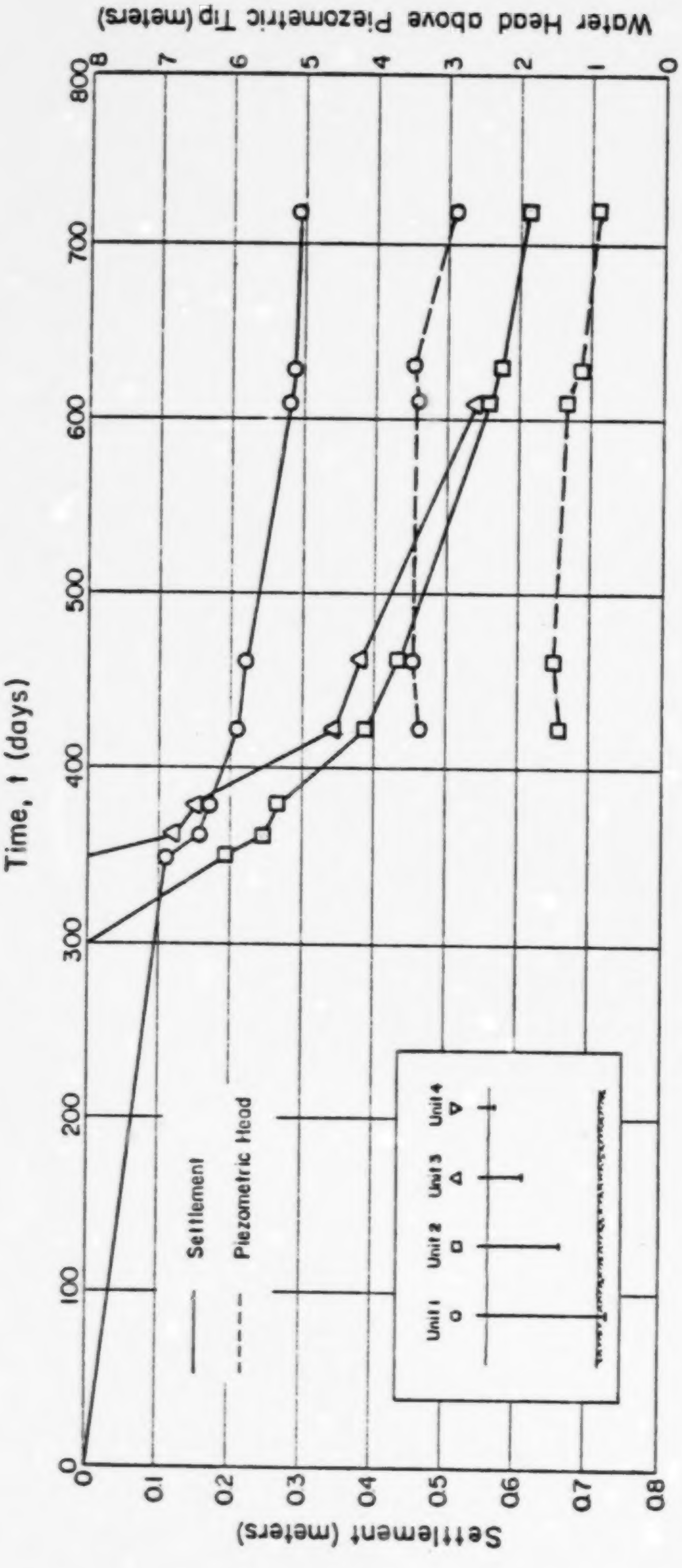

Figure 9-9. Settlement and Piezometric Head versus Time at Location 5/13

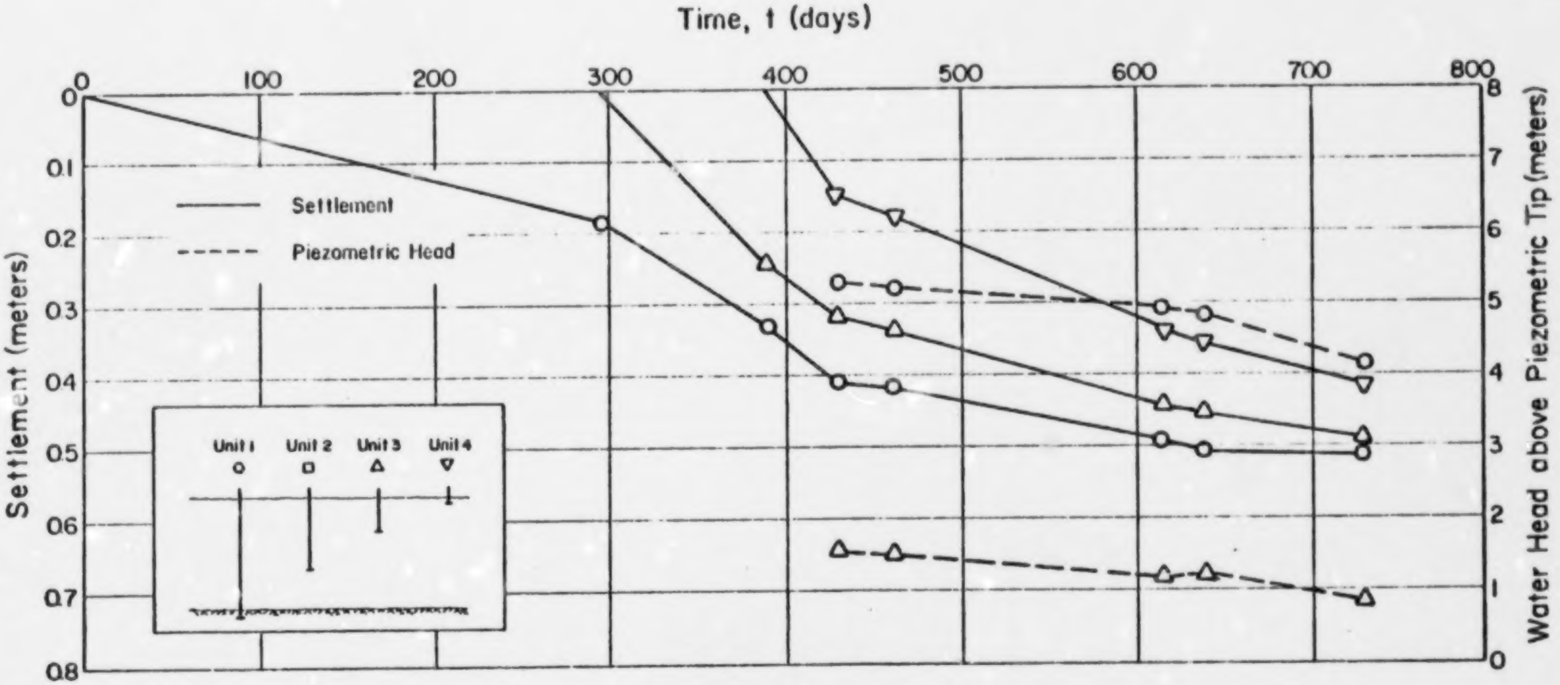

Figure 9-10. Settlement and Piezometric Head versus Time at Location 15/10

days after placing the set of bottom settlement plates and continued thereafter for about 440 days. Some of the units were destroyed at the times indicated in Table 9-2, and therefore complete sets of data are not available for all locations. Observed settlements varied between about 8 to 20 inches (0.2 to 0.5 meters) for bottom units and about 8 to 32 inches (0.2 to 0.8 meters) for plates near the surface of the fill. Piezometric heads above the mid-height of the porous tips indicated values near to the elevation of the fill surface for a long time, but a considerable drop was measured in August of 1974. The observed values of settlements and piezometric heads will be discussed in Chapter 11.

TRAVERSE AND LEVEL SURVEY OF DIKE

A traverse and level survey along the top of the Penn 7 dike was conducted in July 1972, September 1973, and April 1974 to investigate the possible movement of the dike in both the horizontal and vertical directions. The elevations of the traverse points were measured by conventional surveying techniques, starting from benchmark BM1 (elevation 588.25 feet according to the Department of Public Service, Division of Engineering and Construction, Toledo) shown in Figure 9-11 in front of the St. Regis Paper Company on Summit Street. Hydrants H1 through H7 on Summit Street were used as turning points to establish the elevations of two temporary benchmarks near the site. These benchmarks are designated in Figure 9-11 as BM2 (elevation 594.12 feet), the top of a drain pipe at the A. P. Parts Corporation, and BM3 (elevation 593.30), the top of a horizontal pipe mounted in a wall of the Continental Coffee Company; they were checked every time the crest of the dike was surveyed, and no vertical movement of either benchmarks was detected.

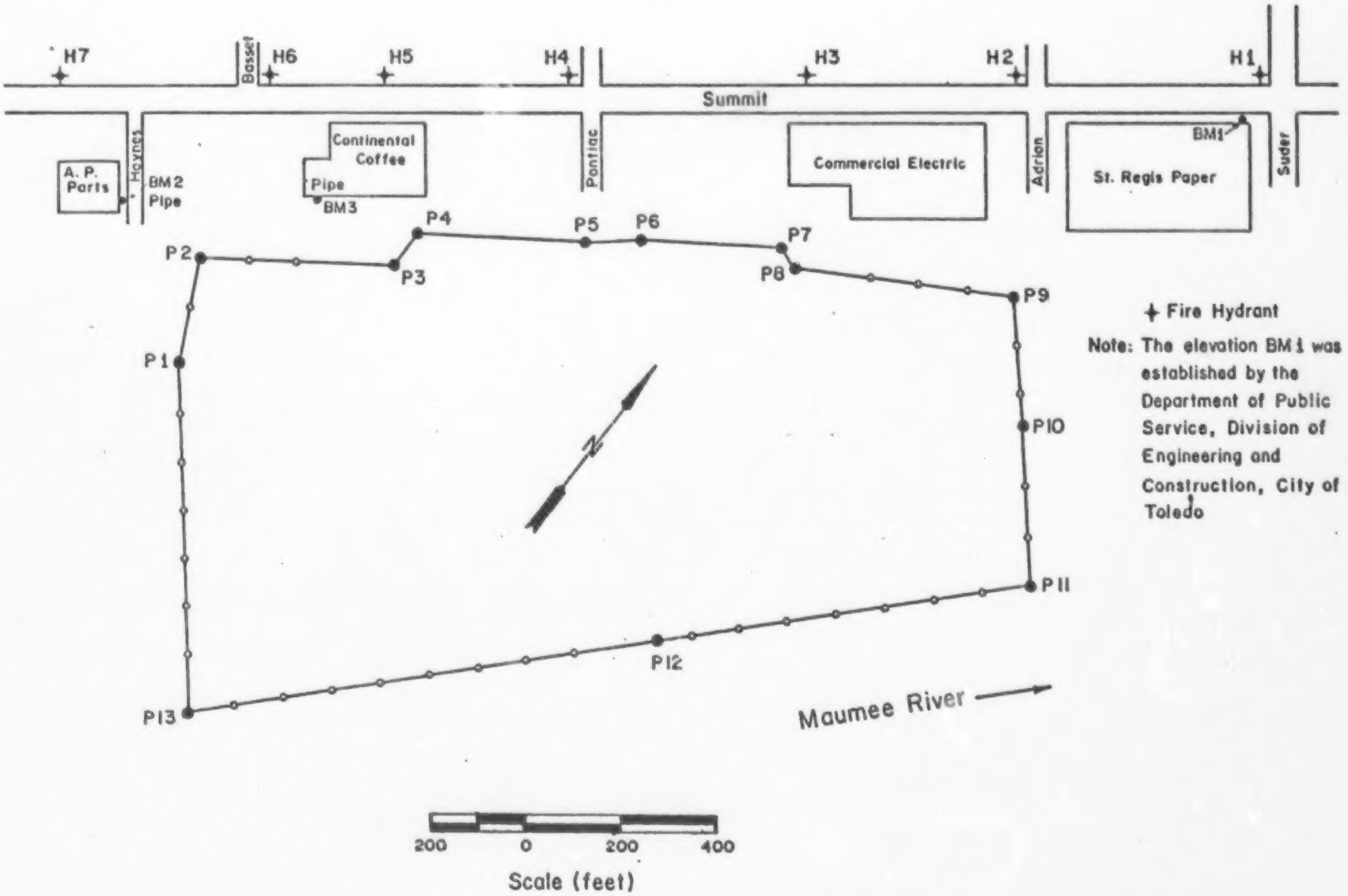
H7
H6
H5
H4
H3
H2
H1
Basset
Summit
Haynes
Pontiac
Adrian
Suder
A. P. Parts
BM2 Pipe
Continental Coffee
Pipe
BM3
Commercial Electric
St. Regis Paper
BM1
P1
P2
P3
P4
P5
P6
P7
P8
P9
P10
P11
P12
P13
N
Maumee River
✦ Fire Hydrant
Note: The elevation BM1 was established by the Department of Public Service, Division of Engineering and Construction, City of Toledo
200
0
200
400
Scale (feet)

Figure 9-11. Plan View of Penn 7 with Locations of Benchmarks and Reference Points

Based on traverses conducted around the crest of the dike in three consecutive years, no horizontal displacements could be detected. Vertical movements at 44 points along the approximate centerline of the dike are given in Figure 9-12. The large apparent settlements of the dike along the south and southeast sides of the containment area occurred primarily between 1972 and 1973; since many of the original traverse points were missing at the time of the 1973 survey, these large apparent settlements can be reasonably (though not definitely) attributed to the scraping of material from the top of the dike by heavy equipment or the possible compaction caused by this equipment at the end of the 1972 dredging season while in the process of raising dike elevation around the discharge pipe (shown by the hatched area in Figure 9-12) and relocating the discharge pipe after it was moved towards the river by a severe storm.

SURVEY OF GRID IN LANDFILL

Soon after the site was filled (at least temporarily) in August 1973, elevations of the fill surface were determined at essentially the node points of the original grid established on the foundation soil in the summer of 1972. The initial surface elevations were taken on September 14, 1973, at which time the consistency of most of the material in the landfill varied between a heavy slurry and a thick mud with a relatively soft soil capable of supporting a person being found in about 20 percent of the site around the discharge pipe. With the use of "mudshoes" to afford a larger bearing area to aid in supporting the weight of a person, stakes were placed at about 40 percent of the grid points near the discharge pipe and elevations (based on BM2 and BM3) were determined. Additional surveys were conducted on October 25, 1973 and December 5, 1973

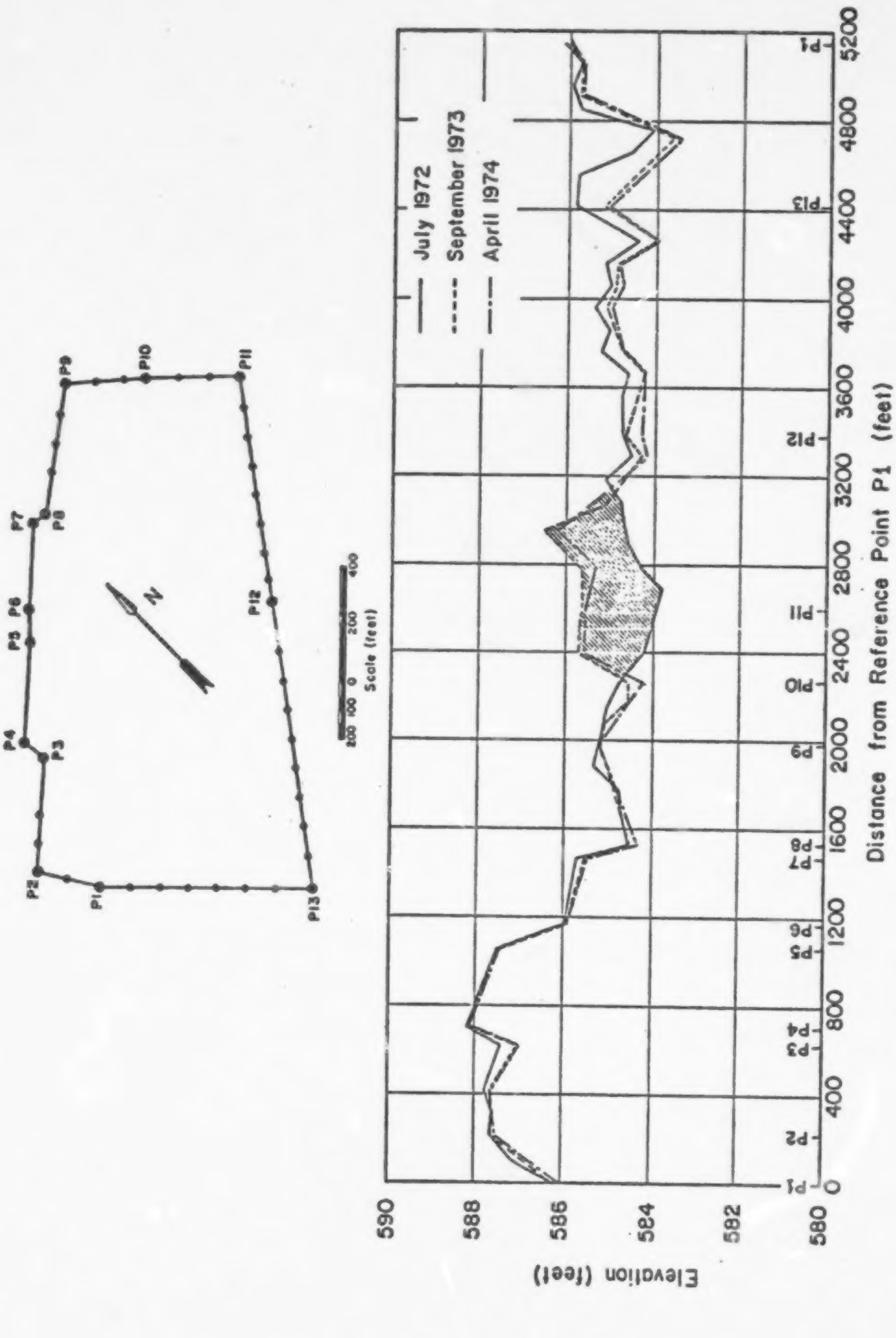

Figure 9-12. Longitudinal Section along the Centerline of Dike

on about 70 percent of the site. On April 19, 1974, and May 21, 1974, the complete area was surveyed. A final survey was attempted on August 20, 1974, but the high (5 to 10 feet or 1.5 to 3.0 meters) dense vegetation covering the site obstructed access to most points of the grid. In this case two lines were cleared (mainly for field vane strength tests) and surveyed along with a few scattered points, and settlement plate units were monitored at all locations.

Data from six topographic surveys (3 in 1973 and 3 in 1974) of the grid were interpolated, and contour lines representing these data for individual surveys, in addition to the original topographic survey prior to the placement of dredgings, are shown in Figure 9-13. Incomplete contour lines are indicated for the early surveys because some portions of the site were inaccessible at these times. Figure 9-14 shows the elevations of a longitudinal section along the base line of the landfill area; it includes the 1972 elevations for the original foundation soil and the surface elevations of the landfill at the time of the previously mentioned six surveys in 1973 and 1974.

SUMMARY AND RECOMMENDATIONS

The design of the field instrumentation and the methods used to install and monitor field response are explained in this chapter. Despite considerable effort to protect this equipment, over one-half of the units were destroyed by vandalism or adverse weather conditions. Such a situation can likely be prevented in the future only by the use of 24-hour-a-day surveillance.

The placement of the discharge pipe caused the formation of a high delta in its immediate vicinity and a rapid transition in the surface

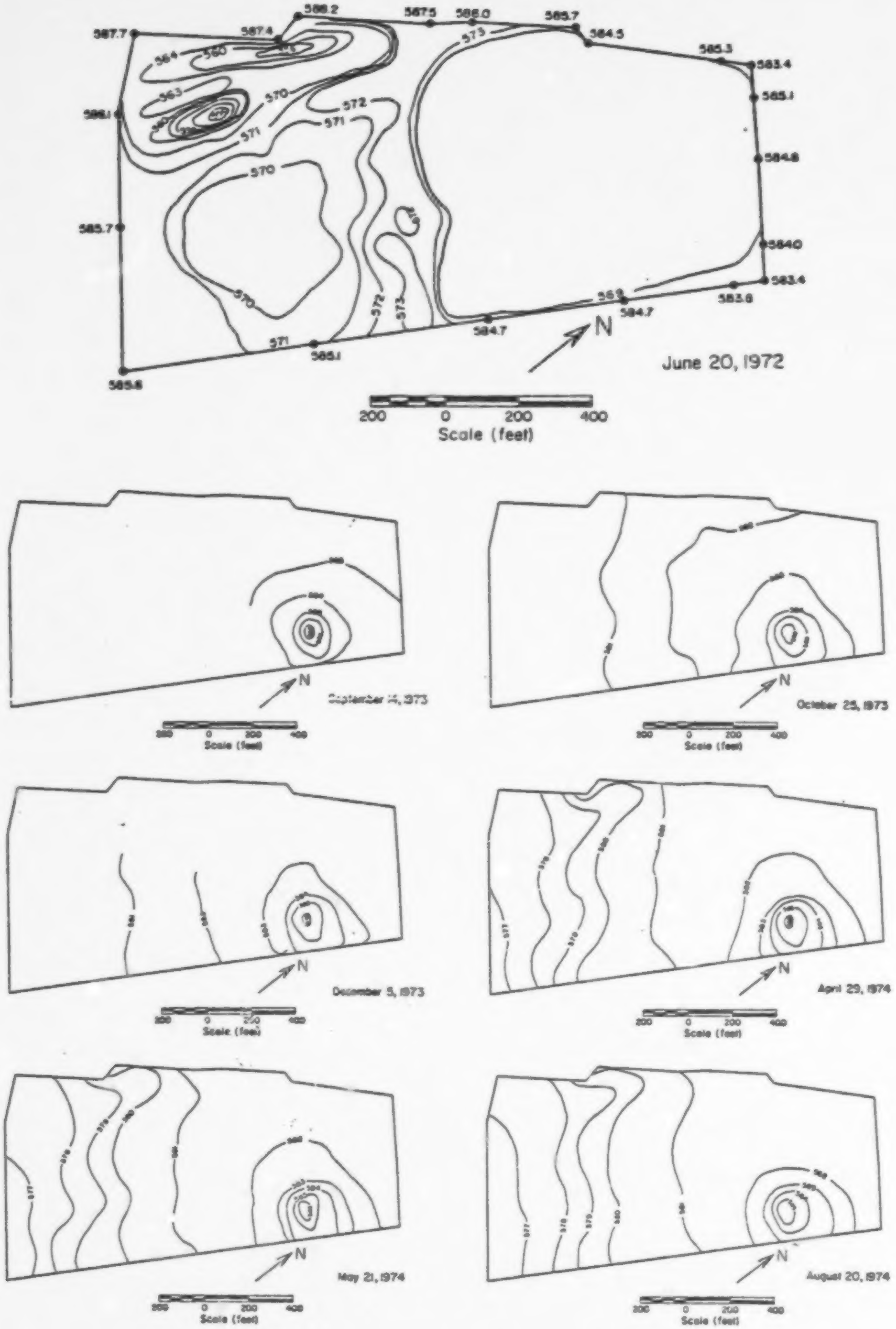
588.2
587.5
588.0
585.7
587.7
587.4
584.5
585.3
583.4
585.1
584.8
584.0
583.4
583.8
584.7
584.7
585.1
585.8
585.7
586.1
564
560
563
570
572
571
573
569
N
June 20, 1972
200 0 200 400
Scale (feet)
September 14, 1973
October 25, 1973
December 5, 1973
April 29, 1974
May 21, 1974
August 20, 1974

Figure 9-13. Variations in Topography of Penn 7 during Disposal Operation

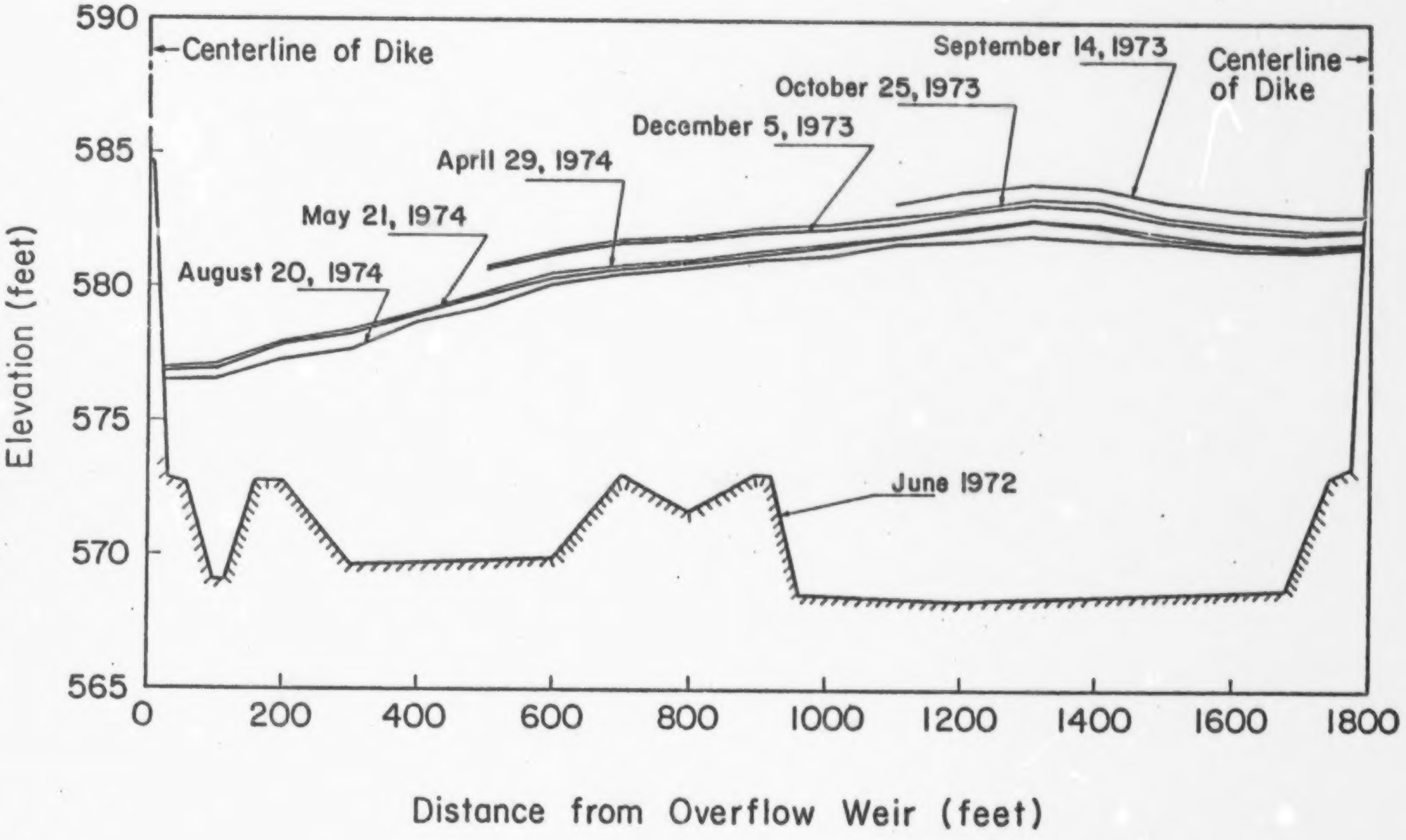

Figure 9-14. Longitudinal Section along Base Line of Penn 7

elevations of the landfill with increasing distance from the pipe. This resulted in little or no depth of water above the mud surface at many locations where the placement of instrumentation was desired; hence, these points were not accessible by either raft or mudshoes. This condition could be improved (a) by modifying the discharge pipe geometry with respect to the site configuration to obtain a more-or-less evenly distributed layer of dredged material and overlying water, or (b) by use of an amphibian type of vehicle to traverse the site. However, in the latter case extreme care would have to be taken to avoid disturbing the instrumentation as it was approached.

The permeability of the foundation soil ranged from about 10^{-2}cm/sec to 10^{-6} cm/sec with most of the values lying between 10^{-3} cm/sec and 10^{-4} cm/sec. Relative to the permeability values of 10^{-4} cm/sec to 10^{-8} cm/sec for dredged materials given in Chapter 6, it can be seen that the permeability of the foundation soil is orders of magnitude higher than that of the dredged material, which indicates that bottom drainage should be relatively unimpeded, provided the foundation soil can be adequately drained.

No horizontal displacements of the dike were observed, and the small vertical settlements could be attributed to the self-weight of the dike and the possible compaction caused by the movement of heavy equipment over the dike. It must be appreciated that the depth of dredged material was only about 10 or 12 feet (3 or 4 meters) in most places, and the situation may be different if the depth of material was greater.

The settlements of the foundation soils at some locations were much higher than expected; this is probably due in part to the relatively small area and large weight of the steel base plates that were used for the bottom units, which may have punched into the soft surface layer of the foundation soil. In retrospect, it would have been desirable to use lighter plates with a larger area at these locations. The rapid decreases in piezometric heads observed in August of 1974 were due mainly to the dense vegetation and relatively dry 1974 summer, which were jointly conducive to a high rate of evapo-transpiration.

CHAPTER 10

FIELD PROBLEMS

Various field problems, some normal and some abnormal, were encountered throughout virtually all phases of this study, thereby requiring extra expenditure of effort in some cases and reducing the amount of available data in other cases. Some of the major hardships and difficulties categorized according to the different aspects of the field work are discussed in the following sections and illustrated pictorially in Figures 10-1 through 10-5.

LOGISTICS

Accessibility to the sites and transportation of equipment and personnel posed an expected, but nonetheless difficult, problem. The local base of operations for this investigation was the Toledo Field Office of the U. S. Army Corps of Engineers, and the field sites were generally located a mile or two from this office. Accessibility to the Island Site was particularly difficult and had to be accomplished by small boats with outboard motors; this posed special problems when samples and heavy equipment had to be transported. Despite the excellent cooperation and support furnished by personnel from the U. S. Army Corps of Engineers, the problems encountered during this phase of the operation were frequently disconcerting.

Once personnel and equipment reached a given site, significant difficulties were met in gaining access to a desired test location within the site. In general, either the fill materials were too soft to support the weight of a person (see Figures 10-1 and 10-2) or the vegetation provided a virtually impenetratable jungle (see Figure 10-3) which had to be cut manually with machetes, since heavy equipment could not traverse the surface. While a site was being filled, accessibility presented an even more difficult problem because the materials were usually either too soft to walk on or too thick to pass over in a raft (see Figure 10-1); near the overflow weir the water was normally a few feet deep and a rubber raft, perhaps in conjunction with a guide rope anchored at each end in the surrounding dike, could be used to gain access to these points (see Figure 10-2). Much of the equipment and instrumentation was heavy or awkward, and it was often difficult to transport it over hundreds or thousands of feet.

Although the surveys were rather routine in nature, considerable problems were encountered in clearing the lines of sight through the dense vegetation (see Figures 10-3) or in gaining access to distant points surrounded by soft dredged material. Walkie-talkies were used effectively to provide lines of communication between personnel separated by large distances. Finally, the frequently encountered and normally simple task of making equipment repairs or modifications in the field led to considerable frustration and loss of time, since local welders, machinists, etc did not want to interrupt their routine work to render emergency repairs to our equipment.

SAMPLING

Numerous difficulties were encountered in the sampling of dredged materials with various consistencies and in the obtaining of groundwater

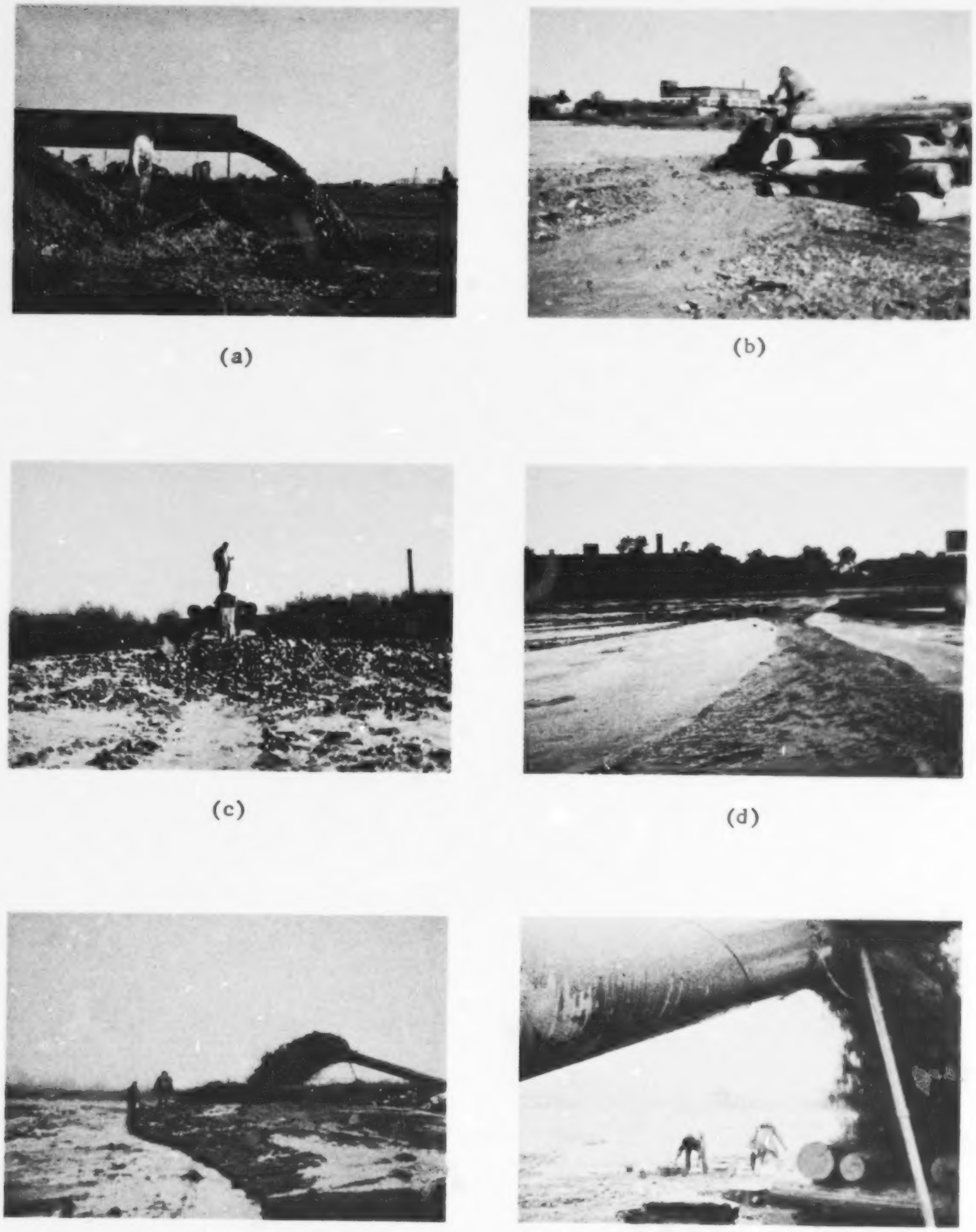

(a)

(b)

(c)

(d)

(e)

(f)

Figure 10-1. Conditions Associated with Inflow Pipe

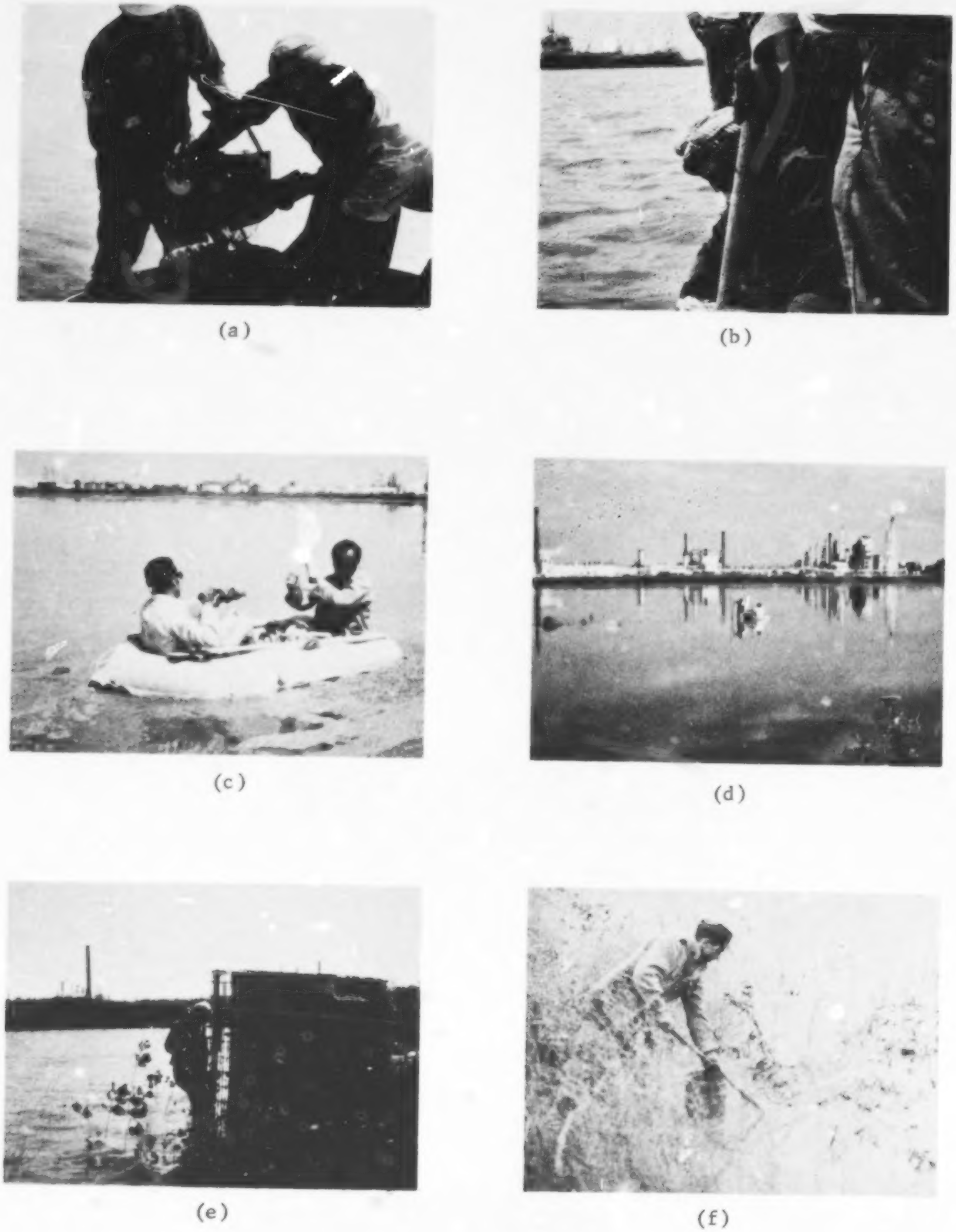

(a) (b) (c) (d) (e) (f)

Figure 10-2. Sampling Difficulties

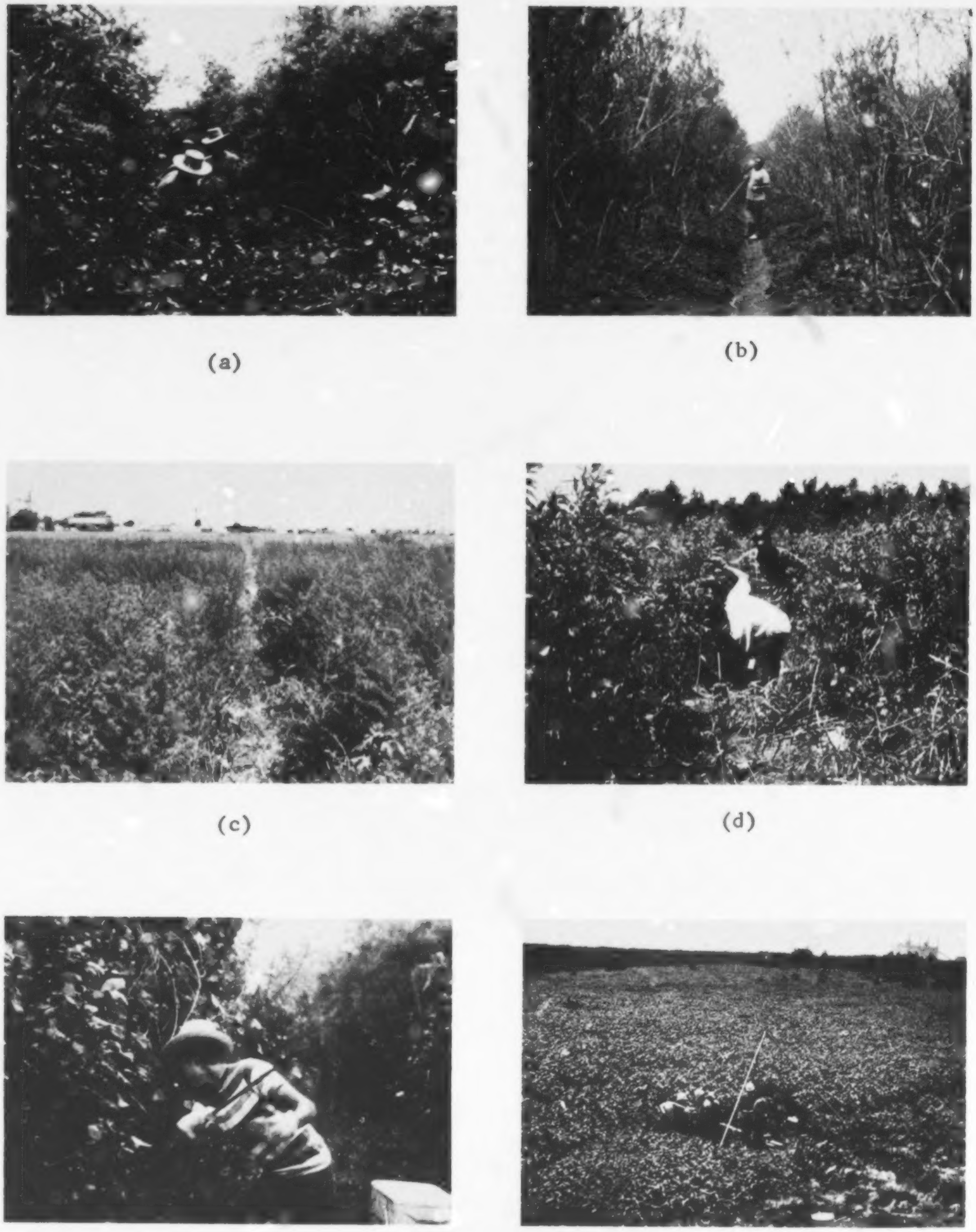

(a) (b)

(c) (d)

(e) (f)

Figure 10-3. Rapid Growth of Vegetation

samples from the observation wells. These problems were mainly concerned with the accessibility of a sampling site and the representativeness of a given sample. These problems have been discussed in detail by Hummel and Krizek (1974) and Raphaelian and Krizek (1974), and only brief summaries will be given here.

Inflow Pipe

In the case of large diameter inflow pipes with high velocity flows, the sampling problem may very well involve various aspects of personnel safety, since the thrust of the discharging jet may be sufficiently large to injure a worker if proper precautions are not taken (see Figures 10-1a, 10-1b, and 10-1e). After considerable experimentation, slurry samples from the inflow pipe were finally taken by introducing a 3-inch diameter tube with a 90-degree elbow into the stream at various locations (see Figure 10-1f); the tube was held in place by a strong rope attached to the inflow pipe, and samples were collected in a container positioned below the pipe. After the dredgings were pumped into the fill area and before they had desiccated to the point where they could be traversed by foot, samples were taken by shovel and bucket (see Figure 10-2f).

Fill and Foundation Materials

Since conventional heavy truck-mounted sampling equipment could not be used on these soft landfills to sample the in-place dredged materials, special manually-operated sampling equipment had to be designed and constructed. As normally happens with the development of any new piece of equipment, a variety of small, but bothersome, problems (such as O-ring seals, leaks between liner tubes, deffective vacuum release, undesired rough edges, weak points in the supporting frame, etc) were

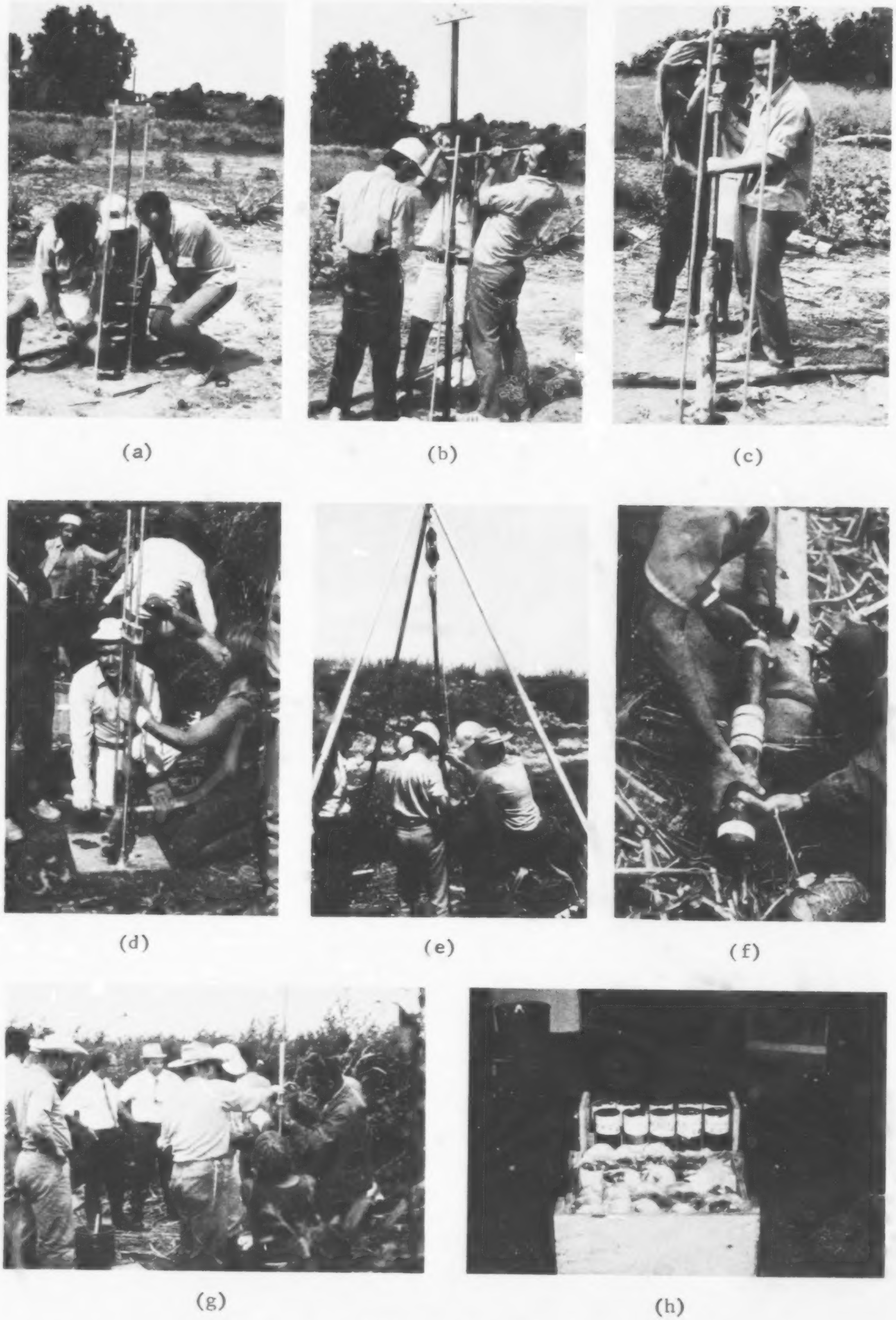

(a) (b) (c)

(d) (e) (f)

(g) (h)

Figure 10-4. Piston Sampling Operation

encountered before the piston sampler was rendered routinely operational. In another situation split spoon samples of the foundation material in the Penn 7 Site were obtained prior to the deposition of any spoil in this area, but during an unguarded late-evening break in the sampling operation the samples were stolen and the field reports were destroyed.

Several steps in the piston sampling operation are illustrated in Figure 10-4. In general, the sampler was pushed manually (Figure 10-4a and 10-4d) into the landfill material; then, if possible, it was recovered by the reverse operation (Figures 10-4b and 10-4c). In other cases where the suction release did not function properly or if the sidewall friction was too large to retract the sample manually, a tripod and block-and-tackle system (Figure 10-4e) was employed. The inner lining of the sampler consisted of two one-foot sections (Figure 10-4f), and the joint between these sections caused a loss of vacuum in the early stages of sampling before precautions were taken to remedy this condition. Upon completion of the field sampling operation, the tubes were properly identified and transported in carrying cases (Figure 10-4h) to the laboratory for chemical and mechanical tests.

Observation Wells

One of the biggest problems associated with obtaining samples from the observation wells centered around accessibility and the difficulty of working from a rather unstable rubber raft (see Figures 10-2c and 10-2d). Other difficulties stemmed from the malfunction and ultimate loss of a plunger mechanism used to recover the samples. These problems were aggravated somewhat by the fact that time was a significant factor in the obtaining, transporting, and testing of these samples, since bacteriological analyses were conducted. In one unfortunate case the samples were iced

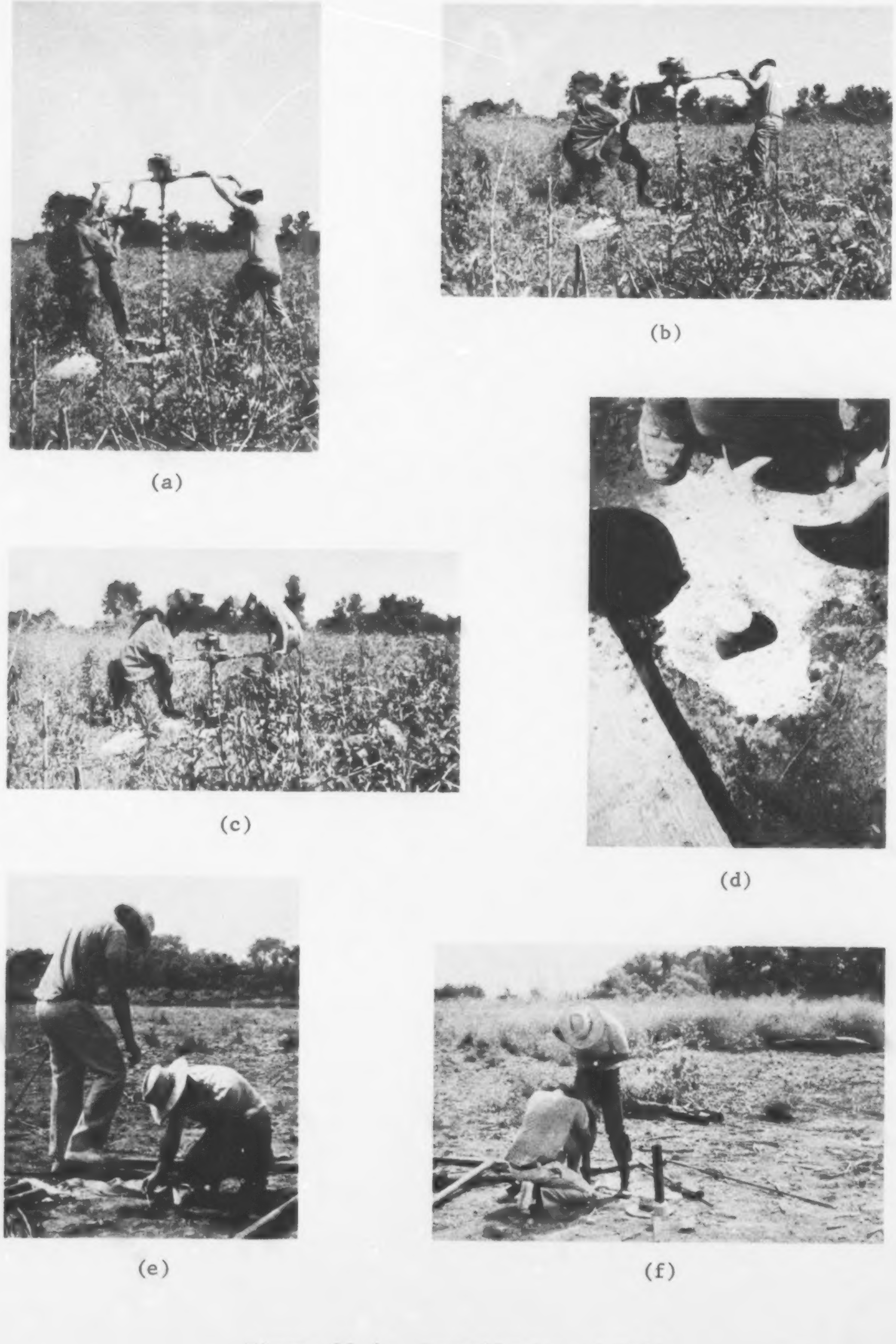

(a)

(b)

(c)

(d)

(e)

(f)

Figure 10-5. Installation of Wells

down and shipped via Greyhound Bus from Toledo, Ohio to Milwaukee, Wisconsin, where they were to be tested, but they were lost in shipment and have never been located.

Bottom Sediments and Overflow Weir

Shallow (6-inch depth) bottom sediments were sampled by means of an Ekman dredge (see Figure 10-2a), and a custom designed flap-valve sampler (see Figure 10-2b) was used to obtain samples of deeper (2-foot depth) bottom sediments. However, the flap valve sampler was very difficult to utilize if the current was swift, and this was the reason for losing one such sampler in the Milwaukee harbor. Samples of the effluent from the disposal area were taken directly from the overflow weir (see Figure 10-2e) by climbing down a grillage of welded reinforcing bars. Although this sampling operation seems rather routine, it presented many anxious moments.

INSTALLATION OF OBSERVATION WELLS

Difficulty with the installation of the observation wells in the foundation soils of the Penn 7 site started with the inaccessibility of the truck-mounted rig to many of the desired locations. For example, while attempting to gain access to the area near the overflow weir, the truck became stuck and more than one-half day and additional equipment were required to free it. During the ensuing night the truck and drilling equipment were seriously vandalized, and another full day was needed to render it operational. The wells at the locations that were inaccessible by truck-mounted drilling equipment were drilled by means of a manually operated power auger, which was reasonably effective but extremely difficult to operate (see Figure 10-5). Due to the nature of the dike material (clayey sand with gravel and boulders), it was very difficult and time-consuming to advance observation wells in the dike; in one case it required one full day to drill a 10-foot deep well and in another case the well could only be drilled about 2 feet deep, despite the expenditure of considerable time and effort. After installation, the risers of several observation wells were vandalized very early in the history of the site; these wells were repaired, but were destroyed again shortly thereafter. Finally, an abnormally severe storm late in 1972 destroyed the risers of a few wells and damaged several others, some of which were subsequently repaired.

INSTALLATION OF SETTLEMENT PLATES

Although no problems were encountered in installing the settlement plates in most areas of the foundation soil, some difficulties were experienced in the submerged regions, especially one area (location 5/16) which was covered with about 14 feet of water. The final installation procedure at this latter location involved the use of styrofoam boards to float ballast material to the vicinity of the unit and swimming in the water to place the unit and surround it with the ballast for stability. The difficulties associated with the installation of the intermediate units on the mud surface were explained in Chapter 9. Despite their location within the disposal area, many of these units were vandalized and destroyed early in the history of the site. In addition, the 1972 storm damaged the risers of several other units and destroyed a large raft which was constructed to install and monitor the units; thereafter, a small rubber raft (see Figure 10-2c) was used for this purpose, but it was not nearly as stable as desired. A corollary problem caused by the same severe storm resulted when the discharge pipe was moved to a new position in line with the settlement plates at location 12/8, thereby causing them to be destroyed by the jet of influent slurry.

Freezing before the end of the 1972 dredging season caused an ice jam at the overflow weir, and the dredgings and associated water accumulated to a level about 3 feet higher than the normal level of the overflow weir. Hence, the risers of the settlement plates (and the observation wells) were beneath or surrounded by the sheet of ice that formed. When the water finally flowed over the weir, the ice above or around the risers caused them to tilt from the vertical, and serious difficulties (explained in Chapter 9) were encountered in realigning them. During periods when it was desired to install new units or monitor the existing ones, the level of the water surface had to be raised in order to be able to maneuver the raft (see Figure 10-2c); this was accomplished by raising the level of the overflow weir by adding boards. However, these boards were sometimes removed, thereby allowing the site to drain and the water level to lower; the boards had to be replaced, and it was frequently necessary to wait several days (depending on the rate of disposal in the area) until the water level was again high enough to maneuver the raft to the desired locations. Several additional units were vandalized during the 1972-73 winter and after the materials in the site had dried enough for persons to walk on the surface.

FIELD EVAPORATION TESTS

Several man-days were expended to design and prepare a series of field evaporation tests in cut-off 55-gallon drums to study the effects of evaporation and infiltration under prevailing weather conditions in the field (Krizek, Roderick, and Jin, 1974). After a little more than a week, the drums were found tipped over and riddled with bullet holes, and the contents were scattered around the discharge pipe. It was decided for security reasons to reconstruct the experiment on the premises of the Toledo Field Office of the U.S. Army Corps of Engineers; however, this site was about one mile from the Penn 7 disposal area, and considerable hardship was experienced in transporting over this distance the large amounts of material needed to set up the test series.

WATER QUALITY STUDY

As explained by Krizek, Gallagher, and Karadi (1974), a water quality study of the Penn 7 disposal site involved monitoring the precipitation and evaporation in the vicinity and the quantity of water passing over the weir. At one point during the monitoring process the sensing electrode mounted on the sill of the overflow weir (see Figure 10-2e) was found hanging in the weir shaft, thereby resulting in a discontinuous record of the outflow quantity. On another occasion the recording equipment (which was locked inside a metal box that was, in turn, fastened to the inside of the weir which was covered by a heavy metal grating composed of welded reinforcing bars) was stolen by breaking the lock on the metal grating and then the clamps on the box. The rain measuring pan and its associated recording equipment, which was located on the grounds of the Corps of Engineers Toledo Field Office, were damaged by the 1972 storm. The more-or-less routine problems of obtaining water samples from the observation wells were already discussed in a previous section.

SUMMARY

As explained above, a variety of problems and difficulties were encountered during the course of this study; in general, these may be categorized in the following way. Problems of accessibility, though largely anticipated, nevertheless caused considerable difficulty from time to time. The logistics of obtaining and transporting representative samples and of providing for field repairs of equipment frequently led to much anxiety and loss of valuable time. By far, however, the worse problem encountered was that of vandalism, which was responsible for the destruction or damage of many risers for the observation wells and settlement plates, the evaporation tests, and the instrumentation for monitoring the outflow quantity, as well as for the loss of several samples and boring logs. Of considerable concern throughout the study were the extraordinary measures that had to be taken to secure, insofar as possible, various aspects of the work; hence, even in situations where direct acts of vandalism did not occur, their effect was felt in the extra effort that had to be expended to prevent it. Many of these cases were reported to the Toledo Police Department, and they agreed to increase their frequency of visits to the site; however, such increased protection did not serve to measurably decrease the incidence of vandalism, and the project suffered accordingly. Another act of nature that was unexpected and caused considerable problems was an unusually severe storm that occurred in late 1972; this storm damaged or destroyed virtually all the instrumentation (weather station at the Toledo Field Office, large raft, risers of settlement plate units, etc) that was installed at the time. Despite these problems, most of the work during the course of the project proceeded reasonably well, and it is felt that sufficient information was accumulated to accomplish the major objectives of this investigation.

CHAPTER 11

SYNTHESIS OF RESULTS

In this chapter the results reported in the previous chapters are synthesized and interpreted to deduce guidelines and observations of engineering significance regarding the use of dredgings for landfills. Settlements predicted from two mathematical models are compared with the measured settlements at various locations in the Riverside and Penn 7 disposal areas. Based on topographic surveys of the Penn 7 site before and after the deposition of dredgings in the area, its initial storage capacity is evaluated in terms of the in-situ volume of bottom sediments and the bin-measure volume of the material aboard the dredge. Density measurements on undisturbed samples taken from the four Toledo sites allow the anticipated time-dependent increase in storage capacity over an 8-year period to be assessed. The advantages of compacting dredgings in the disposal site are studied in terms of the increased storage capacity of the site and the improved usefulness of the associated fill. Various empirical expressions are deduced to relate shear strength, dry density, and time. A study is undertaken to identify the particle size distribution in the vicinity of the discharge pipe and along a line between the discharge pipe and the overflow weir. And finally, a preliminary cost study is presented for the Toledo disposal sites, and the potential usefulness of landfills composed of maintenance dredgings is discussed.

SETTLEMENTS

Time-dependent settlements and piezometric heads were measured at various depths at five locations in the Penn 7 area, and these data have been given in Figures 9-6 through 9-10. Settlement measurements began about 280 days after installation of the bottom units and continued for about 440 days thereafter. The observed settlements varied from about 0.2 to 0.5 meters (8 to 20 inches) for bottom units and from about 0.2 to 0.8 meters (8 to 32 inches) for plates near the surface of the fill. Settlement records at location 2/10 (Figure 9-6) are incomplete because the bottom settlement plate was destroyed before any measurements were taken and two intermediate units were vandalized soon after installation.

The unusually high settlements of 0.17, 0.26, 0.30, and 0.51 meters for the bottom units at locations 5/8, 5/10, 5/13, and 15/10, respectively (Figures 9-7 through 9-10) are attributed in large part to the softening of the foundation soil after being inundated by the dredging slurry; the 5/8-inch thick, 18-inch square, steel plates were relatively small and heavy, and they very likely punched into the soft foundation soil after it became wet and soft. In particular, the foundation soil at location 15/10 was very soft for a depth of about 0.6 meters (2 feet), and this plate ultimately showed the highest settlement (0.51 meters) of all the bottom units.

Since the plates that were placed within the fill material were much larger and lighter (two 1/8-inch thick crossed sheets of corrugated fiberglass 30 inches square), their possibility of punching into the mud was minimized. The surface unit at location 5/8, which is the closest location to the dike (about 6 meters away), indicated the highest settlement compared to the surface units at the other locations; this is probably due to the better drainage conditions and therefore faster rate of consolidation near the dike than at more distant locations. The piezometric heads at all locations were essentially equal to the elevation of the fill surface for a long time, but a considerable drop in all values was noticed in August of 1974; this drop was due mainly to the evaporation that took place during the summer and the transpiration associated with the dense, fast-growing vegetation.

In addition to the settlements measured at the Penn 7 site, surface settlements were monitored at various locations at Riverside Site for several years. The measured settlements at both sites are compared with settlements calculated from a simple model based on the classical theory of consolidation, and a more sophisticated model (Krizek and Casteleiro, 1974) that accounts for both consolidation and desiccation, as well as a nonhomogeneous distribution of mechanical properties in the vertical direction, is used to compute comparative settlements for the Penn 7 data. In each case the input information was determined, insofar as possible, by laboratory and field tests; when appropriate test data were unavailable or inconclusive, engineering judgment was used to select the input parameters.

Model Based on Classical Theory of Consolidation

The classical theory of consolidation was used to obtain a first-order approximation for the rate of settlement that would likely occur in a typical hydraulically-placed landfill. However, since the conditions associated with this problem are considerably different than those that exist in most conventional consolidation problems, several key adaptations and assumptions had to be made. The parameters needed to estimate the total settlement and its time rate for a typical layer of dredged material (Figure 11-1) are obtained from the results reported in Chapter 5 for conventional consolidation tests conducted on sixty-four undisturbed tube samples obtained from the Island, Riverside, and Penn 8. The compression index, C_c, varied between 0.3 and 0.7; the initial void ratio, e_o, varied from 1.2 to 2.0; and the average value for the coefficient of consolidation, c_v, was found to be 0.0006 cm^2/sec. The assumed average thickness of the dredged material in the landfills under consideration was 3.6 meters (12 feet), and the initial and final levels of the groundwater table were taken to be at the ground surface and at the mid-height of the layer, respectively; these water levels were commonly observed at different locations of all four sites. In order to simplify calculations, the 1.8-meter (6-foot) drop in water level was assumed to take place suddenly. Based on the relationship

$$c_v = \frac{Th^2}{t} \quad , \qquad (11\text{-}1)$$

where T is the time factor (function of the degree of consolidation), t is the time, and h is the shortest drainage path (equal to one-half the layer thickness for a double drainage condition, or the total thickness for a single drainage condition), the time required for 90 percent consolidation of the 3.6-meter layer due to its own weight and the effect of capillary tension is about 6 years for double drainage and 1.5 years for single drainage. The total expected settlement, S, can be evaluated from the relationship

$$S = \frac{C_c}{1 + e_o} (H) \log \frac{p_o + \Delta p}{p_o} \quad , \qquad (11\text{-}2)$$

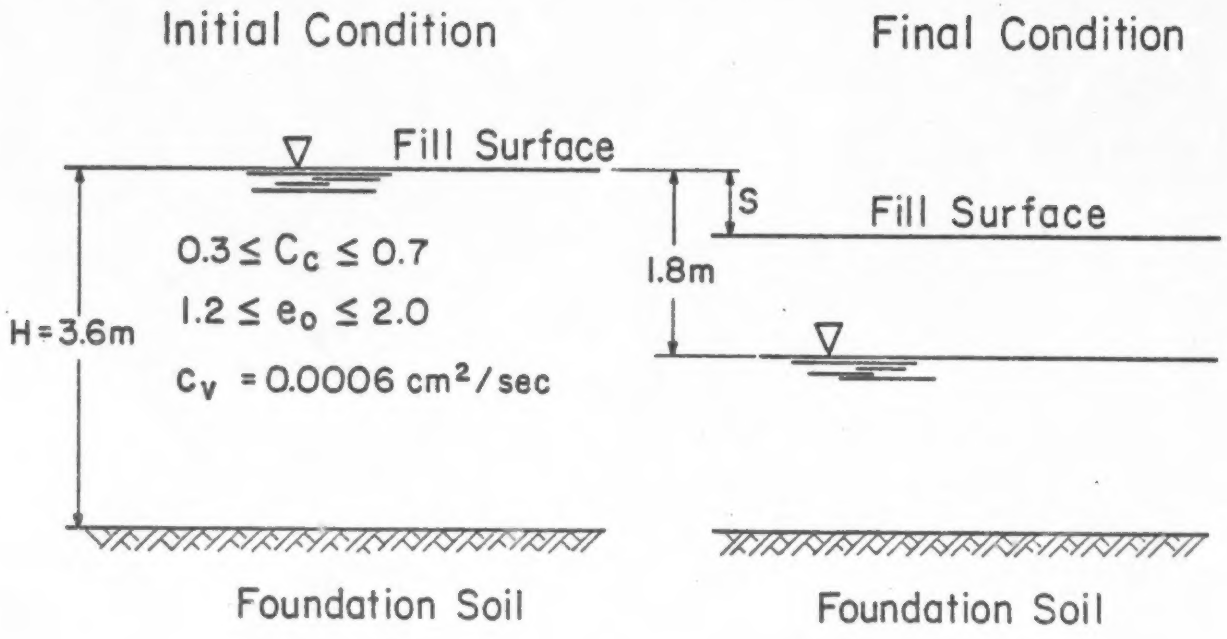
Initial Condition
Final Condition
Fill Surface
S
Fill Surface
$0.3 \leq C_c \leq 0.7$
$1.2 \leq e_0 \leq 2.0$
$c_v = 0.0006\ cm^2/sec$
H = 3.6m
1.8m
Foundation Soil
Foundation Soil

Figure 11-1. Assumed Initial and Final Conditions for Typical Layer of Dredgings

where p_o is the initial effective stress at mid-height of the layer and Δp is the developed effective (or consolidation) stress. The surface settlement of the 3.6-meter (12-foot) layer is determined by adding the one-dimensional volume changes of the portions of the layer above and below the assumed final groundwater table. For the 1.8-meter (6-foot) layer above the final water table, p_o is taken to be the initial effective stress at mid-height of this layer (0.9 meters from ground surface) and Δp is the sum (at the mid-height of the layer) of (a) the overburden stress increase due to lowering the water table and (b) the tensile stress developed due to surface tension or capillary action. The initial effective overburden stress, p_o, of the layer below the final water rable is that stress which existed at the mid-height (2.7 meters from ground surface) of this layer before the water table is lowered, and Δp for this layer is due only to the lowering of the water table by 1.8 meters (6 feet). The maximum expected settlement would logically correspond to $C_c = 0.7$ and $e_o = 2.0$, and the minimum expected settlement would correspond to $C_c = 0.3$ and $e_o = 1.2$. Accordingly, the maximum and minimum values of the settlement ratio, S/H, are found to be 0.12 and 0.06, respectively. The relationships for the associated values of the settlement ratio at any time, t, are shown in Figure 11-2 for both single and double drainage conditions; although the actual drainage conditions are not known, the field settlements should lie within the indicated extremes if the assumed model is reasonably applicable. The time origin for Figure 11-2 is taken as the time corresponding to the assumed sudden drop of the water table.

Also given in Figure 11-2 are the average values and ranges of data from periodic level surveys of the fill surface at three locations

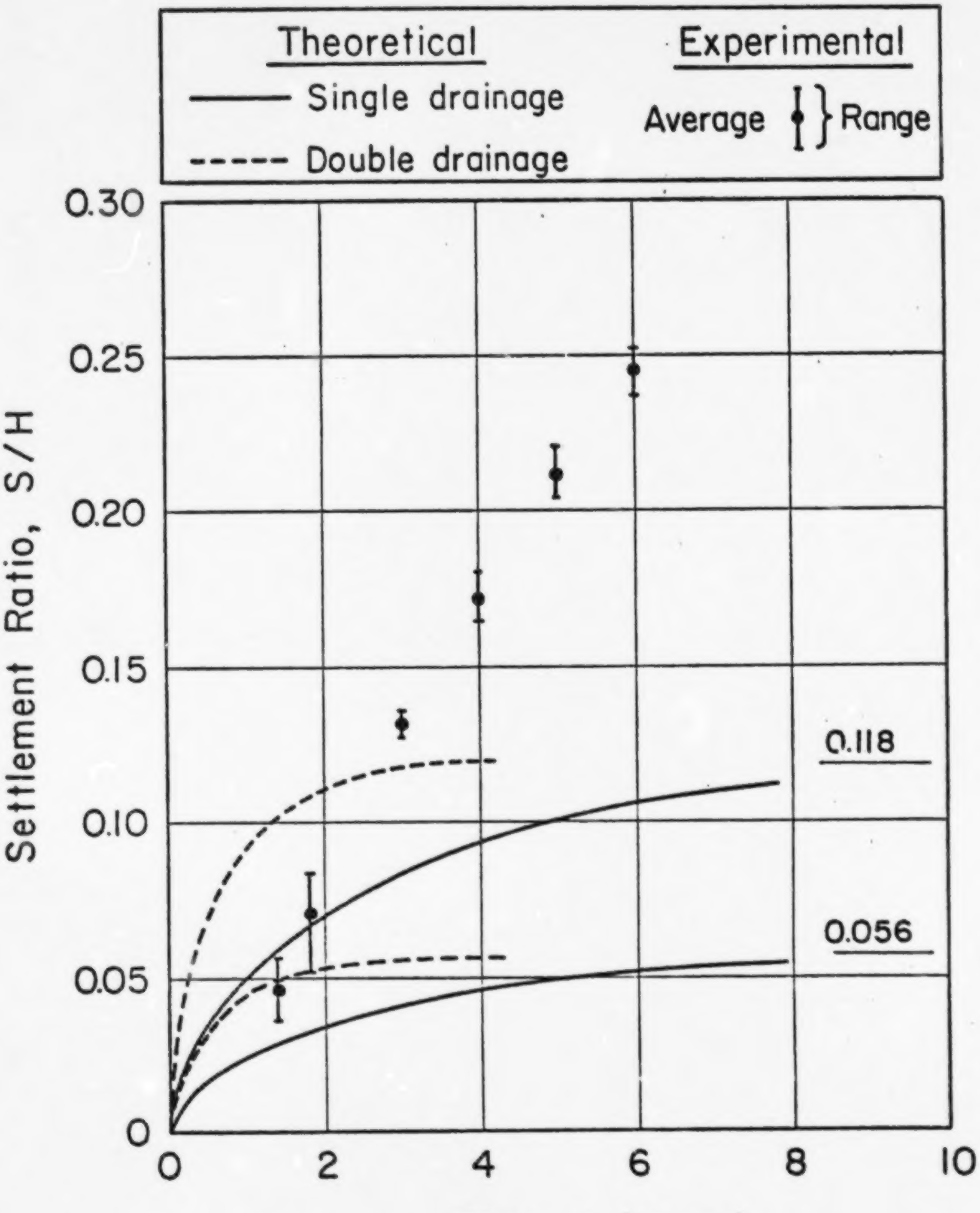

Figure 11-2. Comparison between Observed Settlements and Predictions Based on Classical Consolidation Theory

in Riverside Site and seven locations in Penn 7; the time origin for these data is the same as that described in Chapter 8, namely, t = 0 when a given disposal site is about one-half filled. As can be seen, the measured settlements (or settlement ratios) are considerably higher than those calculated by classical consolidation theory, even for the so-called maximum settlement conditions. Although there are many possible reasons for this observed discrepancy, two of the most probable reasons are (a) the initial conditions are not known with any degree of certainty (for example, in view of the fact that these sites were filled discontinuously, what is the proper time origin and what is really the initial void ratio), and (b) all of the physical phenomena that occur are not properly taken into account in classical consolidation theory.

Model Based on Consolidation and Desiccation

In an attempt to model more correctly the actual conditions that occur after dredged material is placed in a landfill, Krizek and Casteleiro (1974) developed a more comprehensive mathematical model that accounts for impeded bottom drainage conditions, nonhomogeneous variations in material properties in the vertical direction, and one-dimensional consolidation and desiccation of successive layers of dredged materials as they are periodically deposited in a diked containment area. The governing boundary value problem, defined in terms of pore water pressures, consists of two field equations (one for the saturated domain and one for the unsaturated domain), drainage boundary conditions, an evapotranspiration boundary condition, and a series of continuity conditions at the interfaces between different layers. A number of simplifying assumptions were made to render the field equations tractable, and a step-by-step numerical procedure was used to solve the linearized boundary value problems; at the end of each step, the errors introduced by the simplifying assumptions were corrected. Then, established empirical relationships for the permeability (Chapter 7), water retention (Krizek and Casteleiro, 1974), and volume change characteristics of typical dredged materials (Chapters 4 and 5) were employed in conjunction with this mathematical model to calculate settlements of the dredged materials in the Penn 7 disposal area.

The accuracy of these calculated settlements was evaluated by direct comparison with corresponding settlements measured at various points in the Penn 7 Site, and one typical example of such a comparison is illustrated in Figure 11-3. In this example the coefficient of permeability of the foundation soil, k_f, is taken to be 10^{-5} cm/sec (based on values obtained from field tests reported in Chapter 9), the thickness of the non-consolidating foundation soil, H_f, is assumed equal to 4.57 meters, and the coefficient of transpiration, β, was considered to be 0.2. The average thickness of the dredged material was taken to be 2.35 meters for the first dredging season (from August 28, 1972 to December 19, 1972) and 1.44 meters for the second dredging season (from June 11, 1973 to August 20, 1973). The thickness of each layer is not actually constant over the entire site, but the assumption of a one-dimensional process at any given point provides a reasonable approximation to the actual conditions.

Although this mathematical model is capable of handling vertical nonhomogeneities in the material characteristics within a layer (and these variations would almost certainly exist in a practical problem), available data are insufficient to delineate readily identifiable vertical variations in the engineering properties of the dredged material at a

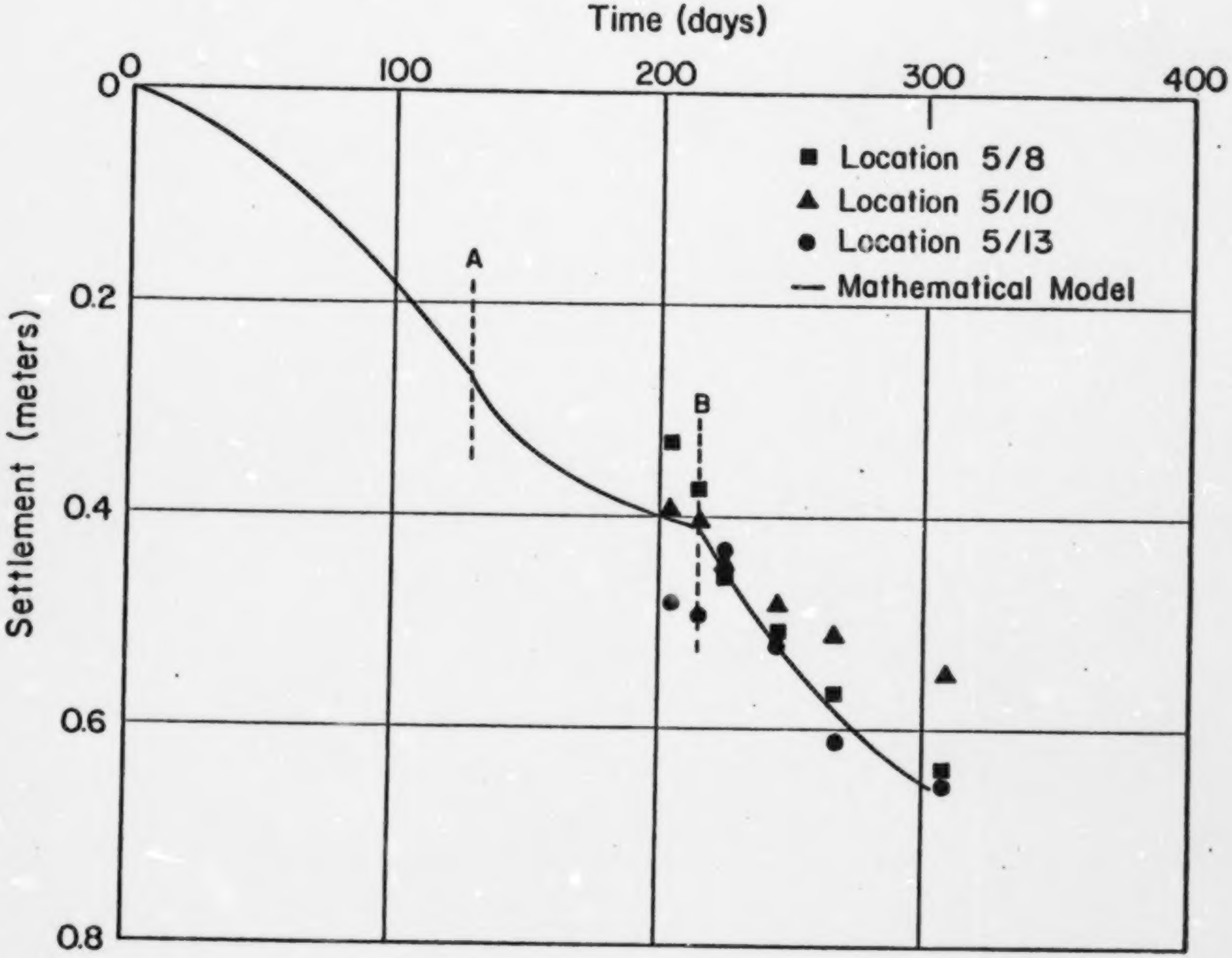

Figure 11-3. Comparison between Observed Settlements and Predictions of Mathematical Model

given location in either the Penn 7 area or similar nearby sites; hence, the dredged material at a given location was assumed to be homogeneous in the vertical direction. Despite this assumption of initial homogeneity, it is clear that the dredgings will be heterogeneous as soon as the consolidation and desiccation processes begin, since variations in the void ratio, water content, and pore water pressure will produce variations in all soil characteristics, such as permeability, compression index, etc.

In the settlement versus time curve shown in Figure 11-3, three distinct time zones can be distinguished. The zone extending from the origin to point A represents the desiccation of the first layer; at point A the deposition associated with the second cycle begins, and the zone beyond point B depicts the volume change due to evapotranspiration through the top boundary of the second layer. The time origin for this curve is February 3, 1973, and points A and B represent June 11, 1973 and September 5, 1973, respectively. From the origin to point B the indicated settlement represents the volume change of the first layer of sediments, whereas beyond point B it represents the volume change of both layers. Therefore, the calculated settlement prior to point B must be compared with the observed settlement of the first layer (difference between the settlements recorded at the top and bottom of the first layer), ,while comparisons beyond point B must be made with the total settlement data (difference between settlements recorded at the top of the second layer and the bottom of the first layer). Due to the fact that the settlement plates at the top of the first layer were placed on June 13, 1973, the comparisons between the calculated and observed settlements must be made in terms of relative, rather than absolute, values. To facilitate this comparison it is assumed that points A and B represent values that agree with the measured settlements, and the plotted points are the relative values with respect to these initial values.

The actual settlements in each layer were measured by means of settlement plates that were placed at the bottom and top of the first layer and at the top of the second layer. Due to the difficulties described in Chapter 10, complete records are available at only four locations (5/8, 5/10, 5/13, and 15/10), and the accuracy of the data for location 15/10 is suspect because of the unusually large settlements of the bottom settlement plate. Nevertheless, the predictions determined from this mathematical model agree reasonably well with the measured values, thereby suggesting that this more comprehensive mathematical model is reasonably capable of characterizing the physical processes that occur in a typical dredging disposal operation as considered herein.

STORAGE CAPACITY OF CONTAINMENT AREAS

Although the specific costs of diked disposal depend strongly on local conditions, it is frequently much more expensive than open water disposal and the availability of disposal sites near highly industrialized areas surrounding deep water harbors is usually very limited. Accordingly, the economics of diked disposal operations require that appropriate consideration be given to all aspects relating to the planning and use of the sites. Since one particular problem encountered in the planning of diked containment areas, especially for long-term operations, concerns the amount of dredged bottom sediment that can be deposited in a given site, an attempt was made to provide some guidelines by which the storage capacity of disposal sites can be reasonably estimated.

In the process of dredging and disposing of bottom sediments by means of a hopper dredge, three volumes are of interest. The first is the volume of the in-situ bottom sediment to be dredged (as determined, for example, by soundings); the second is the so-called bin-measure volume, that volume occupied by the sediment in the hopper of the dredge; and the third is the volume that the material occupies after it is placed in a disposal site. Although the bin-measure volume provides a convenient quantitative parameter which can be used to determine payment, it serves no other function in the dredging and disposal operation, except possibly to relate bottom sediment volume to disposal site volume. The basic problem involves a given volume of in-situ bottom material that must be dredged and deposited in a diked containment area to comprise some disposal site volume. As the sediment in the containment area is dewatered and/or consolidated by some combination of external loading, drainage, evaporation, and transpiration, the dry density increases and the disposal site volume decreases. The rate at which this process takes place depends strongly on local conditions (weather, types of plants, bottom drainage, conditioning, etc), and broad generalizations must be viewed cautiously. If disposal sites are at a premium in a given area or if rapid utilization of the landfill is desired, certain conditioning procedures (such as accelerated dewatering and compacting) of the spoil may be justified to densify the material and obtain additional storage capacity or improved mechanical properties.

The volumes of dredgings deposited in the four Toledo sites (Riverside, Island, Penn 7, and Penn 8) during each of the past ten years are reported in Chapter 2. The work described here involves the synthesis of (a) over 100 dry density determinations taken from undisturbed piston-tube samples of the deposited dredgings in each of the four sites, (b) a comprehensive survey of the Penn 7 site prior to the placement of dredgings and after the site was essentially filled, and (c) the results of compaction tests on typical dredged materials. Although the qualitative interpretations of these data are expected to be generally applicable to a variety of bottom sediments and disposal site configurations, the quantitative values are associated specifically with the Toledo area.

Experimental Program

The sampling procedures described by Hummel and Krizek (1974) were used to take nine sets of undisturbed piston-tube samples from the four disposal sites, and over 100 field dry densities were determined. Riverside Site was sampled in the summers of 1971, 1972, 1973, and 1974; the Island Site in 1971, 1973, and 1974; Penn 8 in 1973 and 1974; and Penn 7 in 1974. Quite detailed topographic surveys were made of the Penn 7 site in 1972 prior to the placement of any dredgings and in 1974 after the site was essentially filled; readings in both cases were taken at the node points of a rectangular grid with 100 foot (30 meter) intervals, and details of these surveys are described in Chapter 9.

Dredgings taken from three different locations at Riverside Site were compacted in the laboratory with compactive efforts of 2,480 ft-lb/ft^3 or 119,000 m-N/m^3 (20% of Standard Proctor-ASTM D698), 12,400 ft-lb/ft^3 or 593,000 m-N/m^3 (Standard Proctor-ASTM D698), and 56,300 ft-lb/ft^3 or 2700,000 m-N/m^3(Modified Proctor-ASTM D66T). The maximum dry densities obtained in these tests provide the basis for assessing the relative merits of dewatering and compacting dredged material in a disposal area.

Analysis and Interpretation of Results

The primary objective of this analysis is to relate the time-dependent storage capacity of a given disposal site to the volume of bottom sediment that can be deposited in the site. The first step of the dredging process involves removing the sediments from the bottom of the waterway and placing them in the dredge. For a hopper dredge the volume conversion factor often employed is 0.82 (Powell, 1973), where the volume of dredged bottom sediment divided by 0.82 equals the bin-measure volume of the material in the dredge. Although this factor has not been explicitly verified in this study, it is based on numerous before-and-after sounding records and considerable experience by the U.S. Army Corps of Engineers, Detroit District. Alternatively, the in-situ density of the bottom sediments could be measured by a technique similar to that described by Poloncsik, Langdon, Nedved, and Fochtman (1972) and compared with the density of the sediments in the dredge hopper.

When the dredgings are pumped hydraulically into a disposal area, they are accompanied by large quantities of water that acts as a carrier; hence, the actual pumped volume is much larger than the bin-measure volume, and it is not important in this study. However, after the solids settle out of suspension and the excess water exits the area, the disposal site volume is considerably less than the bin-measure volume. Based on the bin-measure volume of 920,527 cubic yards that was deposited into Penn 7 (Boresch, 1974) and the actual in-place spoil volume of about 570,000 cubic yards that was calculated from the 1972 and 1974 surveys, it is found that the conversion factor between bin-measure volume and disposal site volume is 0.62. This is quite comparable to the factor of 0.65 commonly used by the Corps of Engineers (Powell, 1973) for this purpose, especially when consideration is given to the fact that the calculated factor is determined from measurements that were taken in 1974 -- 1.5 years after the majority of the material had been placed in the site. If some adjustment is made for the fact that some densification (consolidation) occurred during this period, a factor somewhat larger than 0.62 would be obtained.

Since the dry density of the dredgings in each of the four sites is time-dependent and varies in both the horizontal and vertical directions, the data must be interpreted within the framework of certain assumptions. First, it is assumed that the dredge spoil deposited in each of the sites is basically similar; this is quite reasonable because all the material was dredged from the Toledo harbor area. Second, some time datum must be selected for each of the four sites, and for purposes of this work this time reference (as explained in Chapter 8) is chosen as the year in which the site was half filled; reference to Figure 2-3 indicates that the time bases for Riverside Site, the Island Site, Penn 8, and Penn 7 were 1968, 1967, 1966, and 1972, respectively. Third, the spatial variations are hopefully handled by obtaining a number of samples from throughout each area and working with average values. Within the context of these assumptions, the average densities determined on the basis of a specified number of samples taken from a given site in a given year are referred to the respective time datum for each and plotted in Figure 11-4 (for example, the 1972 average dry density for 15 samples taken at Riverside Site,

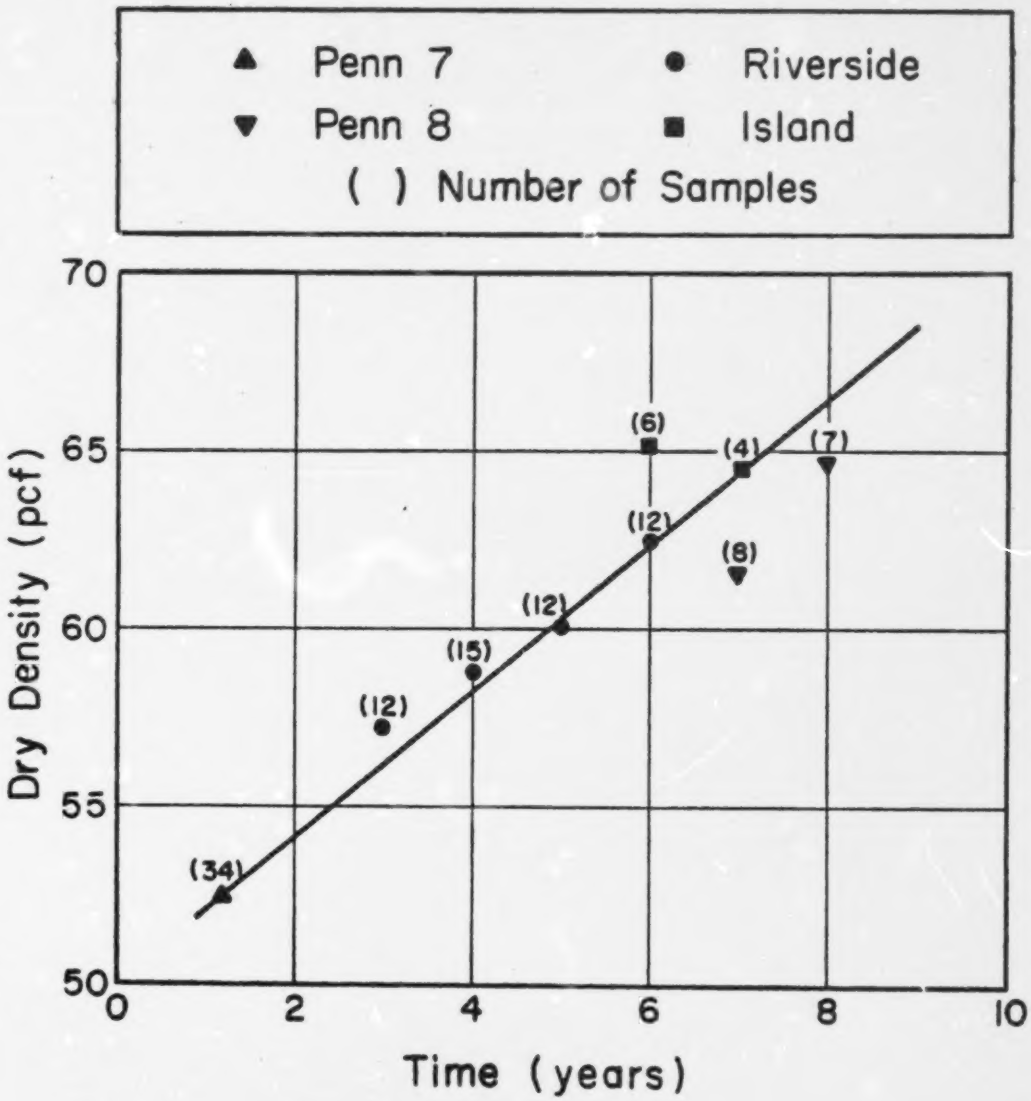

Figure 11-4. Increase in Dry Density with Time

when adjusted for the 1968 time datum, is plotted at a time increment of 4 years).

One exception to this rule occurs for the case of Penn 7, the youngest and most closely monitored of the four sites; since the density determinations were actually made about 1.50 years after 60% of the site was filled and 0.75 years after the other 40% was filled, the average dry density (measured in 1974) for Penn 7 was plotted at an average time of $[0.6(1.50) + 0.4(0.75)] = 1.2$ years. These data can be reasonably well and conveniently described by a straight line with a reference density of 50 pcf at zero time and a slope of 2 pcf per year; this implies that a given disposal area will increase in storage capacity at a rate of approximately 4% per year of the volume of confined material. Of course, this trend would not continue for very long times, because some limiting density would ultimately be attained; however, it appears that the trend does exist for at least the first eight or ten years. In comparison, it was found that the surface of the Penn 7 site settled an average of about 6% of the spoil thickness during a 9-month period prior to May of 1974.

If the results of the foregoing determinations are synthesized, a time-dependent relationship between the volume of dredged bottom sediments and the volume occupied by the material in a disposal site can be advanced. Using the 4% per year average increase in dry density and projecting the measured factor of 0.62 obtained for Penn 7 in 1974 back to 1972 (when it was impossible to obtain samples and measure densities), it can be reasonably hypothesized that the actual ratio of disposal site volume to bin-measure volume was $0.62[1 + 0.04(1.2)]$ or 0.65, which is exactly the factor used by the Corps of Engineers. Now, if the disposal site volume and the bottom sediment volume are related through their respective relationships with the bin-measure volume, we find that the required disposal area volume is 0.65/0.82 or about 0.8 times the bottom sediment volume. When adjusted for the observed 4% per year densification, the relationship between the disposal site volume, V_D, and the bottom sediment volume, V_B, can be expressed as

$$V_D = 0.8(1 - 0.04\ t)V_B \quad , \tag{11-3}$$

where t is time expressed in years. The direct implication of Equation (11-3) is that the initial required storage capacity of a diked disposal area must be about 80% of the anticipated volume of the bottom sediments to be dredged; however, after a period of 5 years, for example, about 20% of the initial volume of deposited sediment would be available for disposal of additional dredgings.

If disposal areas are extremely scarce or if rapid utilization of the landfill is desired, it may be economically justified to dewater the spoil and compact it in place; although the costs would be quite high, the benefits may be sufficient to warrant this approach. The first benefit would be a substantially reduced disposal site volume necessary to contain a given volume of bottom sediments. Referring to Figure 11-5, the maximum dry density, $(\gamma_d)_{max}$, can be related to the compactive effort, E_c, by the empirical expression

$$(\gamma_d)_{max} = 15(1 + \log_{10} E_c) \quad , \tag{11-4a}$$

where $(\gamma_d)_{max}$ and E_c are units of pcf and ft-lb/ft^3, respectively, or by

$$(\gamma_d)_{max} = 240(\log_{10} E_c - 0.67) \quad , \tag{11-4b}$$

where $(\gamma_d)_{max}$ and E_c are in units of kg/m^3 and m-N/m^3, respectively. For a Standard Proctor effort of 12,400 ft-lb/ft^3 or 593,000 m-N/m^3,

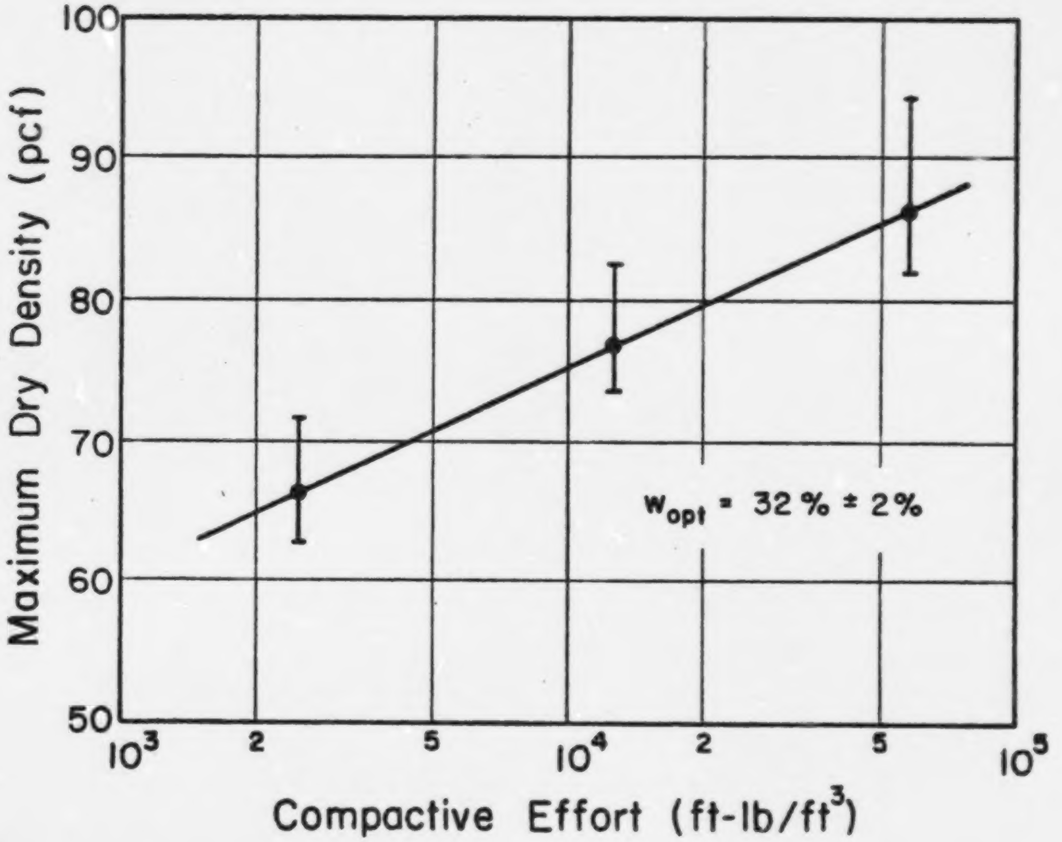

Figure 11-5. Increase in Maximum Dry Density with Compactive Effort

$(\gamma_d)_{max}$ equals 76.5 pcf or 1230 kg/m^3, which, when compared to the densities depicted in Figure 11-4, is seen to be much higher. Based on an initial disposal site dry density of about 50 pcf or 800 kg/m^3 for the hydraulically placed dredgings, the compacted Standard Proctor density of 76.5 pcf or 1230 kg/m^3 is seen to be about 50% higher, which means that about 50% more dredged material can be placed in the disposal site. If a Modified Proctor compactive effort is used, the initial storage capacity is increased on the order of 70%, and approximately a 30% increase is realized for only 20% of the Standard Proctor compactive effort. A major problem and expense would be encountered, however, when attempting to decrease the water content of the spoil to approximately the optimum water content, and such an approach would probably be justified only in very unusual circumstances. Of course, since increases in density improve most engineering properties (such as compressibility, shear strength, etc), some additional benefits, besides an increase in storage capacity, would be obtained, and the economic value, if any, of these benefits would have to be treated appropriately.

As an alternative to conventional dewatering and compaction, the type of site conditioning recently reported by the Office of Dredged Material Research (1974) may be useful for increasing greatly the storage capacity of containment areas and enhancing the possibilities of developing the landfills for industrial parks or other useful purposes. Briefly stated, the procedure involves the almost continuous conditioning of a layer of dredged material slurry by a tracked vehicle to accelerate the evaporation of water in order to create a layer of soil from the slurry; the soil layer is then compacted with conventional construction equipment. In two test areas located close to Toledo, Ohio the initial water contents of the slurries were 245% and 386%, and these were reduced to 68% in 8 days with 250 coverages and 39% in 30 days with 350 coverages, respectively, whereas the water content of 425% in a control pond decreased to 186% in 30 days with no conditioning. Since these materials were probably saturated throughout most of this conditioning process, reductions in water content can be readily used to approximate increases in dry density. The application of such a procedure would probably involve staged planning to permit filling operations to be undertaken in partitioned areas of a larger containment site while previously filled areas were being conditioned.

RELATIONSHIPS BETWEEN DRY DENSITY, SHEAR STRENGTH, AND TIME

The observed linear increase in dry density, γ_d, with time, t, as shown in Figure 11-4, can be expressed by

$$(\gamma_d/\gamma_w) = 0.8 + 0.032\ t \quad , \qquad (11\text{-}5)$$

where t is expressed in years and γ_w is the unit weight of water. In Chapter 8 the relationships between (a) the field vane strength, s_{fv}, and dry density, and (b) the average field vane shear strength, s_{avg}, time, and distance were found to be

$$\log s_{fv} = 2.6[(\gamma_d/\gamma_w) - 0.58] \qquad (8\text{-}6)$$

and

$$s_{avg} = \left[2.9 + 2\left(\frac{x}{\ell}\right)\right](t - 1) \qquad (8\text{-}13)$$

where s_{fv} and s_{avg} are expressed in kN/m^2, and $\frac{x}{\ell}$ is the ratio between the distance of the test location from the overflow weir and the distance between the discharge pipe and the overflow weir. In Equation (8-13) the parameter x/ℓ varied between 0 and 0.6; hence, if an average value of 0.3 is assumed for sake of simplicity, the average shear strength can be expressed in terms of time only as

$$s_{avg} = 3.5\ (t - 1) \quad . \tag{11-6}$$

The elimination of time, t, from Equations (11-5) and (11-6) yields

$$s_{avg} = 109\ (\gamma_d/\gamma_w) - 91 \quad . \tag{11-7}$$

Figure 11-6a shows the variation of the average shear strength, s_{avg}, with normalized dry density, γ_d/γ_w, as expressed by Equations (11-7) and (8-6). The difference in the values calculated from each of these equations can be attributed primarily to the manner in which the two equations were developed. The logarithmic relationship represents the "best fit" of numerous individual values of field vane strength and dry density (hence, profile variations of strength are taken into account), whereas the linear formulation given by Equation (11-7) reflects the combination of two relationships that are both based on average values.

Similarly, the elimination of the normalized dry density, γ_d/γ_w, from Equations (11-5) and (8-6) yields

$$\log s_{fv} = 0.083\ t + 0.57 \quad , \tag{11-8}$$

which, together with Equation (11-6), is plotted in Figure 11-6b. The higher average shear strength values given by Equation (11-6), except for very short times (less than about 2 years), can not be explained by the same argument outlined above, because the density-time relationship given by Equation (11-5) is based on average values of dry density (very similar to profile averages of shear strength). Hence, when such average values of dry density are substituted into Equation (8-6), they should yield an average value of the field vane strength. The difference

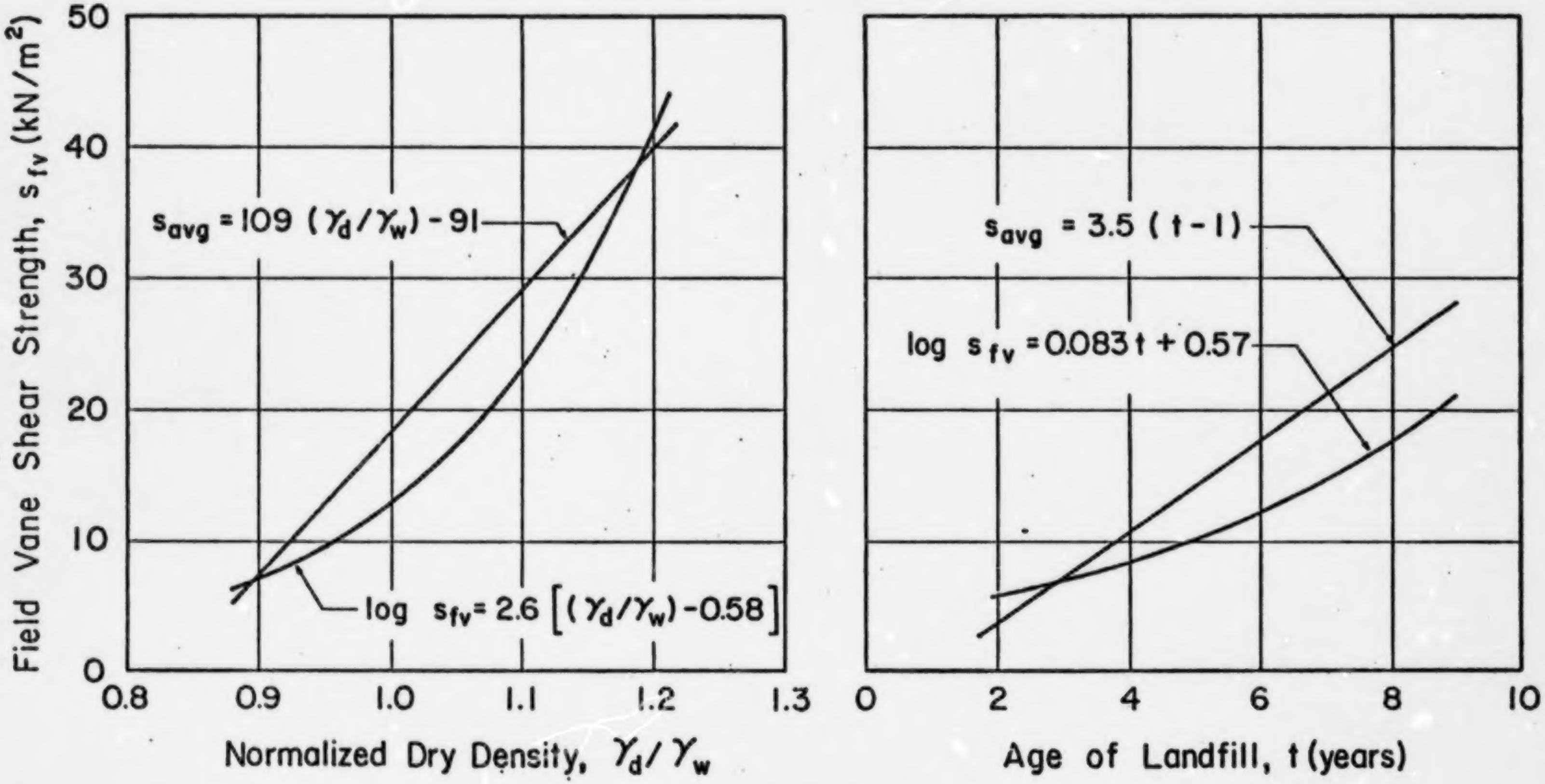

Figure 11-6. Development of Shear Strength with Dry Density and Time

between the two relationships depicted in Figure 11-6b must be interpreted as simply the variation that must be expected when two different approaches are taken to empirically quantify an observed trend. Although each individual empirical expression given by Equations (8-6), (8-13), and (11-5) is based on a substantial amount of experimental data and therefore considered to be reasonably valid, the comparisons given in Figure 11-6 suggest the caution that must be exercised when combining two of these empirical relationships to form a third one. In the process of "too much averaging" there is a tendency to obscure the physical nature and the associated sensitivites of the phenomenon being described.

PARTICLE SIZE DISTRIBUTION

The shear strength and dry density at a given site in a given year were found to generally increase with horizontal distance from the overflow weir. In addition, visual observations over a period of four years indicated that the fill material was usually soft near the weir and relatively strong in the vicinity of the inflow pipe. These variations in engineering properties are due in large part to the spatial variation in the grain size distribution of the dredged materials as they are deposited hydraulically in a disposal area, because the coarser particles tend to settle near the inflow pipe while the finer particles settle closer to the weir. Grain size data were obtained from tube samples taken from different elevations at various sampling locations at Riverside and Penn 7 and from auger samples taken from Riverside, and these data were combined to develop an appreciation for the actual distribution of particles sizes between the inflow pipe and the overflow weir. These experimental observations are supplemented by investigating the extent to which available relationships for stream bed movement and sedimentation velocity can be used to explain the manifested spatial variation of particle sizes in a containment area.

Actual Variations

Documented in Figure 11-7 are the spatial variations in the average grain size characteristics of the samples taken from the Riverside and Penn 7 disposal areas. Thirty-seven tube samples were obtained from Riverside Site from seven boreholes along Line I, which connects the overflow weir with the inflow pipe, and auger samples were obtained from three boreholes along each of Lines II, III, and IV, which emanate radially at 45° spacings for a short distance from the end of the inflow pipe; thirteen tube samples were also taken from the Penn 7 site at four locations along the base line designated in Figure 2-2. All samples were tested in accordance with the procedures explained in Chapter 3.

Longitudinal Line -- Tube samples were obtained from Riverside Site at locations 1, 4, 5, 6, 7, and 8 (see Figure 2-2) in 1971 and at locations 1, 6, and 8 in 1972, 1973, and 1974, and from Penn 7 at locations 2/10, 5/10, 8/10, and 12/10 in 1974. The actual spatial variation of particle size characteristics was evaluated by plotting average values of the effective size, D_{10}, uniformity coefficient, C_u, percent clay ($< 2\mu$), and percent fines (< 0.074 mm) for each location versus the horizontal distance of each respective location from the inflow pipe, and the results are given in Figure 11-7. The effective size, D_{10}, is seen to decrease from about 0.3 mm to 0.0015 mm in a distance of 30 meters (100 feet). In the following 300 meters (1000 feet) the effective size fluctuates between 0.0005 mm and 0.001 mm with no definite trend;

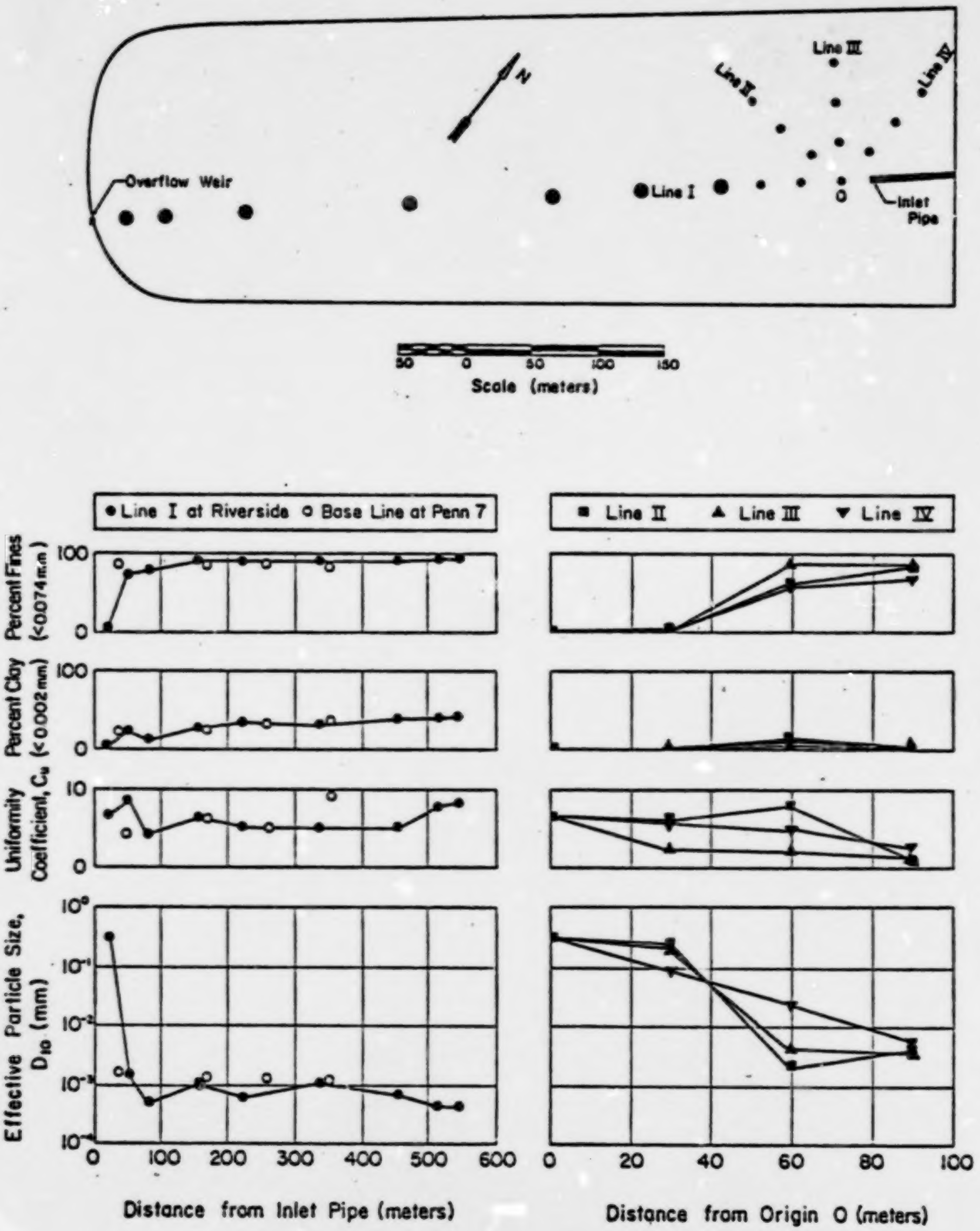

Figure 11-7. Spatial Variations of Average Grain Size Characteristics

this can be explained by the fact that particles may travel horizontally at different velocities while sedimentation is taking place. A gradual decrease in D_{10} from about 0.001 mm to about 0.0005 mm is noted in the vicinity of the overflow weir where the water normally covers the site. The coefficient of uniformity, C_u, has an average value of about 5 in the middle 400 meters (1300 feet) of the site and about 7 near the inflow pipe and the overflow weir. The clay sizes are generally missing near the inflow pipe, but they gradually increase with distance to a maximum of about 40 percent. The abnormally high percent clay (25 percent) at Borehole 1 may be due to a pool of stagnant water at this location. The fines (< 0.074 mm) increase from virtually zero to about 90 percent in 160 meters (500 feet) and remain practically constant thereafter for a distance of about 300 meters (1000 feet), after which they increase slightly to about 95 percent near the overflow weir. Analogous data from the Penn 7 site manifested generally similar trends; the observed differences are probably due in large part to the different flow patterns that prevailed (see Figure 2-2) at the two sites.

Vicinity of Discharge Pipe -- Six samples from Line II, thirteen from Line III, ten from Line IV, and one surface sample from the origin, O, were analyzed, and the average values of the pertinent parameters at each borehole are plotted in Figure 11-7 versus the distance from the origin. The effective size, D_{10}, decreased from 0.3 mm to about 0.005 mm in about 90 meters (300 feet), and the coefficient of uniformity, C_u, decreased from about 13 at the origin to an average of about 4 at 90 meters (300 feet). The clay fraction increased from zero in the first 30 meters (100 feet) to about 5 to 10 percent in the following 60 meters (200 feet), but the fines (< 0.074 mm), which were almost zero in the first 30 meters (100 feet), increased dramatically to an average of 70 percent at 60 meters (200 feet) and then slightly more to an average of about 80 percent at 90 meters (300 feet).

Theoretical Variations

An attempt was made herein to assess the extent to which an extremely simplified model, based on empirical and theoretical relationships documented in the literature, can be used to estimate the spatial variation of particle sizes. This model is arbitrarily centered around the mean particle size, D_{50}; the experimental mean particle size at a given distance is taken as the average of the mean sizes obtained from different samples at each location, and the results are plotted in Figure 11-8. For the first 120 meters (400 feet) from the inflow pipe, the plotted values represent the average values of D_{50} for all samples obtained from different boreholes along Lines I, II, III, and IV (see Figure 11-7) at the same distance from the inflow pipe. As can be seen, the mean particle size, D_{50}, decreased rapidly from about 4 mm to 0.6 mm in a distance of about 30 meters (100 feet); this is followed by a gentle decrease with distance up to about 200 meters (700 feet), after which the size remains nearly constant. Since two clearly different physical phenomena predominate in different areas of the disposal site, the model was assumed to consist of two parts, one of which was considered to be related to the bed load movement of a flowing stream and the other of which was considered analogous to sedimentation in a slowly flowing body of water; these component parts were assumed to apply near the inflow pipe and throughout the major portion of the site, respectively.

Vicinity of Inflow Pipe -- The elevation of the fill surface was assumed to vary linearly with distance from the inflow pipe; hence, the flow depth, z, at a radial distance, r, can be expressed by

$$z = (z_o r)/R \quad , \tag{11-9}$$

where z_o is the flow depth at a radial distance, R, as illustrated in Figure 11-9a. If the flow pattern is assumed to encompass an angle θ, the cross-sectional area, A, of flow may be expressed as

$$A = (r^2 \theta \, z_o)/R \quad . \tag{11-10}$$

Typically, the flow quantity, Q, passing over the weir of the Riverside or Penn 7 disposal areas varied from practically zero to several hundred thousand cubic feet per day. One simple empirical relationship to characterize the stability of coarse bed material in open channel flow has been given by Neill (1967) as

$$v_r = 6.37 \, D^{0.4} \, z^{0.1} \quad , \tag{11-11}$$

where D is the particle diameter in meters (assumed to be equal to the mean size, D_{50}), z is the depth of flow in meters, and v_r is the flow velocity in meters per second. The combination of Equation (11-11) with Equations (11-9), (11-10), and the continuity equation

$$Q = v_r \, A \tag{11-12}$$

yielded

$$D_{50} = \left[\frac{Q}{6.37 \left(\frac{z_o}{R}\right)^{1.1} r^{2.1} \, \theta} \right]^{2.5} \quad . \tag{11-13}$$

The mean particle size, D_{50}, calculated from Equation (11-13) is plotted in Figure 11-8 versus distance, X = r, for points close to the inflow pipe for values of Q equal to 0.15 m^3/sec (460,000 cubic feet per day), 0.03 m^3/sec (92,000 cubic feet per day), and 0.003 m^3/sec (9,200 cubic feet per day). The radial distance, R, was assumed to be 100 meters

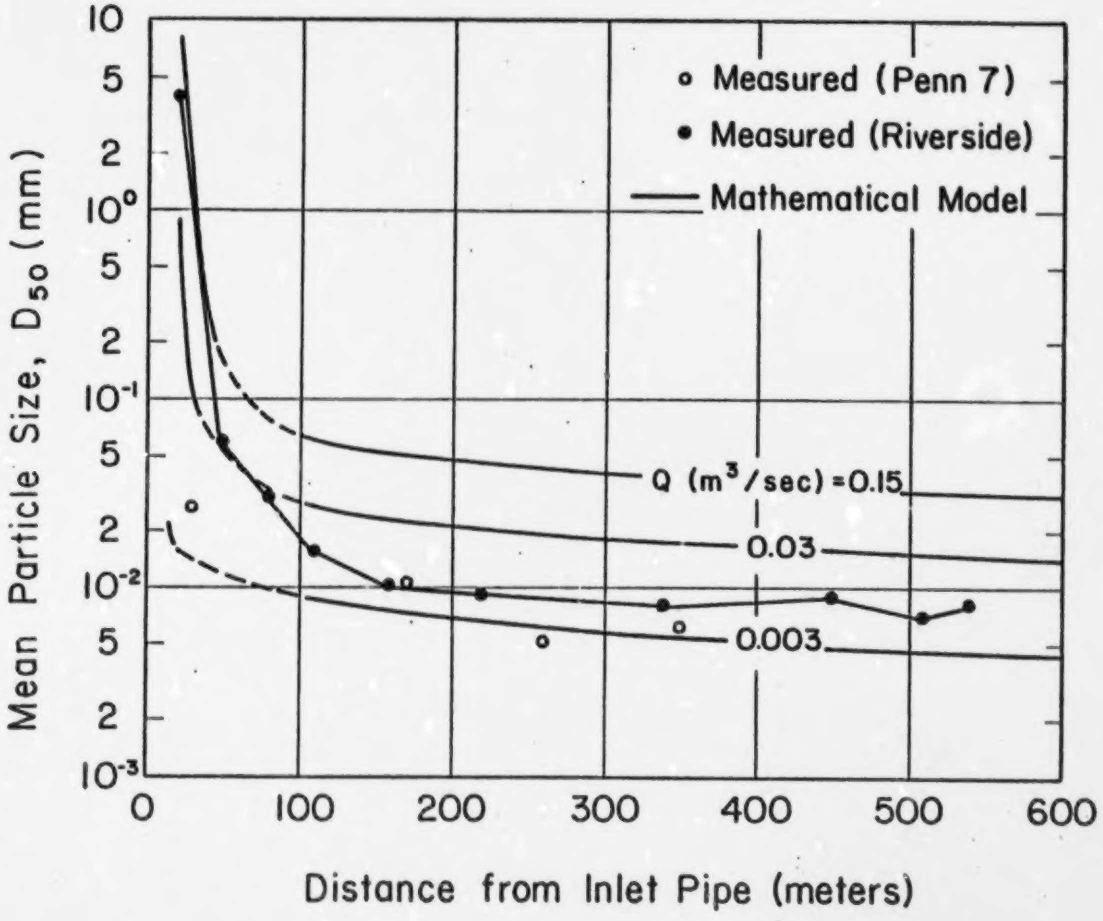

Figure 11-8. Observed and Predicted Values for Spatial Variation of Mean Grain Size

(330 feet), and the flow depth, z_o, at R was selected as 0.2 meters (8 inches). Due to the formation of a delta in front of the inflow pipe, small rivulets tended to form and the flow area in the immediate vicinity of the pipe usually encompassed only a small portion of the total possible flow area; this is expressed by the angle, θ, which may vary from virtually zero at very low flow rates to a larger value at higher flow rates; based on many observations of pumping operations the angle θ was selected to be $\pi/12$, $\pi/24$, and $\pi/48$, respectively, for each of the three aforementioned flow rates.

Open Water Domain -- At a sufficient distance from the inflow pipe (assumed to be 100 meters or 330 feet), the flow pattern is presumed to be such that Stoke's law may be applied to calculate the time necessary for a particle to settle out of suspension. At this distance it was also assumed that the discharge, Q, is evenly distributed across the total width, B, of the site for the total distance, L, to the overflow weir. The horizontal distance travelled by a D_{50} soil particle (which settles at the same rate as a spherical particle of diameter D) before it settles on the bottom of a disposal area may be calculated by equating the time necessary for it to travel a horizontal distance, $\bar{x}$, and the time required for it to fall to the bottom at $\bar{x}$. Figure 11-9b shows graphically the conditions assumed in this mathematical derivation. The steady-state settling velocity of a particle can be expressed by Stoke's law (Means and Parcher, 1963) as

$$v = \frac{2}{9}\frac{(\gamma_s - \gamma_f)}{\eta}\left(\frac{D}{2}\right)^2 \quad , \qquad (11\text{-}14)$$

where v is the velocity, γ_s is the unit weight of the solid particle,

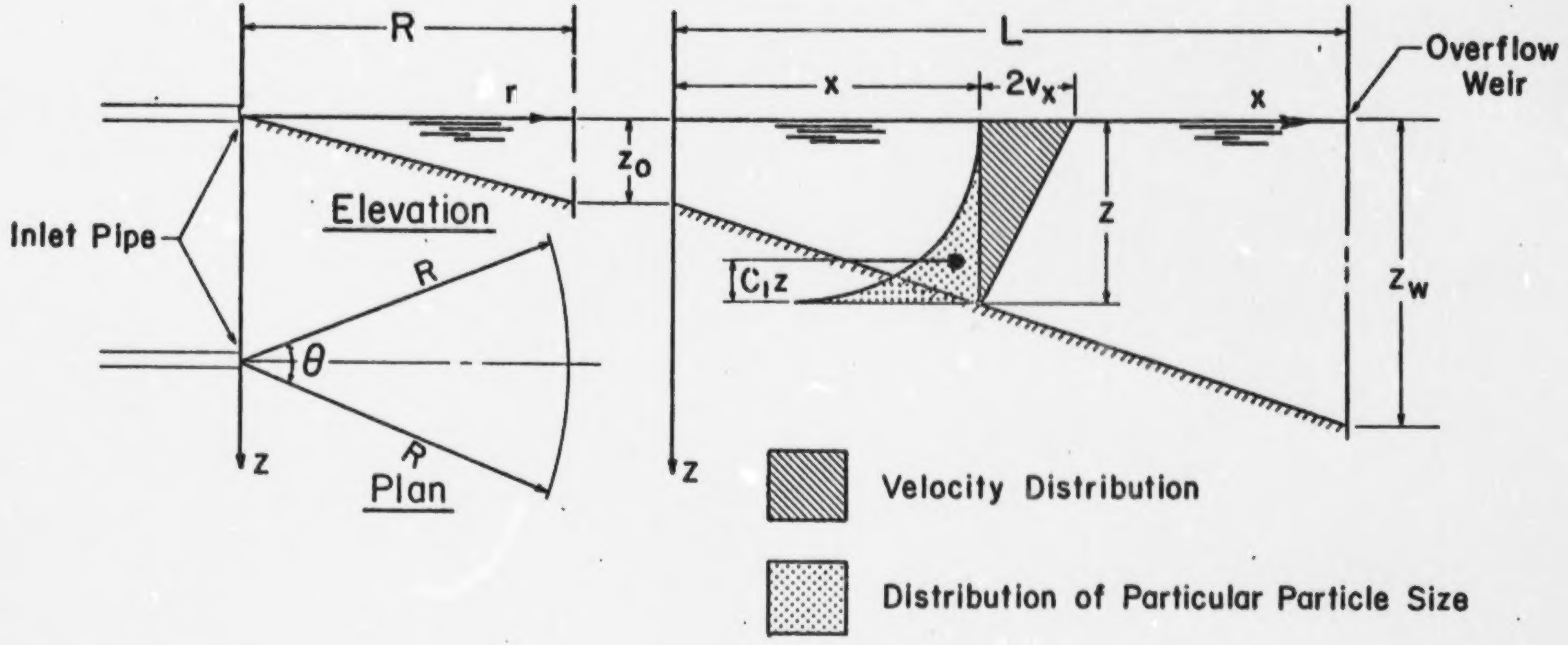
R
r
L
x
2v_x
x
Overflow Weir
z_o
Elevation
Inlet Pipe
R
θ
R
z
Plan
z
Z
z_w
C_1z
Velocity Distribution
Distribution of Particular Particle Size

(a) Model Based on Bed Load Movement

(b) Model Based on Sedimentation Velocity

Figure 11-9. Assumed Conditions for Development of Model to Characterize Spatial Distribution of Mean Grain Size

γ_f is the unit weight of the suspending fluid, η is the absolute viscosity of the suspending fluid, and D is the equivalent diameter of the particle. If it is assumed that a stream line maintains its same relative position in the velocity distribution as the flow depth increases, a particle of soil in suspension at height $C_1 z_o$ at $x = 0$ (Figure 11-9b) would actually fall a distance $C_1 \bar{z}$ in order to settle on the bottom at a distance $\bar{x}$. Based on this assumption the height of fall, h_f, can be expressed as

$$h_f = C_1 \bar{z} = C_1 \left[z_o + \left(\frac{z_w - z_o}{L} \right) \bar{x} \right] \quad , \qquad (11\text{-}15)$$

where z_w is the flow depth at the weir (or as close to the weir as the model can be reasonably applied). Assuming a linear distribution of flow velocity with an average value, v_x, and a parabolic distribution of a certain particle size throughout a vertical cross-section, the average horizontal flow velocity, $\bar{v}_h$, of a particle can be expressed as $C_2 v_x$, which is the mean of its value at $x = 0$ and its ultimate zero value. In terms of the discharge, Q, and the dimensions, B and z, of a cross-section of flow, the mean horizontal velocity of the particle at time t and distance x is

$$\bar{v}_h = \frac{dx}{dt} = C_2 v_x = \frac{C_2 Q}{B\, z} \quad , \qquad (11\text{-}16)$$

which can be rearranged to yield

$$dt = \frac{B\, z\, dx}{C_2 Q} = \frac{B}{C_2 Q} \left[z_o + \left(\frac{z_w - z_o}{L} \right) x \right] dx \quad . \qquad (11\text{-}17)$$

By equating the time required for the particle to fall to the bottom (which is determined by combining Equations (11-14) and (11-15)) to the time needed for the particle to reach the distance $\bar{x}$ (which is calculated by integrating Equation (11-17)) and assuming that D_{50} is the representative particle size, the resulting expression may be rearranged to yield

$$D_{50} = \left\{ \left[\frac{36\ C_1 C_2\ Q\eta}{B(\gamma_f - \gamma_s)} \right] \left[\frac{L\ z_o + (z_w - z_o)\bar{x}}{2L\ z_o\bar{x} + (z_w - z_o)\bar{x}^2} \right] \right\}^{\frac{1}{2}} \quad . \qquad (11\text{-}18)$$

If a triangular velocity distribution is assumed, as shown in Figure 11-9b, C_1 equals C_2; furthermore, if a third-order parabolic distribution of a given particle size is assumed to exist in the vertical cross-section, both coefficients C_1 and C_2 are equal to one-fifth. For an average temperature of 20°C, the absolute viscosity, η, of water equals approximately 0.1 gm sec/cm^2 (Means and Parcher, 1963); furthermore, for γ_s and γ_f values of 2.7 and 1.0 gm/cm^3, respectively, an average site width of about 200 meters, initial and final flow depths, z_o and z_w, of 0.2 meters (8 inches) and 1.2 meters (4 feet), respectively, and a site length, L, of 500 meters (1700 feet), Equation (11-18) can be rewritten in the simplified form

$$D_{50} = \left\{ \frac{Q}{47500} \left(\frac{10{,}000 + \bar{x}}{100{,}000 + 5\ \bar{x}^2} \right) \right\}^{\frac{1}{2}} \quad , \qquad (11\text{-}19)$$

and D_{50} values computed therefrom for the three different flow rates previously mentioned (0.15, 0.3, and 0.03 m^3/sec) are plotted in Figure 11-8; predictions from the two component models are joined together by dashed lines. For the high flow rate (0.15 m^3/sec), which is approximately equal to the average flow rate measured during a 26-day period at Penn 7 (Krizek, Gallagher, and Karadi, 1974), the predicted D_{50} values agree with observed values for only the first 40 meters. In general, the predicted mean particle sizes at a given location are considerably larger than those actually measured. Although there are many possible reasons for these differences, the most probable explanation lies in the fact that the model described is grossly oversimplified and does not truly simulate the actual phenomena that take place in the field situation.

PRELIMINARY COST STUDY

Based on (a) data furnished by Boresch (1974) for the volumes of dredgings deposited in the four Toledo sites, (b) the unit costs of confined disposal (including dike cost) for each dredging period, and (c) the estimated minimum unit costs of depositing these dredgings in the open water, a comparison can be made between the total costs of confined disposal and open water disposal and the cost per unit area of the field sites can be determined. The range of unit costs in dollars per cubic yard (including dike cost) is 0.59 to 1.07, 0.37 to 1.06, 0.81 to 2.01, and 0.53 to 0.65 with an average value of 0.68, 0.53, 1.14, and 0.55 for Riverside, the Island, Penn 7, and Penn 8, respectively. The corresponding estimated range of minimum unit costs in dollars per cubic yard if these materials were dumped in the open water are respectively 0.50 to 1.35, 0.43 to 1.40, 0.69 to 1.96, and 0.46 to 0.96 with average values of 0.70, 0.63, 1.06, and 0.59.

The first point worthy of note is that the corresponding unit costs are essentially the same, provided the price of the land needed for disposal areas and/or the value of the resulting landfills are ignored. Subject to these latter conditions, the total cost of the dredging and disposal operations (including the cost of the dike) in millions of dollars is 1.34, 2.63, 1.05, and 0.51 at Riverside, the Island, Penn 7, and Penn 8, respectively, and the corresponding cost per acre in thousands of dollars is 40, 17, 31, and 20. It must be emphasized that these cost figures are applicable to the Toledo area only during the period under consideration. There are a multitude of highly localized factors that manifest their influence in any such cost analysis, and these are not in any way reflected in the foregoing figures. Moreover, even these results for the Toledo sites will change in the next few years, because more dredgings will be deposited in the Island, Penn 7, and Penn 8.

USES OF RESULTING LANDFILLS

The placement of dredgings in diked containment areas has the potential to serve two useful purposes at the same time -- disposal of the dredgings and creation of needed landfill for community development projects. In general, the use of landfill for industrial, residential, or recreational purposes involves considerations of settlement and stability, both with respect to time, and the ultimate usefulness of the landfill will be governed to a large degree by these considerations. Since maintenance dredgings of the type studied herein are very compressible and weak when hydraulically placed in a containment area, the effectiveness and economy of the landfill operation are often hampered by the time-consuming process of consolidation and the resulting man-made land is usually of marginal quality.

Based on results reported herein, the dry density increased about 4 percent per year and the shear strength increased about 4 kN/m^2 (0.6 psi) per year for the 8-year period covered by the observations of a hypothetical representative site composed of four individual field sites at different stages in their history. After about 6 or 8 years a 3 or 4 meter (10 or 12 foot) layer of hydraulically placed dredged material with no special treatment or extraordinary dewatering measures may be expected to attain an average dry density and shear strength of about 1050 to 1100 kg/m^3 (66 to 70 pcf) and 25 to 30 kN/m^2 (about 4 psi), respectively. The expected total settlement due to a surface load equal to the shear strength of the soil at this time would be about 10 cm (4 inches). In view of the low densities and shear strengths after such a long time (6 or 8 years), it is apparent that landfills composed of hydraulically placed dredged materials can not support shallow foundations for even light residential structures without special treatment, such as dewatering coupled with either compaction or preloading. These sites seem most suitable for parks, wildlife refuges, recreational areas, and parking lots and access roads for industrial buildings which would be founded on piles or caissons extending to deeper and more competent soils. However, even if the sites were used for buildings with deep foundations, special care would have to be taken to account for the inevitable differential settlements that would occur between the buildings and their accessories (pipes, parking lots, sidewalks, etc).

SUMMARY

Although a simple model based on the classical theory of consolidation underestimated considerably the measured settlements at Riverside and Penn 7, a more extensive mathematical model that accounts for impeded bottom drainage, evaporation, transpiration, and a vertical variation in material properties was found to predict quite well the measured settlements at three locations in the Penn 7 area. Topographic surveys of Penn 7 before and after the placement of dredgings verified that the ratio between the initial disposal site volume and the bin-measure volume is about 0.65; this ratio is useful when estimating the storage capacity of a given containment area. Nine sets of density determinations from four disposal sites encompassing about an eight-year history indicated that the dry density of deposited dredgings increases at a rate of about 4 percent per year, thereby commensurately increasing the storage capacity of the containment area. Compaction of the dredgings in a disposal area has the ability to significantly increase the dry density of the dredgings and the related storage capacity of the site, but the costs of dewatering and compacting these materials would probably be prohibitive in all except the most unusual cases. A significant spatial variation in particle size characteristics was observed, and other engineering properties (such as shear strength, dry density, compressibility, etc) were affected accordingly. The percent clay increased from zero near the inflow pipe to about 40 percent near the overflow weir. The percent fines increased sharply in the first 80 to 100 meters from the inflow pipe and then attained an approximately constant value of about 90 percent for the major portion of the disposal area. Typical D_{10} sizes were about 0.0008 mm over the mid-portion of the landfill and about 0.0004 mm near the overflow weir. A simple mathematical model was used to evaluate the extent to which the spatial distribution of particle sizes could be estimated, but results were not too encouraging from a quantitative point of view. In general, predicted mean particle sizes at a given location are several times larger than the measured sizes.

A preliminary cost study on the four disposal sites at Toledo indicated that the cost of confined disposal (including dike cost) is approximately the same as the estimated minimum cost of open water disposal, provided the land costs and/or value of the resulting landfill are ignored; although the indicated figures give some appreciation for the economics of the situation, it must be emphasized that these figures are valid only for the Toledo area. The low values and slow increase in the dry density and shear strength of hydraulically placed dredgings in diked containment areas with relatively impervious foundation soils near the water table limit to large extent the potential usefulness of sites composed of these materials. Such landfills would likely be most suitable for wildlife refuges, parks, recreational areas, and parking lots and access roads for industrial buildings supported on deep foundations; in this latter case, however, attention would have to be given to differential settlements between the buildings and service facilities located in or on the landfill material.

CHAPTER 12

SUMMARY AND CONCLUSIONS

The behavioral characteristics of landfills composed of hydraulically placed dredged materials were investigated during an extensive four-year field and laboratory experimental program. The field work was conducted at four sites (Riverside, the Island, Penn 7, and Penn 8) in the vicinity of Toledo, Ohio and consisted of (a) performing periodic vane shear tests, (b) obtaining undisturbed tube samples and disturbed samples of dredged materials for laboratory tests, (c) measuring the in-situ permeability of a dredging landfill, and (d) surveying various aspects of the containment areas and their surrounding dikes; in addition, the Penn 7 area was instrumented with settlement plates and piezometers to obtain data on the time-dependent variations of settlements and pore water pressures. The laboratory program included (a) the evaluation of time-dependent volume changes by means of slurry consolidation, conventional consolidation, and long-term secondary compression tests, (b) strength determination by use of miniature vane, fall cone, and unconfined compression tests, and (c) various classification and characterization tests.

Based on the results of the characterization and classification tests, the dredged materials in each of the four sites were found to be essentially the same. Data from twelve slurry consolidation tests and sixty-four conventional consolidation tests on undisturbed tube samples were used to correlate the consolidation characteristics of these dredgings with their index properties, void ratio, and consolidation pressure. Compressibility parameters were determined from the results of conventional consolidation tests and related to various index properties and dry density. The secondary compression characteristics were studied by means of long-term slurry and conventional consolidation tests, and the deflection-log time response was found to exhibit a consistent, but unusual, pattern wherein the rate of secondary compression, after being constant with log time for a considerable length of time, started to increase and form a second S-shaped curve similar to that of primary consolidation. The parameters which characterize the secondary and total compressions, including the coefficient of secondary consolidation, were correlated with the index properties and consolidation stress.

Laboratory and field shear strength measurements of the dredged materials in each of the four Toledo disposal sites, together with the basic assumption that the materials in each of the four sites are essentially the same, allow the development of a meaningful empirical relation that expresses the gain in shear strength with time for a period of about ten years. In addition, various empirical relationships were established to provide guidance in predicting the strength of similar dredgings as a function of water content, dry density, and liquidity index. However, the developed empirical relationships must be used with caution because the variation is often quite large for a given property and the equations are only applicable within the observed ranges of the independent variables. The measured settlements at the Penn 7 area compared reasonably well with the settlements calculated by a mathematical model which simulates the physical phenomena that occur during the desiccation and one-dimensional consolidation of successive layers of dredged materials as they are preiodically deposited in a diked containment area.

Based on the analysis and interpretation of the data obtained from the field and laboratory testing programs, the following conclusions can be advanced:

1. In view of the complex and unusual nature of this problem, which involves a heterogeneous landfill that is preferentially segregated upon deposition in layers and seasonally desiccated with interspersed fibers due to growth of vegetation, a methodology is established to obtain and interpret the appropriate data required to assess the long-term usefulness of such landfills and to identify measures that might be taken to improve these conditions. This methodology consists mainly of (a) performing several series of laboratory and field tests to determine both characterization indices and behavioral properties of these materials, (b) correlating these parameters to enable estimates to be advanced regarding the response of landfills composed of similar materials, and (c) synthesizing the characteristics of four Toledo disposal sites with different histories to predict the long-term (10 year) behavior of similar disposal areas.

2. Most of the dredgings encountered in this study can be classified as either a mixture of organic silts and clays of medium to high plasticity or inorganic clays of high plasticity; furthermore, all of the materials deposited in each of the four Toledo disposal sites are essentially the same, thus justifying the consideration of data from all four sites as representative of one site spanning a time period of almost a decade.

3. The compression index lies between 0.3 and 0.7 and increases linearly with both water content and liquid limit; for all practical purposes a value of 0.0006 cm^2/sec can be assumed to represent the average coefficient of consolidation.

4. The constrained tangent modulus increases linearly with consolidation stress, and the modulus number lies between 8 and 20, increasing linearly with the dry density and decreasing linearly with the water content and percent clay.

5. Despite the significant difference in the proportions of secondary and primary compressions obtained from slurry and conventional consolidation tests, the total settlement per unit height associated with corresponding stress levels is about the same for both tests; the times necessary to reach ultimate settlements are shorter for slurry consolidation tests than for conventional tests, and this suggests that the times needed to reach ultimate settlements in the field may be much shorter than those predicted from conventional consolidation tests.

6. The coefficient of permeability, as obtained from conventional consolidation tests and from direct permeability tests, ranges from about 10^{-7} to 10^{-8} cm/sec for dredged materials with void ratios on the order of 1 to 2; however, field infiltration tests on materials with comparable void ratios yielded permeability coefficients about three orders of magnitude higher.

7. The logarithm of shear strength varies exponentially with water content and linearly with dry density and liquidity index.

8. The shear strength of the four landfills investigated was found to increase at an average rate of about 4 kN/m^2 per year (about 0.6 psi per year) for a period of about a decade.

9. The storage capacity of a field site can be improved by modifying the positions of the discharge pipe and the overflow weir with respect to the site configuration to obtain a more-or-less evenly distributed layer of dredged material and overlying water; this may be achieved by using a longer discharge pipe with valves at different locations or by installing two discharge pipes and two overflow weirs to allow periodic reversal of the flow in the containment area.

10. Topographic surveys of one diked containment area before and after the placement of dredgings verify that the ratio between the initial disposal site volume and the bin-measure volume is about 0.65.

11. Dry density determinations at four disposal sites encompassing about an eight year history indicate that the dry density of hydraulically deposited dredgings increases at the rate of about 4 percent per year, thereby increasing the storage capacity of the containment area.

12. Compacting the dredgings in a disposal area will significantly increase their dry density and the related storage capacity of the site, but the costs of dewatering and compacting these materials will probably be prohibitive in all except the most unusual cases.

13. The simple model based on available theories of bed load movement and particle settling was inadequate for predicting the spatial variation of particle sizes within a dredgings containment area; in general, model predictions overestimated the actual particle size at a given location by a factor of 5 to 10, and a more sophisticated model is necessary to realistically represent the true field situation.

14. The low initial shear strength of these dredged materials, together with their slow rate of increase in shear strength and associated large volume change, indicate that, unless steps are taken to add stabilizing agents or accelerate the process of dewatering, the use of landfill sites composed of such materials will be limited to wildlife refuges, parks, recreational areas, parking lots, access roads, and light structures with flexible structural joints and flexible floors which would allow several inches of total settlement and a few inches of differential settlement. Special precautions would be required to ascertain that embedded utilities are sufficiently flexible to accommodate the inevitable differential movements. The improvement of such landfills may be accomplished by use of chemical additives or mechanical methods, such as preloading, sand drains, sand blankets, vacuum drainage, electro-osmosis, or combinations thereof, but in each case the cost would have to be analyzed in terms of the benefits expected; controlled preloading may increase the bearing capacity sufficiently to construct small to medium size buildings, warehouses, shopping centers, storage tanks, airport facilities, and other similar structures.

REFERENCES

Adams, J. I. (1965), "The Engineering Behavior of a Canadian Muskeg," Proceedings of the Sixth International Conference on Soil Mechanics and Foundation Engineering, Montreal, Canada, Volume 1, pp. 3-7.

Andresen, A., and Bjerrum, L. (1958), "Vane Testing in Norway," Contributions from Scandinavia, Discussion, Norwegian Geotechnical Institute, Publication Number 28.

Arman, A. (1970), "Engineering Classification of Organic Soils," Highway Research Record 310, pp. 75-89.

Atterberg, A. (1911), "Uber die physikalishe Bodenuntersuchung und uber die Plastizitat der Tone" (On the Investigation of the Physical Properties of Soils and on the Plasticity of Clays), Int. Mitt. fur Badenkunde, 1, pp. 10-43.

Barber, E. S. (1961), "Notes on Secondary Consolidation," Proceedings of the Highway Research Board, Volume 40, pp. 663-675.

Barden, L. (1965), "Consolidation of Clay with Non-linear Viscosity," Geotechnique, Volume 15, Number 4, pp. 345-362.

Benjamin, J. R., and Cornell, C. A. (1970), Probability, Statistics and Decision for Civil Engineers, McGraw-Hill Book Company, New York.

Bjerrum, L., Jonson, W., and Ostenfeld, C. (1957), "The Settlement of a Bridge Abutment on Friction Piles," Proceedings of the Fourth International Conference on Soil Mechanics and Foundation Engineering, London, England, Volume 2, pp. 14-18.

Boresch, U. W. (1974), Personal Communication.

Buisman, A. S. (1936), "Results of Long Duration Settlement Tests," Proceedings of the First International Conference on Soil Mechanics and Foundation Engineering, Cambridge, Massachusetts, Volume 1, pp. 103-106.

Cadling, L., and Odenstad, S. (1950), "The Vane Borer: An Apparatus for Determining the Shear Strength of Clay Soils Directly in the Ground," Proceedings of the Royal Swedish Geotechnical Institute, Number 2, Sweden.

Carlson, L. (1948), "Determination in Situ of the Shear Strength of Undisturbed Clay by Means of a Rotating Auger," Proceedings of the Second International Conference on Soil Mechanics and Foundation Engineering, Rotterdam, Holland, Volume 1, pp. 265-270.

Cadagrande, A. (1932), "Research on the Atterberg Limits of Soils," Public Roads, October.

Casagrande, A. (1936), "The Determination of the Pre-consolidation Load and its Practical Significance," Proceedings of the First International Conference on Soil Mechanics and Foundation Engineering, Cambridge, Massachusetts, Volume 3, pp. 60-64.

Casagrande, A. (1948), "Classification and Identification of Soils," Transactions of the American Society of Civil Engineers, Volume 113, pp. 901-930.

Corps of Engineers, Buffalo District (1969), Dredging and Water Quality Problems in the Great Lakes, Twelve-Volume Technical Report, New York.

Corps of Engineers, Philadelphia District (1969), Long Range Spoil Disposal Study, Six-Volume Technical Report, Pennsylvania.

Cozzolino, V. M. (1961), "Statistical Forecasting of Compression Index," Proceedings of the Fifth International Conference on Soil Mechanics and Foundation Engineering, Paris, France, Volume 1, pp. 51-53.

Croney, D., and Coleman, J. D. (1954), "Soil Structure in Relation to Soil Suction (pF)," Journal of Soil Science, Volume 5, p. 75.

Crow, E. L., Davis, F. A., and Maxfield, M. W. (1960), Statistics Manual, Dover Publications, Inc., New York.

Draper, N. R., and Smith, H. (1966), Applied Regression Analysis, John Wiley & Sons, Inc., New York.

Garbe, C. W., and Jeno, J. J. (1968), "Reclamation of Hydraulic Dredge Spoil," Dames and Moore Technical Topics, San Francisco, California, pp. 1-5.

Gibbs, H. J. (1956), "An Apparatus and Method of Vane Shear Testing of Soils," American Society for Testing and Materials, Special Technical Publication Number 193, pp. 9-15.

Gibbs, H. J., Hilf, J. W., Holtz, W. G., and Walker, F. C. (1960), "Shear Strength of Cohesive Soils," Proceedings of the Research Conference on Shear Strength of Cohesive Soils, American Society of Civil Engineers, University of Colorado, Boulder, Colorado, pp. 33-168.

Gibson, R. E., and Lo, K. Y. (1961), "A Theory of Consolidation of Soils Exhibiting Secondary Compression," Norwegian Geotechnical Insttitue, Publication Number 41.

Giger, M. W., Franklin, A. G., and Krizek, R. J. (1973), "Electrical Resistivity Survey of Two Dredging Disposal Sites," Bulletin of the Association of Engineering Geologists, Volume 10, Number 2, pp. 107-119.

Goldberg, D. (1964), Discussion of "Subsurface Stabilization of Organic Silty Clay," by E. Jonas, Proceedings of the Conference on Design of Foundations for Control of Settlement, American Society of Civil Engineers, Evanston, Illinois, pp. 463-467.

Haefeli, R., and Schaad, W. (1948), "Time Effect in Connection with Consolidation Tests," Proceedings of the Second International Conference on Soil Mechanics and Foundation Engineering, Rotterdam, Holland, Volume 3, pp. 23-29.

Hansen, J. B., and Inan, S. (1969), "Tests and Formulas Concerning Secondary Consolidation," Proceedings of the Seventh International Conference on Soil Mechanics and Foundation Engineering, Mexico City, Mexico, Volume 1, pp. 45-53.

Hartzell, E. P. (1968), Disposal of Shoal Material from the Dredging Operation in the Delaware River, Corps of Engineers, Philadelphia District, pp. 240-260.

Hummel, P. L., and Krizek, R. J. (1974), "Sampling of Maintenance Dredgings," Journal of Testing and Evaluation, American Society for Testing and Materials, Volume 2, Number 3, pp. 139-145.

Hvorslev, M. G. (1949), Subsurface Exploration and Sampling of Soils for Civil Engineering Purposes, U.S. Waterways Experiment Station, Vicksburg, Mississippi, (Reprinted by Engineering Foundation, New York).

Janbu, N. (1963), "Soil Compressibility as Determined by Oedometer and Triaxial Tests," Proceedings of the First European Conference on Soil Mechanics and Foundation Engineering, Wiesbaden, Germany, Volume 1, pp. 19-25.

Keene, P. (1964), Discussion of "Settlement of Buildings on the MIT Campus," by H. Horn and T. W. Lambe, Proceedings of the Conference on Design of Foundations for Control of Settlement, American Society of Civil Engineers, Evanston, Illinois, pp. 232-244.

Krizek, R. J., and Casteleiro, M. (1974), Mathematical Model for One-Dimensional Desiccation and Consolidation of Dredged Materials, Technical Report Number 3, by Northwestern University to the Environmental Protection Agency, EPA Grants 15070-GCK and R-800948, Evanston, Illinois

Krizek, R. J., Franklin, A. G., and Soriano, A. (1974), "Seismic Survey of a Hydraulic Landfill Composed of Maintenance Dredgings," Bulletin of the Association of Engineering Geologists, Volume 11, Number 3, pp. 173-202.

Krizek, R. J., Gallagher, B. J., and Karadi, G. M. (1974), Water Quality Study for a Dredging Disposal Area, Technical Report Number 4, by Northwestern University to the Environmental Protection Agency, EPA Grants 15070-GCK and R-800948, Evanston, Illinois.

Krizek, R. J., Karadi, G. M., and Hummel, P. L. (1973), Engineering Characteristics of Polluted Dredgings, Technical Report Number 1, by Northwestern University to the Environmental Protection Agency, EPA Grants 15070-GCK and R-800948, Evanston, Illinois.

Krizek, R. J., and Katz, B. M. (1974), "Comparative Determinations of Organic Matter in Polluted Maintenance Dredgings," Proceedings of the International Symposium on Water Resources Instrumentation, International Water Resources Association, Chicago, Illinois, Volume 2, pp. 492-504.

Krizek, R. J., Parmelee, R. A., Kay, J. N., and Elnagger, H. A. (1971), Structural Analysis and Design of Pipe Culverts, National Cooperative Highway Research Program, Report Number 116, Washington, D. C.

Krizek, R. J., Roderick, G. L., Jin, J. S. (1974), Stabilization of Dredged Materials, Technical Report Number 2, by Northwestern University to the Environmental Protection Agency, EPA Grants 15070-GCK and R-800948, Evanston, Illinois.

Lambe, T. W. (1951), Soil Testing for Engineers, John Wiley & Sons, Inc., New York.

Lambe, T. W., and Whitman, R. V. (1969), Soil Mechanics, John Wiley & Sons, Inc., New York.

Leonards, G. A., and Ramiah, B. K. (1959), "Time Effects in the Consolidation of Clays," American Society for Testing and Materials, Special Technical Publication Number 254, pp. 116-130.

Lo, K. Y. (1961), "Secondary Compression of Clays," Journal of the Soil Mechanics and Foundations Division, American Society of Civil Engineers, Volume 87, Number SM4, pp. 61-87.

Lowe, J., Jonas, E., and Obrician, V. (1969), "Controlled Gradient Consolidation Test," Journal of the Soil Mechanics and Foundations Division, American Society of Civil Engineers, Volume 95, Number SM1, pp. 77-97.

McNely, D. J. (1966), Hydraulic Fill Area 2, Mariner's Island, Dames and Moore Office Memorandum, San Francisco, California, pp. 1-24.

Means, R. E., and Parcher, J. V. (1963), Physical Properties of Soils, Charles E. Merrill Publishing Company, Columbus, Ohio.

Mesri, G. (1973), "Coefficient of Secondary Compression," Journal of the Soil Mechanics and Foundations Division, American Society of Civil Engineers, Volume 99, Number SM1, pp. 123-137.

Neill, C. R. (1967), Stability of Coarse Bed Material in Open Channel Flow, University of Alberta Press, Edmonton, Canada.

Newland, P. L., and Allely, B. H. (1960), "A Study of the Consolidation Characteristics of a Clay," Geotechnique, Volume 10, Number 2, pp. 62-74.

Nichols, C. (1972), Personal Correspondence, Dames and Moore, San Francisco, California.

Norman, L. (1958), "A Comparison of Values of Liquid Limit Determined with Apparatus with Brass of Different Hardness," Geotechnique, Volume 8, Number 1, pp. 79-91.

Office of Dredged Material Research (1974), Spoil Compaction Method Tested, World Dredging and Marine Construction, Volume 10, Number 6, pp. 57-58.

Osterberg, J. O. (1952), Discussion of "Field Compaction," by R. Phillipe, Proceedings of the Conference on Soil Stabilization, Massachusetts Institute of Technology, Cambridge, Massachusetts, pp. 167-168.

Poloncsik, S., Langdon, W. M., Nedved, T. K.,and Fochtman, E. G. (1972), "In-place Measurement of Shoal Density," Journal of the Water Pollution Control Federation, Volume 44, Number 12, pp. 2334-2341.

Powell, K. C. (1973), Personal Communication.

Raphaelian, L. A., and Krizek, R. J. (1974), "Collection and Analysis of Representative Samples of Dredging Slurries," Proceedings of the International Symposium on Water Resources Instrumentation, International Water Resources Association, Chicago, Illinois, Volume 1, pp. 400-408.

Salazar, J. H. (1973), Regression Analysis of Soil Compressibility, M.S. Thesis, Department of Civil Engineering, Northwestern University, Evanston, Illinois.

Schultze, E., and Kotzias, P. (1961), "Geotechnical Properties of Lower Rhine Silts," Proceedings of the Fifth International Conference on Soil Mechanics and Foundation Engineering, Paris, France, Volume 1, pp. 329-333.

Seed, H. B., Woodward, R. J., and Lundgren, R. (1964), "Clay Mineralogical Aspects of the Atterberg Limits," Journal of the Soil Mechanics and Foundations Division, American Society of Civil Engineers, Volume 90, Number SM4, pp. 107-131.

Seed, H. B., Woodward, R. J., and Lundgren, R. (1964), "Fundamental Aspects of the Atterberg Limits," Journal of the Soil Mechanics and Foundations Division, American Society of Civil Engineers, Volume 90, Number SM6, pp. 75-105.

Sheeran, D. E., and Krizek, R. J. (1971), "Preparation of Homogeneous Soils Samples by Slurry Consolidation," Journal of Materials, Volume 6, Number 2, pp. 356-373.

Skempton, A. W. (1953), "The Colloidal Activity of Clays," Proceedings of the Third International Conference on Soil Mechanics and Foundation Engineering, Zurich, Switzerland, Volume 1, pp. 57-61.

Skempton, A. W., and Bishop, A. W. (1950), "The Measurement of the Shear Strength of Soils," Geotechnique, Volume 2, Number 2, pp. 90-108.

Smith, R. E., and Wahls, H. E. (1969), "Consolidation Under Constant Rate of Strain," Journal of the Soil Mechanics and Foundations Division, American Society of Civil Engineers, Volume 95, Number SM2, pp. 519-539.

Stamatopoulos, A. C., and Kotzias, P. C. (1973), "The Specific Constrained Modulus," Proceedings of the Eighth International Conference on Soil Mechanics and Foundation Engineering, Moscow, Russia, Volume 1, Part 2, pp. 397-402.

Taylor, D. W. (1942), Research on Consolidation of Clays, Technical Report, Department of Civil and Sanitary Engineering, Massachusetts Institute of Technology, Cambridge Massachusetts, Serial 82.

Taylor, D. W. (1948), Fundamentals of Soil Mechanics, John Wiley & Sons, Inc., New York.

Taylor, D. W., and Merchant, W. (1940), "A Theory of Clay Consolidation Accounting for Secondary Compression," Journal of Mathematics and Physics, Volume 19, Number 3, pp. 167-185.

Terzaghi, K. (1923), "Die Berechnung der Durchässigkeitsziffer des Tones aus dem Verlauf der hydrodynamischen Spannungserscheinungen, Akademie der Wissenschaften in Wien, Mathematisch-naturwissenschaftliche Klasse, Sitzungsberichte, Abteilung II a, Volume 132, Number 3/4, pp. 125-138.

Terzaghi, K. (1926), "Simplified Soil Tests for Subgrades and Their Physical Significance," Public Roads, October.

Terzaghi, K. (1941), "Undisturbed Clay Samples and Undisturbed Clays," Journal of the Boston Society of Civil Engineers, Volume 28, Number 3, pp. 211-231.

Terzaghi, K. (1944), "Ends and Means in Soil Mechanics," Engineering Journal (Canada), Volume 27, pp. 608-615.

Terzaghi, K., and Peck, R. B. (1948), Soil Mechanics in Engineering Practice, First Edition, John Wiley & Sons, Inc., New York (Second Edition was published in 1968).

Van Zelst, T. W. (1948), "An Investigation of the Factors Affecting Laboratory Consolidation of Clay," Proceedings of the Second International Conference on Soil Mechanics and Foundation Engineering, Rotterdam, Holland, Volume 7, pp. 52-61.

Wahls, H. E. (1962), "Analysis of Primary and Secondary Consolidation," Journal of the Soil Mechanics and Foundations Division, American Society of Civil Engineers, Volume 88, Number SM6, pp. 207-231.

Wissa, A. E. Z., Christian, J. T., Davis, E. H., and Heiberg, S. (1971), "Consolidation at Constant Rate of Strain," Journal of the Soil Mechanics and Foundations Division, American Society of Civil Engineers, Volume 97, Number SM10, pp. 1393-1413.

APPENDIX

DESCRIPTIONS OF SAMPLES

Summarized in this Appendix are all the undisturbed and remolded samples of relatively solid dredged materials that were obtained subsequent to the list published in the report by Krizek, Karadi, and Hummel (1973). In accordance with the identification system explained in this latter report, these samples are designated by a letter which refers to the consistency of the sample (E indicates a solid material that is capable of maintaining a given shape), a chronological number, and two letters which represent the first letters of the city and state from which the samples were taken (TO stands for Toledo, Ohio). The sampling equipment and techniques have been described in detail by Hummel and Krizek (1974), and the sample locations are illustrated in Figures A-1 and A-2. Various laboratory tests (consolidation, strength, grain size distribution, Atterberg limits, dry density, etc.) were conducted on most of these samples, and the results are given in different sections of this report.

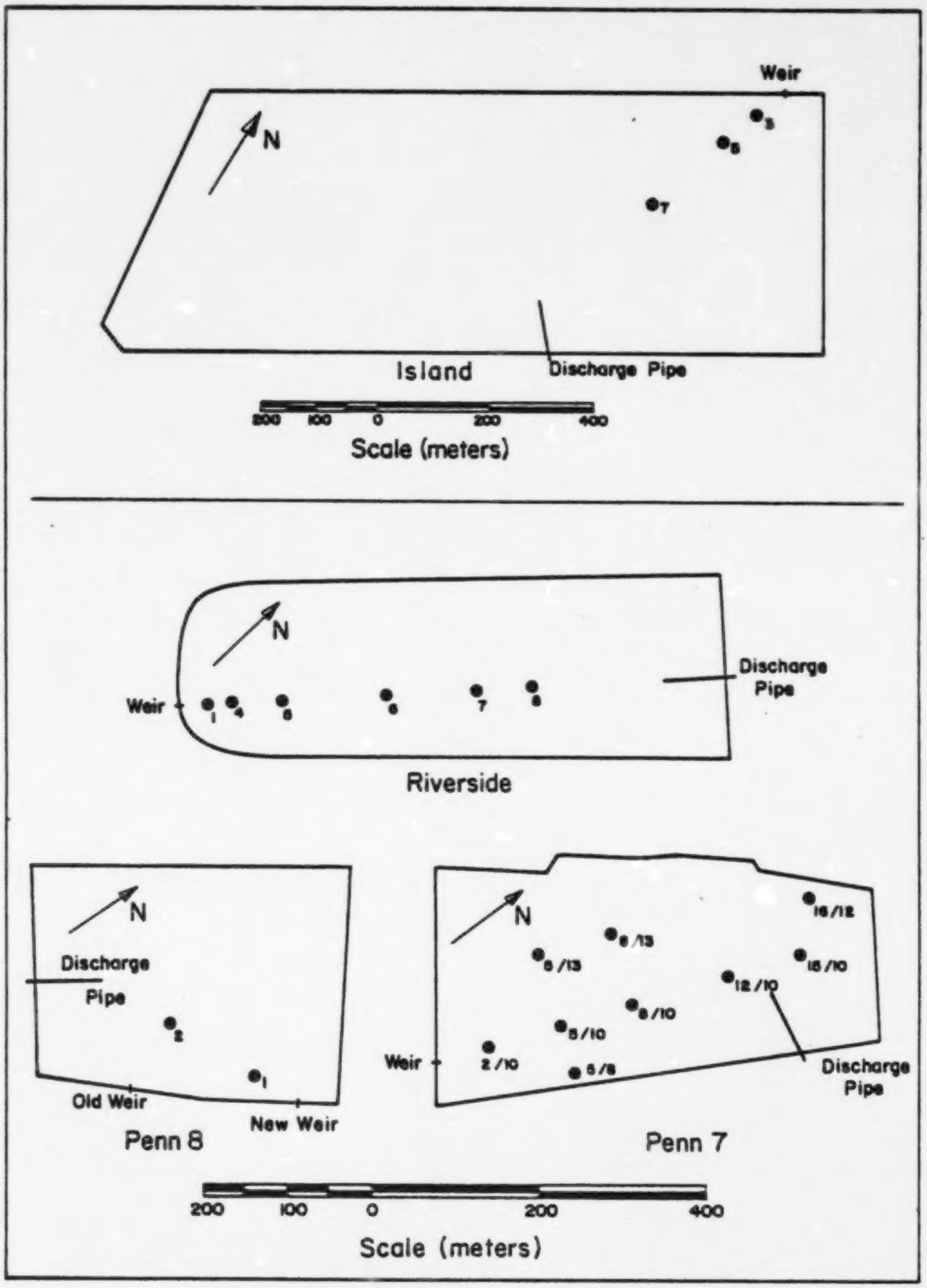
Weir
N
3
5
7
Island
Discharge Pipe
200 100 0 200 400
Scale (meters)
N
Weir
1
4
5
6
7
8
Discharge Pipe
Riverside
N
Discharge Pipe
2
1
Old Weir
New Weir
Penn 8
N
16/12
6/13
3/13
15/10
12/10
8/10
5/10
Weir
2/10
5/8
Discharge Pipe
Penn 7
200 100 0 200 400
Scale (meters)

Figure A-1. Test Locations at Toledo Disposal Areas

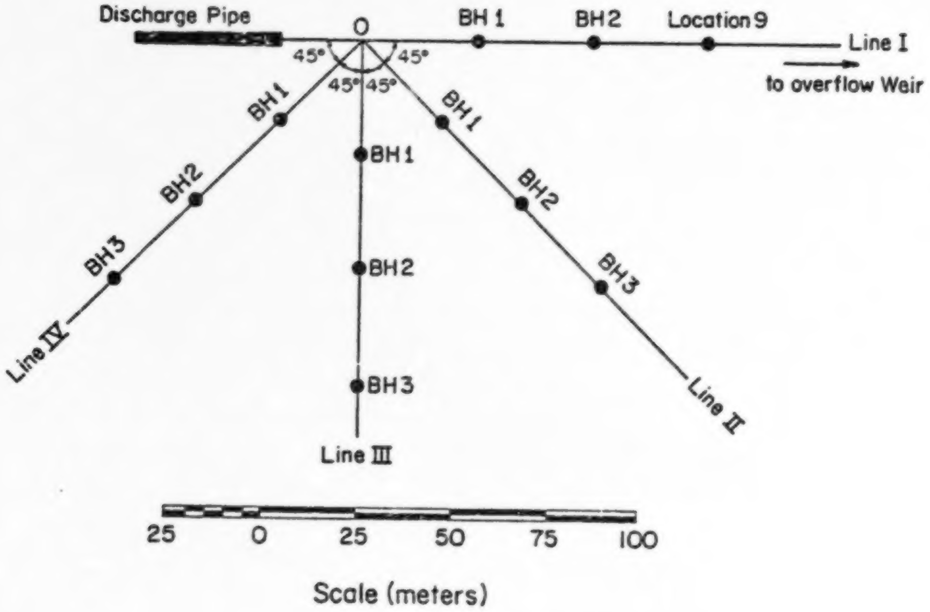

Discharge Pipe
O
BH 1
BH 2
Location 9
Line I
to overflow Weir
45°
45°
45°
45°
BH1
BH2
BH3
Line IV
BH1
BH2
BH3
Line III
BH1
BH2
BH3
Line II
25
0
25
50
75
100
Scale (meters)

Figure A-2. Sampling Locations in Vicinity of Inflow Pipe at Riverside

Table A-1

Summary of "E" Samples

Sample Number	Date Obtained	Brief Description
E153TO	7/18/72	Split spoon sample from Location 8/8 at depth of 10 feet at Penn 7
E154TO	7/18/72	Split spoon sample from Location 8/8 at depth of 20 feet at Penn 7
E155TO	7/19/72	Split spoon sample from Location 6/10 at depth of 9 feet at Penn 7
E156TO	7/19/72	Split spoon sample from Location 9/10 at depth of 9 feet at Penn 7
E157TO	7/19/72	Split spoon sample from Location 9/10 at depth of 19 feet at Penn 7
E158TO	7/19/72	Split spoon sample from Location 9/14 at depth of 9 feet at Penn 7
E159EI	12/21/72	Mixture of various samples from different sites
E160TO	7/9/73	Tube sample from Location 1 at depth of 1.8 feet at Riverside Site
E161TO	7/9/73	Tube sample from Location 1 at depth of 2.8 feet at Riverside Site
E162TO	7/9/73	Tube sample from Location 1 at depth of 4.2 feet at Riverside Site
E163TO	7/9/73	Tube sample from Location 1 at depth of 5.2 feet at Riverside Site
E164TO	7/9/73	Tube sample from Location 1 at depth of 6.2 feet at Riverside Site
E165TO	7/9/73	Tube sample from Location 1 at depth of 7.2 feet at Riverside Site
E166TO	7/9/73	Tube sample from Location 1 at depth of 8.2 feet at Riverside Site
E167TO	7/9/73	Tube sample from Location 1 at depth of 9.2 feet at Riverside Site

Table A-1 (cont.)

Summary of "E" Samples

Sample Number	Date Obtained	Brief Description
E168TO	7/9/73	Tube sample from Location 1 at depth of 10.2 feet at Riverside Site
E169TO	7/9/73	Tube sample from Location 1 at depth of 11.0 feet at Riverside Site
E170TO	7/10/73	Tube sample from Location 6 at depth of 2.5 feet at Riverside Site
E171TO	7/10/73	Tube sample from Location 6 at depth of 3.5 feet at Riverside Site
E172TO	7/10/73	Tube sample from Location 6 at depth of 4.5 feet at Riverside Site
E173TO	7/10/73	Tube sample from Location 6 at depth of 5.5 feet at Riverside Site
E174TO	7/10/73	Tube sample from Location 6 at depth of 6.5 feet at Riverside Site
E175TO	7/10/73	Tube sample from Location 6 at depth of 7.5 feet at Riverside Site
E176TO	7/10/73	Tube sample from Location 6 at depth of 8.5 feet at Riverside Site
E177TO	7/10/73	Tube sample from Location 6 at depth of 9.5 feet at Riverside Site
E178TO	7/11/73	Tube sample from Location 8 at depth of 2.5 feet at Riverside Site
E179TO	7/11/73	Tube sample from Location 8 at depth of 3.5 feet at Riverside Site
E180TO	7/11/73	Tube sample from Location 8 at depth of 4.5 feet at Riverside Site
E181TO	7/11/73	Tube sample from Location 8 at depth of 6.0 feet at Riverside Site
E182TO	7/11/73	Tube sample from Location 8 at depth of 7.5 feet at Riverside Site

Table A-1 (cont.)

Summary of "E" Samples

Sample Number	Date Obtained	Brief Description
E183TO	7/11/73	Tube sample from Location 8 at depth of 8.5 feet at Riverside Site
E184TO	7/11/73	Tube sample from Location 8 at depth of 9.5 feet at Riverside Site
E185TO	7/11/73	Tube sample from Location 3 at depth of 1.5 feet at Island Site
E186TO	7/11/73	Tube sample from Location 3 at depth of 2.5 feet at Island Site
E187TO	7/11/73	Tube sample from Location 3 at depth of 3.5 feet at Island Site
E188TO	7/11/73	Tube sample from Location 3 at depth of 4.5 feet at Island Site
E189TO	7/11/73	Tube sample from Location 3 at depth of 5.5 feet at Island Site
E190TO	7/11/73	Tube sample from Location 3 at depth of 6.5 feet at Island Site
E191TO	7/11/73	Tube sample from Location 3 at depth of 7.5 feet at Island Site
E192TO	7/11/73	Tube sample from Location 3 at depth of 8.5 feet at Island Site
E193TO	7/11/73	Tube sample from Location 3 at depth of 9.5 feet at Island Site
E194TO	7/11/73	Tube sample from Location 3 at depth of 10.5 feet at Island Site
E195TO	7/11/73	Tube sample from Location 3 at depth of 11.5 feet at Island Site
E196TO	7/11/73	Tube sample from Location 3 at depth of 12.5 feet at Island Site
E197TO	7/12/73	Disturbed sample from Borehole 1 on Line I at depth of 2.0 feet at Riverside Site

Table A-1 (cont.)

Summary of "E" Samples

Sample Number	Date Obtained	Brief Description
E198TO	7/12/73	Disturbed sample from Borehole 1 on Line I at depth of 2.5 feet at Riverside Site
E199TO	7/12/73	Disturbed sample from Borehole 1 on Line I at depth of 4.0 feet at Riverside Site
E200TO	7/12/73	Disturbed sample from Borehole 1 on Line I at depth of 6.0 feet at Riverside Site
E201TO	7/12/73	Disturbed sample from Borehole 2 on Line I at depth of 4.0 feet at Riverside Site
E202TO	7/12/73	Disturbed sample from Borehole 2 on Line I at depth of 6.0 feet at Riverside Site
E203TO	7/12/73	Disturbed sample from Borehole 2 on Line I at depth of 8.0 feet at Riverside Site
E204TO	7/12/73	Disturbed sample from Borehole 2 on Line I at depth of 10.0 feet at Riverside Site
E205TO	7/12/73	Disturbed sample from Borehole 1 on Line II at depth of 0.0 feet at Riverside Site
E206TO	7/12/73	Disturbed sample from Borehole 2 on Line II at depth of 4.5 feet at Riverside Site
E207TO	7/12/73	Disturbed sample from Borehole 2 on Line II at depth of 6.5 feet at Riverside Site
E208TO	7/12/73	Disturbed sample from Borehole 3 on Line II at depth of 1.0 feet at Riverside Site
E209TO	7/12/73	Disturbed sample from Borehole 3 on Line II at depth of 3.0 feet at Riverside Site
E210TO	7/12/73	Disturbed sample from Borehole 3 on Line II at depth of 5.0 feet at Riverside Site
E211TO	7/12/73	Disturbed sample from Borehole 3 on Line II at depth of 7.0 feet at Riverside Site
E212TO	7/12/73	Disturbed sample from Borehole 1 on Line III at depth of 0.0 feet at Riverside Site

Table A-1 (cont.)

Summary of "E" Samples

Sample Number	Date Obtained	Brief Description
E213TO	7/12/73	Disturbed sample from Borehole 2 on Line III at depth of 1.0 feet at Riverside Site
E214TO	7/12/73	Disturbed sample from Borehole 2 on Line III at depth of 2.0 feet at Riverside Site
E215TO	7/12/73	Disturbed sample from Borehole 2 on Line III at depth of 3.0 feet at Riverside Site
E216TO	7/12/73	Disturbed sample from Borehole 2 on Line III at depth of 4.0 feet at Riverside Site
E217TO	7/12/73	Disturbed sample from Borehole 2 on Line III at depth of 5.0 feet at Riverside Site
E218TO	7/12/73	Disturbed sample from Borehole 2 on Line III at depth of 7.0 feet at Riverside Site
E219TO	7/12/73	Disturbed sample from Borehole 2 on Line III at depth of 8.0 feet at Riverside Site
E220TO	7/12/73	Disturbed sample from Borehole 2 on Line III at depth of 9.0 feet at Riverside Site
E221TO	7/12/73	Disturbed sample from Borehole 3 on Line III at depth of 1.0 feet at Riverside Site
E222TO	7/12/73	Disturbed sample from Borehole 3 on Line III at depth of 2.0 feet at Riverside Site
E223TO	7/12/73	Disturbed sample from Borehole 3 on Line III at depth of 3.0 feet at Riverside Site
E224TO	7/12/73	Disturbed sample from Borehole 3 on Line VI at depth of 5.0 feet at Riverside Site
E225TO	7/12/73	Disturbed sample from Borehole 3 on Line III at depth of 6.0 feet at Riverside Site
E226TO	7/12/73	Disturbed sample from Borehole 2 on Line IV at depth of 1.0 feet at Riverside Site
E227TO	7/12/73	Disturbed sample from Borehole 2 on Line IV at depth of 2.0 feet at Riverside Site

Table A-1 (cont.)

Summary of "E" Samples

Sample Number	Date Obtained	Brief Description
E228TO	7/12/73	Disturbed sample from Borehole 2 on Line IV at depth of 3.0 feet at Riverside
E229TO	7/12/73	Disturbed sample from Borehole 2 on Line IV at depth of 4.0 feet at Riverside
E230TO	7/12/73	Disturbed sample from Borehole 2 on Line IV at depth of 4.5 feet at Riverside
E231TO	7/12/73	Disturbed sample from Borehole 2 on Line IV at depth of 5.0 feet at Riverside
E232TO	7/12/73	Disturbed sample from Borehole 2 on Line IV at depth of 6.0 feet at Riverside
E233TO	7/12/73	Disturbed sample from Borehole 3 on Line IV at depth of 1.0 feet at Riverside
E234TO	7/12/73	Disturbed sample from Borehole 3 on Line IV at depth of 2.0 feet at Riverside
E235TO	7/12/73	Disturbed sample from Borehole 3 on Line IV at depth of 3.0 feet at Riverside
E236TO	7/12/73	Disturbed sample from Borehole 3 on Line IV at depth of 4.0 feet at Riverside
E237TO	7/12/73	Disturbed sample from Borehole 3 on Line IV at depth of 5.0 feet at Riverside
E238TO	7/12/73	Disturbed sample from Borehole 3 on Line IV at depth of 6.0 feet at Riverside
E239TO	7/12/73	Disturbed surface sample from Point 0 at Riverside Site
E240TO	7/30/73	Tube sample from Location 1 at depth of 1.5 feet at Penn 8
E241TO	7/30/73	Tube sample from Location 1 at depth of 2.5 feet at Penn 8
E242TO	7/30/73	Tube sample from Location 1 at depth of 3.5 feet at Penn 8
E243TO	7/30/73	Tube sample from Location 1 at depth of 4.5 feet at Penn 8

Table A-1 (cont.)

Summary of "E" Samples

Sample Number	Date Obtained	Brief Description
E244TO	7/30/73	Tube sample from Location 1 at depth of 5.5 feet at Penn 8
E245TO	7/30/73	Tube sample from Location 1 at depth of 6.5 feet at Penn 8
E246TO	7/30/73	Tube sample from Location 1 at depth of 7.4 feet at Penn 8
E247TO	7/30/73	Tube sample from Location 1 at depth of 8.2 feet at Penn 8
E248TO	7/30/73	Tube sample from Location 2 at depth of 2.0 feet at Penn 8
E249TO	7/30/73	Tube sample from Location 2 at depth of 4.0 feet at Penn 8
E250TO	7/30/73	Tube sample from Location 2 at depth of 5.0 feet at Penn 8
E251TO	7/30/73	Tube sample from Location 2 at depth of 7.5 feet at Penn 8
E252TO	7/30/73	Tube sample from Location 2 at depth of 8.5 feet at Penn 8
E253TO	7/30/73	Tube sample from Location 2 at depth of 10.0 feet at Penn 8
E254TO	5/20/74	Tube sample from Location 1 at depth of 1.0 feet at Riverside
E255TO	5/20/74	Tube sample from Location 1 at depth of 3.0 feet at Riverside
E256TO	5/20/74	Tube sample from Location 1 at depth of 4.5 feet at Riverside
E257TO	5/20/74	Tube sample from Location 1 at depth of 5.5 feet at Riverside
E258TO	5/20/74	Tube sample from Location 1 at depth of 8.5 feet at Riverside

Table A-1 (cont.)

Summary of "E" Samples

Sample Number	Date Obtained	Brief Description
E259TO	5/20/74	Tube sample from Location 1 at depth of 9.5 feet at Riverside
E260TO	5/20/74	Tube sample from Location 6 at depth of 1.8 feet at Riverside
E261TO	5/20/74	Tube sample from Location 6 at depth of 3.0 feet at Riverside
E262TO	5/20/74	Tube sample from Location 6 at depth of 4.0 feet at Riverside
E263TO	5/20/74	Tube sample from Location 6 at depth of 5.0 feet at Riverside
E264TO	5/20/74	Tube sample from Location 6 at depth of 6.0 feet at Riverside
E265TO	5/20/74	Tube sample from Location 6 at depth of 7.0 feet at Riverside
E266TO	5/20/74	Tube sample from Location 6 at depth of 8.0 feet at Riverside
E267TO	5/20/74	Tube sample from Location 6 at depth of 9.0 feet at Riverside
E268TO	5/20/74	Tube sample from Location 6 at depth of 10.0 feet at Riverside
E269TO	5/20/74	Tube sample from Location 8 at depth of 4.5 feet at Riverside
E270TO	5/20/74	Tube sample from Location 8 at depth of 5.0 feet at Riverside
E271TO	5/20/74	Tube sample from Location 8 at depth of 5.5 feet at Riverside
E272TO	5/20/74	Tube sample from Location 8 at depth of 7.0 feet at Riverside
E273TO	5/20/74	Tube sample from Location 8 at depth of 8.5 feet at Riverside

Table A-1 (cont.)

Summary of "E" Samples

Sample Number	Date Obtained	Brief Description
E274TO	5/20/74	Tube sample from Location 8 at depth of 9.5 feet at Riverside
E275TO	5/20/74	Tube sample from Location 8 at depth of 10.5 feet at Riverside
E276TO	5/20/74	Tube sample from Location 8 at depth of 11.5 feet at Riverside
E277TO	5/20/74	Tube sample from Location 1 at depth of 1.0 feet at Penn 8
E278TO	5/20/74	Tube sample from Location 1 at depth of 3.0 feet at Penn 8
E279TO	5/20/74	Tube sample from Location 1 at depth of 4.5 feet at Penn 8
E280TO	5/20/74	Tube sample from Location 1 at depth of 5.5 feet at Penn 8
E281TO	5/20/74	Tube sample from Location 1 at depth of 6.5 feet at Penn 8
E282TO	5/20/74	Tube sample from Location 1 at depth of 7.5 feet at Penn 8
E283TO	5/20/74	Tube sample from Location 1 at depth of 9.0 feet at Penn 8
E284TO	5/20/74	Tube sample from Location 2 at depth of 3.0 feet at Penn 8
E285TO	5/20/74	Tube sample from Location 2 at depth of 5.0 feet at Penn 8
E286TO	5/20/74	Tube sample from Location 2 at depth of 6.5 feet at Penn 8
E287TO	5/20/74	Tube sample from Location 2 at depth of 7.5 feet at Penn 8
E288TO	5/20/74	Tube sample from Location 2 at depth of 8.2 feet at Penn 8

Table A-1 (cont.)

Summary of "E" Samples

Sample Number	Date Obtained	Brief Description
E289TO	5/20/74	Tube sample from Location 2 at depth of 9.0 feet at Penn 8
E290TO	5/21/74	Tube sample from Location 3 at depth of 2.0 feet at Island
E291TO	5/21/74	Tube sample from Location 3 at depth of 3.5 feet at Island
E292TO	5/21/74	Tube sample from Location 3 at depth of 4.5 feet at Island
E293TO	5/21/74	Tube sample from Location 3 at depth of 5.5 feet at Island
E294TO	5/21/74	Tube sample from Location 3 at depth of 6.5 feet at Island
E295TO	5/21/74	Tube sample from Location 3 at depth of 7.5 feet at Island
E296TO	5/21/74	Tube sample from Location 3 at depth of 8.5 feet at Island
E297TO	5/21/74	Tube sample from Location 3 at depth of 9.5 feet at Island
E298TO	5/21/74	Tube sample from Location 3 at depth of 10.5 feet at Island
E299TO	5/21/74	Tube sample from Location 3 at depth of 11.5 feet at Island
E300TO	5/21/74	Tube sample from Location 3 at depth of 12.5 feet at Island
E301TO	5/21/74	Tube sample from Location 3 at depth of 13.5 feet at Island
E302TO	5/21/74	Tube sample from Location 2/10 at depth of 3.5 feet at Penn 7
E303TO	5/21/74	Tube sample from Location 2/10 at depth of 5.5 feet at Penn 7

Table A-1 (cont.)

Summary of "E" Samples

Sample Number	Date Obtained	Brief Description
E304TO	5/21/74	Tube sample from Location 5/8 at depth of 2.5 feet at Penn 7
E305TO	5/21/74	Tube sample from Location 5/8 at depth of 4.5 feet at Penn 7
E306TO	5/21/74	Tube sample from Location 5/8 at depth of 6.5 feet at Penn 7
E307TO	5/21/74	Tube sample from Location 5/8 at depth of 8.5 feet at Penn 7
E308TO	5/21/74	Tube sample from Location 5/8 at depth of 10.5 feet at Penn 7
E309TO	5/21/74	Tube sample from Location 5/8 at depth of 11.5 feet at Penn 7
E310TO	5/21/74	Tube sample from Location 5/10 at depth of 2.5 feet at Penn 7
E311TO	5/21/74	Tube sample from Location 5/10 at depth of 6.5 feet at Penn 7
E312TO	5/21/74	Tube sample from Location 5/10 at depth of 8.5 feet at Penn 7
E313TO	5/21/74	Tube sample from Location 5/13 at depth of 2.0 feet at Penn 7
E314TO	5/21/74	Tube sample from Location 5/13 at depth of 4.5 feet at Penn 7
E315TO	5/21/74	Tube sample from Location 5/13 at depth of 6.5 feet at Penn 7
E316TO	5/21/74	Tube sample from Location 5/13 at depth of 9.0 feet at Penn 7
E317TO	5/21/74	Tube sample from Location 8/10 at depth of 1.8 feet at Penn 7
E318TO	5/21/74	Tube sample from Location 8/10 at depth of 4.5 feet at Penn 7

Table A-1 (cont.)

Summary of "E" Samples

Sample Number	Date Obtained	Brief Description
E319TO	5/21/74	Tube sample from Location 8/10 at depth of 6.5 feet at Penn 7
E320TO	5/21/74	Tube sample from Location 8/10 at depth of 9.0 feet at Penn 7
E321TO	5/21/74	Tube sample from Location 8/10 at depth of 10.0 feet at Penn 7
E322TO	5/21/74	Tube sample from Location 8/13 at depth of 2.5 feet at Penn 7
E323TO	5/21/74	Tube sample from Location 8/13 at depth of 4.5 feet at Penn 7
E324TO	5/21/74	Tube sample from Location 8/13 at depth of 6.5 feet at Penn 7
E325TO	5/21/74	Tube sample from Location 8/13 at depth of 9.5 feet at Penn 7
E326TO	5/21/74	Tube sample from Location 12/10 at depth of 2.5 feet at Penn 7
E327TO	5/21/74	Tube sample from Location 12/10 at depth of 4.5 feet at Penn 7
E328TO	5/21/74	Tube sample from Location 12/10 at depth of 6.5 feet at Penn 7
E329TO	5/21/74	Tube sample from Location 15/10 at depth of 2.5 feet at Penn 7
E330TO	5/21/74	Tube sample from Location 15/10 at depth of 6.5 feet at Penn 7
E331TO	5/21/74	Tube sample from Location 15/10 at depth of 11.5 feet at Penn 7
E332TO	5/21/74	Tube sample from Location 16/12 at depth of 2.5 feet at Penn 7
E333TO	5/21/74	Tube sample from Location 16/12 at depth of 4.5 feet at Penn 7

Table A-1 (cont.)

Summary of "E" Samples

Sample Number	Date Obtained	Brief Description
E334TO	5/21/74	Tube sample from Location 16/12 at depth of 6.5 feet at Penn 7
E335TO	5/21/74	Tube sample from Location 16/12 at depth of 11.5 feet at Penn 7